

UNCLASSIFIED

AD NUMBER
AD830971
NEW LIMITATION CHANGE
TO Approved for public release, distribution unlimited
FROM Distribution authorized to U.S. Gov't. agencies and their contractors; Administrative/Operational Use; FEB 1968. Other requests shall be referred to Air Force Rocket Propulsion Laboratory, Edwards AFB, CA 93524.
AUTHORITY
AFRPL, per ltr dtd 27 Oct 1971

THIS PAGE IS UNCLASSIFIED

AD830971

AFRPL-TR-68-42

**AIR FORCE ROCKET PROPULSION LABORATORY
SCIENTIFIC AND ENGINEERING
SEMINAR ABSTRACTS-1967**

Edited By

LAWRENCE J. EDWARDS

and

CHARLES M. STONE, LT, USAF

FINAL REPORT

TECHNICAL REPORT AFRPL-TR-68-42

February 1968

THIS DOCUMENT IS SUBJECT TO SPECIAL EXPORT CONTROLS AND EACH TRANSMITTAL TO FOREIGN GOVERNMENTS OR FOREIGN NATIONALS MAY BE MADE ONLY WITH PRIOR APPROVAL OF AFRPL (RPPR-STINFO), EDWARDS, CALIFORNIA 93523.

**AIR FORCE ROCKET PROPULSION LABORATORY
AIR FORCE SYSTEMS COMMAND
UNITED STATES AIR FORCE
EDWARDS, CALIFORNIA**

MAY 1 1968

BEST AVAILABLE COPY

20050722050

340

AFRPL-TR-68-42

AIR FORCE ROCKET PROPULSION LABORATORY
SCIENTIFIC AND ENGINEERING SEMINAR ABSTRACTS - 1967

Edited By

LAWRENCE J. EDWARDS

and

CHARLES M. STONE, Lt, USAF

This document is subject to special export controls and each transmittal to foreign governments or foreign nationals may be made only with prior approval of AFRPL (RPPR-STINFO), Edwards, California 93523.

NOTICES

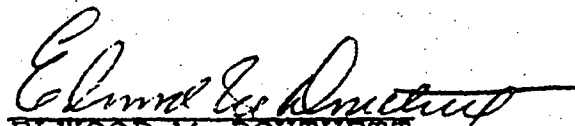
When U.S. Government drawings, specifications, or other data are used for any purpose other than a definitely related Government procurement operation, the Government thereby incurs no responsibility nor any obligation whatsoever, and the fact that the Government may have formulated, furnished, or in any way supplied the said drawings, specifications, or other data, is not to be regarded by implication or otherwise, or in any manner licensing the holder or any other person or corporation, or conveying any rights or permission to manufacture, use, or sell any patented invention that may in any way be related thereto.



FOREWORD

This report is a compilation of abstracts and papers presented at scientific and engineering seminars conducted by the Air Force Rocket Propulsion Laboratory, Edwards, California, from 10 January 1967 through 23 August 1967.

This report has been reviewed and approved.



ELWOOD M. DOUTHETT

Colonel, USAF

Commander, Air Force Rocket Propulsion Laboratory

ABSTRACT

Opportunities for personal growth through intellectual stimulation and the acquisition of new knowledge should be available to scientists, engineers and managers regardless of their field of experience or geographical location. Such opportunities are readily available when colleges and universities are located in the immediate vicinity. However, at the Air Force Rocket Propulsion Laboratory (AFRPL) the nearest university is approximately two hours distant by automobile. Accordingly, in September 1964 a seminar program was initiated as a lecture series for the scientists and engineers. In the first three years, over 100 seminars were conducted on a wide range of subjects dealing with both technical and management aspects of research and development. The emphasis in this program has been on subjects relating to the mission and the career development requirements of the Laboratory personnel.

In the first three years of operation, many of the seminar speakers have been provided by UCLA on contracts from AFRPL and have included authorities from various government agencies, universities and industry. In addition, Laboratory personnel served as speakers for the program on subjects ranging from technical discussions on in-house experimental studies to reviews of management and planning activities.

TABLE OF CONTENTS

	<u>Page</u>
ABSTRACTS (In Chronological Order)	1
Recent Advances in Solid Propellant Development	1
Fluorine Technology	13
Advanced Thrust Chamber Cooling	19
Rocket Performance Prediction and Analysis;	39
Nuclear Rocket Engine Reactors and Engine/Vehicle Integration;	45
Thermal Control of Space Propulsion Systems;	49
Plasma Physics and Application to Rocketry;	57
Electric Propulsion for Space Vehicles	61
Solid Propellant Mechanical Properties Testing, Failure Criteria and Aging;	67
Effect of Design on Booster Characteristics;	159
Advanced Propellants;	177
Human Factors and Maintenance in Space;	207
Concepts of Hypersonic Ablation;	213
Digital and Analog Simulation of Distributed Parameter Systems;	223
Principles of Cryogenic Engineering;	227
Deformation and Fracture of Viscoelastic Materials;	243
The Challenge of Effective Technical Speaking;	259

→ Paper

Table of Contents (Cont'd)

	<u>Page</u>
FM Systems;	267
Hey, Wait for Me; I'm Your Leader	275
Trajectory and Orbital Mechanics	281
Operations Research and Decision Making	295
The New Industrial Economics - An Adjustment Process;	301
Communication and the Managerial Process;	317
Solid Propellants (Oscillatory and Unstable Combustion). . .	323
ARPA Liquid Programs - A Critical Review	329
Shocks and Their Effects on Propellants	333

DISTRIBUTION LIST

FORM 1473

SPEAKER INDEX

<u>Speaker</u>	<u>Subject</u>	<u>Page</u>
Bussard, R. W.	Nuclear Rocket Engine Reactors and Engine/Vehicle Integration	45
Collins, Samuel C.	Principles of Cryogenic Engineering	227
Coulbert, Clifford D.	Advanced Thrust Chamber Cooling	19
Crow, Jack H.	FM Systems	267
Dellinger, David C.	Operations Research and Decision Making	205
Forbes, Forrest S.	ARPA Liquid Programs - A Critical Review	329
Gent, A. N.	Deformation and Fracture of Visco-Elastic Materials	243
Hand, Harry E.	The Challenge of Effective Technical Speaking	259
Jasinski, Frank J.	Hey, Wait for Me; I'm Your Leader	275
Karplus, W. J.	Digital and Analog Simulation of Distributed Parameter Systems	223
Kelley, Frank N.	Solid Propellant Mechanical Properties Testing, Failure Criteria and Aging	67
Landsbaum, Ellis M.	Advanced Propellants	177
Lyman, John	Human Factors and Maintenance in Space	207
Mager, Artur	Effect of Design on Booster Characteristics	159
Meyer, Rudolf X.	Electric Propulsion for Space Vehicles	61
Neumark, Hans R.	Fluorine Technology	13

Speaker Index (Cont'd)

<u>Speaker</u>	<u>Subject</u>	<u>Page</u>
Ryan, Norman W.	Solid Propellants: Oscillatory and Unstable Combustion	323
Salveson, M.E.	The New Industrial Economics - An Adjustment Process	301
Scala, Sinclair M.	Concepts of Hypersonic Ablation	213
Schmidt, Warren H.	Communication and the Managerial Process	317
Seely, Leslie B., Jr.	Shocks and Their Effects on Propellants	333
Sutton, G.W.	Plasma Physics and Application to Rocketry	57
Svenson, F.C.	Thermal Control of Space Propulsion Systems	49
Thompson, Grant	Recent Advances in Solid Propellant Development	1
Thompson, W.T.	Trajectory and Orbital Mechanics	281
Valentine, R.S.	Rocket Performance Prediction and Analysis	39

RECENT ADVANCES IN SOLID PROPELLANT DEVELOPMENT

(10 January 1967)

by
Grant Thompson

Mr. Thompson received his B.A. Degree in Chemistry in 1950 and Ph.D. in Organic Chemistry in 1953 from University of Utah. Formerly with DuPont Company doing research in the field of organic and polymer chemistry, he is now Manager of Propellant Development at Wasatch Division of Thiokol Chemical Corporation.

INTRODUCTION

A solid propellant rocket motor is well known for simplicity of design and operation. This reputation has been adequately demonstrated over the years with thousands of motor firings. Recently, the requirements dictated by missions that solid motors are being called on to perform have become more complex and the designs are therefore less simple. As a result the propellant properties that are now being specified are very sophisticated and therefore much more difficult to meet.

It is necessary for some missions that the solid motor have on-off capability and the propellant must have properties that will allow it to extinguish and reignite readily. Other applications specify throttling thus requiring propellant to possess a high burning rate-pressure slope. Some missions make it mandatory that the exhaust plume have low radar attenuation or low radar cross section; thus electron densities, afterburning and etc. must be controlled. Motors for volume limited applications may use end burning grain designs requiring very high burning rates and yet maintaining structural integrity over wide temperature extremes. The usual excellent properties of the solid propellants must be maintained while obtaining

these special properties.

Composite and double base are the two common types of solid propellants, both having their advantages and disadvantages. Composite propellants are safer to manufacture and use, can be stored and fired over wider temperature ranges, are cheaper, and are easier to case bond. Double base propellants, on the other hand, deliver a few seconds more of specific impulse in aluminized propellants, and are more effective with the hydride fuels primarily because performance optimizes at higher binder levels.

There are many considerations that are taken into account when selecting a new propellant ingredient or when deciding whether a new propellant can be useful. These include properties that affect performance, such as heat of formation or I_{sp} , density, and burning rate. Compatibility of a new ingredient with the other ingredients in the propellant or the compatibility of a new propellant with liner and insulation must be studied. The processability of the propellant has a large influence on the propellant selection, as well as mechanical properties, aging and safety characteristics. Cost and availability of ingredients must not be neglected.

Binders

The binder system for a solid propellant has several important functions. It provides a continuous matrix for the solid oxidizer and fuel with sufficient strength to maintain structural integrity during handling, storage and operation. It also serves as a fuel and in some cases as an oxidizer.

The double base binder consists primarily of nitrocellulose and an energetic nitrate plasticizer such as nitroglycerine (NG), diethyleneglycol dinitrate (DEGDN), triethyleneglycol dinitrate (TEGDN) or trimethyloethane trinitrate (TMETN).
(1)

Stabilizers such as nitrodephenyl amine are used to inhibit the decomposition of the nitrate compounds. The nitrocellulose which is a high polymer is swollen by the plasticizer to yield a viscoelastic gel which is somewhat thermoplastic since it is not crosslinked. Recent work has improved the mechanical properties by crosslinking the nitrocellulose with isocyanates through the free hydroxyl groups.

(2)

The most commonly used binders for composite propellants are hydrocarbon and polyurethane liquid polymers while polysulfides have lost favor because of low energy. Recently interest has been shown in fluorocarbon binders and in fluorine containing binders.

Composite binders are chain extended and crosslinked, chemically, with curing agents to give a network which is at least partially three dimensional. Random carboxylated hydrocarbon polymers which are cured with epoxides and aziridines do not give the ultimate in mechanical properties because of their dangling chain ends. Carboxyl-terminated hydrocarbon polymers give better mechanical properties and much higher gel fractions than the random carboxylated polymers when trifunction epoxides and aziridines are used because the dangling chain ends are eliminated. Hydroxyl terminated hydrocarbons which have lower viscosities at the same molecular weight than the carboxyl analog are cured with isocyanates to give urethane linkages. Polyurethane propellants are prepared by two methods: (1) a hydroxyl-terminated polyether is reacted with an isocyanate or (2) an isocyanate terminated polyether or polyester is reacted with diols and/or triols.

A hydrogenated polybutadiene binder yields the highest theoretical I_{sp} performance with ammonium perchlorate and aluminum while the polybutadiene type is a close second. Polyurethanes yield slightly lower I_{sp} values and the optimum values shift to lower total solids. Nitratoplasticized polyurethane or polyesters

and double base propellants optimize for I_{sp} at much higher binder levels but the peak values are not as high as with the hydrocarbon system. Since the nitratoplasticized propellants optimize for I_{sp} at higher binder levels, this allows them to accept high concentrations of light metal hydrides and still be processable.

Oxidizer

Perchlorates are used almost exclusively as solid oxidizers and, of the perchlorates, ammonium perchlorate is used for almost all propellants. Because ammonium perchlorate is non-hygroscopic, safe to handle, available in large quantities and cheap, it has been difficult to find a higher energy oxidizer to replace it even in a few of the applications.

Recent emphasis has been placed on nitronium perchlorate (NP), hydroxyl-ammonium perchlorate (HAP), and hydrazinium diperchlorate (HP2) since these materials have favorable heats of formation and reasonable thermal stability. All three are hygroscopic, but NP decomposes in the presence of moisture which makes it more difficult to work with. Compatibility of the oxidizers with binders has been a problem but solid progress has been made. HAP and HP2 can be used with either functionally terminated polybutadiene binders or with functionally terminated saturated hydrocarbon binders. NP requires a saturated hydrocarbon binder and even then great pains must be taken to remove trace impurities from the binder.

(1)

Theoretical calculations show that NP yields significantly higher I_{sp} (> 15 sec) than NH_4ClO_4 for an aluminized system; with beryllium the increase

is only about 6 sec, with aluminum hydride the increase is 24 and with BeH_2 , 10 sec. From the reported heats of formation for HP2 and HAS, it is predicted that theoretical performance will be between ammonium perchlorate and NP.

Fuels

A fuel as used in solid propellants is a reducing agent that improves performance by increasing the enthalpy of system or by decreasing the molecular weight of the gaseous products or both. The fuels are usually metals or metal hydrides with the important ones being aluminum, beryllium, aluminum hydride and beryllium hydride. Of these, aluminum is the only one used in an operational solid rocket motor.

Since aluminum is cheap, readily available, inert and yields non-toxic exhaust products, there has been reluctance to accept higher performing replacements. It appears that it is more desirable to increase the size of the motor rather than using a higher energy fuel. Beryllium can be used in place of aluminum in either composite or double base propellants rather easily but cost and toxicity of exhaust products have apparently prevented its use in an operational motor. Aluminum hydride does not have the toxicity problem of beryllium but it is expensive and the thermal stability of the material is borderline. Beryllium hydride is more thermally stable than aluminum hydride, but it is also expensive and high specific impulse efficiencies have been elusive. Good specific impulse efficiencies have been achieved recently in double base propellants. Beryllium hydride, of course, suffers from the same toxicity problems as beryllium.

Techniques of Propellant Characterization

There are numerous techniques of characterizing solid propellant which have been developed over the years. This discussion will be limited to the more recent promising techniques.

Extinguishment

Propellant extinguishment has recently become an important characteristic which must be evaluated according to the extinguishment method being used. To evaluate the pressure deflagration limit (P_{dl}) of a propellant, a 5/8 in. diameter strand is burned in a large bomb of essentially infinite L^* .⁽⁴⁾ The pressure is reduced slowly (5 psia/sec) while recording pressure and luminosity time traces. P_{dl} is the pressure at which the luminosity drops to zero. The validity of this test has been verified by many motor firings.

Techniques have also been devised to study propellant extinguishment using dp/dt and L^* methods. The first method requires rapid depressurization while the second uses a variable volume device that can change L^* as the propellant burns.

Plume Properties

The radar attenuation and reflection characteristics of solid propellant exhaust plumes are very important considerations for guidance and tracking of missiles using solid propellant motors. These properties are influenced by propellant flame temperature, afterburning, alkali metal impurities and chemi-ionization. Techniques of measuring and improving these characteristics have been developed.

Processability

The ability to cast propellants into motors is becoming more and more complex as propellant total solids increase and grain designs become more unorthodox. It is seldom that a simple viscosity from a Brookfield instrument will predict propellant processability. To completely predict the propellant flow characteristics it is necessary to measure the rate of shear as a function of both shear stress and temperature. In addition, a knowledge of the process life (pot life) is essential, so that perfect motors can be obtained from the casting. The Sivers Extrusion Rheometer and the Brookfield Viscometer can be utilized to obtain the desired information.

Mechanical Properties

With the trend toward higher propellant loading densities in motors and the use of plastic cases, the need for reliable grain structural analysis is even more important than it has been. The specific material properties which are required for analysis are (1) the maximum stress, strain at maximum stress and maximum strain to define large deformation and failure properties; (2) equilibrium modulus, relaxation modulus, Poisson's ratio, and multiaxial properties to define the visco-elastic functions; (3) coefficient of thermal expansion, specific heat, glass transition temperature, and thermal conductivity to define thermal properties; (4) creep modulus to define slump properties; and (5) dynamic modulus and fatigue to define cyclic and dynamic properties. Only the more recent methods of measuring properties such as these will be discussed.

Uniaxial properties are determined by deforming the specimen at constant rate of deformation at various temperatures and strain rates and measuring the

load through the specimen. Recent work has been shown that the problem of changing effective gage length with strain can be alleviated by using an end-bonded JANAF specimen. Application of the time-temperature superposition principle yields curves of reduced stress or strain versus time. A Smith type failure envelope can be defined which shows uniaxial properties of propellant independent of temperature and time. The effect of motor operating pressure can be determined by testing under pressure and then treating the data in the same manner. At the same time a multiaxial effect is observed due to the hydrostatic pressure on the specimen. The stress field is changed by testing at several pressures.

The motor grain experiences biaxial and triaxial forces and since the multiaxial field product on a uniaxial specimen by pressurization is not the only multiaxial field experienced in the motor, some multiaxial testing must be performed at ambient pressure.

The biaxial rail test has been shown to have a true biaxial field at the center of the specimen and it is commonly used to obtain correlation between biaxial and uniaxial data. Pressure can be imposed during the test to more nearly simulate motor operation. A more recent method uses a hollow sphere specimen and deforms it in either a biaxial or triaxial field. This method has advantages over the biaxial rail test.

Poisson's ratio which is the ratio of lateral contraction to the axial elongation is known to decrease with increasing strain. It can be determined by elongating a cylindrical bonded tab-end specimen and determining the change in cross-sectional area with an Opscan or optical micrometer. This instrument projects a beam of light across the specimen and the change in volume is detected by change in the shadow cast on photoelectric cells. (5)

Cyclic loads below the failure strain cause a decrease in the propellant ultimate properties similar to fatigue in metals. It is necessary to know the effect of these repeated loads upon the motor grain capability; therefore, fatigue testing is performed. The tests are made at a constant cyclic strain and the strain vs. number of cycles to failure plotted to show propellant capability.

A recent promising technique for the prediction of aging life of propellant as determined by mechanical properties is based on a superposition method. This method utilizes uniaxial data obtained after aging at several temperatures for various periods of time. The property-time data are superposed to give master curves of uniaxial properties versus log storage time. Properties after long term storage at lower temperatures have been successfully predicted using this method.

Hazard Tests

Because of the increase in higher energy materials in the propellant industry, several tests are performed to ascertain the potential hazard of the propellant or its ingredients. Two relatively new techniques are worthy of discussion: one to determine friction sensitivity and the other to determine detonability. The friction sensitivity test is conducted by pulling one strip of an assembly consisting of two thin metal strips with the sample sandwiched between the strips. The use of a seismometer with the standard card gap detonation test has improved results.

Illustrative Example

The development of a solid propellant that can be readily extinguished by pressure deflagration limit (P_{dl}) technique is a good example of how a propellant is developed. A set of requirements which included a P_{dl} of >15 psia were

established as targets for the program. A theory of extinguishment by the P_{dl} mechanism was proposed and experimental work was conducted along the lines that the theory predicted would be most useful. A propellant was developed with a P_{dl} of >30 psia and characterized by numerous tests including a 150 lb. motor firing.

REFERENCES

S. F. Sarner, Propellant Chemistry, New York, Rheihold, 1966

M. S. Cohen, Advanced Propellant Chemistry, Washington, American Chemical Society, 1966

B. Siegel and L. Schieder, Energetics of Propellant Chemistry, New York, Wiley, 1964

J. A. Peterson, R. Reed, Jr. and A. J. McDonald, AIAA Second Propulsion Joint Specialist Conference, Colorado Springs, Colorado 13-17 June 1966

D. Saylak, Investigations of Broad Spectrum Volumetric Response in Solid Propellants, AFRPL-TR-65-113, June 1965

E. A. Platt and J. A. Ford, Handling and Testing Unstable Materials,

Chemical Engineering Progress 62, 98 (1966).

FLUORINE TECHNOLOGY

24 January 1967

by

Hans R. Neumark

Dr. Neumark received his Ph.D. in electrochemistry from the Technische Hochschule, Munich, Germany. He has been with Allied Chemical Corporation since 1938, where he is presently Director of Government Liaison. He has directed activities in the field of fluorine propellants and nuclear energy and initiated the production of uranium hexafluoride. At the conclusion of World War II, he visited Germany as a civilian expert with the chemical warfare services to study fluorine installations employed in the German war effort. Dr. Neumark's present position includes the corporate coordination of research and development contracts with DOD and NASA in the field of propellants and special materials such as plastics and refractory metals.

Fluorine, the most powerful chemical oxidizer, has been of interest to the rocket engineer for almost a decade. In addition to its superior specific impulse, major performance advantages are high density and hypergolicity which eliminates the need for a separate ignitor system. The use of fluorine as a chemical oxidizer permits maximum payload capabilities using existing booster configurations. A brief history of the element fluorine is presented, and a description is given of the physical and chemical properties of the element. Fluorine reacts with practically all organic and inorganic substances with the exception of metal fluorides or fully fluorinated inorganic or organic compounds such as sulfur hexafluoride or tetrafluorethylene.

The manufacture of fluorine from initial laboratory stages carried out in 1886 to present large-scale multi-ton commercial operations are discussed in detail. The basic raw material for fluorine is calcium fluoride or fluorspar which is treated with sulfuric acid to form hydrofluoric acid. Fluorine gas is then produced by electrolysis of a solution of anhydrous hydrofluoric acid and potassium bifluoride subsequently liquified by refrigeration. The major impurities contained in fluorine gas are HF and CF_4 which are solids at liquid fluorine temperature and have to be

removed prior to the liquefaction step in order to avoid plugging of lines and orifices in rocket engine systems. The only other impurities are oxygen and nitrogen which do not interfere with the use of fluorine as rocket oxidizer.

Present liquid fluorine specifications are 99% F_2 minimum.

The basic design of fluorine tanks and of tank trucks for the shipment of 5,000 to 25,000 tons of liquid fluorine is described.

In spite of the high reactivity of fluorine, many metals and materials are compatible for handling of gaseous and liquid fluorine without difficulty. Most common metals can be used as well as fluorinated hydrocarbons under certain specified operating conditions. Temperature and flow velocity are important factors that affect the compatibility. The flow velocity has little effect on the corrosion of metals; however, it is extremely important in the case of plastic materials. Research studies carried out at elevated temperature indicate that nickel has the highest temperature compatibility followed by monel, aluminum, stainless steel and steel. The resistance of all materials used in fluorine service depends on the cleaning and passivation of the system. This is one of the most critical steps in all fluorine operations and cannot be over-emphasized. Its purpose is to remove the last traces of foreign matter and to form a passive fluoride film on the metal surface. In brief, after applying a standard cleaning method, the passivation procedure consists of slowly displacing the nitrogen in the system with gaseous fluorine. If at all possible, it is recommended the fluorine pressure be raised to the working pressure level of the equipment.

In addition to cleaning and passivation procedures, the welding specification for tanks or any equipment in contact with fluorine is of extreme importance. Welding must be carried out by the tungsten inert gas process, and no back-up strips are permitted. X-ray examination of the weld must show no cracks,

undercuts or lack of fusion. Maximum porosity of slag inclusion parameters are specified.

Recommendations are made for materials of construction to be used in system components. For piping and fittings carbon steel can be used for gaseous fluorine service and stainless steel 300 series, aluminum or monel for liquid service. Carbon-steel or bronze-body gate and globe valves are recommended for gaseous service and packless valves of the bellows type or packed valves with tetrafluorethylene packing for liquid service. Valve plugs and seats should be of dissimilar materials such as stainless steel, monel, aluminum or copper. For gaskets soft aluminum or copper is recommended in gaseous or liquid fluorine service. Liquid fluorine pumps have been designed and demonstrated by NASA and many rocket engine manufacturers.

One major concern of personnel unfamiliar with the handling of fluorine has been the safety hazards associated with the use of the oxidizer. Experience has shown that this concern has been unwarranted. Over a hundred million pounds of fluorine have been produced, handled and used during the past two decades, and during the last 20 years of industrial experience no single serious injury caused by fluorine has been reported either by the industrial producers or the Atomic Energy Commission. If proper precautions are taken, fluorine proved to be no more difficult to handle than other reactive or toxic chemicals commonly used. There is no protective clothing that affords complete protection under all conditions, but for short intervals of contact with low-pressure gas or splashes of liquid fluorine, neoprene gloves, coats and boots are recommended. Safety glasses must be worn at all times. Face shields preferably made from transparent fluorinated polymers are recommended. The most important point to remember is that all

protective clothing should be designed and used in such a manner that it can be shed easily and quickly. Another important item of general concern is the toxicity of fluorine. The harmful effects on the human body are essentially non-cumulative, and limited exposures can be repeated daily. The pungent odor of fluorine is detectible in concentrations as low as 20 parts per billion which is considerably below the safe working level. This characteristic can be considered as a built-in alarm system which makes it impossible for personnel to inhale dangerous concentrations of fluorine unless they are unable to escape the area of the gas contamination. In contrast to many other toxic propellants, the effect of fluorine on the human body is clearly predictable. It is limited to the lungs and has no insidious side effects on other organs of the blood stream and the nervous system. Evaluation of animal toxicity data suggests that exposure to 12 ppm fluorine for 5 minutes will cause no permanent respiratory damage and that at least 5 ppm should be tolerable for short single exposures from the comfort standpoint. The very latest information is presented on short-term animal toxicity tests with fluorine from 5 minutes to one hour which were carried out in 1966 at the Department of Pharmacology, School of Medicine, University of Miami, Florida. As a result of this investigation it is expected that the presently recommended EEL limits will be revised. There are various commercial detecting devices available for the continuous monitoring of fluorine in the atmosphere. The Tracer Lab analyzer is based on the reaction of fluorine with the quinol clathrate containing krypton 85, and the MSA billionaire depends on the use of an ionization chamber to detect an aerosol. The clathrate detector is more specific to fluorine than the MSA analyzer. Other detectors have been developed on the laboratory scale but

are not available commercially.

Accidental spillages of liquid fluorine can be controlled either with water in the form of a fine spray, or fog, and smaller spills can be decontaminated with powdered soda ash or bicarbonate. The heat of reaction with water causes the light gaseous HF to rise almost vertically and to diffuse quickly into the atmosphere.

In addition to fluorine, OF_2 , FLOX and halogen fluorides such as ClF_3 and ClF_5 are being considered as oxidizers in the rocket program. The compatibility with metals, handling and safety procedures are very similar for all these oxidizers. Oxygen difluoride is in a different category regarding its toxicity. Since it is less reactive and irritating than fluorine, it can be inhaled unknowingly in dangerous concentrations. In that respect it can be compared with the boranes. Because of its higher toxicity, considerably more stringent precautions are required for the handling of OF_2 . For decontamination of OF_2 water is unsuitable since it does not react with the compound, but dilute ammonia solutions are recommended for that purpose.

It is concluded that fluorine can be readily produced, shipped, stored and handled if proper precautions are taken. The present state of the art permits the design and development of fluorine engine propulsion systems and ground handling equipment through a straight-forward engineering approach.

ADVANCED THRUST CHAMBER COOLING

Clifford D. Coulbert

THE MARQUARDT CORPORATION

Van Nuys, California

February 7, 1967

Mr. Coulbert received the MS in Mechanical Engineering at UCLA where he spent some years on the research staff. He joined the Marquardt Corporation in 1953 and is now Manager of Advanced Technology Programs in the Rocket Systems Division. His research encompasses spacecraft rocket engine cooling techniques, including applications of pyrolytic graphite and related materials.

All rocket engines have one problem in common: The energy released by the propellants must be contained, and the thrust chamber and any surrounding structure must be protected and/or cooled. Concepts developed to cope with this problem, either singly or in combination, include regenerative cooling, radiation cooling, film or transpiration cooling, ablation, and inert or endothermic heat sinks. In addition to this primary requirement for cooling during firing, the design of thrust chambers for launch, space or tactical applications pose additional special problems related to (1) long time storage on earth or in space, (2) starting and intermittent operation or throttling, (3) shut-down and postrun soaking in a space environment, and (4) entry at high velocity into planetary atmospheres.

Furthermore, the various cooling concepts may be used separately or combined in different ways for each of the thrust chamber components, such as the combustion chamber, the nozzle throat and the expansion nozzle.

The objective of this lecture is to present the ranges of applicability and the limitations imposed on these various cooling concepts. New materials,

composites, and more sophisticated combined cooling designs are providing increased cooling capability for the advanced high energy propellants including fluorinated oxidizers and metal containing fuels.

The function and size of the engine establish several important cooling design parameters, such as engine location, thrust level, burn time, and duty cycle.

The propellant choice determines the combustion gas temperature and composition. Several propellants are excellent coolants (such as hydrogen) while others are thermally unstable (such as diborane), and the combustion gas constituents vary widely in their compatibility with candidate thrust chamber materials. Typical operating characteristics and propellant choices associated with five different propulsion requirements are shown in Figure 1.

What dictates the choice of cooling scheme? As the severity of the operating conditions increase, the choice of cooling technique becomes limited or material capability must increase or cooling techniques may be combined. Factors which increase the severity of operating conditions are:

- . Increased run times
- . Higher chamber pressures
- . Hotter propellants
- . Chemical reactivity with structural materials
- . Buried installation or chamber outer wall temperature limits
- . Throttling and restarts

These are desirable directions because they usually provide greater mission capability, increased payloads, high specific impulse, etc.

As we survey the capability of the available cooling techniques, it's hard to generalize completely but one can show trends as in the chart of Figure 2 which outlines the general operating regimes of several cooling techniques as a function of chamber pressure and gas temperature. Increased gas temperatures are attained by going to hotter propellants, such as from cold gas to monopropellants, such as peroxide and hydrazine to LOX/RP, N_2O_4 , Fluorine and on to the OF_2 and metal fuel combinations including lithium and beryllium systems.

Typical propellant flame temperatures and exhaust products are shown in Figure 3. Temperatures above $7000^\circ F$ will exist in high performance systems. Temperatures approaching $9000^\circ F$ may be attained in lithium combustion.

A more detailed review of the advantages and limitations of each cooling concept is presented below. Of course, the limitations described may be overcome as materials improve and cooling techniques are combined.

Radiation Cooling

The equilibrium temperatures reached by the walls of a refractory metal thrust chamber cooled only by radiation to the surroundings may be expressed in simplified form by the familiar steady-state equation

$$q/A = h(T_g - T_w) = \epsilon \sigma (T_w^4 - T_{\infty}^4)$$

A graphical presentation of this relationship is shown in Figure 4.

Where conditions permit steady-state operation, radiation-cooled engines have the advantages of lightweight, simple structure, and long operating life. They are capable of high-frequency pulsing or variable-thrust operation and are not subject to dimensional change during operation.

Experimental heat transfer rates in small thrust chambers can be controlled by injector design (leading to film cooling or combustion stratification) to permit chamber pressures well above theoretical limits.

The characteristic limitation on radiation cooling is availability of coatings and materials that can operate at equilibrium temperatures above 3000°F in the combustion environment. Disilicide coated refractory metals have demonstrated the best performance with propellant gases containing water vapor. At higher temperatures a promising material system is an alloy of hafnium and tantalum. For propellant gases containing fluorine products, the most promising materials are the carbons while silicon bearing materials are not usable.

Regenerative Cooling

Regenerative cooling has long been the conventional method for cooling liquid rockets. The coolant(s) (one or both of the propellants) is (are) circulated through cooling jackets or through contoured thin-walled tubes that form the chamber walls.

The metal walls operate at relatively low temperatures ($< 2000^{\circ}\text{F}$) compared to the gas temperatures (450°F - 6000°F); heat fluxes range from 1-10 Btu/in.²-sec. Basic advantages are: 1) continuous long run times are possible, 2) there is negligible heat loss from the propulsion cycle due to cooling, and 3) with modern fabrication techniques, the chamber structure is relatively light compared to typical uncooled structure.

Three factors describe the nature of the operating limits for regenerative cooling: pressure, fabrication limits, and coolant heat capacity. The results of specific studies of chamber pressure limits vs. engine thrust

capabilities for various propellant combinations are shown in Fig. 5.

Three lines define the boundaries of feasibility in Fig. 5. The maximum chamber pressure line is fixed by the available propellant supply pressure, which must be greater than the sum of the chamber pressure, the propellant injector pressure, and the coolant circuit pressure loss. Propellant supply pressure, in turn, depends on the result of a system weight optimization, and whether the propellants are pump-fed or pressure-fed. The upper-left line which limits minimum thrust depends on the minimum practical coolant passage height at the nozzle throat, assumed to be 0.060 in. for this plot. (The heat flux capability of the liquid propellants is directly related to coolant pressure and velocity; velocity may be increased by decreasing the flow area, subject to pressure loss and fabrication limitations.) The lower line which limits minimum thrust is determined by the allowable bulk temperature rise for the coolant. For propellants such as N_2O_4 , the bulk temperature limit is the saturation temperature, whereas for fuels such as pentaborane, hydrazine or RP-1, the limit is the thermal decomposition temperature which would cause solids formation or an explosion; e. g., the coolant-side wall temperature limitation for Aerozine 50 (0.5 N_2H_4 -0.5 UDMH) is 500° - 600° F. For hydrogen, the limit is determined only by the required temperature difference (to achieve heat transfer) between the wall and the hydrogen; the lower curve in Fig. 5 is drawn for a hydrogen temperature limit of 1000° F. These coolant temperature limitations determine how much of the thrust chamber area can be cooled. In Fig. 5 the thrust limit curves are drawn for the case of cooling the chamber, the nozzle throat, and the expansion section to an area ratio of 5; greater

relative areas can be cooled for engines falling above the line, and vice versa.

Specific design conditions could alter the locations of these regenerative cooling envelopes, but the trends would remain the same. It is seen that regenerative cooling is best suited to high-thrust, pump-fed, main-propulsion engines. Current design studies indicate that chamber pressures from 2000-5000 psia are feasible and that cooling limits may be extended further through the use of auxiliary film cooling and/or refractory metals.

Ablative Cooling (Char-Forming Plastics)

The thrust chamber can be lined with a solid matrix containing a substance that pyrolyzes to form gases which in turn act as a transpiration coolant. (This technique has been extensively used to protect re-entry vehicles.) For engines using N_2O_4 /hydrazine blends and O_2/H_2 propellants, the oriented-silica-fiber reinforced phenolics have consistently shown superior performances over many other ablative materials.

This has been attributed to the formation of a very viscous protective film of molten silica and to the favorable structural and insulating qualities of the char. Numerous thermodynamic processes are involved: heat absorption, heat conduction, resin depolymerization, silica-carbon reaction, transpiration cooling, evaporation, radiation, etc. A variety of analyses have been developed to account for these phenomena and facilitate calculation of charring and surface recession rates.

An analysis of transient temperature response data on several ablative nozzle firings at the NASA Lewis Research Laboratory and at Marquardt, and a comparison with a slab heat conduction analysis carried

out with the IBM 704 digital computer, assuming only conduction heat transfer, revealed that the experimental char depth and transient temperature response could be predicted approximately, neglecting the other phenomena. The correlation of a large amount of data has produced the following relationship between char depth δ , an effective thermal diffusivity α , and run time θ :

$$\delta = 2.0(\alpha \theta)^{1/2}$$

The successful prediction of surface recession rates on so simple a basis has not been accomplished for any general case, but useful empirical correlations have been achieved for limited ranges of applications.

For chamber applications involving fluorine containing oxidizers, the carbon reinforced phenolics have proved superior to the silica-phenolics. Newer carbon composites such as carbon fiber based graphite or pre-charred and impregnated carbon fiber materials appear most promising.

Heat Sink Cooling

The primary limitation on this transient heating approach is the run time available before one of two limiting surface temperatures is reached: 1) the melting, subliming, or softening temperature at which the material would flow or erode rapidly, or 2) the temperature at which the oxidation or reaction rate with the combustion gases would be excessive. Heat sink materials should have high heat capacity, high thermal conductivity, high structural temperature limits, and compatibility with combustion gases. Pyrolytic graphite, isotropic graphite, and tungsten top the list for use with high-temperature propellants. Oxidation of these materials is the critical problem with all combustion gases containing CO_2 and H_2O . Surface coatings for graphite and tungsten offer only a partial solution to this problem, since

available coatings are limited to temperatures of less than 4000°F.

Effects of various parameters on heat-sink run time capability are shown by Fig. 6. A dimensionless heat-transfer parameter, hr_i/k , is plotted against a dimensionless run-time parameter, $\alpha\theta/r_i^2$, for various values of the wall-thickness to inside-radius ratio, t/r_i . Here θ is the time required to raise the wall temperature by an amount equal to half the initial temperature difference between the gas and the wall. The limiting or "envelope" curve represents the locus of points for which increased wall thickness could not increase the run time parameter; in other words, for a given value of hr_i/k , this curve gives the maximum value of $\alpha\theta/r_i^2$ achievable regardless of wall thickness.

For example, if $\alpha\theta/r_i^2 = 0.1$ is desired, nothing would be gained by making t/r_i greater than 0.67, and the maximum hr_i/k that could be handled for that run time would be 3. From the individual curves, it can be seen that for the relatively thin-walled cylinders that one would consider acceptable for the combustion chamber ($t/r_i \rightarrow 0.1$), the run time parameter is inversely proportional to the heating parameter. For very thick walls, which might be acceptable only in the nozzle throat, i. e., working along the envelope curve, it is seen that the run time can be increased by a factor near 5 if the convective heat-transfer coefficient is halved.

The over-all conclusions from Fig. 6 is that the inert heat sink approach is applicable for small engines with low to moderate chamber pressures (low h). The use of limited film cooling to extend run time may be attractive for special applications. Theoretically, run times for heat sink nozzles can also be extended through the use of endothermic materials.

such as subliming salts, lithium compounds, and low-melting-point metals, which can absorb large amounts of heat through a phase change. The endothermic materials may be impregnated into porous refractory wall materials or used to back up the walls as an insulator as well as a heat sink.

Film and Transpiration Cooling

In film cooling, the fluid is introduced directly into the thrust chamber through slots or holes and directed along the walls. This layer of liquid or gas absorbs heat and thickens the effective boundary layer, thus reducing the heat flux to the walls. Cooling films may be supplied from several sources. One source is a propellant injector designed such that a separate supply of fuel is injected along the chamber walls during firing, thus producing a fuel-rich boundary zone. Alternatively, a fraction of the fuel or oxidizer can be routed directly to slots or holes in the chamber wall just ahead of the critical nozzle cooling area. Or, a separate supply of coolant (liquid, gas, or solid) can be metered separately or controlled by the heat flux (causing melting, expansion, or evaporation) to provide flow through slots or holes in the nozzle surface. Cooling of this latter type has been studied for solid-propellant motor application.

Transpiration cooling may be thought of as a special case of film cooling in which the slot or hole spacing becomes very small (porous surface). Many of the same design considerations apply, but the available analytical design equations differ. Coolant sources are usually 1) pressure-fed fuel, water, hydrogen, or other coolant or 2) a material such as copper, lithium, or a subliming salt with which the porous refractory wall has been impregnated. Transpiration cooling is most applicable to one-shot, constant-

thrust engines due to the problems of flow control and shutdown effects.

There are no inherent limitations on the coolant capability, run time, or chamber pressure with either film or transpiration cooling. If one of the propellants or an inert fluid is used as a coolant at the nozzle throat, there may be a performance penalty (I_{sp} loss, where coolant flow is counted as added propellant flow in the I_{sp} calculation). However, coolant introduced well ahead of the nozzle throat may completely mix and react, thus causing no loss.

Application to engines is limited by possible coolant waste in starting and residual flow from coolant passages after shutdown. Plugging of film cooling passages or transpiration media may be caused by either thermal decomposition during operation or by freezing between firings.

Current research on the practical application of transpiration cooling to high chamber pressure engines has led to the development of transpiration cooled walls composed of a stack of many thin discs with multiple slots on the surface of each disc.

Combined Cooling Techniques and Advanced Concepts

There are several propellant systems for which no completely satisfactory cooling technique for reasonable run times has yet been developed. Examples are fluorine-based oxidizers, such as OF_2 and ClF_3 , used with fuels containing such metals as boron, aluminum, beryllium, and lithium. These propellants give combustion gas temperatures in the 6000° - $8000^{\circ}F$ range, and the combustion products may be highly erosive and corrosive on the available refractory metals and carbides. Throat heat fluxes may fall in the 15-25 Btu/in.² second range for a chamber pressure

of 600 psia (and increase with pressure, of course). At these conditions, the very best inert heat sinks would reach temperatures of 5000°F in less than 20 sec. The other cooling techniques, which do not involve a performance loss such as regenerative, ablative, and radiation, will not do the job alone; some form of film or transpiration cooling is required.

When film or transpiration cooling is required, the objective is to minimize the required coolant flow, which depends on the surface area to be cooled and also the wall temperature. Therefore, the engine surfaces should be held at the highest temperatures consistent with structural integrity. Materials with the highest temperature capabilities are the graphites, tungsten, and the carbides of hafnium and tantalum. Structurally, graphite and tungsten are capable of operation above 5000°F (the structural capability of the carbides has not been demonstrated), but all of these materials are subject to oxidation and erosion by the combustion gases even at 5000°F, so that they must be cooled to somewhat lower temperatures.

Most advanced cooling studies now in progress are related to ways of generating coolant films either on a transient or steady-state basis. Development problems lie in the areas of refractory material formulation, nozzle design and fabrication, coolant selection and supply techniques. Particular problems include passage plugging by coolant or combustion products, coolant distribution, starting and shutdown phenomena, limits on run time and thrust variability, and thermal expansion and sealing provisions.

Concluding Remarks

Most of the material included in this lecture summary has been extracted from the article by the author published in the JOURNAL OF SPACECRAFT

AND ROCKETS of March, 1964. This article, "Selecting Cooling Techniques for Liquid Rockets for Spacecraft" also includes an extensive unclassified bibliography.

MISSION AND COOLING CRITERIA

MISSION	OPERATING CHARACTERISTICS	TYPICAL PROPELLANTS	TYPICAL COOLING CONCEPTS
LAUNCH	HIGH THRUST PUMP FED 1-5 MINUTE FIRING ONE START	LOX/RP SOLIDS	REGENERATIVE HEAT SINK ABLATIVE
UPPER STAGE PLANETARY TAKE-OFF	HIGH ISP SPACE IGNITION SPACE STORAGE ONE START	O ₂ /H ₂ F ₂ /H ₂ N ₂ O ₄ /50-50 TRIPROPELLANTS	REGENERATIVE ABLATIVE HEAT SINK FILM-COMBINED
SECONDARY - ΔV MANEUVERING	HIGH ISP MULTIPLE STARTS THROTTLING SPACE STORAGE BURIED INSTALLATION	O ₂ /H ₂ F ₂ /H ₂ N ₂ O ₄ /50-50 OF ₂ /LPG	ABLATIVE FILM-COMBINED RADIATION HEAT SINK TRANSPARATION
ATTITUDE CONTROL	LOW THRUST SMALL SIZE LONG RUNS COMPLEX DUTY CYCLE SPACE STORAGE RE-ENTRY HEATING SPACE IGNITION	COLD GAS MONOPROPELLANTS N ₂ O ₄ /MMH OF ₂ /LPG O ₂ /H ₂ F ₂ /H ₂	RADIATION FILM-REGENERATIVE FILM-RADIATION FILM-ABLATIVE FILM-HEAT SINK
TACTICAL	PREPACKAGED STORAGE AND HANDLING SHORT FIRING HIGH CHAMBER PRESSURE VOLUME LIMITED	SOLIDS SLURRIES CTF/MAF N ₂ O ₄ /MAF	HEAT SINK FILM TRANSPARATION ABLATIVE ENDOTHERMIC COMBINED

FIGURE 1

NOMENCLATURE

A_*	nozzle throat area, in. ²
A	combustion chamber cross-sectional area, in. ²
A_e	nozzle exit plane area, in. ²
h	heat-transfer coefficient, Btu/hr-ft ² -°R
I_{sp}	specific impulse, lbf/(lbm/sec)
k	thermal conductivity, Btu/hr-ft-°R
q/A	heat flux, Btu/hr-ft ²
r_i	inside radius, in., ft
T_g	gas recovery temperature, °R
T_w	wall temperature, °R
T	effective heat sink temperature, °R
t	wall thickness, in.
ΔT	temperature difference between gas and wall
θ	time, sec
ϵ	exterior wall emissivity
α	effective thermal diffusivity, in. ² /sec
δ	char depth, in.
σ	Stefan-Boltzmann constant, Btu/ft ² -°R ⁴ -hr

COMBUSTION CHAMBER COOLING (U) OPERATING REGIMES

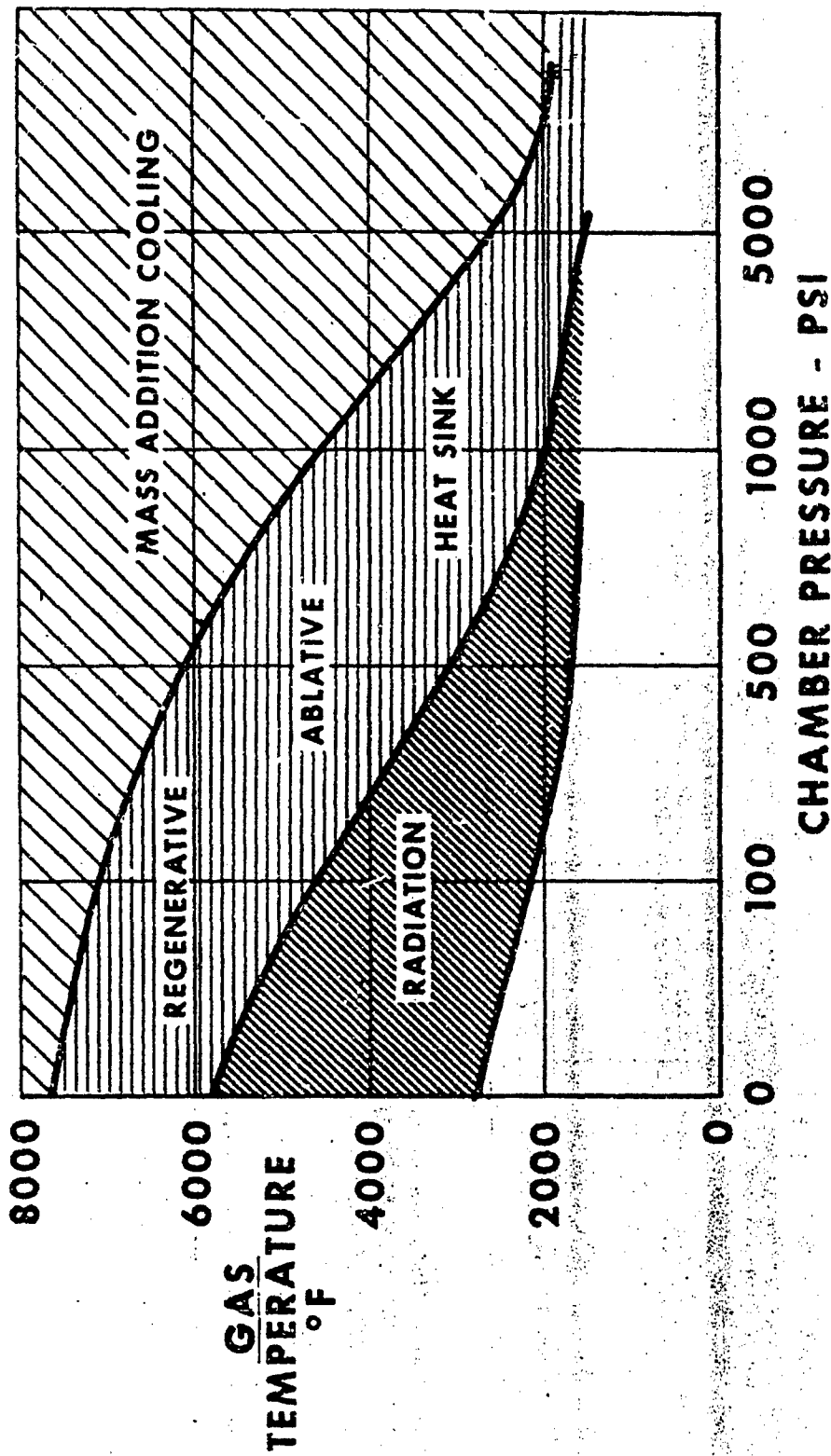


FIGURE 2

V2020-3
9-14-55

PROPELLANT PROPERTIES

PROPELLANTS	PERFORMANCE		FLAME TEMPERATURE	PRINCIPLE EXHAUST PRODUCTS
	Pc	isp		
EARTH STORABLE N ₂ O ₄ / N ₂ H ₄ N ₂ O ₄ / 0.5N ₂ H ₄ - 0.5 UDMH N ₂ H ₄ / B ₅ H ₉	50 PSI	343	5400°R	H ₂ O, H ₂ , N ₂
	50 PSI	335	5400°R	H ₂ O, H ₂ , N ₂ , CO
	150 PSI	393	4800°R	H ₂ , BN
CRYOGENIC O ₂ / H ₂ F ₂ / H ₂ OF ₂ / H ₂	50	456	5300°R	H ₂ O, H ₂
	300	478	7300°R	HF, H ₂
	300	477	6600°R	HF, H ₂ , H ₂ O, H
SPACE STORABLE OF ₂ / B ₂ H ₆ OF ₂ / CH ₄	300	437	8000°R	HF, H ₂ , BOF, H
	300	420	7600°R	HF, CO, H

FIGURE 3

COMPARISON OF HEAT FLUX WITH WALL TEMPERATURE
 $N_2 O_4 / 0.5 N_2 H_4 - 0.5$ UDHM -
 $P_c = 100$ psia

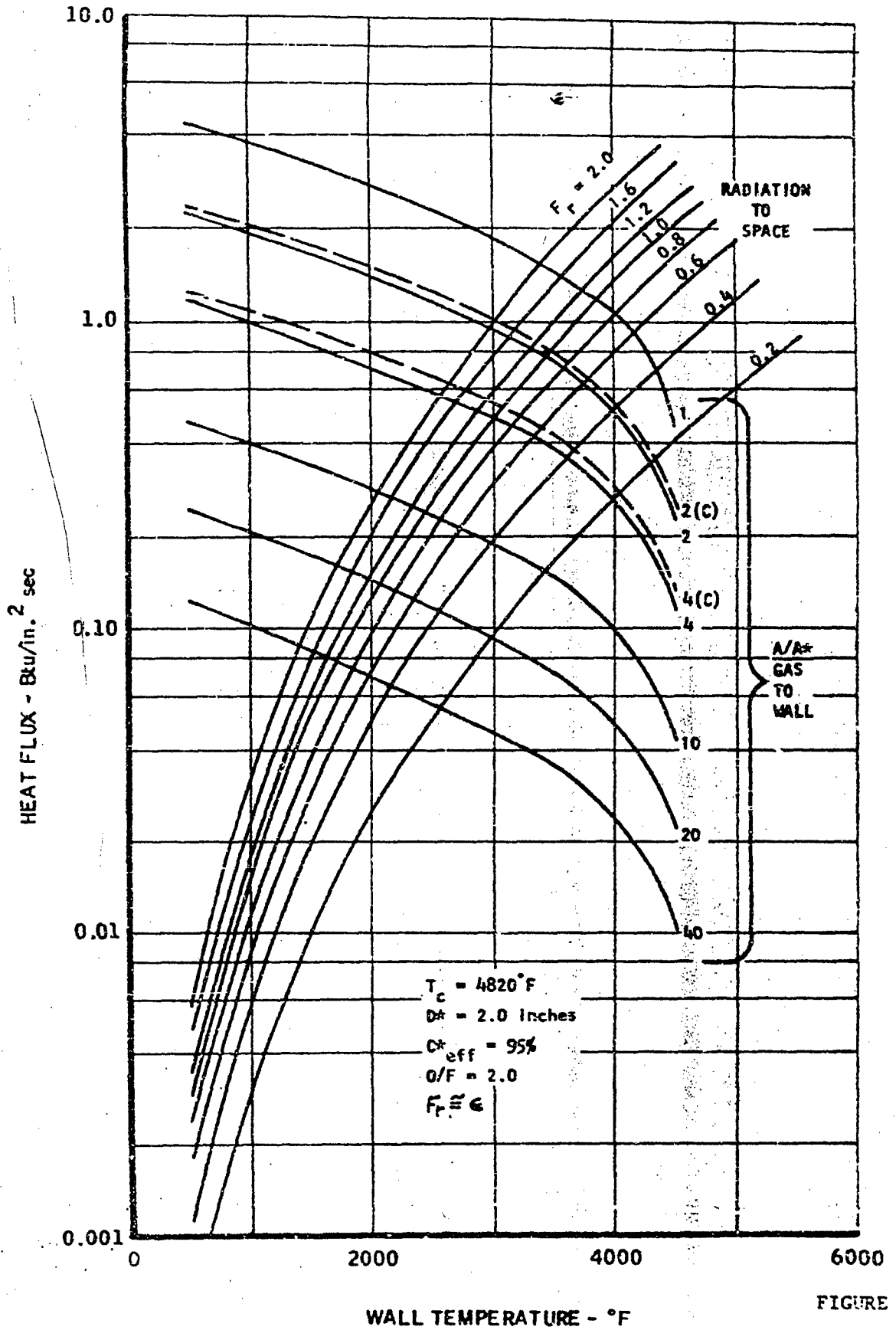
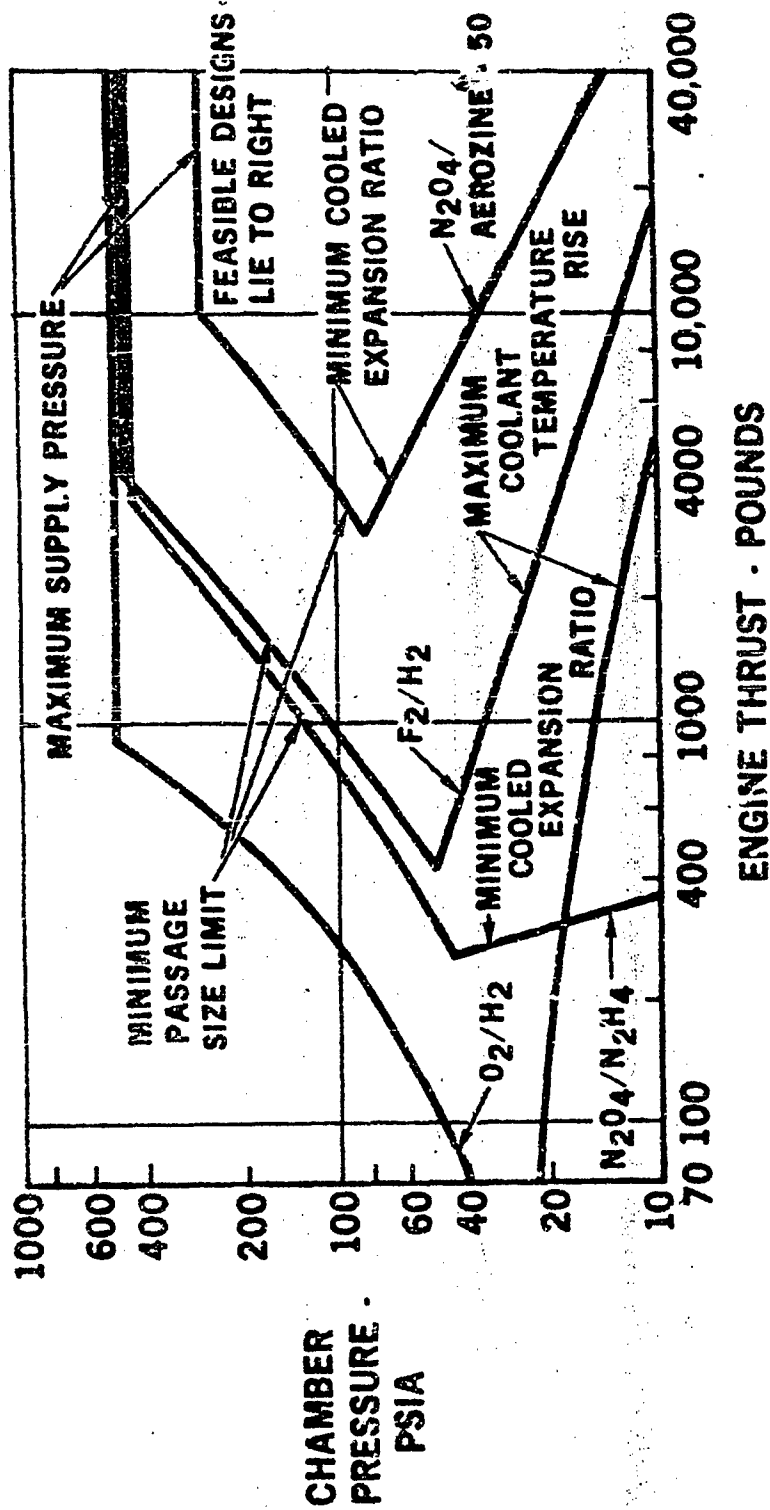


FIGURE 4

FEASIBILITY MAP FOR REGENERATIVE COOLING WITH THE PROPELLANTS O₂/H₂, F₂/N₂O₄/N₂H₄ AND N₂O₄/AEROZINE-50



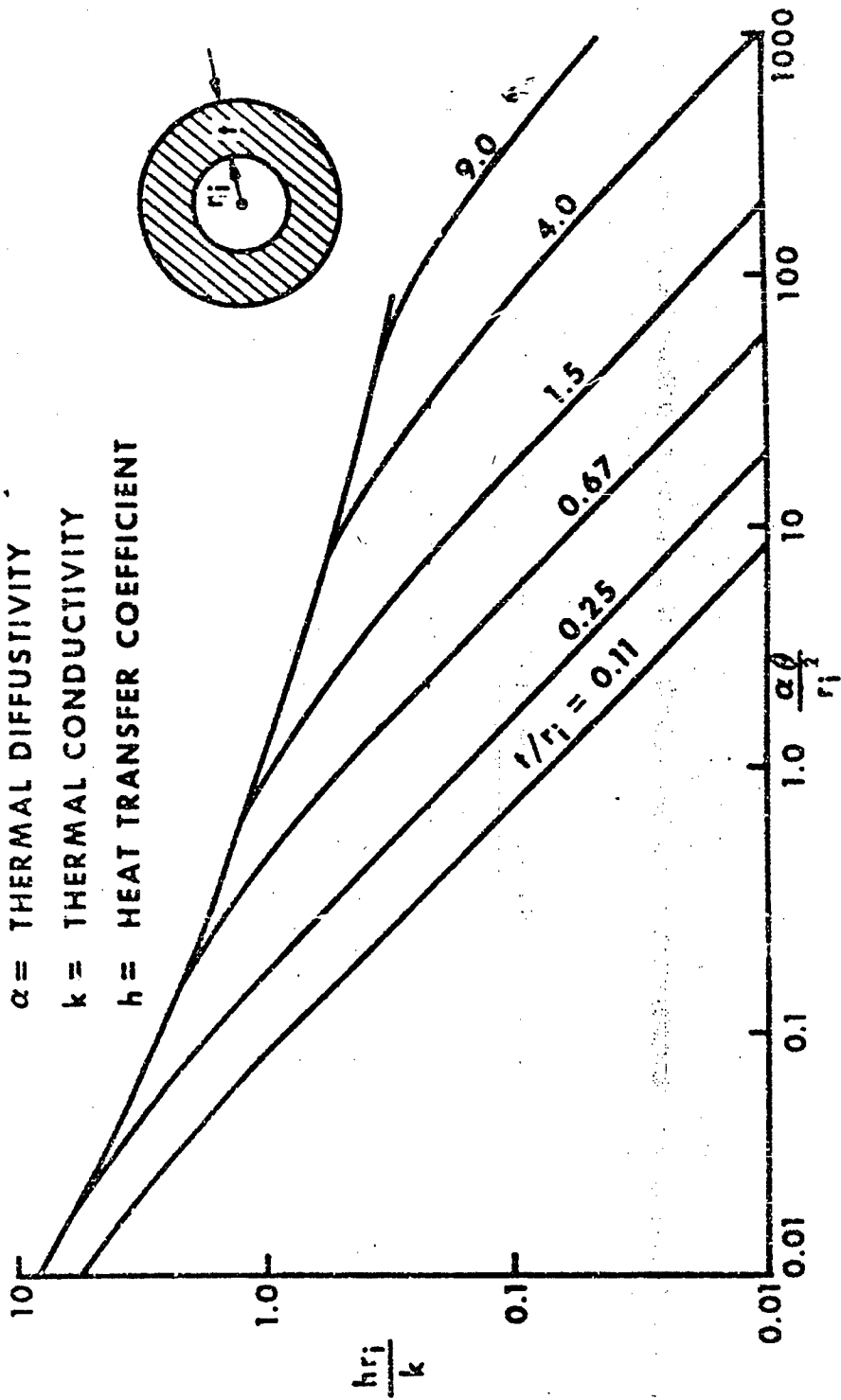
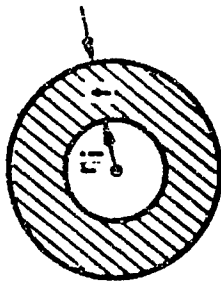
HEAT SINK DESIGN CAPABILITY

$\theta =$ TIME TO REACH $(T_s - T_o) / (T_g - T_o) = 0.5$.

$\alpha =$ THERMAL DIFFUSIVITY

$k =$ THERMAL CONDUCTIVITY

$h =$ HEAT TRANSFER COEFFICIENT



A1410-1

FIGURE 6

ROCKET PERFORMANCE PREDICTION AND ANALYSIS

SUMMARY

by

R. S. Valentine

(February 14, 1967)

Dr. Valentine holds the MS degree from the University of Illinois and the PhD degree from the University of Washington - both in Chemical Engineering. After five years with Chevron Research Corporation where he was engaged in petrochemical research, he joined Aerojet-General where he is now Manager of the Fluid Dynamics Section, Liquid Rocket Operations. He holds 12 patents and has authored extensive publications.

Rocket engine performance is determined by the potential of the propellant system, the operating conditions and the physical design characteristics of the thrust chamber. The variations between the ideal performance of a perfect engine and that actually attained by a real engine is the result of such physical conditions as boundary effects, heat losses, curvature, finite reaction rates, two phase flow and non-homogeneous mass and mixture ratio distribution.

Perfect Engine Concept

Liquid rocket performance calculations are greatly simplified if one assumes a "perfect engine" condition, i. e., perfect injector, chamber, and nozzle operation. For this model, specific impulse is only a function of the propellant combination and the combustion products, because complete combustion of the propellant and ideal expansion of the combustion gases are presumed. Thus, for the perfect engine the following conditions are applicable:

- (1) One-dimensional flow

(2) Adiabatic and reversible flow

(3) Chemical equilibrium among the combustion products throughout the entire expansion process.

- (4) Equilibrium multiphase flow
- (5) Homogeneous composition of combustion products
- (6) Complete combustion

On the basis of the above conditions or assumptions, thermochemical calculations can be made to determine the composition and properties (density, temperature, pressure, and velocity) of the combustion gases at any point in the expansion process.

Perfect Injector Concept

The perfect injector concept represents the maximum performance attainable in a rocket engine assuming ideal performance up to the throat, but taking into account expansion nozzle losses for a specific configuration and area ratio. For this concept, the following conditions are applicable.

- (1) Three-dimensional flow
- (2) Boundary layer effects (friction and heat transfer)
- (3) Finite reaction and relaxation rates
- (4) Nonequilibrium multiphase flow
- (5) Homogeneous composition of combustion products
- (6) Complete combustion

The first four of the above conditions represent deviations from the first four conditions of the perfect engine concept, and the remaining two conditions are identical to the perfect engine concept. These deviations will result in the following performance loss definitions:

(1) Nozzle curvature and divergence performance loss - This represents the difference in performance between the one-dimensional and three-dimensional flow conditions.

(2) Boundary layer performance loss - This represents the difference in performance between isentropic and nonisentropic flow due to friction and heat transfer effects.

(3) Finite rate performance loss - This represents the difference in performance between total shifting equilibrium expansion and nonequilibrium expansion because of finite reaction and relaxation rates.

(4) Gas/Particle flow performance loss - This represents the difference in performance between equilibrium and nonequilibrium multiphase combustion product flow.

Real Engine Concept

The real engine concept considers specific impulse to be a function of the propellant combination, the injector/chamber design and operation, the combustion products, and the nozzle expansion design and operation. For the real engine concept, the following conditions are applicable:

- (1) Three-dimensional flow
- (2) Boundary layer effects
- (3) Finite reaction and relaxation rates
- (4) Nonequilibrium multiphase flow
- (5) Nonhomogeneous composition of combustion products
- (6) Incomplete energy release

The first four of the above conditions are identical to the perfect injector conditions and thus can be accounted for by the performance losses defined in the discussion of the perfect injector concept. The remaining two conditions, however, represent deviations from the last two conditions of both the perfect injector and perfect engine conditions, and, as such, will result in the following performance loss definitions:

(1) Mixture ratio distribution performance loss - This represents the difference in performance between homogeneous and nonhomogeneous combustion products.

(2) Energy release performance loss - This represents the difference in performance between complete and incomplete energy release.

Sources of Losses

The performance losses which determine the performance of a real rocket engine are the result of the physical conditions noted, and their mutual interactions. For example, consider kinetic losses, which occur when the rate of recombination reactions is insufficient to allow recovery of the energy of dissociation in the residence time available. This phenomenon is a function of the chemical species present, and thus the mixture ratio. Therefore, non-homogeneous mixture ratio distribution will have an effect on the overall kinetic loss. In addition, since dissociation is temperature dependent, a reduction in energy release efficiency from the theoretical maximum will result in a lower stagnation temperature in the chamber, and in turn, lower kinetic losses. Similar interactions exist between several of the other physical effects which influence performance.

As a result of these interactions, a loss can occur in the expansion nozzle because of a condition which exists in the combustion chamber. For this reason, parameters such as c^* and C_F can be grossly misleading. The best parameter for evaluation of performance is I_{sp} , which contains the overall effects of losses from each source as well as the interaction effects.

Effects of Operating Variable

The magnitude of the performance losses which result from the physical conditions associated with the real engine concept is a function of the operating conditions. Losses such as boundary effects, finite rate and two phase flow effects are a function of the thrust level. The pressure level and area ratio have a significant influence on, for example, kinetic losses. The loss resulting from non-homogeneous mixture ratio distributions may change by an order of magnitude as the overall mixture ratio of the engine is varied. Because of these factors and the interactions mentioned previously, the performance of an engine over a wide throttling range can exhibit characteristics which would defy prediction by use of c^* and C_F as performance parameters.

Experimental Measurements

Performance related parameters which can be measured in experimental tests include thrust, chamber pressure, ambient pressure, throat area, exit area, weight flows and temperatures. These parameters, with the exception of chamber pressure, can be used to determine the actual measured I_{sp} of a rocket engine with sufficient information to convert it to vacuum performance. Chamber pressure, or any parameter derived from it, can only be used for comparative tests on identical units or for engine

balancing. It is not generally useful for evaluating absolute performance levels.

Design Constraints

For each propellant system, set of operating conditions and envelope there is an optimum injector/chamber/nozzle design which will maximize performance consistent with satisfactory stability and reliability. Trade-offs between high steady-state performance, transient performance, cooling and factors affecting stability must be made consistent with system requirements. General statements can be made however about the desirability of even mixture ratio distribution, the relationship between pattern design and chamber volume requirements and the effects of mass distribution on compatibility and stability. These general rules can be used as preliminary criteria for establishing chamber length, nozzle area ratio and length, contraction ratio, choice of element design, and hydraulic characteristics of the injector manifolds.

Performance Standardization

Recently, a committee of the ICRPG Performance Standardization Working Group has undertaken the task of selecting the best available methods for evaluating rocket engine performance. The committee has tentatively chosen the interaction theory approach discussed above as its recommendation for a proposed national standard. The problems associated with a standardized procedure include choice of calculation method for individual losses and insuring that best methods are available to all users. The goal is to devise a workable program which will allow performance prediction within 1% of the true value for systems operating at steady state at over 100 lbs. thrust.

Nuclear Rocket Engine Reactors

and

Engine/Vehicle Integration

The aim of this lecture is to survey the physical bases of nuclear rocket reactors and to show from these bases the motivation for or reason why nuclear rocket reactors, engines, and vehicles have the characteristics which characterize them and differentiate them from chemical rocket engines and vehicles.

This is accomplished at three successive levels of nuclear rocket systems. First, a summary is given of the principal features of nuclear rocket reactors, with emphasis on their characteristics as arising from basic physical principles. This background is related to detailed engineering characteristics of current nuclear rocket engine programs. Next, a survey is given of engine/vehicle interaction effects and integration problems, again emphasizing fundamental physical bases and limitations on integration areas, illustrating considerable differences from chemical rocket practice. Finally, constraints in operational employment of nuclear rocket vehicles are reviewed and directions for their best use indicated.

In order to accomplish this it is necessary to examine these features in three different frameworks of analysis and design: (1) Flight Mechanics, (2) Reactor Physics, and (3) Radiation Leakage and Shielding. Overall systems and integration aspects are discussed as appropriate for each area. **

*

For reference purposes these areas of study are covered in Chapters 2, 4, and 5 of Fundamentals of Nuclear Flight (FNF), by R. W. Bussard and R. D. DeLauer, McGraw-Hill, 1965. Chapter, page and equation numbers referenced further in these notes are to FNF as a source.

**

See also Chapter 7, FNF.

1. Flight Mechanics.

Equation (2-6),
(2-65)

(a) Mass-ratio equation with gravity loss terms
($g \sin \theta t_b$).

Use to show unfavorable features of nuclear rocket vs. chemical for (ground) launching against gravity fields.

Equation (2-69),
(7-11) and Table 7-3

(b) Same equation with drag, turbine-drive, and back-pressure losses.

Use to show unfavorable features of nuclear rocket vs. chemical for operation in atmosphere, and for need for highly efficient bleed-gas or topping cycle turbine device (gas generator not competitive).

Sec. C, Ch. 2,
p. 72 ff., and
eqs. (2-135, 137)

(c) Performance analysis equation relating engine system internal parameters to (mass-ratio equation) ballistic external performance parameters.

Use to show rationale for "minimum" reactor specific mass (λ_r), shows favorable features of nuclear rockets for use in orbit or "free-fall" launching vs. ground-launching, and illustrates greater allowable I_{sp} and easier reactor development (higher λ_r) for optimum low- a_0 operation.

Eqs. (2-138 to 142)
and Table 2-7.

(d) Same equation but with shield + engine mass as parameter of interest.

Use to show effect of shielding on manned space operations and impossibility of shadow shielding over 4π .

2. Reactor Physics.

Sec. B-1, Ch. 4,
eq. (4-31) and ff,
and Sec. C-2, Ch. 4,
eqs. (4-118 to 121).

(a) Basic one-velocity flux shapes, and reflector-savings equations.

Use to illustrate need for reflectors to achieve low fuel loading, and flat fission density distribution (and thus optimum heat exchange performance, with minimum specific weights, λ_r).

(Cont'd) 2. Reactor Physics

Eq. 4-161 and
Table 4-10

(b) Time-dependent reactivity equation, with delayed neutrons.

Use to illustrate need for and problems of rocket reactor control. Rapid start up, need for delayed neutrons and precursor retention, and for high frequency response (10 - 100 cps) control rod drive systems.

Ch. 4, Sec. A and
Sec. D.

(c) Nature of cross-sections, energy dependence, and neutron energy distribution. Fast and slow group extremes. Slowing-down process and simple theory. Fast and slow group flux shapes in reflected reactors.

Use to illustrate need for multi-group, multi-region calculations, employing electronic computers and sophisticated calculational codes. Use to show unique problems in reflected reactors with cold reflectors -- i. e. neutron "speeding-up".

3. Radiation Leakage and Shielding.

Eqs. (5-1 to 10)

(a) Operating leakage and dose rate equations; point sources.

P. 270

Use to illustrate biological hazards and leakage power levels in sample situations; e. g. orbit launching, ground testing, and associated operational systems problems.

(b) Post-shutdown radiation; power and dose-rate equations.

Use to show need for cooling, and difficulties of operational use of nuclear rockets for manned surface landing missions, and of post-shutdown in-flight maintenance, etc. Difficulty of long-time cooling and reactor re-use; the modular stage (including engine) throw-away concept.

Ch. 5, Sec. B;
Sec. C, p. 312 ff.

(c) Leakage radiation interaction with matter; heating and activation from neutrons, gammas, in and from finite sources.

(Cont'd) 5. Radiation Leakage and Shielding.

Use to illustrate totality of engine/vehicle integration problems and fundamental differences of nuclear vs. chemical systems with respect to those problems. Appropriate materials choices from activation point of view, heating rates in vehicles, tankage, pumps; test-stand, etc. structure and associated pump system design problems and shield requirements. Ionization of air around air-launched vehicles, and consequent e.m. communications problems. Shielding requirements for crew, use of chemical stage propellants as shielding, comparison with solar flare shielding, to show crew shield needs are generally satisfied by requirements imposed by sources other than the reactor, and satisfied by materials on-board for purposes nominally other than shielding.

In general, the main points in conclusion are:

A. Nuclear rockets are best used in orbit launching for inter-orbit transfer, and least effectively used for surface launching or landing.

B. Many engine/vehicle integration problems are entirely different with nuclear rockets from past experience with chemical rockets, and careful attention must be paid to all of these. Past experience does not provide any sure guide for their solution, but solutions are seen for every major problem area.

C. Nuclear radiation imposes new constraints on the use of nuclear rocket vehicles relative to those evolved for in-space application of chemical rockets. New methods must be evolved and adopted, different from but just as practical as those developed for non-nuclear systems.

THERMAL CONTROL OF SPACE PROPULSION SYSTEMS

7 March 1967

by

F. C. Svenson

Mr. F. C. Svenson, who received his BSME from the University of Cincinnati, is the Supervisor of Apollo RCS and SPS Technology, Research, Engineering and Test, Space and Information Systems, North American Aviation. He is responsible for the thermal analysis of the Thermal Control Systems for the Command and Service Module Reaction Control Systems and the Service Propulsion System. Also, he is responsible for all analysis required to predict the performance of the three Apollo liquid propulsion systems. Prior to joining NAA in 1962, Mr. Svenson was involved with the thermal and performance analysis of propulsion systems at Astropower Inc., The Marquardt Corp., and Douglas Aircraft Co.

Thermal control of a propulsion system is obtained for present spacecraft by balancing the heat gained from the sun and the heat lost to space with the addition of heat from electrical heaters. If the allowable propellant temperature range was wider, the need for electrical heaters could be eliminated for most missions by the proper choice of optical properties on the rocket engine and adjacent spacecraft structure. Since this range is relatively narrow, the optical properties have been selected to reduce the net environmental heating thus eliminating any over temperature problem. However, this built-in cold bias must be eliminated by the addition of heat from electrical heaters during periods of earth, lunar or spacecraft shadowing.

In order to size a thermal control system optimally with respect to weight and energy usage, extensive thermal models must be developed to describe the heat transfer to and from the components, propellant tanks, helium bottles, rocket engines and adjacent structure. These models which consist of hundreds of nodes, resistors and capacitors can only be solved by

thermal analyzer type computer programs. Every use of spacecraft orientation is required and should be used to aid in thermal control. A thermal control roll of 1 or 2 RPH imparted to the spacecraft during most of the mission greatly reduces the thermal control requirements.

One of the major heat losses is the rocket engine. Because it is designed to reject heat during firing periods and has a great amount of exposed surface area, it can be responsible for losing over eighty percent of the heat lost from the propulsion system. Present engine designs generally do not consider this factor and thus have not been optimized to reduce the heat loss during non-firing periods.

The thermal control of the feed and pressurization systems have been achieved by passive techniques consisting of optical property selection use of high thermal resistance for structural materials and spacecraft orientation constraints. However, thermal control of the engines require the use of electrical heaters which have on-off control in addition to optical property selection and spacecraft orientation constraints.

Propellant Temperature Range

The temperature range of storable hypergolic propellants in the tanks of large and small pressure fed propulsion systems is about 40 to 85°F. The temperature range of the propellants in the lines is about 25 to 175°F for small systems and about 25 to 135°F for large systems. The temperature ranges of propellant valves vary from 20°F to 225°F depending on the engine. The temperature range for the tanks present no serious thermal control problem although wider limits could reduce spacecraft orientation constraints.

The temperature ranges on the lines and engine valves do result in the addition of electrical heaters and many spacecraft orientation constraints.

Use of propellants which have wide usable temperature ranges would reduce the thermal control requirements, possibly resulting in passive methods with no orientation limits. Development of engines with wide temperature ranges for the propellant and valves could eliminate the need for electrical heaters.

Spacecraft Orientation

Every use of spacecraft orientation relief should be made to reduce the thermal control requirements on the propulsion system. During space flight a steady roll of 1 to 2 revolutions per hour will stabilize almost all components between 60 and 80°F with existing optical coatings. In earth orbit, a random drift mode non-synchronous with the period may be satisfactory for eliminating an active thermal control system. However, the limitation of optical coatings may require that all the solar heating possible be supplied to the rocket engines. This would also be true of lunar orbit or orbits of other planets. In orbit, it is quite difficult to balance the heat lost during shadowing with that gained during solar heating without imposing unacceptable orientation constraints on the spacecraft. Still, proper mission planning can provide spacecraft orientations which will minimize the thermal control requirements.

Computer Programs

Several computer programs are required to aid in thermal analysis of propulsion systems. These programs are a general thermal analyzer

program, a radiosity program and a view factor program. The thermal analyzer program is built around the thermal-electrical analogy using an electrical network with current, electrical capacitors, electrical resistance, and voltage drop replaced by heat flow rate, thermal capacitance, the reciprocal of thermal conductance, and temperature drop respectively. The radiosity program solves a radiation network to determine the interaction of radiation on several adjacent surfaces. The results of this program in the form of thermal radiation resistors are input to the thermal analyzer program. The view factor program defines the configuration or view factor from one surface to another. The output of this program is input to the radiosity program. This program is not necessarily needed as there are extensive tables, equations, and charts defining the view factor between various surfaces.

Thermal Properties

The thermal properties used in the thermal model must be as accurate as possible. A model consisting of hundreds of resistors, capacitors and nodes has the possibility of fairly large errors in predicting temperatures. If the basic data used in the model is also in error, this can result in prohibitively large errors in the predicted temperatures. In addition, correlation of large thermal model with test data is extremely difficult even if the basic data is correct.

The optical properties, contact resistance and the resistance of super insulation are some of the properties with the greatest variation. Any of these that are required for the calculation of an important resistance within the model should be substantiated with laboratory

test data.

Thermal Control of an Entry Propulsion System

Thermal control of an entry propulsion system during earth entry or entry to some other planet was excluded as part of this subject. However, thermal control of the system during spaceflight must be considered. If the propellant is held in the tanks during spaceflight, the thermal control problem is significantly reduced. The tanks can be sufficiently insulated to eliminate the need of active thermal control. The temperature range of the propellant lines, components and engine can be easily expanded for a non-operating system. Thus, any thermal control of propulsion components outside the tanks should not be needed.

Prior to entry the entry propulsion system can be heated to the required minimum temperature by solar heating or the use of electrical heaters. In some cases before activating the system, the engine valves are used as heaters and provide sufficient heat to warm the engine, injector and adjacent propellant lines. Heating times prior to entry of 13 to 20 minutes with a total of 54 watts of heat from the valves of a 100 pound thrust engine is sufficient for certain spacecrafts.

Thermal Control of an ACS for Space

Thermal Control is required of attitude control systems used during a space mission. The heat lost during planet or spacecraft shadowing must be added by electrical heaters or nuclear isotope heating. Present systems use electrical heaters because they can be easily turned off during the periods of engine firing or extensive solar heating. In trans-planet flights, passive thermal control can be readily achieved by imparting a small 1 to 2 rph

roll rate to the spacecraft. However, during orbital conditions heaters with thermal switches are required. A power level of 18 watts per 100 pound thrust engine may be required based on a duty cycle of 60%. Continuous heating would be more reliable but prohibitive orientation constraints would be needed to prevent exceeding the maximum temperature limits. For man rated spacecraft, these heaters and thermal switches must have redundancy. In addition, monitoring information must be supplied to the astronauts. The propellant tanks and components should not need an active thermal control system. Proper selection of thermal insulation and optical properties should enable the feed system to withstand any thermal transient up to 10 hours. Transients longer than 10 hours should be eliminated by mission planning.

Thermal Control of a Main Propulsion System.

Optimum thermal control of a 20,000 lb thrust propulsion system is difficult to achieve. The tanks and components can be easily controlled by thermal insulation and spacecraft orientation. However, the heat loss from the engine can be excessive and difficult to define. Therefore, sophisticated thermal analysis is required of the engine and adjacent spacecraft structure. This analysis can require a thermal model with a network having over 500 nodes and running two to four hours on a 7094 for a single mission. Advantage must be taken of the heat sink capability of the engine, and the additional heat obtained during engine firing to reduce energy and power requirements. Again, active thermal control should not be required during trans-planet flight. But during orbital conditions, heaters may be required on the propellant lines, and the engine propellant valves. The amount of power that may be required

is about 96 watts based on 50% duty cycle. These heaters would also have to have on-off control and must have redundancy for man-rated vehicles.

Conclusion

Thermal control of propulsion systems is an important consideration in spacecraft design and mission planning. The primary loss of heat is from the exposed rocket engines. Therefore, early recognition of the thermal control criteria in an engine and propulsion system design program can result in significant reductions in the thermal control requirements.

ABSTRACT

PLASMA PHYSICS AND APPLICATION TO ROCKETRY

By

G. W. Sutton

Avco Everett Research Laboratory

A plasma is an electrified gas with the following properties: 1) partially or totally ionized; that is, an abundance of charged particles; 2) electrically neutral on the whole; that is, the number of negative charges equals the number of positive charges, and 3) a Debye length much smaller than the macroscopic dimensions. This requirement insures that the plasma will be electrically neutral on size scales larger than the Debye length so that the plasma may be treated as a continuum with local properties, instead of following each charged particle individually, as is done in electron physics. The lecture will consider the special properties of a plasma, its interaction with electric and magnetic fields, and the modes of wave propagation through plasma, and uses for plasmas of interest to rocketry.

The various methods of ionizing gases will be reviewed. Ionization is caused by collisions between molecules, atoms solids, or photons in which sufficient chemical, kinetic, or photon energy is transferred to one of the bound orbital electrons, freeing it from the coulombic attractive field of the nucleus. As a special case, electrical or photon energy can be given to free electrons, which gave them sufficient energy to ionize neutral particles. Thermal and non-thermal ionization will be discussed. Electro-chemical ionization will also be discussed, such as used in the "Q" machine.

In general, the properties of a plasma depend upon three lengths: the mean-free path, the Larmor, radius, and the Debye length and in addition the Magnetic Reynolds number. Two cases of mean-free paths will be considered: very long mean free paths, and very short mean free paths.

When the mean free path in a plasma is very long the electrical conductivity of the plasma is very large and the plasma can be considered to be "collisionless". This plasma is characterized by a very large magnetic Reynold number. Expressions will be derived for the electrical conductivity for this state. With the addition of a magnetic field, the charged particles gyrate around the magnetic lines of flux. The adiabatic invariants for such a gas will be derived, which form the basis for the "magnetic bottle". The limits for escape from such confinement will be derived. The addition of various fields such as electric, gravitational, and magnetic field gradients leads to various drifts across magnetic lines of flux but the number of magnetic lines of flux enclosed by a grating particle remains constant. The constancy of the sum of the magnetic pressure and gas pressure will be shown.

The presence of many collisions of electrons with heavy particles yields a different regime, in which the mean free path is much smaller than dimensions of interest. The plasma is then best described by the velocity distribution function which is obtained from solution to the Boltzmann equation. Several examples will be given of equilibrium states, including the distribution in an electric field, Debye shielding, and Langmuir probes. The non-equilibrium states are usually considered small departures from equilibrium and give rise to typical phenomena of the transport properties of electrical conductivity and thermal conductivity. The dc electrical conductivity will be derived, and the tensor conductivity in a magnetic field. Ion slip and ambipolar diffusion will be illustrated. The electron momentum equation and energy equation will also be given and used to obtain the electrical conductivity and electron heating.

Wave phenomena in plasma will be discussed. The phenomena of acoustic waves and electromagnetic waves become coupled on a plasma and their properties are altered. In addition, in a highly conducting plasma, in the presence of a magnetic field, a new wave discovered by Alfvén (1947) can propagate. Some of the basic properties of these waves will be discussed, including electrostatic longitudinal waves (plasma frequency), electromagnetic waves and their interaction with magnetic fields, cyclotron heating and Alfvén waves.

For typical flow problems, the usual energy and momentum equations of gas dynamics must be modified. Usually, the magnetic Reynold's number is small, so that induced magnetic fields can be neglected (an exception is the Hall accelerator). These modifications are given: the addition of the Lorentz force in the momentum equation and joule heating in the energy equation. These terms make it possible to achieve plasma propulsion by interacting with the Lorentz force, and MHD electrical power generators, in which the joule heating term is negative.

With the Lorentz force in the direction of the flow velocity, momentum is added to the flow; in addition the joule heating heats the flow. If, however, an electrical load is placed in the $\mathbf{V} \times \mathbf{B}$ direction, then the Lorentz force retards the flow, and energy is extracted from the gas.

The Hall effect (tensor conductivity) is usually not negligible in such devices and can decrease the effective electrical conductivity of the flow. This can be remedied by suitable electrode geometries, of which several will be given as illustrations.

It is shown that the joule heating can cause the electron temperature to exceed the gas temperature. This has important applications for increasing the electrical conductivity of the gas for MHD electrical power generators and accelerators.

The remainder of the lecture will consist of examining the applications of plasma physics to rocket applications. One of the most important is the attenuation of telemetry by the exhaust gases from a rocket. On the other hand, at low altitudes the exhaust is highly turbulent and gives rise to turbulent scattering of microwaves. A more recent discovery is the use of electric fields to increasing burning rates of gaseous fuels. Direct uses of plasma physics for rocket application are the plasma propulsion devices. Two will be discussed: the $J \times B$ accelerator and arcs of which the Hall accelerator is a special case, in which the magnetic field give very high efficiencies and specific impulses. The total thrusts are very small, so that this device is very useful for station keeping of synchronous satellites. It is possible that controlled thermo-nuclear reactions may be useful for propulsion, but the success for achieving CTR with fusion has been for limited. On the other hand, combustion fired MHD electrical power generator has achieved operational status on the level of twenty megawatts, and should be capable of much larger sizes. This gives rise to the concept of using a gaseous (Rankine) direct nuclear cycle in which electrical energy is generated in an MHD generator, and then used for propulsion in a large $J \times B$ accelerator. This last application appears to be technically feasible with the existing knowledge of reactive, generators, and $J \times B$ propulsion devices.

ELECTRIC PROPULSION FOR SPACE VEHICLES
(21 March 1967)

by

Rudolf X. Meyer

Dr. Meyer, who received his M.E. degree in 1945 from the Swiss Institute of Technology and his Ph.D. degree in 1955 from Johns Hopkins University in mechanical and aeronautical engineering, is director of the Plasma Research Laboratory, Laboratories Division of Aerospace Corporation. He has been Assistant Professor of Aeronautics at the U.S. Naval Post Graduate School and has also been affiliated with Space Technology Laboratories, Inc. and Ramo-Wooldridge Corporation. Fields in which he has worked are plasma physics and magneto-hydrodynamics, fluid mechanics, particularly internal aerodynamics and hydrodynamics, design of aircraft gas turbines, and propulsion.

INTRODUCTION

The development of electric propulsion is motivated by the need for space vehicle propulsion systems with exhaust velocities far greater than those attainable with chemical rockets or nuclear heat-transfer propulsion. For a fixed thrust, an increase in exhaust velocity results in a smaller expenditure of propellant mass. Depending on the particular mission considered, the ratio of useful payload to initial mass of the rocket is correspondingly increased.

The concept of electric propulsion has a long history. It was considered by R. H. Goddard as early as 1906, but engineering developments did not materialize until the late fifties. First flight tests were conducted several years ago by both NASA and the U.S. Air Force. NASA has operated successfully an electron bombardment type engine on a suborbital flight. A contact cesium ion engine developed under an Air Force contract produced a thrust of 2 mlb in a ballistic test of 30 minute duration.

Most future applications to space vehicles envisage thrust levels of only a fraction of a pound, corresponding to accelerations of 10^{-4} g or less. Chemical or nuclear boosters are therefore needed to put the vehicle first into a low altitude orbit, from which it can ascend slowly in a spiral path until escape velocity is reached. The time required to enter a new orbit about a near-earth planet would exceed several months, and might be as long

as a year.

Anticipated power requirements for future planetary missions are of the order of a few to hundreds of kW, depending upon the application. Nuclear and solar energy sources are being considered. The successful application of electric propulsion hinges largely upon the development of light-weight power conversion devices. The weight of the propulsion unit is typically only a small fraction of the combined weights of energy source and conversion equipment, and therefore often not of critical importance. However, the efficiency with which electric energy is converted into kinetic energy of the propellant is crucial, since it directly affects the weight of the power source.

OPTIMUM SPECIFIC IMPULSE

The exhaust velocity is conventionally expressed in terms of the specific impulse (I_{sp}). It is likely that electric propulsion systems with an I_{sp} ranging from 1000 to 20,000 sec will find wide application in future space missions. The optimum I_{sp} depends mainly on the mission (including the time allowed for the trip) and on the mass/power ratio of the space power source needed to supply the electrical energy. Devices with an I_{sp} of 1000 to 2000 sec are useful for attitude stabilization of satellites and for lifting satellites from a low altitude orbit to a synchronous orbit. An I_{sp} from 3000 to 20,000 sec is optimal for extended missions within the solar system. Systems with an I_{sp} lower than optimum are penalized by excessive propellant weight, whereas systems with higher than optimum specific impulse suffer from an excessive weight of the electric power source.

ELECTROSTATIC THRUSTORS

The most characteristic feature of electrostatic thrusters is the separate acceleration of positive ions and electrons in an electrostatic field. Prominent

thrusters of this type are the electron bombardment (Kaufman) engine and the contact ion engine. Both of these thrusters are relatively highly developed at present, and have demonstrated lifetimes which approach those needed for operational systems, and good efficiency, at least in the higher range of specific impulse.

1. Electron-Bombardment Engine:

The propellant (usually cesium or mercury) is ionized by electron impact, from electrons emitted by a centrally located cathode and accelerated towards a cylindrical anode. The ionization efficiency is greatly improved by the use of an axial magnetic field which provides a partial containment of the electrons, reducing thereby wall losses. The acceleration of the ions takes place in the small gap between two screens (extractor and accelerator electrodes) to which a high electric potential difference is applied. The electrodes are designed in such a way as to minimize erosion through the mechanism of sputtering by the impact of ions, particularly also those resulting from charge-exchange.

2. Contact-Ion Engine:

Historically, this was the first electric thruster type to undergo engineering development. It differs from the electron bombardment engine mostly in the mechanism which is employed for ionization of the propellant. Ionization is achieved through the process of contact ionization (Langmuir-Kingdon effect) on a high-work-function metal surface, such as tungsten. Contact ionization is essentially restricted to the use of alkali metals, particularly cesium, as propellants, and requires that the ionizer be heated to a temperature of 1300°K or higher. The radiation loss from the heated ionizer is the principal power loss sustained by this type of thruster.

The resulting ion beam is space-charge neutralized by the injection of electrons;

A particularly promising device for space-charge neutralization is the recently developed "plasma bridge."

PLASMA PROPULSION

Plasma propulsion is likely to be less efficient in the range of high I_{sp} , but offers the advantage of a wider choice of propellants with good storage and handling characteristics. Other anticipated advantages are a higher thrust per unit area due to the absence of space charge limitations, and possibly a wider useful range of specific impulse.

The propellant is accelerated either by means of expanding an arc-heated plasma through a supersonic nozzle (arc jet), by imparting a momentum to the plasma by means of magnetic fields (crossed-field accelerator, rail accelerator, etc.) or by a combination of both methods. As a consequence of the high particle density, the Debye shielding distance is small compared with the physical dimensions. Except for thin sheaths on electrodes and insulators, electric forces are therefore absent and play no role in the acceleration.

1. Arc Jet:

The usual configuration is coaxial, with the two electrodes separated by an annular gap across which the arc strikes, and through which the propellant flows. The inner electrode is usually the cathode, made of tungsten or some other refractory. Liquid-cooled copper or uncooled refractory metals are used for the anode. In one version, the arc is confined by the throat region formed by the anode and strikes to the diverging portion of the nozzle, resulting in an increased voltage gradient and arc temperature. Anode spot motion to prevent anode burnout can be increased by introducing the propellant with a swirl, or by means of an axial

magnetic field. In the case of polyatomic propellants, the energy required for dissociation represents an important loss mechanism. Due to the relatively low density, recombination in the nozzle is incomplete. 1000 to 2000 sec specific impulse has been obtained with gases of low molecular weight.

In the so-called MPD arc, magnetic forces add greatly to the acceleration. These are produced by the self-magnetic field of the arc current, or else by the magnetic field of a solenoid.

2. Crossed Field Accelerator:

Characteristic for these devices is an externally applied magnetic field, with lines of force substantially perpendicular to the discharge current. The resulting ponderomotive force is perpendicular to both field and current, and is in the direction of motion of the plasma. The propellant flows through a channel, bounded by two electrodes facing each other. Magnetic field strengths of several thousand Gauss are typical.

3. Rail Accelerator:

The electric discharge takes place between two parallel, plane conductors (rails) or two concentric cylinders. The magnetic field associated with the discharge current drives the current from along the rails. In one mode of operation, the space between the electrodes is initially filled with gas at a low pressure; the moving current front then produces a propagating shock wave, which compresses and ionizes the gas. In other devices of this type, a puff of gas is admitted through a fast acting valve, or by sublimation of a solid propellant, and is accelerated by the discharge. Maximum velocities corresponding to a specific impulse of 20,000 sec and higher have been obtained in pulsed operation.

4. Travelling Wave Accelerator:

The principle of operation is somewhat analogous to that of an induction motor.

A time-varying magnetic field is produced either by multi-phase windings, by sequentially switched coils, or by means of a transmission line. An attractive feature of this type accelerator is the absence of electrodes and the possibility of isolating the plasma from the walls by means of magnetic fields.

The lecture terminates with a discussion of laboratory experiments with a Space-Charge-Sheath thruster. In this device, cesium ions are accelerated in the gap between a porous tungsten ionizer and a virtual cathode formed by electrons gyrating in a transverse magnetic field. The magnetic field strength (2500 Gauss) is such that the electron cyclotron radius is comparable to the length of the accelerating region (approximately 1 mm). On the other hand, the ion cyclotron radius which is of the order of 20 cm, is large compared to the characteristic scale length (1 cm) of the magnetic field. A number of experimental and theoretical problems arising in testing this thruster will be discussed.

SOLID PROPELLANT MECHANICAL PROPERTIES TESTING,
FAILURE CRITERIA AND AGING

FRANK N. KELLEY

AIR FORCE ROCKET PROPULSION LABORATORY
EDWARDS, CALIFORNIA

67/65

INTRODUCTION

Solid propellants are structural materials. Today's rocket motors must be designed to meet a variety of mission applications, many of which have placed increasingly severe demands on the structural capability of the propellant grain. Although it is generally recognized that ballistic requirements dictate many aspects of the final grain configuration, structural limitations have become more apparent in recent years. Quantitative measurements of the propellant's physical and mechanical characteristics have become as important to the design engineer as the combustion laws may be to the ballisticians. Unfortunately, the basic character of the material is such that attempts to measure its mechanical properties have posed serious experimental and conceptual difficulties. Techniques of engineering structural analysis have developed to the state where reasonable predictions can be made of loads and deformations in such structures, which may be composed of ninety percent of this unusual material. On the other hand, difficulties in analysis have been greatest in those regions where critical conditions are most likely, such as grain discontinuities, corners and bonded interfaces. That is, prediction of structural failure, where failure is most likely to occur, is in many cases the least satisfactory product of the structural integrity analysis.

There has been substantial progress in the development of methods for solid propellant material characterization over the past decade, however. The propellant has been represented as a linear isotropic viscoelastic material with some success. The necessity for further sophistication is not always obvious but in many instances large errors can be expected if assumptions of linearity and isotropic behavior are retained.

The loading environment which a propellant grain must survive includes thermal cycling, handling and vibration, ignition pressurization, and acceleration. Many

of these conditions may prevail at the same time; such as the imposition of small oscillatory stresses on a grain which has been subjected to large thermal stresses. The resultant deformations may be much greater than a few percent, so finite strains must be considered. The rate at which the material is deformed in some of these cases requires the recognition and proper accounting of its time- and temperature-dependent properties.

The generation of a practical propellant failure criterion has been the object of extensive study for several years. It appears that no completely general analytical criterion is forthcoming, but significant advances in the experimental characterization of ultimate properties in multiaxial stress fields promise more reasonable empirical guidelines.

High-speed computer techniques have provided the means by which material properties, loading environments, and geometry may be considered for a large number of grain configurations. Also, as an important adjunct, it must be recognized that propellant mechanical properties change with time and exposure, and any failure criterion or response characterization applicable to unaged material must also account for these changes to be of any significant value in establishing operational design limitations. Many missile systems must undergo repeated exposure to thermal extremes as well as a wide range of vibrational frequencies and accelerations and are expected to survive for many years without intolerable changes in reliability or operational readiness.

The following sections draw from a very large number of published documents and reports as well as private communications with individual investigators;

however, only the unclassified literature has been surveyed. Several basic source documents have been used liberally. These include: the Interagency Chemical Rocket Propulsion Group (ICRPG) Mechanical Behavior Manual (43), Solid Rocket Structural Integrity Abstracts and the Bulletins of the Joint Army-Navy-Air Force (JANAF) Physical Properties Panel, the ICRPG Working Group on Mechanical Behavior and the JANAF Surveillance Panel.

TESTING

A variety of tests are currently conducted to characterize the mechanical properties of solid propellants. The nature of the test, test mode, and environmental conditions employed depend upon the end use of the data obtained. Certainly, a large portion of all testing is conducted for quality-control purposes; to determine batch variability, and as a check for gross formulation errors. Also, formulation chemists are guided by the recognition that some "standard" tests give reasonable indications of the practicability of experimental propellants. In general, these tests are used for relative comparisons of data, rather than for precise values of stress and strain capability. On the other hand, if the tests are to provide data for engineering analysis, great care must be exercised in the control of test conditions and interpretation of results. The specific tests to be described in this paper will be discussed in terms of their usefulness for both applications described above.

THE UNIAXIAL TEST

This test is by far the most common in use today. The so-called JANAF tensile specimen has received rather wide acceptance for constant strain rate testing since 1957. (65) Figure 1 shows this specimen with dimensions and a typical set of gripping jaws for use with any available tester. The specimen has been prepared

by die-cutting, casting, or milling. The latter procedure usually provides a superior specimen, avoiding the irregularities in dimensions and composition normally produced by the other methods.

It was recognized rather early that although the JANAF specimen has the obvious advantage of preparation ease in large quantities, certain precautions must be taken in order to provide meaningful property data. Since the specimen tends to extrude out of the jaws when a load is applied, strain data based on jaw displacement alone tend to include substantial errors. Figure 2 is an illustration of the extrusion phenomenon. Various techniques have been developed to provide a more accurate measure of strain in the JANAF specimen. One approach is to make a strain measurement which is independent of the jaw displacement, by optical or photographic methods, and to compute an effective gauge length for the specific formulation of interest. Unfortunately, the effective gauge length (EGL) varies with strain and test conditions for most propellants, and a plot of EGL versus strain must be used to correct for this variation.

Other techniques for a more satisfactory measure of strain in the gauge section of the JANAF specimen have been developed. One inexpensive and simple method is the use of a clear plastic film extensometer which is attached to the gauge section of the specimen. A mark on the face of the specimen is pulled past evenly spaced lines on the clear film and the recorder chart is pipped manually as the mark passes each of the lines. Figure 3 illustrates this technique. (Figure not available) Various other methods are also used, such as a spring clip strain gauge developed by Steele and Smith, (1) or the more elaborate extensometer designed by Farris (26) shown in Figure 4. (Figure not available.)

At present there is considerable effort to develop a tensile specimen which does not exhibit a variable gauge length. Most popular is some form of end-bonded

sample. Figure 5 shows some of the specimen configurations presently in use or under development. The end-bonded specimens have been quite satisfactory for response measurements in many cases, but the tendency to fail at one of the bonded joints makes many of the configurations unacceptable for ultimate property determinations. A specimen which has shown considerable promise is that developed by Saylak⁽⁷⁷⁾. The details of this specimen are shown in Figure 6. It is cast in a cylindrical mold and steel washers are bonded to the ends with an epoxy glue. Figure 7 illustrates the improvement in the variation of effective gauge length with strain when this configuration is compared with the JANAF specimen.

The uniaxial test is widely used for quality control and formulation testing for obvious reasons. The JANAF configuration is not likely to be replaced for these purposes, especially since the backlog of information relative to the formulation art is composed primarily of data from this specimen. Grain structural analysts require more precise information, however, and when uniaxial data is obtained for their purposes more elaborate and time-consuming tests may be conducted.

TEST MODES

This discussion applies to various test configurations whether uniaxial or multiaxial and is related, in general, to commercially available testing machines with controlled jaw displacement rates. The characterization of viscoelastic materials requires testing conditions over wide temperature ranges and, at times, a range of strain rates. Although material properties are discussed in some detail in a later section, it should be recognized that the general applicability of time-temperature equivalence principles provides the convenience of temperature variation where very short or extremely long time testing would be impractical.

The constant load-displacement-rate test mode is most frequently employed. This meets most of the requirements for mass testing such as in the quality control situation, but various test analysis methods have made it quite suitable for design as well as research purposes. Displacement rates from 0.2 to 20 inches per minute are normally employed, but some testing equipment provides reasonably controlled rates upwards of 10,000 inches per minute. Extremely low rate tests are very time consuming, of course, but some specialized equipment has been designed to produce strain rates down to 8×10^{-7} inches per minute. (4)

Constant strain for stress relaxation tests, and constant load creep tests, may be conducted in simple devices. In these tests control of temperature is quite critical since the results are usually applied as a spectral representation for structural analysis or research purposes. Figure 8 illustrates a multistation creep tester with automated data recorders. (Figure not available.) Strain and load endurance tests are conducted in similar devices, but the conditions existing at failure and time to failure are normally the only data required. The endurance tests are used frequently to supplement the constant displacement rate tests for routine evaluation purposes.

Other test modes such as constant loading rate and variable strain rate have been employed on a limited basis as research techniques to investigate such phenomena as the path dependence of failure, but no general description of these tests can be provided. Of course the entire area of dynamic testing and fatigue employs a variety of specialized test conditions, but these will be discussed in a later section devoted to that topic.

PROPELLANT PROPERTIES

Some of the more unusual properties of solid propellants result from their basic composition. The two general categories of double-base and composite-rubber-binder

propellants have many sub-categories, but no exhaustive compilation will be attempted here. It should be sufficient to recognize that most modern propellants consist of a deformable binder phase and a crystalline salt filler such as ammonium perchlorate and usually a powdered metallic fuel such as aluminum. Table I gives some typical compositions for both composite rubber-based and composite double-base systems.

A very brief outline of the methods of production of the two general propellant categories is in order at this point to provide a minimal background for following discussions. Much more detailed information may be found in the accompanying articles in this series.

Composite rubber-based propellant ingredients are usually mixed together at somewhat elevated temperatures (ca. 100-160°F) so that a reasonably fluid and uniform mixture results. The filler materials are dispersed in the low-molecular-weight polymer ($\bar{M}_n = 2000-5000$) and other liquid ingredients, and the resultant mixture is poured through de-aerating devices into an evacuated mold. In many instances the mold is the motor case which is suitably fitted with a casting mandrel and lined with an insulating adhesive. The motor is then cured at elevated temperature (ca. 140-160°F) for several hours. The propellant grain retains the geometry of the mold after cure and, therefore, many predetermined ballistic characteristics are built-in. The grain is somewhat rubbery over a wide temperature range and is dimensionally stable within certain physical limits. The ability to deform without rupture, and to recover, is quite important since any cracks or unbonds which develop would result in additional burning surface and an unpredictable chamber pressure during motor operation.

TABLE I

TYPICAL SOLID PROPELLANT FORMULATIONS

HYDROCARBON BINDER COMPOSITE

<u>INGREDIENT</u>	<u>WEIGHT %</u>
Ammonium Perchlorate	70.00
Aluminum Powder	16.00
Poly (butadiene-acrylic acid-acrylonitrile)	11.78
Epoxy Curative	2.22

POLYURETHANE BINDER COMPOSITE

<u>INGREDIENT</u>	<u>WEIGHT %</u>
Ammonium Perchlorate	65.00
Aluminum Powder	17.00
Polyalkylene Glycols	12.73
Diisocyanate	2.24
Triol	0.43
Additives and Plasticizer	2.60

COMPOSITE DOUBLE-BASE

<u>INGREDIENT</u>	<u>WEIGHT %</u>
Ammonium Perchlorate	20.4
Aluminum Powder	21.1
Nitrocellulose	21.9
Nitroglycerine	29.0
Triacetin	5.1
Stabilizers	2.5

The dimensional stability of the propellant grain is the result of the chemically cross-linked polymeric binder. It is to be expected that many of the mechanical properties of the final cured propellant will be dictated by binder characteristics. Another important consideration is the affect of filler, due to its physical presence as well as the degree of interaction with the binder.

Composite double-base propellants are produced by allowing an energetic plasticizer, such as nitroglycerine, to swell and coalesce particles of a high-molecular-weight polymer such as nitrocellulose. The ingredients are dispersed by one of two processes in general use. The first is a casting technique in which the basic ingredients are extruded and chopped into small granules, and these are poured into the motor case or mold. The plasticizer (solvent) is introduced into the evacuated granule-containing mold under pressure with some vibration to aid in the elimination of bubbles. The second technique utilizes a slurry of small premixed granules and plasticizer which is then poured into the grain mold. In each case, curing is accomplished at elevated temperature which aids in the diffusion of plasticizer and subsequent swelling of the polymer. The molecular forces which develop are sufficient to provide rigidity to the final propellant grain, but are secondary in nature and do not provide a continuous covalently bonded network such as that found in rubber-based systems. The individual granules in double-base propellants are identifiable even after swelling and curing, although their boundaries are somewhat diffuse. The precise curing mechanism is not completely understood for these propellants, but the material properties may be controlled by variations in the time-temperature curing cycles.

It can be readily seen that typical composite propellants are highly filled polymers, and, especially in the case of the rubber-based systems, are more nearly

granular media than merely filled rubbers. Certain specific differences between the double-base binder and the elastomeric binder lead to some differences in behavior, but many of the resulting properties show similarities. The relationships between bulk properties and microstructure in the rubber-based systems are much better understood than those of the double-base propellants and, therefore, the following discussions will focus primarily on the former category.

Figure 9 is a schematic representation of a uniaxial stress-strain curve with certain common mechanical property definitions indicated. The gradually decreasing slope and plateau region followed by diminishing stress just before rupture are typical features of the composite propellant stress-strain curve. This behavior is readily understood when one considers the microstructural processes which occur when the material is deformed. (Figure not available.) Figure 10 illustrates the so-called "dewetting" phenomenon which occurs in all composite solid propellants to some extent when a load is applied. The motion of particles imbedded in the matrix produces sufficiently high stresses in the vicinity of the binder-filler interface that rupture occurs and the binder-filler bonds may be pulled loose. The initial point of rupture may be in the binder phase⁽⁷¹⁾, but in many cases the tear propagates to the filler surface and the interface is separated.

As dewetting takes place the reinforcing effects of the filler are reduced and a decreasing modulus results. When this process has proceeded as far as possible any continued deformation is sustained by the binder until the sample breaks.

Propellant behavior is widely varied with respect to this process, however. Differences in formulation or even differences in test conditions may produce very localized dewetting and yielding; or the process may occur uniformly throughout the specimen. Obviously a local yielding condition confuses the interpretation

of test results based on force and jaw displacement curves.

When microscopic destruction occurs within propellant samples, whether by dewetting or by the formation of small cracks in the binder, an overall volume increase may be observed. This phenomenon is shown in Figure 11 by means of a plot of volume change against strain.

The dewetting process may be observed with a microscope if some means is provided to strain the sample during the observation. Hilzinger (41) has produced many excellent photomicrographs using this technique. Various techniques have been employed to monitor the volume change as a function of strain in propellant samples. Rainbird and Vernon (74), Smith (90) and Stedry and Landel and Shelton (97) have shown the general dependence of volume change on strain using simple dilatometers. Kruse (49) examined the rate and temperature effects on Poisson's ratio obtained from uniaxial tests conducted in a dilatometer, and Fishman and Rinde (28) extended this to include several propellant variations as well as humidity affects. Extensive investigations of dewetting have been conducted by Farris (25) who has provided many refinements of the strain-dilatometer. Some of the basic design features are shown (Figure not available.) in Figure 12. Various media have been employed as confining fluids, including silicone oils, air and nitrogen. Some of the earlier work in this area performed by Svob et. al. (101) made use of simple static buoyancy measurements at various strain levels.

One approach which does not utilize a confining fluid has been developed by Saylak (79). This technique involves an optical system which continuously monitors the lateral strain in a uniaxial specimen. The specimen must necessarily be of circular cross section and, obviously, the volume change computation requires uniform dewetting throughout the sample. This method is not rate- and temperature-

limited since no mechanical attachments or fluids are in contact with the sample. A schematic diagram of the lateral strain device is shown in Figure 13. Surland and Olyan⁽¹⁰⁰⁾ describe an electro-optic device which focuses on a rectangular patch on the test surface. A motor-driven slit is interposed between the target and a fine optical grating in the instrument. The precision of this instrument is reported to depend primarily on the quality of the optical system and grating.

Some efforts have been undertaken to study propellant dilatation in multiaxial stress fields and even in small motor configurations. Farris⁽²⁴⁾ has conducted limited investigations along this line and has made approximate correlations between uniaxial and multiaxial tests.

Generally applicable mathematical representations of the dilatational behavior of propellants have not been developed, as might be expected; however Fishman and Hinde⁽²⁸⁾ have derived empirical expressions for the formulations which they studied. These relationships give reasonable description of uniaxial behavior over wide ranges of strain, time and temperature for a number of testing modes. Equation (1) is representative of one of the generalized expressions for the polyurethane and polybutadiene formulations studied.

$$\log V/V_0 = A \left[\log W + B \log t/b_T - C(\log t/b_T)^2 \right]^n \quad (1)$$

where: V_0 = initial sample volume

V = sample volume after time t

W = strain energy (area under stress-strain curve)

b_T = time-temperature shift factor

and A , B , and C are constants for each formulation.

Figure 14 illustrates the relationships between volume change and test conditions for this formulation.

Although dewetting has been, and is currently, the subject of much discussion, its implications with respect to motor performance are not clear. In some cases the propellant burn rate appears to be a regular function of volume change as shown by Saylak⁽⁷⁶⁾. In other cases the onset of extensive dewetting has been considered an operational failure condition. It is quite likely that repetitive environmental cycling may involve dewetting to the extent that the amount of dewetting per loading cycle may be a reasonable measure of damage to structural capability and may be applied to cumulative damage concepts. Colodny⁽⁴⁾ has shown that low-frequency stress-strain cycling below the failure limits of the material produces a general softening until some "equilibrium" condition exists. At somewhat elevated temperatures there appears to be "rehealing" of the relaxed cycled material and the original stress-strain curve may be regenerated. The implications of this to strength capability of the cycled material is not defined at this time, but a general discussion and tentative approach are presented by Torrey and Britton⁽¹⁰³⁾, based on a first-order rate process assumption for the rehealing process.

MULTIAXIAL TESTING

Although the uniaxial test has traditionally received the most attention, it is generally recognized that such tests alone may be insufficient to characterize adequately the mechanical capability of solid propellants. This is especially true in the case of ultimate property determinations where a change in load application from one axis to several at once may have a strong effect on the relative ranking of propellants according to their breaking strains. Since the conditions usually encountered in solid rocket motors lead to the development of multiaxial stress fields, tests which attempt to stimulate these stress fields may be expected to represent more closely the true capability of the material.

Multiaxial test geometries and test conditions may be analyzed with reference to three orthogonal principal stresses as shown in Figure 15.

The various octants in principal stress space are described by considering conditions of tension (+) and compression (-) and their combination. Convention usually takes the upper right hand octant extending out from the page in Figure 15 to be the tension-tension-tension (+++) octant, and, similarly, going diagonally downward and backward through the origin the (---) octant is reached.

Figure 16 illustrates several test specimens which have been used⁽⁴⁵⁾ in the multiaxial characterization of solid propellants. The arrows in the figure indicate the direction of load application. The strip tension or strip biaxial test has been employed rather extensively in failure studies. It can be readily seen that the propellant is constrained by the long bonded edge so that lateral contraction is prevented and tension is produced in two axes simultaneously. The sample is free to contract normal to these axes. The ratio of the two principal tensile stresses may be varied from 0 to 0.5 by varying the bonded length.

The stresses and strains which develop in the center of very long strips are related as follows:

$$\sigma_1 = 2\sigma_2, \sigma_3 = 0$$

$$\epsilon_3 = -\epsilon_1, \epsilon_2 = 0$$

and

$$\tau_1 = \frac{\sigma_2 - \sigma_3}{2} = \frac{\sigma_1}{4}$$

$$\tau_2 = \frac{\sigma_3 - \sigma_1}{2} = -\frac{\sigma_1}{2}$$

$$\tau_3 = \frac{\sigma_1 - \sigma_2}{2} = -\frac{\sigma_1}{4}$$

where τ_1 , τ_2 and τ_3 are the principal shear stresses, and Poisson's ratio is 1/2.

The diametral compression test is performed by compressing a thick disc along a diameter of the specimen. A diameter-to-thickness ratio of approximately 3 is preferred. (Figure not available.) Figure 17 shows this test, including grid lines and gauges for measuring the strains developed as the sample is compressed between the tester platens.

The stress field which is developed at the center of this test specimen is compression-tension, and taking the y axis to be the compression axis the compressive stress, σ_y , is given by^(31, 43)

$$\sigma_y = \frac{-6 F_y}{\pi t d} \quad (2)$$

where d = sample diameter

t = thickness

F_y = Compressive force

and the tensile stress normal to the axis of compression, σ_x is given by

$$\sigma_x = \frac{2F_y}{\pi t d} \quad (3)$$

The corresponding strains are

$$\epsilon_y = \frac{-2 F_y (3 + \nu)}{\pi t d E} \quad (4)$$

$$\text{and } \epsilon_x = \frac{2 F_y (1 + 3\nu)}{\pi t d E} \quad (5)$$

where ν is Poisson's ratio and E is the modulus.

The total deformation \bar{U} along the diameter in the x direction is given by

$$\bar{U} = \frac{F_y}{\pi t E} \left[(1 - \nu)(2 - \pi) + 2(1 + \nu) \right] \quad (6)$$

The simple shear test, also shown in Figure 16, was designed in the "chevron" configuration to eliminate premature tensile failure at the corner between the leading edge and the central plate. It is apparent that the propellant at these corners will be in compression during most of the test.

Another biaxial test which is not shown here utilizes a thin disc of material which is clamped around the edge and inflated by air. The pressure p and the radius r are monitored and if the disc is circular the stress field is

$$\sigma_x = \sigma_y = \frac{pr}{2t} \quad (7)$$

A complete description of this test and certain variations is given by Spangler, (93,94) and Long, Rainbird and Vernon (58).

Triaxial tests usually involve much more elaborate testing equipment and more precise measuring techniques than those normally employed for uniaxial and biaxial measurements. One of the more widely employed tests is the so-called "poker chip" test (32, 57). In this test the faces of a thin circular disc are bonded to rigid plates as shown in Figure 18. (Figure not available.) The specimen is loaded by axial displacement of the plates, normal to the face, and the lateral constraint induces a triaxial stress in the sample. The triaxial stress field approximates hydrostatic (equal triaxial) conditions near the center when (1) the grip plates are very rigid, (2) the disc diameter to thickness is large (>10), and (3) the ratio of shear to bulk modulus is very small compared to unity (Poisson's ratio near $1/2$). The poker chip configuration has been analyzed by Lindsey, Williams, Schapery, Zak (56) and Brisbane (15) and by Messner (64) and the stress and displacement expressions will not be given here.

Refinement of the poker chip test to include a center load cell in one of

the bonded plates is reported by Harbert⁽³⁹⁾. Figure 19 shows the stress-strain curves generated by external measurement, as well as the failure point determined by the center load cell.

A unique and considerably more elaborate multiaxial test employs a thick-walled hollow sphere test specimen which may be pressurized internally or externally with a nearly incompressible liquid. Figure 20 illustrates the essential features of the test device as described by Bennet and Anderson⁽⁵⁾. The specimen is prepared by casting propellant in a mold fitted with a sand-polyvinyl alcohol mandrel inside the sphere which may be easily removed after curing. A constant-displacement-rate instrument drives the piston to pressurize the chamber and apply large deformations. The piston's total displacement volume is transferred to the specimen. It can be seen that simultaneous internal and external pressures may be applied and so adjusted to provide a variety of stress fields. The stress and strain are measured in the hoop and radial directions at the internal boundary of the sphere.

For an externally applied pressure, a compression-compression-compression stress field is obtained with a thick-walled sphere. If the sphere wall is thin a biaxial compression-compression field is produced. If the pressure is applied internally a triaxial tension-tension-compression state is generated, and similarly, if the wall is thin, a biaxial tension-tension field is obtained. A nearly uniform stress field is produced over the entire specimen. The supporting tube is surrounded with a low modulus material to avoid stress concentration and premature rupture in this vicinity. The relative magnitudes of the stresses are varied by changing the thickness of the sphere. One additional feature of this test is ability to examine the effects of pressure on the mechanical properties of propellant. Obviously the various test modes such as constant strain and constant stress may be determined by regulating the pressurizing system.

An apparatus described by Sharma⁽⁸⁶⁾ utilizes a tubular specimen which may be strained longitudinally with internal pressurization. Loading rate can be varied and strains are measured by clip gages. This device permits characterization of propellant-like materials in various biaxial tension-tension and biaxial tension compression stress fields. A schematic diagram of the apparatus is shown in Figure 24.

Uniaxial tension testing with superposed hydrostatic pressure has been described by Vernon,⁽¹⁰⁷⁾ and Surland, Boyden and Givan⁽⁹⁹⁾. Such tests provide response and failure measurements in the triaxial compression or tension-compression-compression octants.

DYNAMIC TESTING

A wide variety of dynamic tests, testers and specimen configurations have been employed in the measurement of solid propellant response to cyclic loading. Table II summarizes many of the techniques and characteristics with appropriate references. In most instances the loading is applied in a regular sinusoidal manner, although other nonsinusoidal time functions may be considered in some tests.

As pointed out by Britton⁽¹⁴⁾, the measurements are useful in design and research studies pertaining to:

- 1- Vibration analysis of structure
- 2- Propellant viscoelastic behavior
- 3- Oscillating combustion
- 4- Internal attenuation of shock waves
- 5- Fatigue life

Test methods can be arranged according to two major categories:

(a) Relatively low amplitude tests (<1% strain) for relatively short times, with response measured in terms of complex or dynamic modulus.

TABLE II (From Ref 14)

SUMMARY OF DYNAMIC TESTS USED FOR SOLID PROPELLANT CHARACTERIZATION

Test and References	Stress/Strain Application	Frequency Range	Response Measured	Date Usually Obtained
Fitzgerald Transducer Fitzgerald, et al (30,27) Landel (43, Section 4.6.2)	Forced sinusoidal nonresonant shear directly applied by pole pieces of electromagnet to sample disk	25--3000 cps	Changes in resistance and capacitance of electrical drive system	G' (ω) G'' (ω)
Oscillating Plate (FIL Tester) Phillipoff (73) Hosbel (42)	Forced sinusoidal shear strain imposed by mechanical drive of clamped annular plate of propellant	0.1--60 cps	Deflection of center ring, applied force	G' (ω) G'' (ω)
Vibrating Plate Baltrukonis (2) Layton, et al (43, Section 4.6.2)	Forced sinusoidal shear strain imposed by vibrating outer ring of annular plate of propellant on an electrodynamic shaker	75--1000 cps	Amplitude ratio, phase angle from two accelerometers, frequency from electrical drive	G' (ω) G'' (ω)
Resonant Weighted Column Britton (103) Burton, et al (16)	Forced sinusoidal uniaxial tension and compression imposed by vibrating weighted rectangular column of propellant on electrodynamic shaker	30--1500 cps	Amplitude ratio, phase angle from two accelerometers, frequency from electrical drive	E' (ω) E'' (ω)

TABLE II
(Continued)

Test and References	Stress/Strain Application	Frequency Range	Response Measured By	Data Usually Obtained
LFC Large Deformation Dynamic Tester Jones, et al (44)	Forced sinusoidal uniaxial tension and shear imposed by mechanical drive to tensile bar or double-lap shear specimen	1--45 cps	Force and displacement by transducers in mounting arrangement	E' (ω) E'' (ω) G' (ω) G'' (ω)
LFC Small Deformation Dynamic Tester Jones, et al (44)	Forced sinusoidal shear imposed by piezoelectric driver to single lap shear specimen	20--1000 cps	Driving force from piezoelectric input voltage, transmitted force from piezoelectric monitor on clamped end of specimen	C' (ω) C'' (ω)
Free Vibrating Reed Tester (AGC) Kostyrko (48) (43)	Free damped sinusoidal vibration of clamped thin rectangular specimen, free end set in motion by deflection and release	4--30 cps	Deflection from strain gauge mounted on sample recorded against time, sample dimensions and mass, Time range extended by using time-temperature superposition	E' (ω) E'' (ω)
Forced Vibrating Reed Tester (HPC) Nicholson, et al (70)	Forced sinusoidal vibration of thin cantilever beam specimen by electrodynamic shaker	10--200 cps	Free end displacement by optical displacement transducers. In-pit from shaker electrical measurements	E' (ω) E'' (ω)

TABLE II
(Continued)

<u>Test and References</u>	<u>Stress/Strain Application</u>	<u>Frequency Range</u>	<u>Response Measured By</u>	<u>Data Usually Obtained</u>
Dynamic Torsion Tester Low Range (STL) Gottenberg, et al (34)	Forced sinusoidal oscillatory torsion imposed by mechanical drive to hollow cylindrical specimen through bell-crank arrangement	0.0002 to 30 cps	Angular displacement sensed by differential transformers; speed indication from electromagnetic sensor on output shaft of drive motor	G' (ω) G'' (ω)
Dynamic Torsion Tester, High Range (STL) Gottenberg, et al (34)	Forced sinusoidal rotary vibration imposed by electrodynamic vibrator to hollow cylindrical specimen through bell-crank arrangement	30--1000 cps	Angular displacement sensed by piezoelectric accelerometers; frequency from vibrator input	G' (ω) G'' (ω)

(b) Relatively high amplitude tests (strains approaching uniaxial rupture) for a time sufficient to cause deterioration and ultimate failure. Time to failure at a given applied stress or strain amplitude is determined.

A general description of the fundamental relationships governing the dynamic response of linear viscoelastic materials may be found in several sources (36, 27, 89) and will not be repeated in detail here. It should be sufficient to note that, in general, sinusoidally applied strains (stresses) result in sinusoidal stresses (strains) that are out of phase. Measurements may be made under uniaxial, shear or dilational loading conditions and the resultant complex moduli or compliance and loss phase angle are computed. Rotating radius vectors are usually taken to represent the stress and strain behavior for graphical analysis on a complex plane. Complex stresses (σ^*) and strains (ϵ^*) may be written as:

$$\sigma^* = \sigma_a \cos \omega t + i \sin \omega t \quad (8)$$

$$\epsilon^* = \epsilon_a \cos (\omega t - \delta) + i \sin (\omega t - \delta) \quad (9)$$

Where:

σ_a = stress amplitude

ϵ_a = strain amplitude

δ = loss phase angle

ω = circular frequency

t = time

The complex modulus may therefore be defined as:

$$E^*(\omega) = \frac{\sigma^*}{\epsilon^*} \quad (10)$$

and in terms of its components

$$E^*(\omega) = E'(\omega) + iE''(\omega) \quad (11)$$

where $E'(\omega)$ is called the storage modulus and $E''(\omega)$ is the loss modulus. The ratio E''/E' is equal to the tangent of the loss angle. The dynamic compliance $D^* = \epsilon^*/\sigma_*$ and storage and loss compliance, $D'(\omega)$ and $D''(\omega)$ may be defined in a similar manner. These symbols are usually applied to uniaxial loading. The designations $G^*(\omega)$ and $J^*(\omega)$ are normally employed for complex shear modulus and compliance, respectively.

Dynamic measurements can be made using either free or forced vibrations, and at resonance or outside of resonance conditions. Since the material is time and temperature dependent, characterization over wide frequency ranges may be greatly simplified by applying the WLF (114) equation for time-temperature equivalence. This relationship has been found to be generally useful in many propellant studies when used with caution under conditions which have established validity.

Sample shape and size are of considerable importance when selecting dynamic test methods for solid propellants. Preparation must take account of surface conditions and precise dimensions. Usually cast specimens retain a polymer-rich surface layer and should be avoided. Additionally the sample dimensions should be large compared to the size of the largest solid particle inclusion in the propellant.

Forced vibrations at large amplitudes may result in propellant deterioration by several mechanisms. Tormey and Britton⁽¹⁰³⁾ examined this problem from the viewpoint of microstructural change as well as engineering mechanics. When a force is applied to the material and deformation results, the mechanical energy may be distributed in several ways, such as: (1) energy stored in recoverable elastic deformation; (2) interphase dewetting; (3) bond breakage; (4) viscous flow; (5) heat generation, etc. New surfaces are formed internally due to

microfractures in the binder as well as binder-filler dewetting. The generation of heat may be quite similar to that experienced in the repeated flexing of rubber tires. During the application of cyclic loading, a certain portion of the mechanical energy of each cycle is lost as heat. If the heat cannot be transferred to the surroundings at a sufficient rate, the temperature of the material will rise.

The energy which is lost in each cycle when an alternating stress is applied to a viscoelastic material may be expressed as follows:

$$W' = \pi E'' \epsilon_a^2 \quad (12)$$

or

$$W' = \pi D'' \sigma_a^2 \quad (13)$$

Where D'' is the loss compliance or the out-of-phase component of the dynamic compliance. The rate is given by

$$W = 1/2 \omega D'' \sigma_a^2 \quad (14)$$

which for N cycles gives

$$W_N = N \pi D'' \sigma_a^2 \quad (15)$$

A vivid example of the resultant deterioration of a solid propellant grain is shown in the report by Tormey and Britton (103), where a grain was subjected to a 5g input at resonant frequency for about 6×10^6 cycles. The propellant degraded so badly that it lost dimensional stability and flowed. Another example illustrated the tendency of vibration to propagate fracture in certain highly stressed regions of the grain. Although the energy loss per cycle may appear as a buildup of heat in the material, this process is related to several governing factors. An increasing temperature in a viscoelastic material generally results in a decreasing modulus. This may lead to larger deformations at a given input vibrational force

if the mass is not amplitude restricted. Since the heat generation in a linear viscoelastic material increases in proportion to the second power of the strain, the process may tend to run away, unless there is a correspondingly large decrease in the loss modulus.

Schapery⁽⁸²⁾ has examined steady-state and transient temperature distributions resulting from energy dissipation in viscoelastic slabs and cylinders subjected to cyclic shear loading. The temperature dependence of the dissipation was introduced through the assumption of thermorheologically simple behavior. A non-linear heat conduction equation resulted, and coupled processes for heat conduction and mechanical deformation were treated by two variational principles. Shapery and Cantey⁽⁸³⁾ studied thermomechanical phenomena, placing particular emphasis on the nature of thermal instabilities. An experimental examination of solid propellant subjected to steady-state sinusoidal shearing was conducted using specimens insulated so that heat transfer was one-dimensional. Loading was accomplished in constant applied strain experiments and in forced vibration with inertia where the attached mass was free to move. Shapery's predictions of dynamic jump instabilities under certain critical conditions were qualitatively verified. Figure 21 shows a schematic drawing of the large deformation sinusoidal test apparatus and specimen configuration which were used.

There is an important aspect involved in large deformation cyclic tests which is related to the amount of damage done in each cycle which may accumulate in a predictable fashion, but which is also dependent on conditions which may allow recovery. These items will be discussed in a latter section dealing specifically with the problem of failure in solid propellants and some implications for cumulative damage.

PHYSICO-CHEMICAL CHARACTERIZATION

While mechanical testing of all types provides a general description of the bulk properties of solid propellants, it is difficult to make generalizations or even extrapolations which may be used in a predictive fashion. When the content or type of solid filler is changed, or curative ratios are altered, there is no simple corresponding material property change which can be defined based on mechanical testing experience. If filler content and type are held constant it may be expected that many mechanical properties are governed by binder cross-linking. Double-base formulations are particularly confounding with respect to variations in degree of "cure" because a continuous chemically cross-linked network is not formed. Pseudo-equilibrium modulus measurements may be employed to characterize the extent of gelation in these materials, but only an "equivalent" cross-link density may be computed. It is not at all clear what benefit, in a predictive sense, is provided by such measurements.

Considerably more satisfactory results have been obtained with composite rubber-based propellants. The binder cross-link density and sol fraction may be determined by employing modified swelling and extraction techniques common to the field of polymer science. The complications introduced by the measurement of such parameters in the presence of very high filler volume fractions are significant, but nevertheless useful techniques have been worked out. The determination of cross-link density in composite solid propellants has been described (47, 3,62) where both swollen tension and compression methods were employed. Previous efforts utilizing "equilibrium" modulus measurements or volume swelling techniques encountered some obvious difficulties. Equilibrium measurements are practically impossible

to obtain since the gradual dewetting of the binder-filler composite structure contributes a relaxation mechanism with very stubborn and non-reproducible characteristics. When high temperatures and very long times are employed, some chemical changes are possible, but a significant factor is the change in moisture content. The moisture effects on solid propellant properties can be considerable and will be discussed in the section on "Aging".

Volume swelling measurements have produced erratic results even under the most carefully controlled conditions. One important contribution in this regard is the work of Bills and Salcedo⁽⁸⁾. These investigations showed that complete release of the binder-filler bond could be obtained with certain solvent systems, and that the volume swelling ratio is independent of the filler content when complete release is achieved. Some thermodynamic problems exist, however, when such techniques are employed to provide a quantitative measure of cross-link density. First, equilibrium swelling is very difficult to achieve since the fragile swollen gel tends to deteriorate with time even under the best of conditions. Second, the solubility of the filler (ammonium perchlorate) and other additives tends to alter the solution thermodynamics of the system in an uncontrollable manner. Non-reproducible polymer-solvent interaction results, and replicate values of cross-link density are not obtained.

Swollen tensile and compression techniques avoid both of these problems since equilibrium swelling is not required and the method is based on interfacial bond release and "plasticization" rather than solution thermodynamics. The technique relies upon the approach to ideal rubberlike behavior which results when lightly cross-linked polymers are swelled. At small to moderate elongations, the stress-strain properties of rubbers have been described by a statistical theory of

rubberlike elasticity⁽¹⁰⁵⁾ resulting in the following expression:

$$\sigma = \nu_e kT(\lambda - 1/\lambda^2) \quad (16)$$

where ν_e is the number of effective network chains per unit volume, k is Boltzmann's constant, T the absolute temperature and λ is the extension ratio. Mooney⁽⁶⁸⁾ and Rivlin⁽⁷⁵⁾ have developed expressions which result in a two-constant description which more nearly approximates real behavior. For simple tension, this is:

$$\sigma = (2C_1 + 2C_2/\lambda)(\lambda - 1/\lambda^2) \quad (17)$$

where $C_1 + C_2$ are empirical constants. The first constant, C_1 , has been related to $\nu_e kT$ of the statistical theory expression, and C_2 to various deviations from the model behavior such as chain entanglement and molecular interactions. A plot of $\sigma/(\lambda - 1/\lambda^2)$ against $1/\lambda$ usually results in a straight line, at small strains, with $2C_1$ as the intercept and $2C_2$ as the slope. This treatment is commonly referred to as a Mooney-Rivlin plot. Obviously, if the slope of the line is zero, the material may be represented by the expression for "ideal" rubbery behavior. Gumbrell, Mullins and Rivlin⁽³⁷⁾ have examined the tensile properties of various rubbers in the swollen condition. They showed that a zero slope could be obtained in a Mooney-Rivlin plot, after only moderate swelling, independent of the swelling solvent.

The application of such techniques to solid propellants has been attempted. But reproducible results depend on the attainment of complete binder filler release and an adequate measure of the binder sol fraction. Preliminary swelling studies to determine a solvent system and conditions which do not degrade the propellant are required. Common extraction techniques are employed to determine the sol fraction. This determination is then applied as a correction in the

computation of cross-link density. The force-deformation relationship for swollen rubbers is

$$F/A = \frac{1}{2} kT (\lambda - 1/\lambda^2) v_2^{-1/3} \quad (18)$$

where F is the force, A is the unstrained unswollen cross-sectional area and v_2 is the volume fraction of rubber in the swollen gel. A correction for v_2 is required for large sol fractions as given by Bills and Salcedo⁽⁸⁾

$$v_2^{-1} = \frac{V_p - V_{st} - V_e}{V_p - V_e/V_r} \quad (19)$$

where V_p is the volume of sample; V_{st} , the volume of solvent in the swollen sample; V_e , the volume of extractable polymer (sol); and V_r , the volume fraction of rubber in the sample.

The average cross-sectional area of rubber in filled samples has been the subject of much discussion. In a filled system which swells to a foam-like material, the average cross-section of effective rubber is given by the initial sample area multiplied by the volume fraction of rubber in the sample and by the area fraction of gel. The volume fraction and area fraction are identical in multi-phase solids.⁽¹⁷⁾

Swollen-tension methods using various sample-gripping techniques have been attempted, but none have been completely satisfactory. Compression methods, on the other hand, avoid the gripping problems, although the attainment of parallel swollen-sample faces is a difficult experimental problem which leads to errors in the determination of strain. Cluff, Gladding and Pariser⁽¹⁸⁾ have described compression techniques for swollen vulcanizates and these methods have been applied in the characterization of propellant cross-link density.⁽⁴⁷⁾

The following expression was employed

$$V_e = h_o S / 3A_o RT \quad (20)$$

where h_o is the height and A_o the cross-sectional area of the undeformed, unswollen sample, and S is the slope of the force deflection curve. Seeley and Dyckes⁽⁸⁵⁾ have performed compression tests on swollen cellular elastomers based on similar techniques.

FAILURE CRITERIA

Structural analysis of the solid rocket case-grain system using experimentally determined propellant response properties may permit a complete description of the combined stresses and resultant deformations, but a statement expressing the ability of the propellant to withstand these stresses is also required. Such a statement, which relates the physical state at which failure occurs to some material parameters, is called a failure criterion. The criterion for failure permits a prediction of the margins of safety to be expected under motor operation and handling conditions, and defines the loading regimes where abnormal operation will occur with intolerable frequency.

The condition termed "failure" may be defined in several ways. An operational definition might involve any deviation from the required motor ballistic performance such as motor pressure, total burn time, burning rate, etc. Several of these abnormalities may be related directly to grain structural integrity. Obviously, a crack or unbond of sufficient size, which is exposed to the hot combustion gases, may result in a catastrophic pressure increase or premature burn-through to the case wall. However, it is quite possible for small changes in burn rate or minor pressure fluctuations to cause mission failure. Since most solid rocket uses

rely upon a pre-programmed thrust-time operation governed by the total burning surface, mid-course thrust corrections may be impossible. Other definitions of failure might include: the first visual crack which forms, sample rupture into two or more pieces, the maximum stress point on a stress-strain curve, a maximum acceptable volume increase, or perhaps a large modulus change resulting in grain slump or bond release.

An important consideration in all failure studies is the influence of material variability. Statistical distributions of failure incidence must be known and properly accounted for if reliability limits are to be set.

Wiegand and co-workers^(109,13) have discussed propellant sample and batch variability, and its effect on failure behavior, in numerous reports. These studies point out the statistical nature of failure and the fact that knowledge of the distributions is required in order to set conservative design values for motor stress and strain capability. Statistical distributions permit the prediction of the probability of failure, but mission considerations dictate the allowable failure frequencies.

Landel and Fedors⁽⁵²⁾ have recently explored the usefulness of extreme value statistics applied to the statistical distribution of rupture in various unfilled polymer specimens. Both breaking stress and breaking strain of natural rubber⁽⁴⁶⁾ and styrene butadiene elastomers⁽⁵²⁾ may be described by the double exponential distribution

$$\Phi = 1 - \exp \left[- \exp A (X - X^*) \right] \quad (21)$$

where Φ is the cumulative distribution of failures, A is the breadth of the distribution and X and X^* are the value of, and the most probable value of stress

(or strain), respectively. It should be clear, therefore, that although the following discussions may be concerned with rupture stress or rupture strain, the inherent variability in rupture processes as well as that of materials in general, requires that all discrete values be viewed as mean values of a distributed population.

The various approaches to the establishment of failure criteria for solid propellants may be divided roughly into two categories. First, simple relationships may be developed which relate actual motor failures to laboratory tests. This produces a pragmatic criterion which may be quite useful when the application is limited to the specific material, motor design, failure mode, and loading conditions which prevailed during the initial correlation testing. Secondly, an analytical criterion may be generated which may be represented in the geometrical form of a "failure surface". The surface represents a boundary, in some specifically defined space coordinate system, between safe mechanical states and unsafe states.

The first category has been traditional in the solid rocket industry and variations on this approach have been many and diverse. The second category is appealing in the sense of its generality and possible mathematical rigor, but has been hampered in its development by the experimental difficulties involved. Until very recently, however, most failure relationships have been based on a single loading history or "first stretch" conditions.

One of the simplest criteria specific to the internal port cracking failure mode is based on the uniaxial strain capability in simple tension. Since the material properties are known to be strain rate and temperature dependent, tests are conducted under a variety of conditions and a so-called failure envelope is generated. Strain at rupture is plotted against a variable such as reduced time and any strain requirement which falls outside of the envelope will lead to

rupture, and any condition inside will be considered safe. Ad hoc criteria have been proposed such as that of Landel⁽⁵³⁾ in which the failure strain ϵ_L is defined as the ratio of the maximum true stress to the initial modulus where the true stress is defined as the product of the extension ratio and the engineering stress, i.e.,

$$\bar{\sigma}_m/E = \lambda_m \sigma_m/E = \epsilon_L.$$

This relationship has been shown to break down at strain rates and temperatures below that at which the strain reaches a maximum. Milloway and Wiegand⁽⁶⁶⁾ suggested the criterion that motor strain should be less than half of the uniaxial tensile strain at failure at 0.74 min^{-1} . This criteria was based on forty-one small motor tests.

The uniaxial failure envelope developed by Smith⁽⁹¹⁾ has proved to be one of the most useful devices for the simple failure characterization of many viscoelastic materials. This envelope normally consists of a log-log plot of temperature-reduced failure stress versus the strain at break. Figure 22 is a schematic representation of the Smith failure envelope. Such curves may be generated by plotting the rupture stress and strain values from tests conducted over a range of temperatures and strain rates. The rupture locus moves counter-clockwise around the envelope as the temperature is lowered or the strain rate is increased. Constant strain, constant strain rate, and constant load tests on amorphous unfilled polymers⁽⁹²⁾ have shown the general path independence of the failure envelope. Studies by Smith⁽⁹³⁾ and Fishman⁽²⁸⁾ have shown a path dependence of the rupture envelope, however, for solid propellants.

Some investigators have shown a preference for plotting strain at maximum stress rather than rupture strain on solid propellant failure envelopes. This is based upon two considerations; first, the onset of cracking or localized

Branching has been observed near the maximum stress point, and second, this value represents a more conservative design limit. Strain at maximum stress data generally shows less scatter in the vicinity of the maximum strain portion of the failure envelope. Limited evidence is also available which indicates the path dependence of the envelope generated in this manner may be somewhat less than that of a rupture boundary.

It should be noted that uniaxial tensile criteria can lead to gross inaccuracies when applied to situations where combined stresses lead to failure in multiaxial stress fields. Often the assumption is made that combined stresses have no influence and that the maximum principal stress governs the failure behavior. A somewhat improved approach applied to biaxial tension conditions relies upon a pragmatic "biaxial correction factor" which is applied to uniaxial data, modifying the strain values to account for the influence of combined stresses. Such factors are based upon extensive testing and comparisons for a single material using uniaxial, strip biaxial or, perhaps, analogue motor tests.

Majerus^(59,60) has approached the failure behavior of highly filled polymers by a thermodynamic treatment in which the ability to resist rupture is related to the propellant's ability to absorb and dissipate energy at a certain rate. An energy criterion which requires failure to be a function of both stress and strain was originally stated by Griffith⁽³⁵⁾ for brittle materials and later adapted to polymers by Rivlin and Thomas⁽⁷⁶⁾. Williams⁽¹¹¹⁾ has applied an energy criterion to viscoelastic materials such as solid propellants where appropriate terms are included for viscous-energy dissipation.

A combination of an energy criterion and the failure envelope has been proposed by Darwell, Parker and Leeming⁽²¹⁾ for various double-base propellants.

Total work to failure was taken from the area beneath the stress-strain curve, but the biaxial failure envelope was seen to deviate from uniaxial behavior depending on the particular propellant formulation. Jones and Knauss⁽⁴⁵⁾ have similarly shown the dependence of failure properties on the stress state of composite rubber-based propellants.

In order to visualize the stress states at which failure occurs, a failure surface may be constructed. The six stress components may be resolved into three orthogonal principal stresses; any stress state which exists in the space containing origin will not cause failure, and conversely, any state outside of this space will lead to failure. A mathematical description of the surface would greatly simplify matters, since the most convenient stress field could be chosen for laboratory testing, and the entire surface could be described from a single failure locus. Such surfaces have been discussed at length by Blatz⁽¹²⁾ and Williams et al⁽¹¹⁰⁾, and the failure surfaces associated with various failure criteria by several authors (38,108,63,104). Nadai⁽⁶⁹⁾ has reviewed eight failure theories which have been proposed for materials (mainly metals) and Marin⁽⁶¹⁾ discusses six of these in a more simplified manner. Simply listed, these are: (1) maximum principal stress or Rankine theory, (2) maximum shear or Coulomb-Tresca criterion, (3) maximum strain or St. Venant's theory, (4) maximum strain energy theory, (5) distortion energy or Von Mises-Hencky theory, and (6) the internal friction theory which is a special case of Mohr's theory.

Mehrdahl⁽⁶³⁾ depicts several failure surfaces by photographs of various three-dimensional models. Figure 25 is an illustration of three such surfaces taken from reference⁽¹⁰⁶⁾ which shows geometries which are symmetrical

about the space diagonal, $\sigma_1 = \sigma_2 = \sigma_3$, and containing the assumption that the triaxial compression octant should be open ("because hydrostatic compression cannot lead to failure in the ordinary sense").

Although the concept of a failure surface in principal stress space seems to provide a descriptive definition of the ultimate capability of materials in any stress state, it should be recognized that in reality there may not be one unique surface for each material. Failure in solid propellants is not only influenced by the stress state, but also by the deformation history. Since a given stress state can be reached by any number of stress-strain paths, a given failure surface may exist for each specific loading history. Sharma⁽⁸⁶⁾ and Jones and Knauss⁽⁴⁵⁾ have produced traces of failure surfaces by maintaining the principal strain rates at equivalent values for the various tests conducted. Little has been said or done about the general problem of multiaxial strain rates and associated multiaxial stresses. A theory has been proposed by Zak⁽¹³⁶⁾ for polymeric materials in which both rate and multiaxial effects are included, but no experimental verification has been attempted. Figure 26 is a representation of parabolic failure surfaces in principal stress space, coaxial with the space diagonal. The two surfaces are shown to illustrate the possibility of several surfaces which might result from changes in the material or the test conditions. Such surfaces need not be concentric as shown; in fact, it would seem possible that significant deterioration could change the basic failure mode of the material, and therefore, the size and shape of the failure surface.

Other coordinate systems may be used for failure surface representations in addition to stress space. Blatz and Ko⁽¹¹⁾ indicate that either stress (σ_1) space, stretch (λ_1) space, or invariant (I_1) space may be appropriate. Stress space is most commonly employed because the failure surface concept was originally applied to metals, for which stress and strain are more simply related. Viscoelastic materials on the other hand may show a multitude of strain values at a given stress level depending on test conditions.

It might be possible for some materials to produce a unique failure surface providing measurements could be conducted under "first stretch" conditions in a state of equilibrium. Tschoegl⁽¹⁰⁶⁾, at the time of this writing, is attempting to produce experimental surfaces by subjecting swollen rubbers to various multi-axial stress states. The swollen condition permits failure measurements at much reduced stress levels and the time dependence of the material is essentially eliminated. Studies of this type will be extremely useful in establishing the foundations for extended efforts into failure of composite materials.

The general inapplicability of the various classic failure theories to solid propellants has been noted by numerous investigators. Jones and Knauss⁽⁴⁵⁾ have shown approximate agreement with the maximum tensile stress theory in the triaxial tension stress octant, while data in other regions indicated an internal friction type of criteria. Figure 23 shows the surface constructed by these authors for a composite rubber-based propellant. Experimental mapping of failure surfaces for solid propellants has been attempted to a limited extent, but difficulties have been encountered, especially in the seven compressive octants. When various analytical criteria are compared to laboratory data it becomes extremely difficult to distinguish the most appropriate criterion in the (+ + +) octant. Scatter in the failure data may be great enough to include several criteria at once since the differences in this octant are not large. In the other octants, however there can be substantial divergences of the analytical failure boundaries and the distinction should be much easier. A few investigators have conducted uni-axial and biaxial tests under superposed hydrostatic pressure. Vernon⁽¹⁰⁷⁾, Kruse⁽⁵⁰⁾, and Surland and co-workers⁽⁹⁹⁾ have discovered that certain

composite propellants exhibit higher strain capability and tensile strength when tested under confining gas pressure. Hazelton and Planck⁽⁴⁰⁾ conducted uniaxial and biaxial tension tests, and simple shear tests on propellants and propellant liner bonds with gas pressures up to 800 psig. They also found increased tensile properties under pressure and interpreted the behavior as due to delayed dilation and to rate effects.

Sharma⁽⁸⁶⁾ has examined the fracture behavior of aluminum-filled elastomers using the biaxial hollow-cylinder test mentioned earlier. Biaxial tension and tension-compression tests showed considerable stress-induced anisotropy, and comparison of fracture data with various failure theories showed no generally applicable criterion at the strain rates and stress ratios studied. Sharma and Lim⁽⁸⁷⁾ conducted fracture studies of an unfilled binder material for five uniaxial and biaxial stress fields at four values of stress rate. Fracture behavior was characterized by a failure envelope obtained by plotting the octahedral shear stress against octahedral shear strain at fracture. This material exhibited neo-hookean behavior in uniaxial tension, but it is highly unlikely that such behavior would carry over into filled systems.

In a recent attempt to bring an engineering approach to multiaxial failure in solid propellants Siron and Duerr⁽⁸⁸⁾ tested two composite double-base formulations under nine distinct states of stress. The tests employed included triaxial poker chip, biaxial strip, uniaxial extension, shear, diametral compression, uniaxial compression, and pressurized uniaxial extension at several temperatures and strain rates. The data was reduced in terms of an empirically defined constraint parameter which ranged from -1.0 (hydrostatic compression) to +1.0 (hydrostatic tension). The parameter (Φ) is defined in terms of

principal stresses and indicates the tensile or compressive nature of the stress field at any point in a structure, i.e.,

$$R = \frac{\sigma_I + \sigma_{II} + \sigma_{III}}{3|\sigma_I|} \quad (22)$$

where σ_I , σ_{II} and σ_{III} are the numerically maximum, intermediate, and minimum principal stresses respectively. Tensile failure stress and tensile failure strain were plotted against the constraint parameter and reasonable correlation was shown for one temperature and strain rate. A preliminary comparison of the failure data with the maximum principal tensile stress, maximum principal tensile strain, maximum shear stress, and maximum distortional-strain energy-failure criteria showed no correlations for these propellants.

CUMULATIVE DAMAGE

The conditions leading to damage accumulation are particularly relevant to the problems of solid rocket structural integrity. It is quite possible for a grain to "wear out" after repeated thermal cycling or vibration through the gradual development and propagation of microscopic tearing or molecular breakdown. If this process could be described analytically and formulated for complex motor geometries, a useful life prediction could be made based on the motor history.

Metal fatigue has been studied extensively for many years, and, more recently, considerable attention has been given to fatigue in plastics and rubbers (6,33,51,23). Williams (112) has suggested that solid propellants might be examined on the basis of Miner's Law (67) which was developed for metal fatigue. This may be represented by the expression

$$\sum_{i=1}^n \left(\frac{R_i}{N_{fi}} \right)^n = 1.0 \quad (23)$$

where M is the number of load levels, N_i is the number of cycles at the i th load level and N_{fi} is the number of cycles to failure at the i th load level. The exponent n can be determined by experiment, but is usually taken to be 1.0, which indicates linear accumulation.

Miner's law has been used to predict failure for sequential loading of solid propellant at different strain rates. The linear form used here is:

$$\sum_{i=1}^M \left(\frac{t_i}{t_{fi}} \right) = 1.0 \quad (24)$$

where t_i is the time at the i th strain rate and t_{fi} is the time to failure at the i th strain rate. Various investigators have examined this relationship for application to solid propellants with only limited success. This is to be expected since the order of loading is not taken into account in Miner's law.

Hillz (7) has applied an adaptation of this law to solid propellants and propellant-liner bonds for discrete, constantly imposed stress levels; considering t_i to be the time at the i th stress level and t_{fi} the mean time to failure at the i th stress level. A probability distribution function P was included to account for the statistical distribution of failures. For cyclic stress tests the time is the number of cycles divided by the frequency, and the i th loading is the amplitude. The empirical relationship

$$\left(\frac{\sigma}{\sigma_0} \right)^B = \frac{t_0}{t_f} f(t) \quad (25)$$

was employed to derive the integral expression

$$P \sum D_i = \frac{1}{\sigma_0^B t_0} \int_0^t \frac{\sigma(t)^B dt}{f[g(t)]} \quad (26)$$

where D_i = incremental damage

t_f = mean time to failure

t_o = unit time to failure

σ_o = stress required to cause failure at t_o

B = an empirical constant

$f[g(t)]$ = viscoelastic time-temperature shift relation with

temperature expressed as a function of time. The various constants were obtained from constant load tests at several temperatures, and specific temperature-stress-time cycles. Integration yields the mean damage per cycle or the number of cycles to failure, N. Figure 27 illustrates the correlation obtained for cyclic tests on propellant-liner bond specimens at temperatures of 40, 77, and 110°F, and sequential stress levels from 40 to 80 psi. The degree of correlation is not completely satisfactory, but at least an estimate can be made of the minimum number of cycles which will cause failure.

An approach suggested by Williams et al.⁽¹¹³⁾ uses an energy balance equation for the initiation of flaw growth in a linearly viscoelastic material. A spherical flaw geometry was selected for simplicity since it was shown that the expressions for the critical values of applied stress to cause fracture were similar for several flaw geometries. The critical conditions are based on a power (energy rate) balance

$$\dot{I} = \dot{F} + 2\dot{D} + \dot{SE} \quad (27)$$

where \dot{I} is the power input, \dot{F} is the rate of increase of strain energy, $2\dot{D}$ is the energy dissipated as heat and \dot{SE} is the rate of increase of surface energy.

dots over the symbols indicate differentiation with respect to time.

The thermodynamic conditions for spherical flaw growth were derived in Ref.(113) for a body with a sinusoidally displaced boundary. The final expression for the oscillatory displacement $u = u_0 \sin \omega t$ is given as:

$$\begin{aligned} & \frac{2}{3\pi} \left(\frac{a}{b}\right)^6 \left(\frac{b}{u}\right)^2 - \frac{E_e}{4} (1 - \cos 2\omega t) + \sum E_1 \left\{ \frac{\omega \tau_1}{1 + \omega^2 \tau_1^2} \right. \\ & + \left[\frac{\omega t}{2} + \frac{\sin 2\omega t}{4} + \frac{\omega^2 \tau_1^2}{1 + \omega^2 \tau_1^2} \left[\exp^{-t/\tau_1} \cos \omega t - 1 \right] \right. \\ & - \left. \frac{\omega^3 \tau_1^3}{(1 + \omega^2 \tau_1^2)^2} \left[\exp^{-t/\tau_1} \sin \omega t \right] \right. \\ & \left. \left. + \frac{\omega^2 \tau_1^2}{4(1 + \omega^2 \tau_1^2)} \left[1 - \cos 2\omega t \right] \right\} \end{aligned} \quad (28)$$

where

a = initial flaw radius

b = outer radius of the spherical body

T = surface energy per unit surface area

and a series expression was introduced for the relaxation modulus of an arbitrary material as given by Schapery⁽⁸⁰⁾. Figure 28 is a plot of flaw growth as a function of time according to Eq 28. Limited experimental results on a well characterized polyurethane elastomer showed a qualitative similarity to the predicted growth-rest cycle of crack propagation. This approach remains to be applied to filled materials such as solid propellants.

AGING

Solid propellants are composed of a large percentage of energetic ingredients so it should be expected that prolonged storage might result in deterioration. Various ingredients may interact with each other or with the atmosphere to produce irreversible changes which can seriously affect both the ballistic and mechanical properties. Some ingredients may simply decompose while others may react to produce chemical products which, by themselves, may be degrading to other materials in the system. Auto-catalytic reactions are common and frequently an ingredient which is a ballistic modifier may produce intolerable changes in the propellant during storage. Plasticizers may migrate and evaporate, gases may be generated, cross-linking and chain cleavage may occur simultaneously. Decomposition of primary ingredients to form products which increase the sensitivity of the propellant is a common problem in double-base systems. These reactions and many more have been examined in numerous studies. Solid propellants are complex mixtures of many possible ingredients so any examination of aging phenomena should consider detailed formulations, expected operational environments, and failure modes. Since detailed formulations are generally revealed only in the classified literature, the following discussions will be restricted to generalizations about typical aging mechanisms and useful test methods for following the aging behavior of solid propellants. Table III (22) lists various interactions and resultant deterioration which must be considered.

This section will deal with the chemical aging problem and related physical phenomena such as diffusion and embrittlement. Apart from the chemical problem there is mechanical deterioration which is also related to long-term environmental effects, but this was covered briefly in the preceding cumulative damage discussion.

TABLE III

FACTORS INFLUENCING PROPELLANT DEGRADATION DURING AGING (Ref 22)

FACTOR	MANIFESTATION	FAILURE MODE
I. <u>Change of Chemical State</u>		
A. Chemical reactivity of propellant components singularly or in combination	Hardening, embrittlement, gassing, accumulation of degradation products, viscous flow enhancement, change of adhesivity.	Increased tendency to crack during storage, ignition or temperature cycling; possible burning rate change, impulse loss, ignition problems, and liner separation.
B. Chemical interaction with environment		
1. Atmosphere		Same as "A"
a. Moisture		
b. Gaseous or solid decomposition products (autocatalysis)		
c. Air (oxygen, ozone, contaminants in air)	Same as "A"; in addition, non-homogeneity of propellant at surfaces and within bulk.	
2. Other materials in motor (liner, metals, etc).		Same as "A"
C. Factors which may influence rate of change		---
1. Temperature		
2. Stress state		
D. Irradiation		
1. Background		
2. Induced	Polymer cross linking or degradation	Same as "A"
E. Bacteriological action	Surface changes	Unknown

TABLE III (CONT'D)

FACTORS INFLUENCING PROPELLANT DEGRADATION DURING AGING

FACTOR	MANIFESTATION	FAILURE MODE
<u>II. Change in Physical State</u>		
A. Reversible physical changes		
1. Phase changes dependent on time and temperature	Hysteresis of temperature dependent physical properties	Increased tendency to crack during storage, ignition or temperature cycling.
2. Recoverable strains	Probably minor	Probably minor
3. Diffusion of materials	Non-homogeneity of propellant properties, oxidizer-poor surfaces, porosity, shrinkage.	Crack development, increased tendency to crack during storage, ignition or temperature cycling.
a. Gases		
b. Plasticizer		
c. Moisture		
B. Irreversible physical changes		
1. Strain beyond reversible limit due to:	Cracks at fillets, liner separation, viscous deformation, de-wetting (blanching)	Increased burning areas and rates.
a. Gravity		
b. Acceleration (during transport)		
c. Thermal gradients		
d. Environmental temperature		

A prediction of useful life for solid propellant rockets is quite important, not only from the standpoint of operational readiness, but also from economic considerations. The premature removal and replacement of deployed systems, based on inaccurate storage life estimates, can be extremely costly. A primary difficulty here is the impossibility of gathering aging data over periods of several years before the systems are committed to production and operation. It is quite possible that obsolescence could overtake a specific missile system and propellant combination while long-term storage data are being compiled. Accelerated aging tests are normally employed to give qualitative indications of storability, but the deficiencies of these tests are rather obvious and will be discussed later.

Chemical aging may be the result of thermal, oxidative or hydrolytic reactions. The changes observed may be: softening, hardening, swelling, discoloration, and gas evolution. These changes may not constitute failure, as such, but should be examined in relation to possible failure modes. Hardening, which is usually accompanied by a decreased strain capability, may result from several conditions. Oxidation may produce discolored and hardened surfaces; continued cure reactions produce overall modulus increases; and loss of volatile plasticizers also leads to higher modulus. Long-term storage at low temperatures may cause embrittlement, whether by binder crystallization or by other mechanisms. Softening is usually the result of binder chain scission or cross-link degradation, and may be produced by hydrolytic reactions or thermal decomposition. Moisture effects are particularly pronounced since they not only relate to hydrolysis, but may interrupt the binder-filler interface. In some cases the solubility of ingredients in the binder may change with moisture content; and phase changes, solution, and precipitation may occur.

Within this morass of complex chemical and physical phenomena, there is little that has not been examined in some detail, but there is also much less which is sufficiently understood to permit predictive estimates of useful propellant life.

The aging characteristics of double-base and composite-rubber-binder propellants are substantially different. The primary changes which occur in double-base propellants relate to stability and are variously concerned with "safe storage life", "safe use life" and "useful life."⁽⁹⁸⁾ The first two categories attempt to define the time beyond which storage or use would constitute a hazard, while the useful life represents the period in which the rocket can be expected to perform reliably. Safe-life tests usually consider such factors as the time to auto-ignition at a given temperature, or the time to the production of fumes of oxides of nitrogen. In some cases the rates of stabilizer depletion at high temperatures are measured and extrapolated to lower temperatures. The time to zero stabilizer concentration is then determined for normal storage temperatures. Depletion rates may be plotted for various temperatures in the form of an Arrhenius plot and the energy of activation determined for a particular stabilizing agent.

So much concentrated effort has been expended on the stabilization of double-base formulations that stability is no longer a limiting factor in the determination of useful life. Some studies^(98) have shown the safe storage life to be in excess of 30 years under ordinary conditions.

Useful-life determinations are similar for both general propellant types since they are primarily concerned with structural integrity. The decomposition or formation of relatively few chemical bonds will normally be undetectable from the viewpoint of ballistic characteristics. On the other hand, the formation of

new cross-links or the cleavage of polymer chains can strongly affect the mechanical properties of polymeric materials. Changes in strength or modulus may cause propellant capability to fall below the structural requirements of particular motor designs. It should be noted, however, that some changes may not be deleterious, but can be, in fact, beneficial.

Many of the tests described in earlier sections have been applied in surveillance studies of solid propellants. Both response and failure characteristics may be followed as a function of time during storage at various conditions. Physico-chemical analysis of specimens before and after exposure to determine sol content and cross-link density changes is particularly useful in correlating gross physical property variations. In conjunction with these tests, various non-destructive techniques may provide additional information. The summary in Table IV was taken from a compilation by DeFries and Johns (22) which shows the large number of techniques and devices applied to solid propellant surveillance. Even this extensive list is not complete and many variations and alternate methods have been proposed through the years. It is especially important to note that non-destructive tests only indicate that a change has taken place in the propellant. They do not provide the decision regarding the acceptability of the material for its intended application. Such decisions require a knowledge of material characteristics and a practical failure criterion. It has been suggested (29) that propellant aging which results in mechanical property changes may be examined in reference to a changing failure surface. The aging material may have an associated failure surface which collapses around the origin similar to a deflating balloon. With the passage of time it is then required that the structural requirements be reviewed with respect to the new failure surface, and the tolerable limits established.

TABLE IV

NON-DESTRUCTIVE TESTING FOR SOLID PROPELLANTS (Ref 22)

<u>CONDITION</u>	<u>DETECTION TECHNIQUE</u>	<u>FOR DETECTION OF</u>	<u>OTHER CONSIDERATIONS</u>
I. <u>Chemical State</u>	<u>Radiation Reflection or Diffraction</u>	Chemical structural groups; quantitative compositional changes	
	Infrared attenuated total reflectance (ATR)	"	Poorer than ATR
	Infrared reflectance	"	
	Ultraviolet spectroscopy	"	
	X-ray diffraction	Appearance of crystalline degradation products	Frequency of crystalline products occurrence unknown
	<u>Resonant Response</u>		
	Nuclear magnetic resonance	Chemical structure and compositional changes	
	Electron paramagnetic resonance	Free radical concentration	Secondary effect; occurrence or correlation not established
	<u>Evolved Gas Analysis</u>		
	Mass spectrometer	Quantitative gases up to mol. wt. of C ₆ hydrocarbons	
	Gas chromatography	"	
	IR transmission		
	Film sensors		
	External Sample Analysis	All components	Does not measure grain

TABLE IV

NON-DESTRUCTIVE TESTING FOR SOLID PROPELLANTS (CONT'D)

II. Physical State

A. Propellant Surface Condition

Visual (Photographic)
Observation

Surface cracks; migration products; roughness; accumulation of degradation products; oxidizer concentration due to moisture; localized dewetting

Subjective observations; traveling mechanisms required

Boroscope

Miniaturized T.V.

Microscope

Radiation Reflectance
or Diffraction

All surface and sub-surface changes that effect reflected radiation density

Photocell (visible)

X-ray diffraction

U.V. reflectance spectroscope

Gamma ray back-scatter

Scintillation read out

Infrared reflectance

Radiation Emission

All physical changes of surface or sub-surface that effect local rate of heat transfer

Infrared Scan

TABIZ IV

NON-DESTRUCTIVE TESTING FOR SOLID PROPELLANTS (CONT'D)

B. <u>Dimensional Stability</u>	<u>Profilometer</u>	Slump, liner separation, sub-surface voids, surface cracks	Residual stresses, porosity
C. <u>Propellant Homogeneity and Density</u>	<u>Radiation Transmission</u>	Porosity (de-wetting) voids, cracks	
	<u>X-ray</u>		
	<u>Gamma ray</u>		
	<u>Scintillation read out</u>		
	<u>Low Frequency Sonic Transmission or Scatter</u>	Porosity (de-wetting) voids, cracks	
D. <u>Propellant Physical Properties</u>	<u>Hardness and Hardness Relaxation</u>	Propellant modulus and relaxation rate changes caused by chemical changes or compositional changes due to migration or absorption	Good potential to provide monitoring of propellant condition at selected points on surface; semi-destructive
	<u>Sonic Transmission Reflection or Scatter</u>	Propellant modulus	Establishment of correlation required
	<u>Propellant Samples in Perforation or External to Motor</u>	All physical properties	Correlation not established
	<u>X-ray Diffraction Micromaya</u>	Crystallinity changes	Occurrence and correlation of crystallinity not established

TABLE IV

NON-DESTRUCTIVE TESTING FOR SOLID PROPELLANTS (CONT'D)

E. <u>Adhesive Interface Integrity</u>	<u>Ultra Sonic Reflection or Transmission</u>	Modulus	At low temperatures except for metal cases
<u>Low Frequency Sonic Reflection or Transmission</u>	Liner separations	Developed system	
<u>Infrared Emission</u>	Liner separations		
<u>Radiation Transmission</u>			Very high energies required for large grains

X-ray

Gamma ray

Microwave transmission or reflection

Laboratory measurements on stored samples are common, but there are many precautions to be observed. It is important to establish confidence that samples are representative of the propellant grain, enclosed in its case-liner-insulation envelope. Since diffusion paths and exposed surface area may be germane to the aging process, these characteristics require duplication in aging samples. There is considerable evidence also that samples stored in sealed containers deteriorate much more rapidly and by different mechanisms than those exposed to the atmosphere.

The aging stability of solid propellants may be evaluated in a gross sense by measuring the change in some prominent property such as modulus or tensile strength at various temperatures. The temperature sensitivity of these changes may then be charted on an Arrhenius plot and extrapolations made to normal storage temperatures. Such accelerated aging tests are useful in establishing degradation patterns and in guiding formulation chemists in the production of propellants with superior aging characteristics. The temptation should be avoided, however, to use these tests in a quantitative, predictive fashion for determining the useful life of propellant systems. In complex materials such as these it is quite possible that some thermally activated mechanisms may prevail at high temperatures, which are relatively unimportant at lower temperatures. Used with caution, accelerated aging tests should be, therefore, an integral part of all propellant development efforts. Figure 29 is an example of the extrapolations which can be made from high-temperature data. The critical storage time is defined in this case as the time to produce an associated change, by a factor of 2, in the initial maximum stress or in the initial strain at maximum stress.

Other conditions may be imposed upon stored propellant to increase the severity of the environment. In some cases the effects of ambient moisture may

is exaggerated by exposure to high relative humidities; and, low temperature embrittlement may be accelerated by the appropriate conditioning temperature. These techniques are particularly difficult to interpret due to the variety of possible interactions and synergistic effects. High humidity has been shown to change the low-temperature properties of propellants in various ways. Polyurethane propellants have undergone severe modulus increases and rupture strain decreases when tested at -40°F after several days exposure to 90% relative humidity at 77°F . This has been interpreted (72) as due to the ion-dipole effects of dissolved ammonium perchlorate, and related to the solubility of water in the binder phase. Other explanations hypothesize "rehealing" (19) of broken binder-oxidizer bonds, or oxidizer dissolution and precipitation of small, high-surface-area crystals (54). Some specialized techniques have been applied to determine the nature of specific degradation reactions, and these have produced very useful insight into the aging process. Chemorheological methods described by Golodny et al (20) have been notable in establishing the relative amount of chain cleavage and cross-linking during exposure to various environments. In some cases the site of degradation may be determined, such as random chain or cross-link scission. These methods are based upon the procedures described by Tobolsky (102) in which both intermittent and continuous stress relaxation measurements are employed. Tests conducted with unfilled binder materials are quite revealing, but when highly filled samples are examined the relaxation process is confused by dewetting and granular interactions.

Many chemical and physical analysis techniques have been applied to the study of solid propellant aging. Valuable contributions have been made in improving formulations and in establishing confidence in the stability of

propellants for a wide variety of applications. Fortunately, many formulations have been developed with exceptional aging stability and predictions of useful life have been exceeded in actual operations. As new, high-energy propellants are developed and enter the inventory, it can be expected that degradation will be a more severe problem and that improved predictive techniques will be required. Progress in the areas of structural integrity analysis, material characterization and failure criteria for solid propellants is continuing and holds the promise that such techniques will be available.

SUMMARY

The preceding discussions have surveyed current approaches and techniques for solid propellant mechanical properties characterization. However, a number of related areas have not been mentioned. The various methods for determining propellant-linear bond strength, and evaluation of bond deterioration with environmental exposure have not been covered, although bond integrity is a critical requirement of solid rocket motors. Another omission is analogue motor testing, a very important area because it partially fills the large gap between laboratory and full-scale motor tests. The determinations of bulk compressibility, thermal conductivity and glass transition temperature are also not described. Certainly the topics included in this paper are extensive in scope and the approaches vary according to a variety of disciplines and viewpoints. Comprehensive treatments of most testing methods and data reduction techniques may be found in reference 43, the ICRPG Mechanical Behavior Manual. Review articles in the "Solid Rocket Structural Integrity Abstracts", currently published by the University of Utah, provide up-to-date surveys of many related topics. These documents are limited in distribution, however, and are generally not available to the public.

ACKNOWLEDGEMENT

The author wishes to express his appreciation to Professor N. W. Tschoegl and Mr. Donald Saylak for many helpful suggestions and discussions during the manuscript preparation.

REFERENCES

1. Aerojet-General Corporation Report No. 0411-10F "Study of Mechanical Properties of Solid Propellant" (1962)
2. Baltrukonis, J. H., Gottenberg, W. G., and Schreiner, R. N., Proc. 4th U. S. National Congress of Applied Mechanics p 867 (1962).
3. Beyer, R. B., Bull. 5th Meeting ICRPG Working Group on Mechanical Behavior, CPIA Pub No. 119 Vol I, p 83 (1966)
4. Beyer, R. B., AIAA Paper No. 65-169 AIAA 6th Solid Propellant Rocket Conference (1965)
5. Bennett, S. J. and Anderson, G. P., Bull. 4th Meeting ICRPG Working Group on Mechanical Behavior CPIA Pub No. 94u, p 121 (1965)
6. Beatty, J. R., Rubber Chemistry and Technology 37, 1341 (1964)
7. Bills, K. W., Steele, R. D., and Svob, G. J., Bull. 5th Meeting ICRPG Working Group on Mechanical Behavior, CPIA Pub. No. 119, Vol I p 547 (1966)
8. Bills, K. W., and F. S. Salcedo, J. Appl. Phys., 32, 2364 (1961)
9. Blatz, P. J., Bull. 18th Meeting JANAF Panel on Physical Properties of Solid Propellants, SPIA Pub. No. PP12, p 17 (1959).
10. Blatz, P. J. Bull., 19th Meeting JANAF Panel on Physical Properties of Solid Propellants, SPIA Pub. No. PP13 p 165 (1960)
11. Blatz, P. J., and Ko, W. L., Trans. Soc. Rheol., 6, 223 (1962)

12. Blatz, P. J., Rubber Chem and Technol. 36 1488 (1963)
13. Briar, H. P. and Wiegand, J. H., Bull. 3rd Meeting ICRPG Working Group on Mechanical Behavior Vol I, CPIA Pub. No. 61u p 455 (1964).
14. Bfitton, S. C., Solid Rocket Structural Integrity Abstracts, Vol 2, No. 4, California Institute of Technology, October 1965.
15. Brisbane, J. J., Bull. 2nd Meeting ICRPG Working Group on Mechanical Behavior, CPIA Pub. No. 27, p 337 (1963).
16. Burton, J. D., Jones W. B., and Frazee, J. D., Bull. 3rd Meeting ICRPG Working Group on Mechanical Behavior. Vol I CPIA Pub. No. 61u p 191 (1964).
17. Chamot, E. M. and G. W. Mason ed., Handbook of Chemical Microscopy, John Wiley and Sons, Inc. New York 1958 pp 483-488.
18. Cluff, E. F., E. K. Gladding, and R. Pariser, J. Polymer Sci., 45, 341 (1960).
19. Colodny, P. C.; Delao, D.; Svob, G. J. and Lou, R. L., Presented at the JANAF Surveillance Panel Meeting, San Francisco, Calif., December 1961.
20. Colodny, P. C., Waddle, L. A., and Wood, J. S., Bull. 3rd Meeting ICRPG Working Group on Mechanical Behavior, Vol III CPIA Pub. No. 61A (1965).
21. Darwell, H. M., Parker, A., and Leeming, H., AIAA Paper No. 65-161, AIAA Solid Propellant Rocket Conference (1965).
22. DeFries, M. and Johns, R. H., Atlantic Research Corporation Report, RTD-TDR-63-1106 August 1963.
23. Dillon, J. H. Advances in Colloid Science, Vol III, p 219, Interscience Publishers, New York (1950).
24. Farris R. J., private communication.

25. Farris, R. J., *Jo. Applied Polymer Sci.* 8, 23 (1964).
26. Farris, R. J. and R. D. Steele, *Bull. 5th Meeting, ICRPG Working Group on Mechanical Behavior*, Vol 1 CPIA Pub. No. 119 p 1 (1966).
27. Ferry, J. D., Viscoelastic Properties of Polymers, John Wiley and Sons, Inc. New York (1961).
28. Fishman, N., Rinde, J. A., *Bull. 3rd Meeting (ICRPG Working Group on Mechanical Behavior, Vol I, CPIA Pub. No. 61u* (1964).
29. Fishman, N., Solid Rocket Structural Integrity Abstracts, Calif Inst. of Technology, Vol III No. 1, January 1966.
30. Fitzgerald, E. R., and Ferry, J. D., *J. Colloid Sci.* 8, 1 (1953).
31. Fitzgerald, J. E., *Bull. Joint Meeting JANAF Panels on Physical Properties and Surveillance of Solid Propellants*, SPIA Pub. No. pp-13/SPSP-8 p 155 (1960).
32. Gent, A. N., and Lindley, P. B., *Proc. Royal Soc.*, 249A, 195 (1959).
33. Gent, A. N., Lindley, P. B. and Thomas, A. G., *Jo. Applied Polymer Sci.* 8, 455 (1964) and *Rubber Chemistry and Technology* 38, 292 (1965).
34. Gottenberg, W. G. and Christensen, R. M., *Space Technology Laboratories Technical Report No. 6121-6777-RU000*.
35. Griffith, A. A., *Trans. Roy. Soc. (London) Series A*, Vol 221, 163 (1921).

36. Gross, B., Mathematical Structure of the Theories of Viscoelasticity Chap. 3, Hermann and Co. Paris (1953).
37. Gumbrell, L. Mullins, and R. S. Rivlin, Trans. Faraday Soc., 49, 1495 (1953).
38. Haigh, B. P., Engineering, 190 158 (1920).
39. Harbert, B. C., Bull 4th Meeting, ICRPG Working Group on Mechanical Behavior, CPIA Pub. No. 94u, p 217 (1965).
40. Hazelton, I. G., and Plank, R. W., Bull. 4th Meeting ICRPG Working Group on Mechanical Behavior, CPIA Pub. No. 94u, p 287 (1965).
41. Hilzinger, J. E., Bull. 5th Meeting ICRPG Working Group on Mechanical Behavior Vol. 1, CPIA Pub. No. 119., p. 169 (1966).
42. Hoebel, J. F., Bull. 20th Meeting JANAFAN Panel on Physical Properties of Solid Propellants, Vol II, SPIA PP/14u p 13 (1961).
43. ICRPG Solid Propellant Mechanical Behavior Manual, CPIA Pub. No. 21 (1963).
44. Jones, J. W. and Cantey, D. E., Bull. 3rd Meeting, ICRPG Working Group on Mechanical Behavior, Vol I, CPIA Pub. No. 61u p 203 (1964).
45. Jones, J. W., and Knauss, W. G., AIAA Paper No. 65-157 AIAA 6th Solid Propellant Rocket Conference (1965).
46. Kase, S., Jo. Polymer Sci., 11 425 (1953).
47. Kelley, F. N., Appl. Polymer Symposia 1 229 (1965).

48. Kostyrko, G. J., Aerojet TN229, Aerojet-General Corp. (August 1963).
49. Kruse, R. B., Bull. 1st Meeting ICRPG Working Group on Mechanical Behavior, CPIA Pub. No. 2, p 337 (1962).
50. Kruse, R. B. and Jones. T. M., AIAA Paper No. 65-156. AIAA 6th Solid Propellant Rocket Conference (1965).
51. Lake, G. J. and Lindley, P.B., Jo. Applied Polymer Sci. 8, 707 (1964) and Rubber Chemistry and Technology 38, 301 (1965).
52. Landel, R. F., Solid Rocket Structural Integrity Abstracts, Vol. 2, No. 1, California Institute of Technology, January 1965. See also, Landel, R. F., and Fedors, R. F., Trans. Soc. Rheol 9, 195 (1965).
53. Landel, R. F., CBS66, Jet Propulsion Laboratory, California Institute of Technology, Pasadena, California (Aug 1958).
54. Landel, R. F., and Mozer, B. G., Tech. Report No. 32-389, Jet Propulsion Laboratory, Pasadena, California (Feb 1963).
55. Layton, L. H., Addendum to Bull. 2nd Meeting ICRPG Working Group on Mechanical Behavior. CPIA Pub. No 27A p 155 (1964).
56. Lindsey, G. H., Shapery, R. A., Williams, M. L., and Zak, A. R., Report ARL 63-152 on Contract AF 33(616)-8399 to USAF Aerospace Research Laboratories (1963).
57. Lindsey, G. H., Bull. 3rd Meeting ICRPG Working Group on Mechanical Behavior, CPIA Pub. No. 61u, p 573 (1964).

58. Long, E. F., Rainbird, R. W., and Vernon, J. H., Bull. 1st Meeting ICRPG Working Group on Mechanical Behavior, CPIA Pub. No. 2, p 317 (1962).
59. Majerus, J. N., Jo. Polymer Sci., 3 No. 10, 3361 (1965).
60. Majerus, J. N., Jo. Spacecraft and Rockets, 2 883 (1965).
61. Marin, J., Mechanical Behavior of Engineering Materials, Chap. 3., pp 104-168. Prentice Hall, Inc., New Jersey (1962).
62. Martin, D. L., Bull. 5th Meeting ICRPG Working Group on Mechanical Behavior, CPIA Pub. No. 119, Vol I, p 191 (1966).
63. Melidahl, A., Brown Boveri Rev., 31 260 (1944).
64. Messner, A. M., Bull. 2nd Meeting ICRPG Working Group on Mechanical Behavior, CPIA Pub. No. 27, p 109 (1963).
65. "Method for Determining the Tensile Properties of Solid Rocket Propellants", SPIA/PP8 Part I Nitrocellulose Base Propellants (1956) Part II Composite Propellants (1957).
66. Milloway, W. T., and Wiegand, J. H., Bull. 20th Meeting JANAF-ARPA-NASA Panel on Physical Properties of Solid Propellants, Vol I, SPIA Pub. No. 147, p 341 (1961).
67. Miner, M. A., Jo. Applied Mechanics 12, A159 (Sep 1945).
68. Mooney, M., Jo. Applied Physics 11, 582 (1940); 19, 434 (1948).

69. Nadai, A., Theory of Flow and Fracture of Solids, Vol. I Chap. 15, pp 175-220. McGraw-Hill Book Co., Inc., New York (1950).
70. Nicholson, D. E., Blomquist, D. S., and Lemon, R. H., Bull. 20th Meeting JANAF Panel on Physical Properties of Solid Propellants. Vol I, SPIA Pub. No. 14u p 271 (1961).
71. Oberth, A. E., and Bruenner, R. S., Trans. Soc. Rheology 9:2, 165 (1965).
72. Oberth, A. E., and Bruenner, R. S., Bull. 5th Meeting ICRPG Working Group on Mechanical Behavior, CPIA Pub. No. 119, (1965).
73. Phillippoff, W., Jo. of Applied Physics 24, 685 (1953).
74. Rainbird, R. W., and Vernon, J. H. C., Bull. 19th Meeting JANAF Panel on Physical Properties of Solid Propellant, SPIA Pub. No. PP-13, p 39 (1960).
75. Rivlin, R. S., Trans. Roy. Soc. (London), A240, 459, 491, 509 (1948); 241, 379 (1948).
76. Rivlin, R. S., and Thomas, A. G., Jo. Polymer Sci. 10 291 (1952).
77. Saylak, D., Bull. 1st Meeting ICRPG Working Group on Mechanical Behavior, CPIA Pub. No. 2, p 54 (1962).
78. Saylak, D., Bull. 2nd Meeting ICRPG Working Group on Mechanical Behavior, CPIA Pub. No. 27, p 423 (1963).
79. Saylak, D., Appl. Polymer Symposia 1; High Speed Testing, Vol V, 247 (1965).
80. Schapery, R. A., 4th U. S. Natl. Congr. Appl. Mech. 2, 1075 (1962).

81. Schapery, R. A., Solid Rocket Structural Integrity Abstracts, Calif. Inst. of Technology, Vol III No. 4., (Oct 1966).
82. Schapery, R. A., ASME Applied Mechanics and Fluids Engineering Conference, Wash., D. C., Paper No. 65-APM-15, June 1965.
83. Schapery, R. A., and Cantey, D., AIAA Jo. 4, No. 2, 255 (1966).
84. Schwarzl, F., and Staverman, A. J., in Die Physik der Hochpolymeren; ed. Stuart, H. A., Springer, Berlin, (1956).
85. Seeley, R. D., and Dyckes, G. W., Jo. Appl. Polymer Sci., 9, 151 (1965).
86. Sharma, M. G., Bull. 4th Meeting ICRPG Working Group on Mechanical Behavior, CPIA Pub. No. 94u, p 297 (1965).
87. Sharma, M. G., and Lim, C.K., Bull. 5th Meeting ICRPG Working Group on Mechanical Behavior, CPIA Pub. No. 119, Vol I, p 625 (1966).
88. Siron, R. E., and Duerr, T. H., Bull. 5th Meeting ICRPG Working Group on Mechanical Behavior, CPIA Pub. No. 119, Vol. I, p 657 (1966).
89. Smith, T. L., Trans. Soc. Rheology 2, 131 (1958).
90. Smith, T. L., Trans Soc. Rheology 3, 113 (1959)
91. Smith, T. L., and Stedry, F. J., Jo. Applied Physics 31, 1892 (1960); Rubber Chem. Technology, 34, 897 (1961).
92. Smith, T. L., Jo. Polymer Sci., 1, 3597 (1963); Rubber Chem. Technology, 37, 777 (1964).
93. Smith, T. L., and Smith, J. R., Stanford Research Institute Technical Rpt. No. NOW-61-1057-d, (Oct 1962).

94. Smith, T. L., *Journal Applied Physics*, 35, 27 (1964).
95. Spangler, R. D., *Bull. 20th Meeting JANAF-ARPA-NASA Panel on Physical Properties of Solid Propellants, Vol II*, SPIA Pub. No. 14c, p 23 (1961).
96. Spangler, R. D., *Bull. 2nd Meeting ICRPG Working Group on Mechanical Behavior*, CPIA Pub. No. 27, p 221 (1963).
97. Stecny, P. J.; Landel, R. F.; Shelton, H. T., *Bull. 20th Meeting JANAFAN Panel on Physical Properties of Solid Propellants, Vol II*, SPIA Pub. No. 14c, p 43 (1961).
98. Steinberger, R., "Preparation and Properties of Double-Base Propellants" *The Chemistry of Propellants*, Pergamon Press (1965).
99. Surland, C. C.; Boyden, J. R.; Givan, G. R., *Bull. 20th Meeting JANAF-ARPA-NASA Panel on Physical Properties of Solid Propellants, Vol I*, SPIA Pub. No. 14u, p 323 (1961).
100. Surland, C. C., and Givan, G. R., *Bull. 3rd Meeting ICRPG Working Group on Mechanical Behavior, Vol III*, CPIA Pub. No. 61A, p 85 (1965).
101. Svob, G. J.; Colodny, P. C.; Waddle, L. A.; and Lefferdink, T. B., *Bull. 20th Meeting JANAF-ARPA-NASA Panel on Physical Properties of Solid Propellants, Vol. I.*, SPIA Pub. No. 14u, p 307 (1961).
102. Tobolsky, A. V., *Properties and Structure of Polymers*, John Wiley & Sons, New York, (1960).
103. Torrey, J. F., and Britton, S. G., *AIAA Jo.* 1, (1963).

104. Torre, C., Schweiz. Arch. angew. Wiss. Techn., 15, 116, 145 (1949).
105. Treloar, L. R. G., The Physics of Rubber Elasticity, 2nd Ed. Chap. IV and VII, Oxford, Clarendon Press (1958).
106. Tschoegl, N. W., California Institute of Technology Materials Science Report MAT-SCET PS 66-6, Quarterly Report No. 8, Contract AF 04(611)-9572, May 1966.
107. Vernon, J. H. C., Bull. 19th Meeting JANAF Panel on Physical Properties of Solid Propellants, SPIA Pub. No. PP13, p 1 (1960).
108. Westergaard, H. M., J. Franklin Institute 189, 627 (1920).
109. Weigand, J. H., Am. Rocket Soc. J., 521 (April 1962) and Rubber Chem. and Technol. 37 542 (1964).
110. Williams, M. L.; Blatz, P. J.; and Schapery, R. A., "Fundamental Studies Relating to Systems Analysis of Solid Propellants", Graduate Aeronautical Lab., California Institute of Technology SM 61-5 (Feb 1961).
111. Williams, M. L., "The Fracture of Viscoelastic Material", Fracture of Solids, Interscience Publishers, New York, ; 157 (1963).
112. Williams, M. L., Addendum to Bull. 17th Meeting JANAF Panel on Physical Properties of Solid Propellants, SPIA Pub. (1959).
113. Williams, M. L., Knauss, W. G., and Wagner, F. R., Bull. 5th Meeting ICRPC Working Group on Mechanical Behavior, CPIA Pub. No. 119, Vol I, p 681 (1966).

114. Williams, M. L., Landel, R. F. and Ferry, J. D., *Jo. American Chemical Society*, 77, 3701 (1955).

115. Wibe, J. S., *Bull. 20th Meeting JANAFAN Panel on Physical Properties of Solid Propellants*, Vol I SPIA/PP 14u, p 209 (1961).

116. Zak, A. R., *Bull. 3rd Meeting ICREG Working Group on Mechanical Behavior*, CPIA Pub. No. 6lu, p 501 (1964).

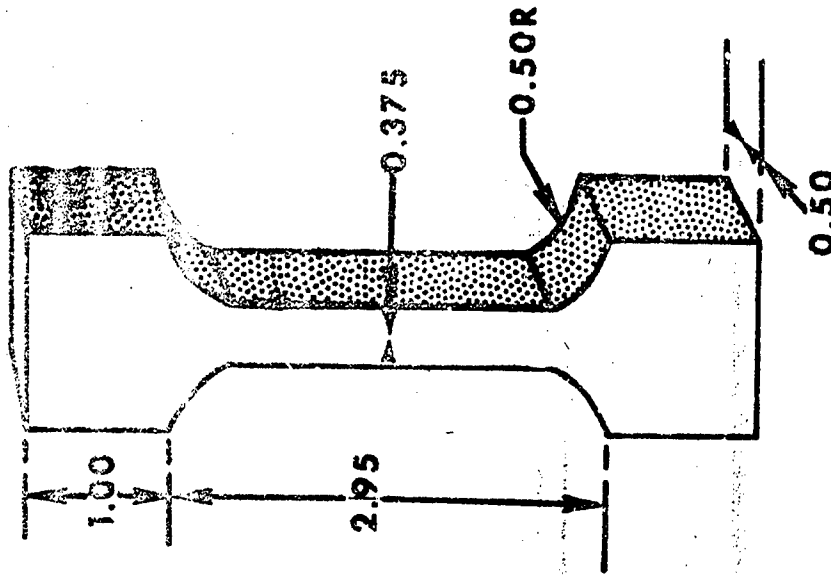
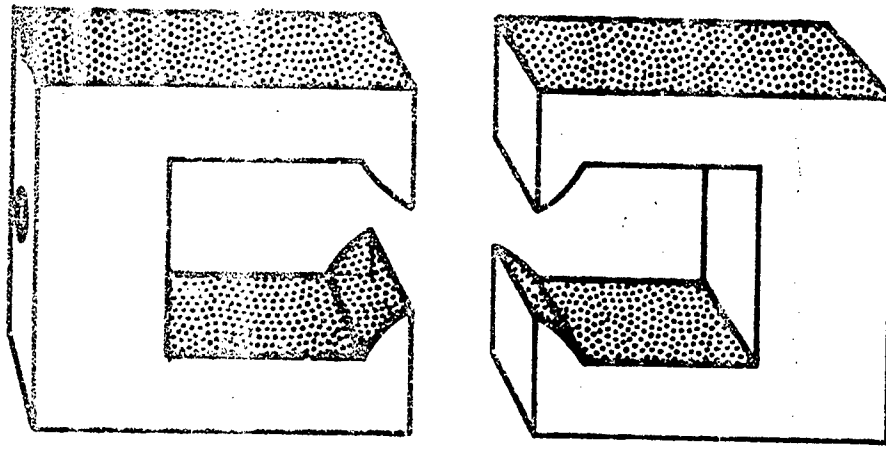


FIGURE 1. JANAF uniaxial solid propellant tensile specimen with typical gripping jaws. Dimensions are in inches.

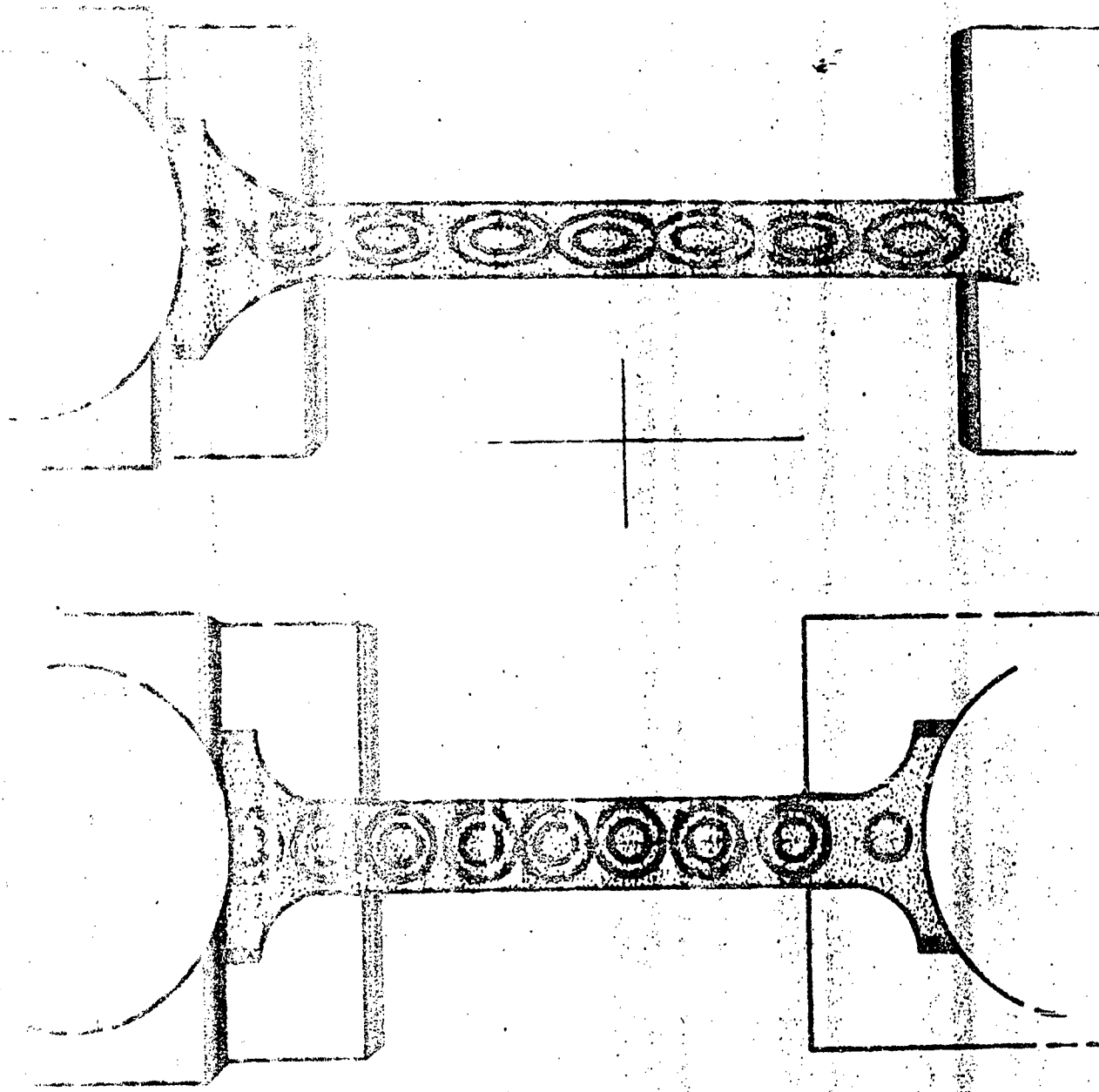


Figure 2. Schematic representation of the extrusion behavior of the JANA specimen. The extended sample ($\lambda = 1.57$) on the right shows a distribution of the oval markings through the jaw area. Drawing was taken from photographs in Reference 11.

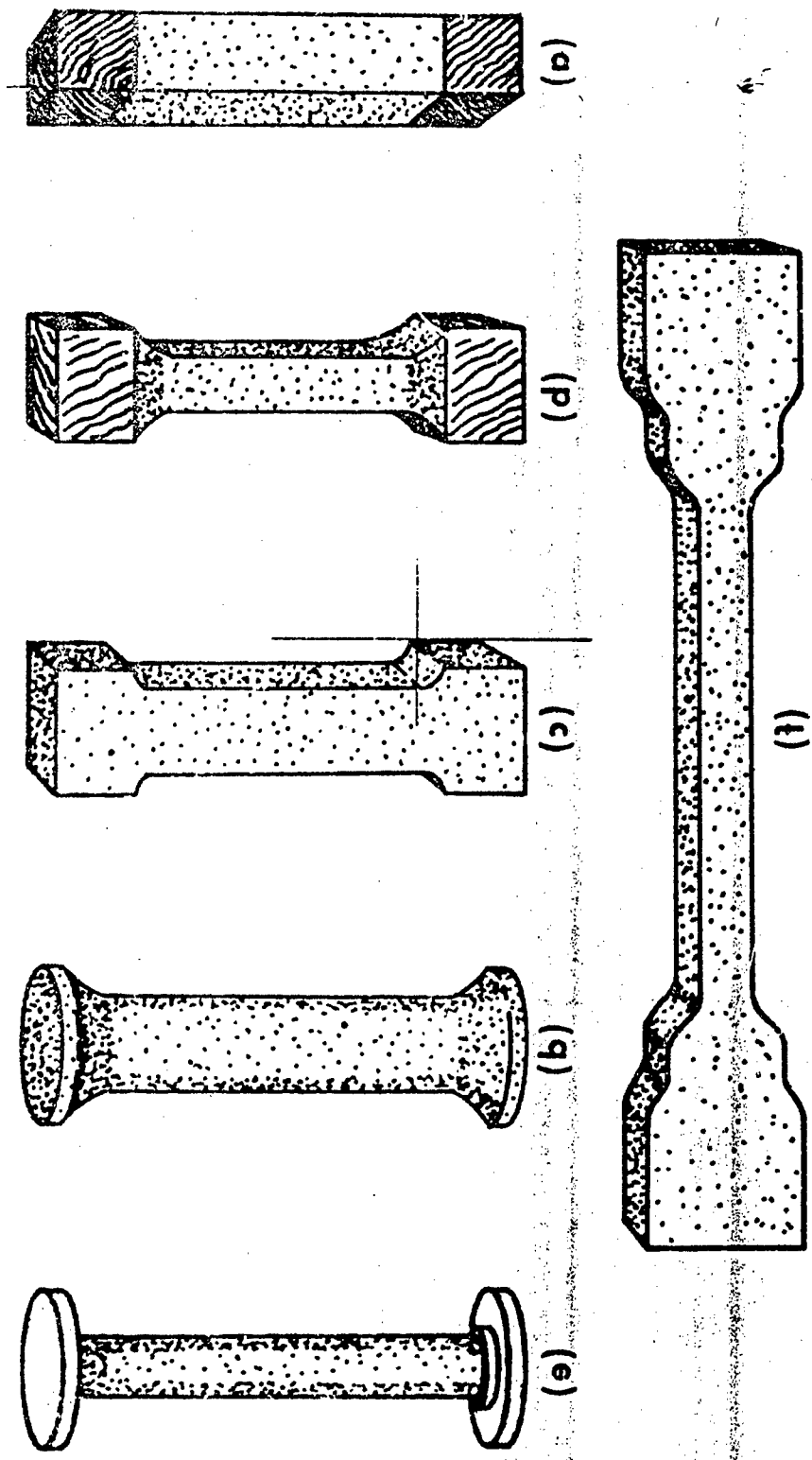


FIGURE 5. Several uniaxial specimen configurations. (a) Thiokol end-bonded, (b) cylindrical, (c) Stanford Research Institute configuration, (d) JANAF/Tab end hybrid, (e) rectangular tab end (f) Flow Reservoir (115) configuration.

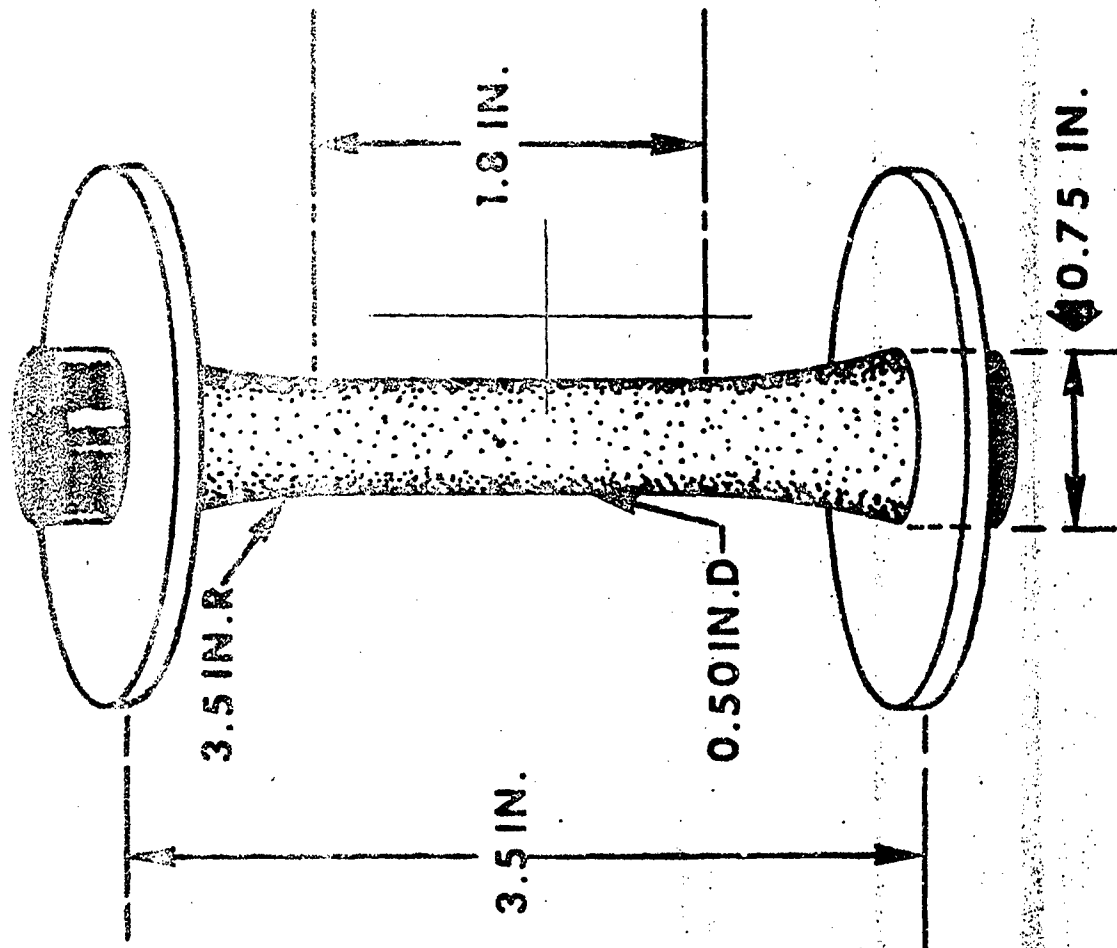


FIGURE 6. Saylak Cylindrical Specimen. Special jaws are required to fit the circular end plates.

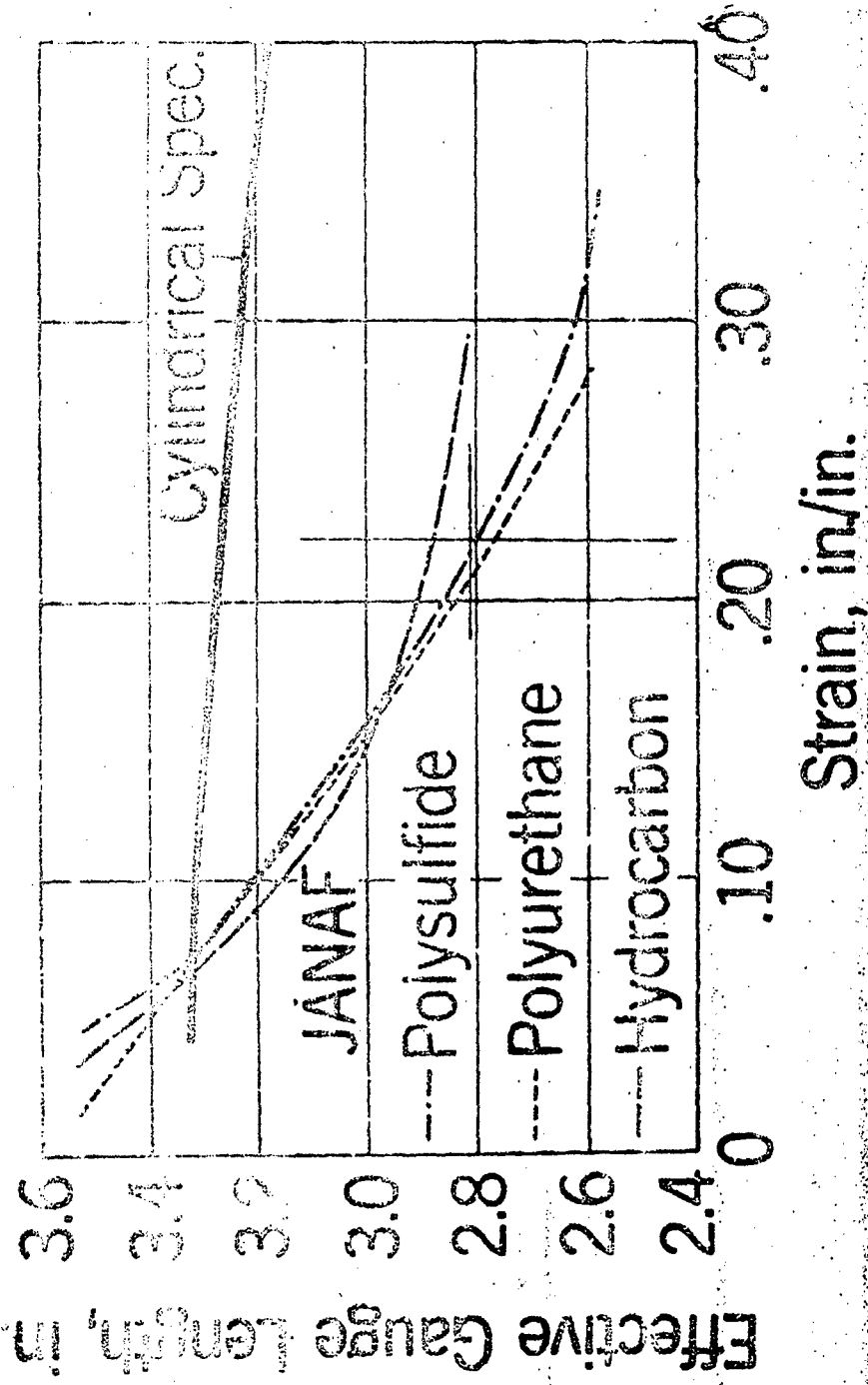
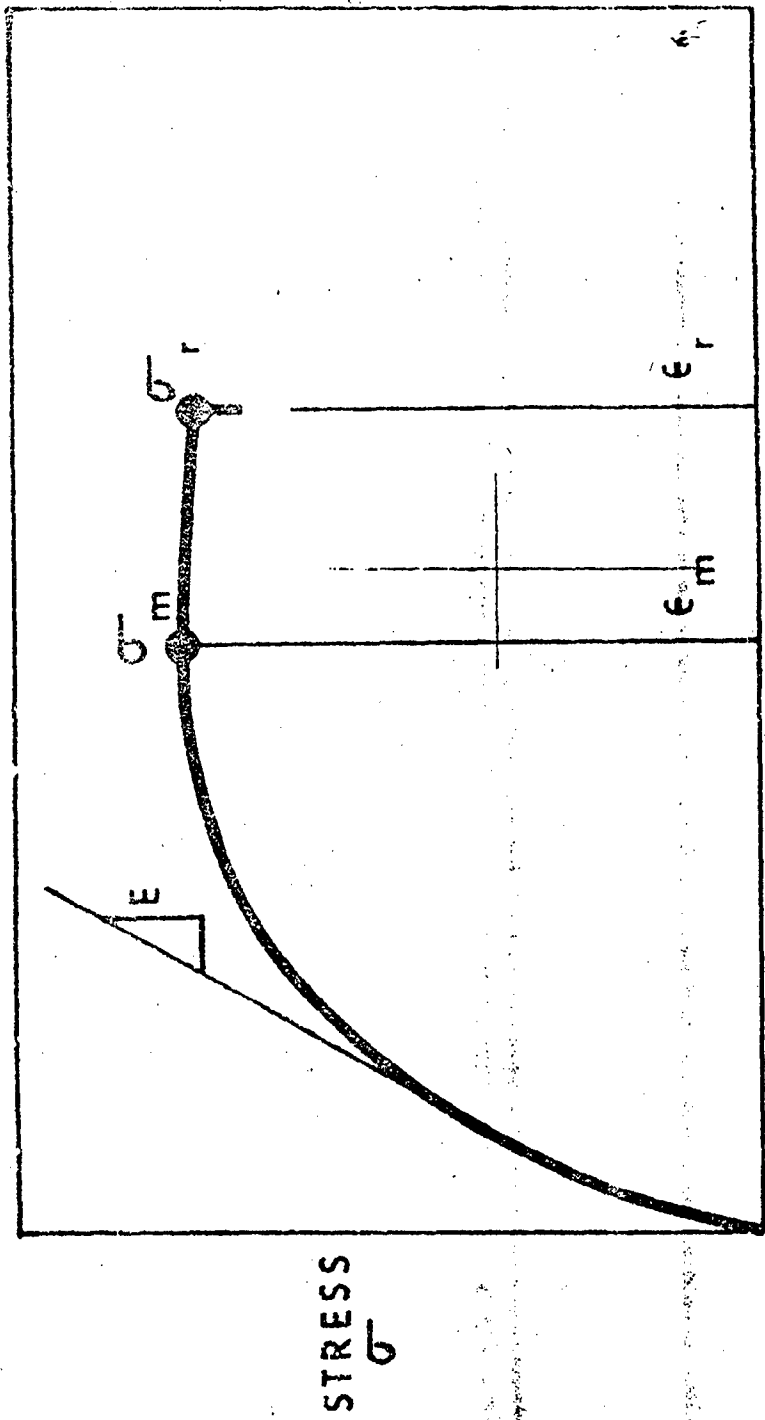


FIGURE 7. Plot of Effective Gauge Length (EGL) vs. strain comparing the Saylak cylindrical specimen with the JANAF specimen. Three propellant formulations were tested (Ref. 19).



STRAIN, ϵ

FIGURE 9. Typical stress-strain curve for solid propellants at 0.77 inches/min. and 80°F. E is the slope of the tangent to the initial portion of the curve. A wide variety of curve shapes are possible depending on specific formulations and test conditions.

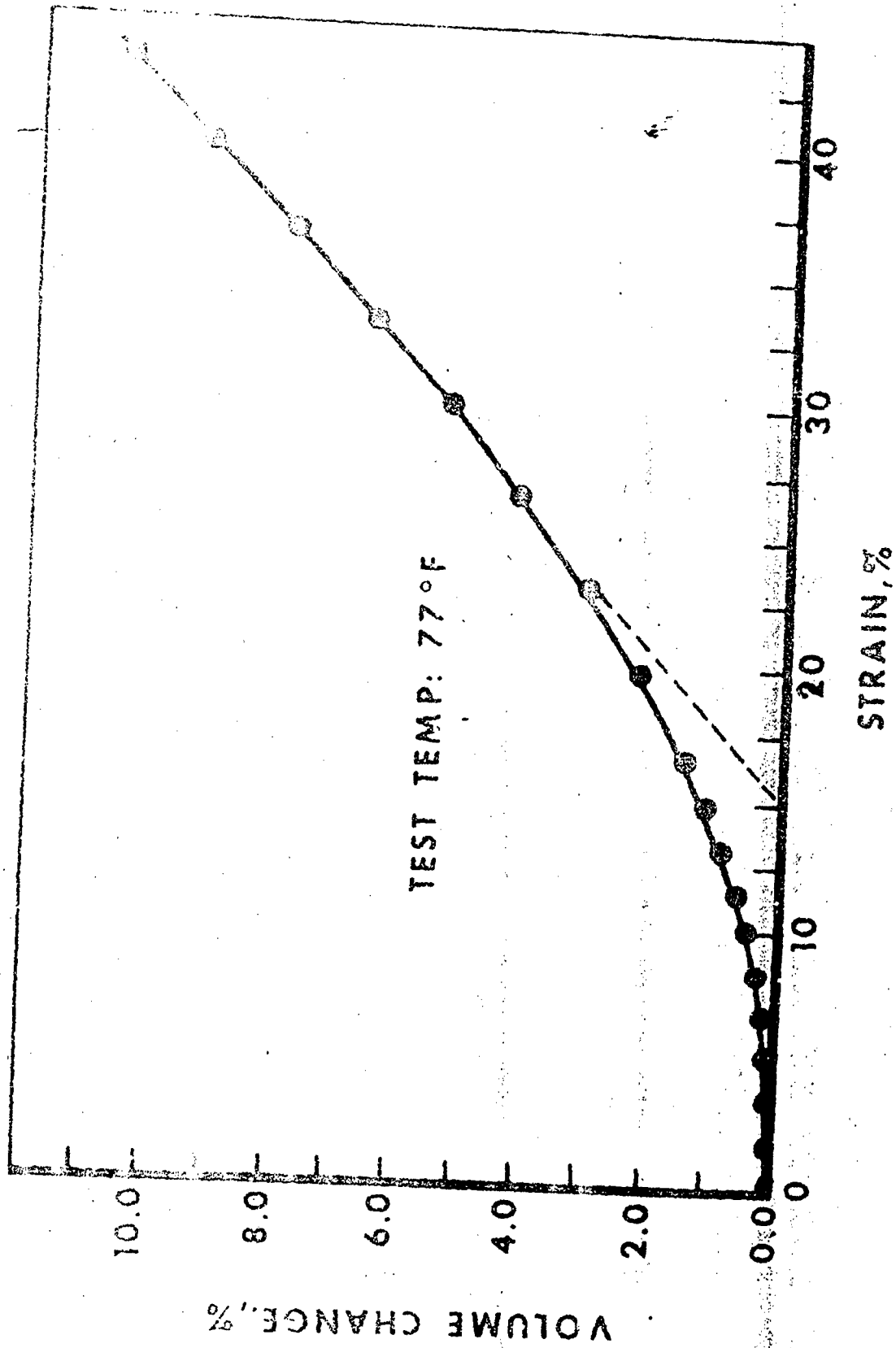


Figure 11. Volume change versus strain for a polyurethane propellant. Curve taken from Reference 101. Volume change was determined by static buoyancy measurements.

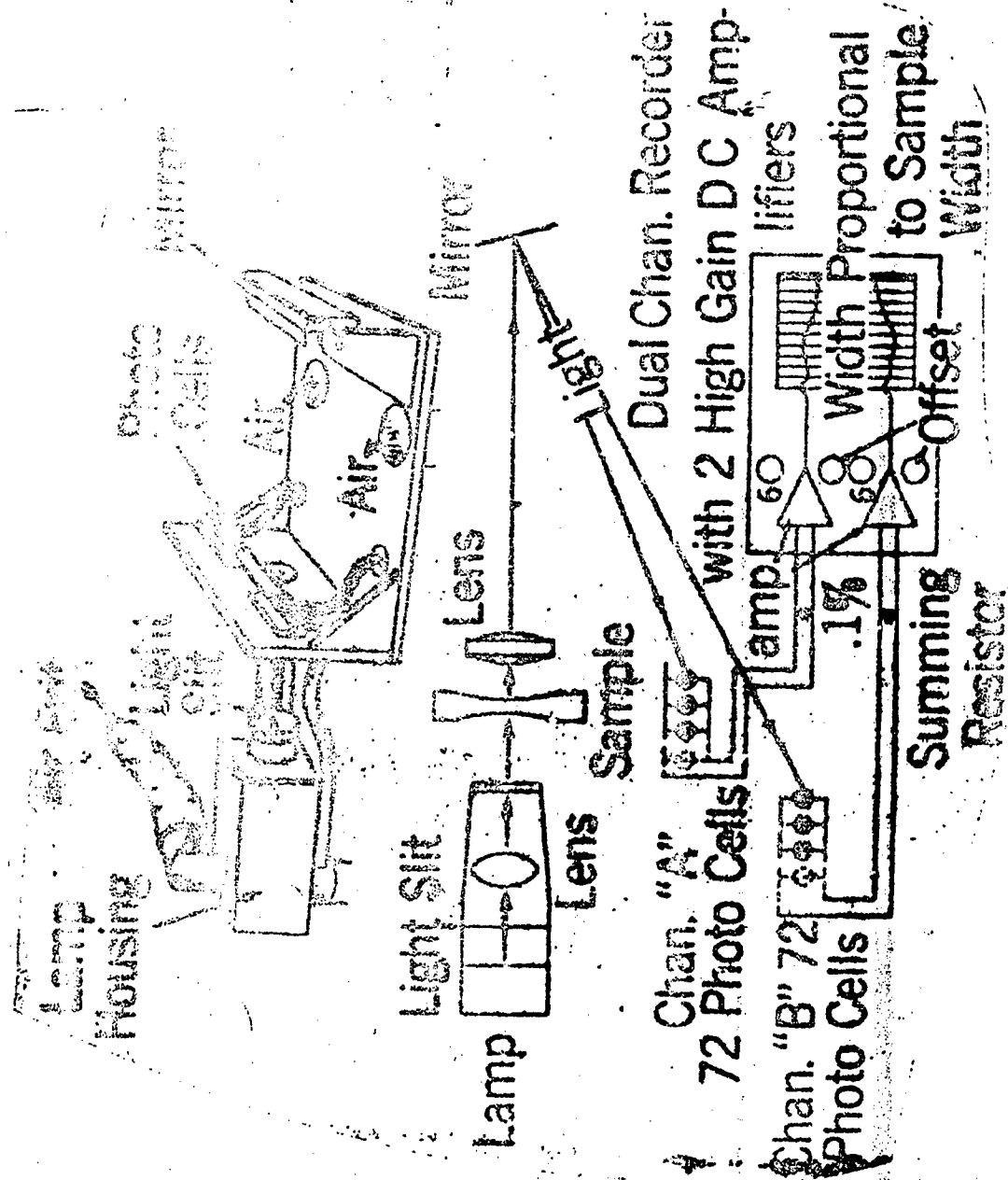


Figure 13. Optical scanning cross-sectional area recorder. Cylindrical sample shadow is magnified and monitored during extension by a bank of linearized photocells. (Reference 79)

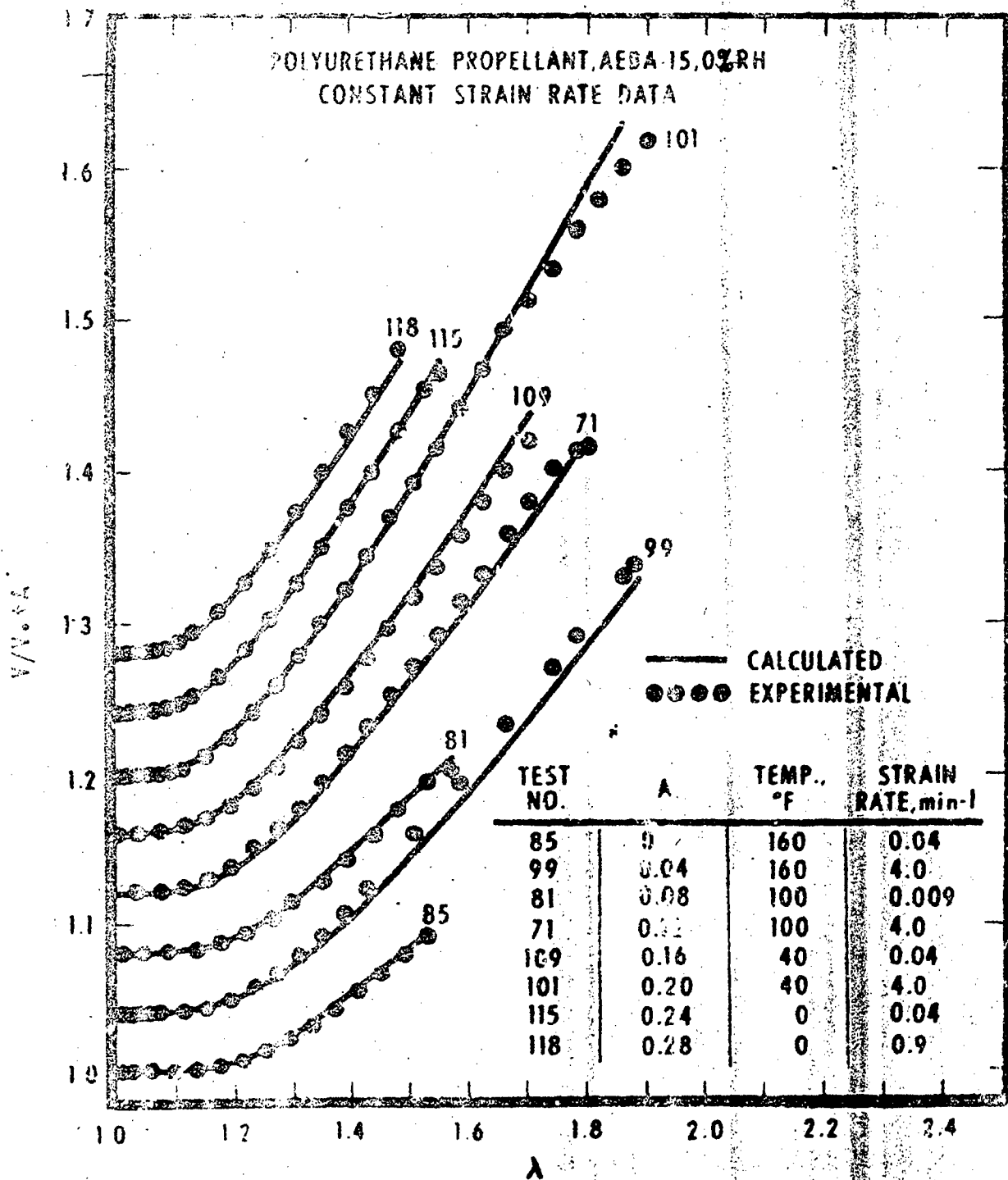


Figure 14. Comparison of calculated versus experimental dilatometric data for a polyurethane composite propellant. Curves have been displaced by a constant A for convenience. The quantity V/V_0 is the ratio of sample volume to initial volume. Data from Reference 28.

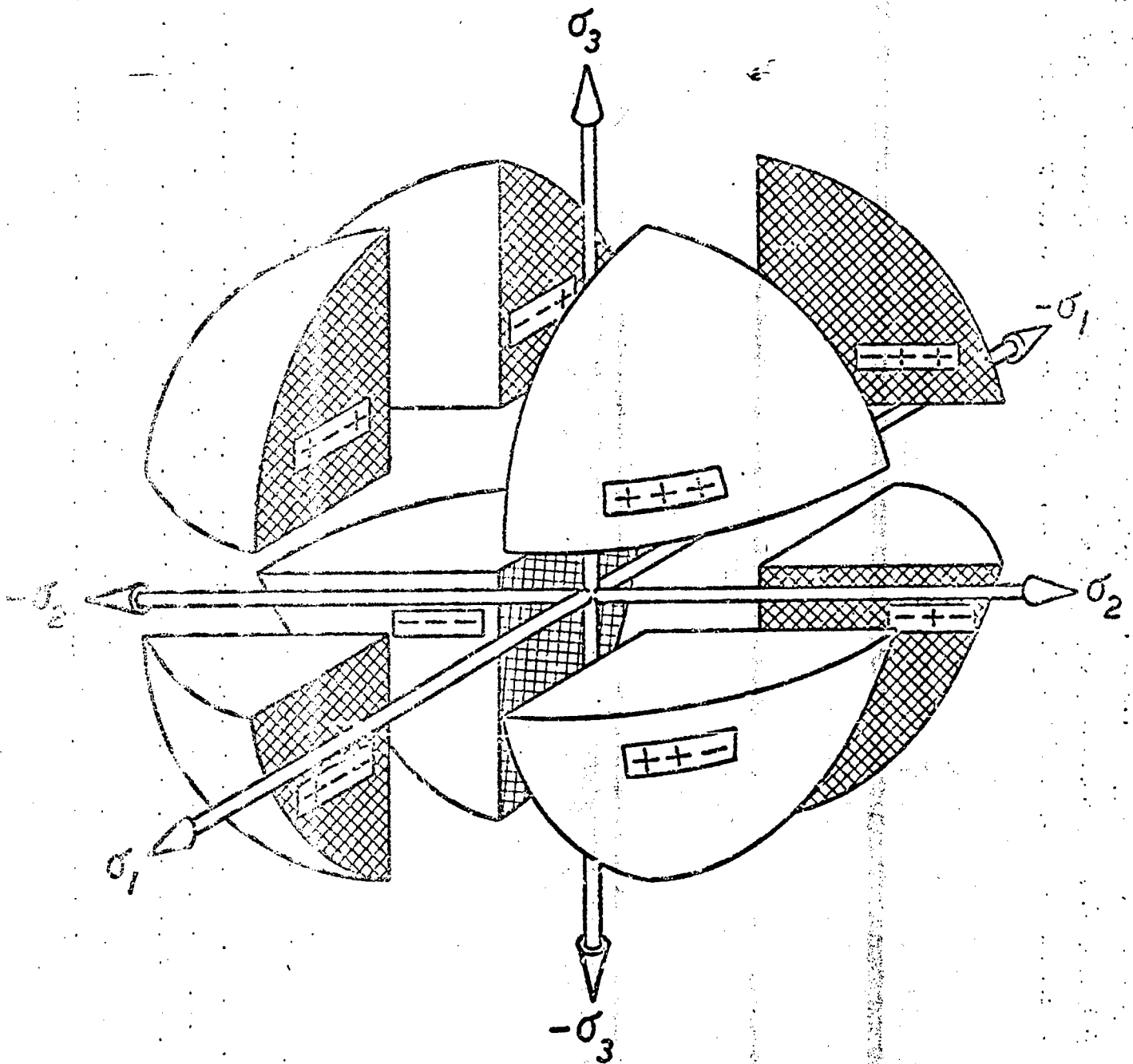


Figure 15. Schematic representation of the octants of principal stress space; where (+) indicates tension and (-) is compression.

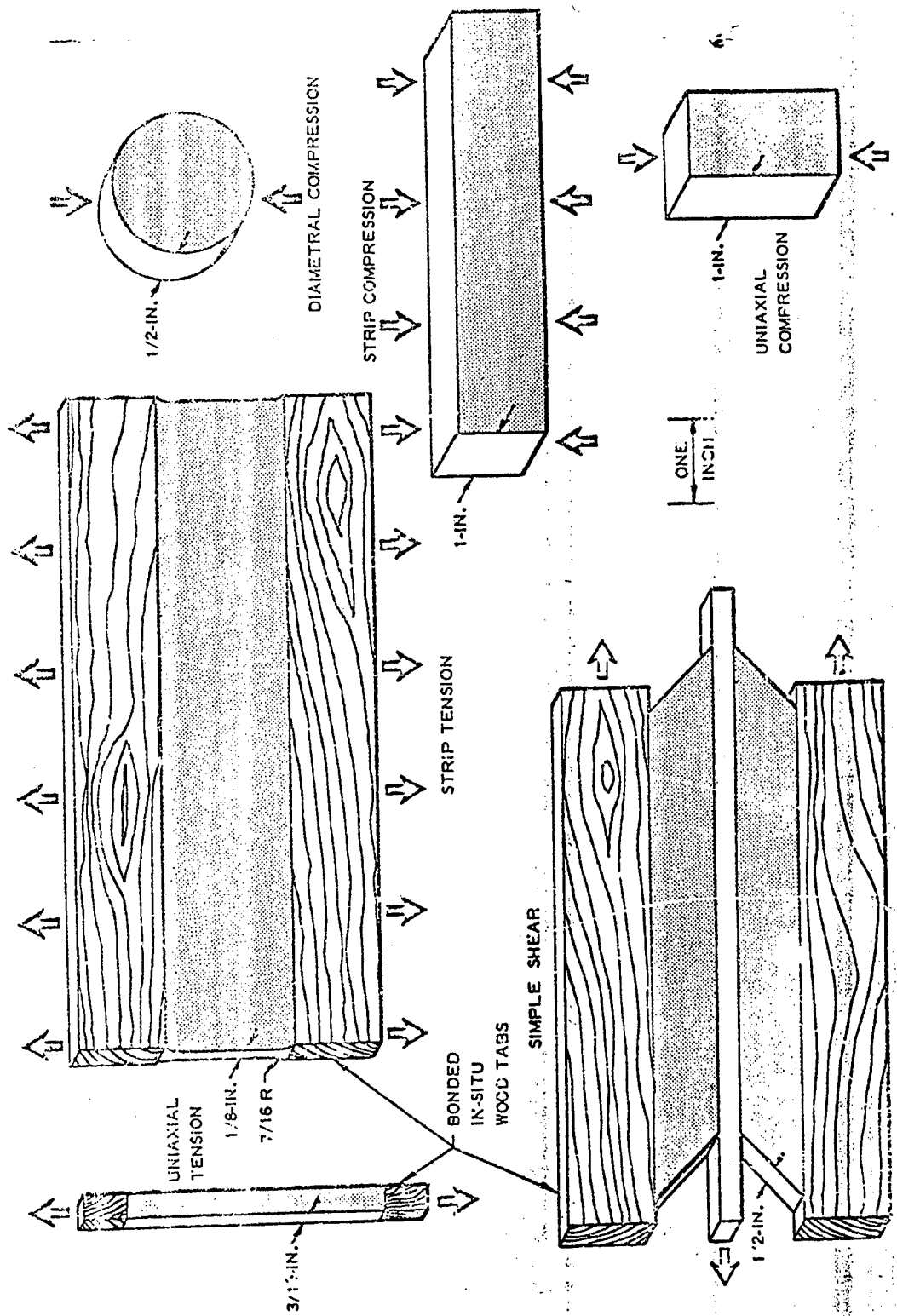


Figure 16. Various specimens used in the multiaxial characterization of solid propellants. Figure courtesy of Lockheed Propulsion Company.

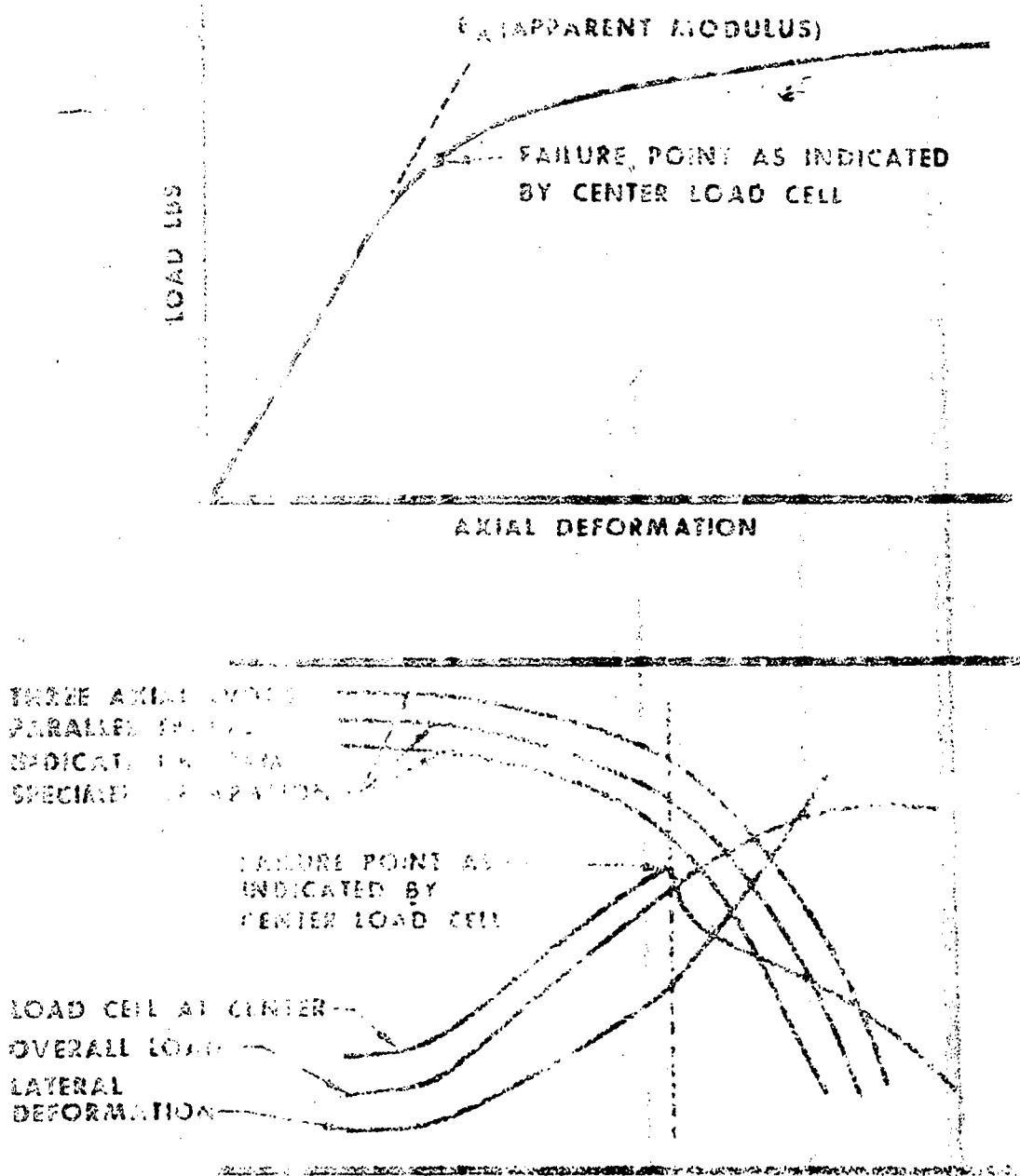


Figure 39. Poker Chip test data. Small center load cell in one of the bonded plates provides an indication of the rupture point which would not be obvious from overall load recording instruments. Curves from Reference 39.

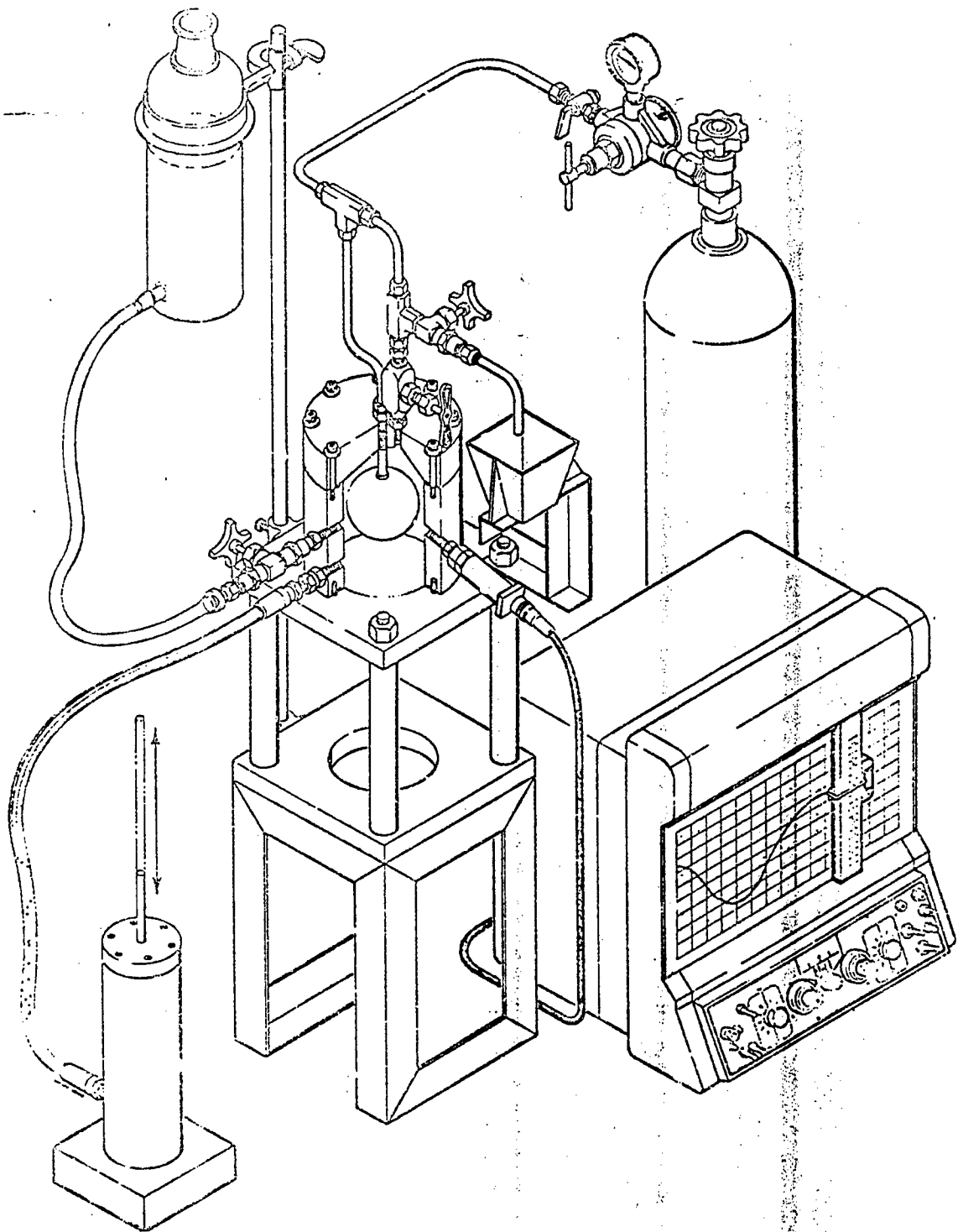
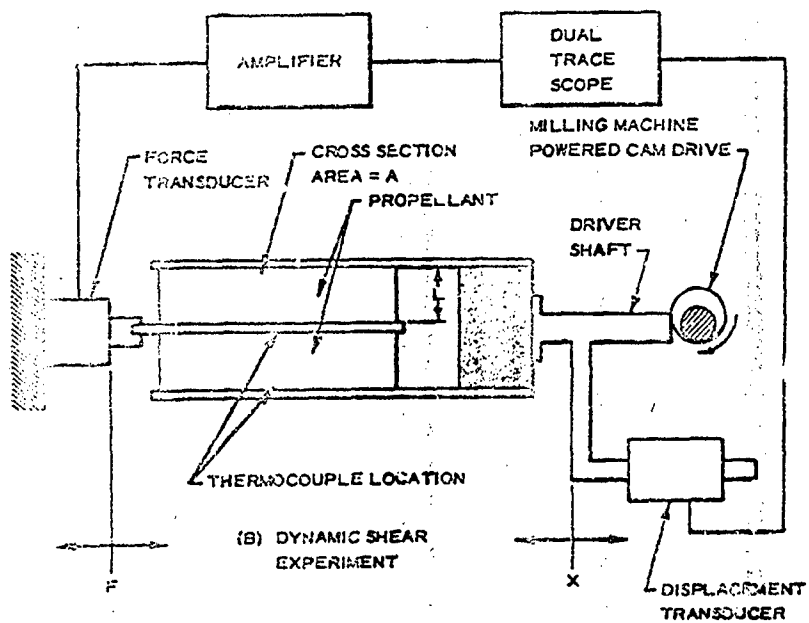
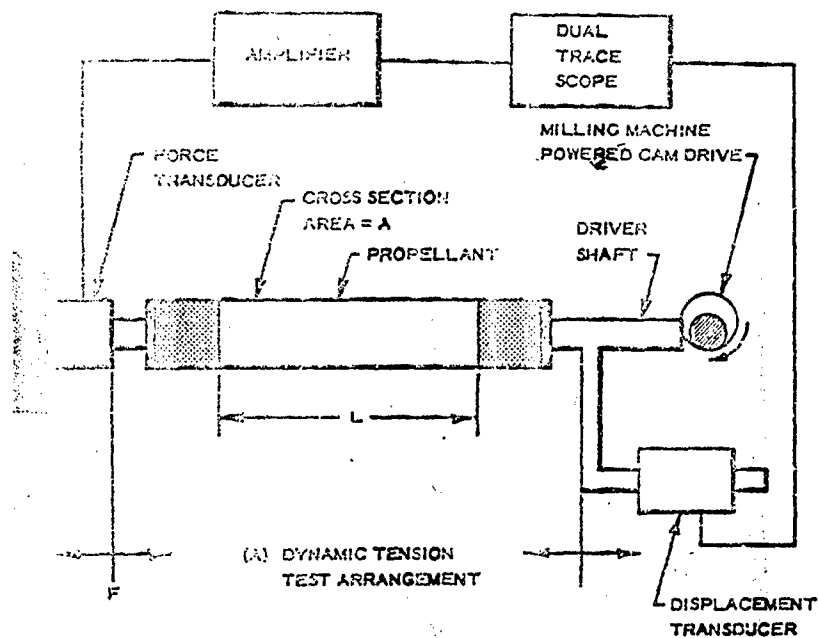


Figure 20. Spherical test assembly. Propellant sphere may be pressurized externally or internally and wall thickness may be varied. Drawing courtesy of Thicol Chemical Corporation, Wasatch Division.



LPC LARGE DEFORMATION SINUSOIDAL TEST APPARATUS

Figure 21. Schematic of large deformation dynamic tension and shear apparatus. Drawing courtesy of Lockheed Propulsion Company.

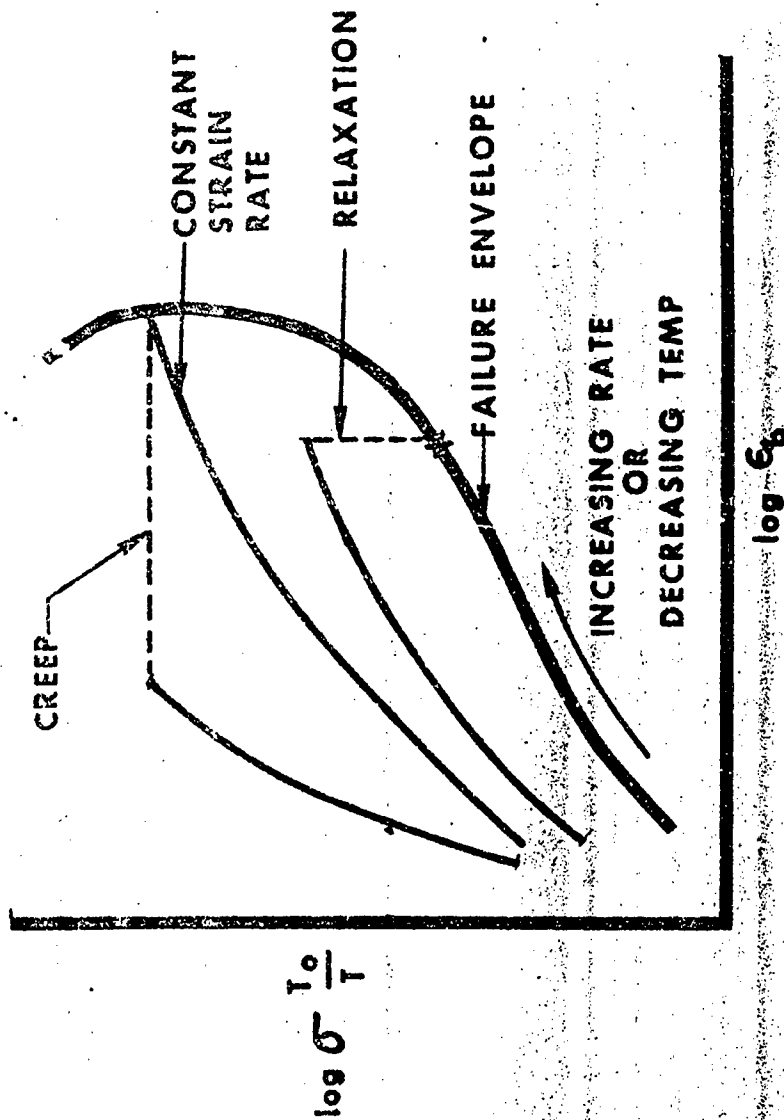
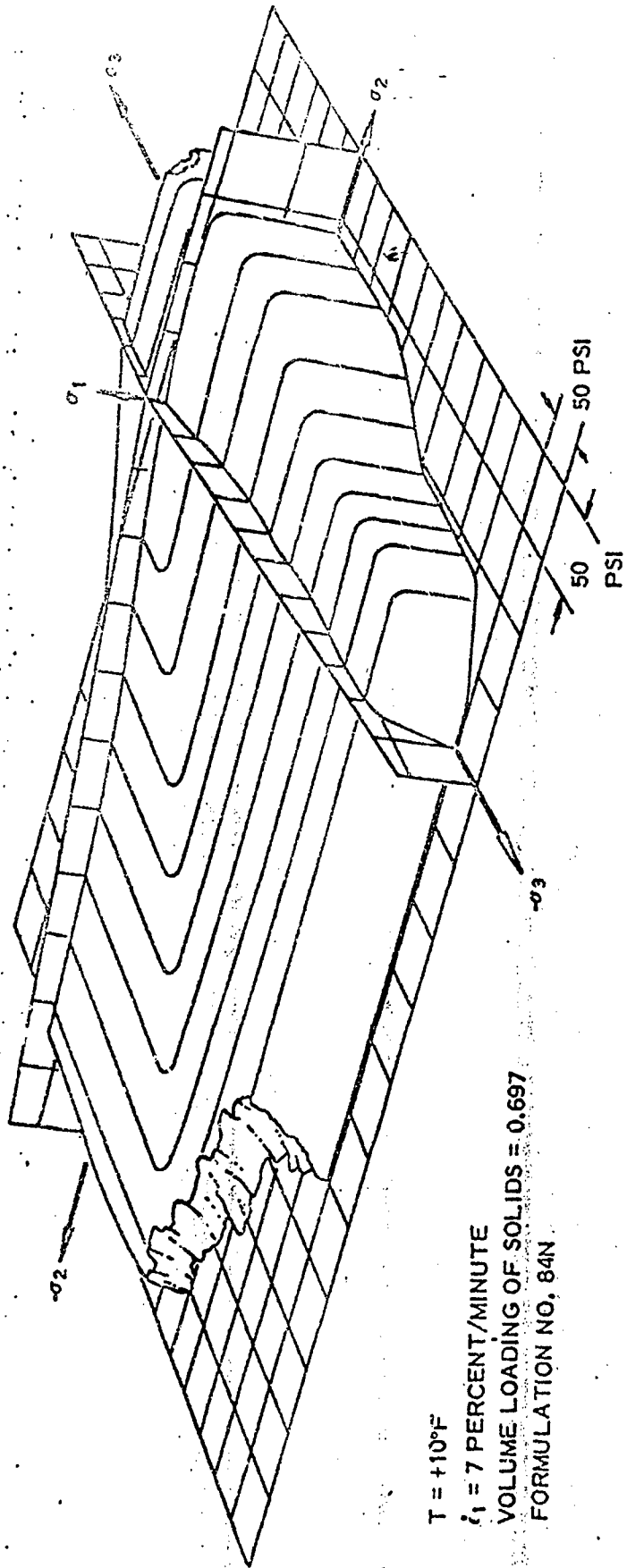


FIGURE 22. Schematic representation of the Smith Failure Envelope. Stress is corrected for kinetic theory temperature effects by the ratio of the reference temperature T_0 to the test temperature T .



$T = +10^{\circ}\text{F}$
 $\dot{\epsilon}_1 = 7 \text{ PERCENT/MINUTE}$
 VOLUME LOADING OF SOLIDS = 0.697
 FORMULATION NO, 84N

1.52

FIGURE 23. Failure surface in principal stress space for a composite solid pro-
 pellent. Diagram is taken from Ref. 45.

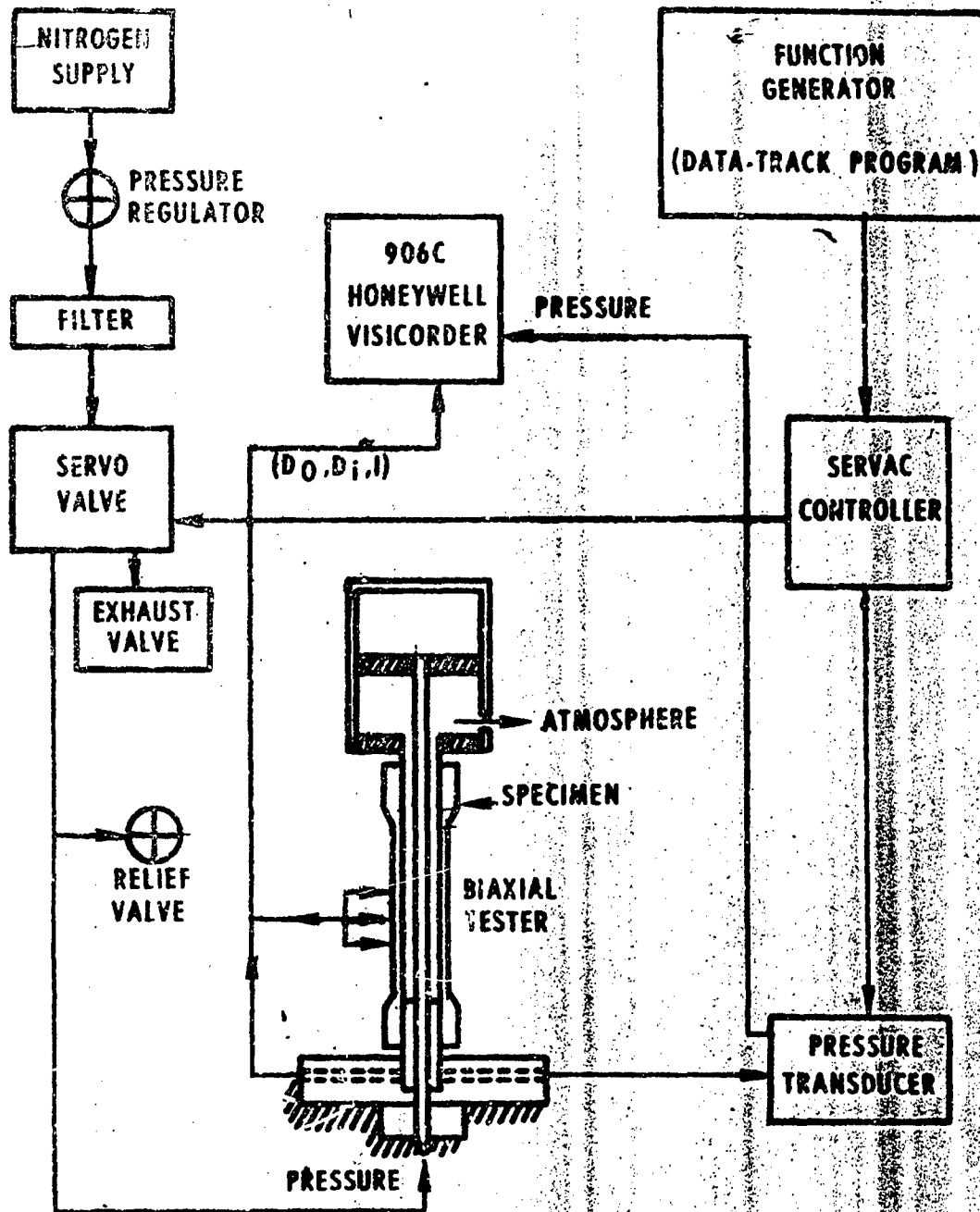


FIGURE 24. Schematic diagram of hollow cylinder biaxial tester as given by Sharma (86).

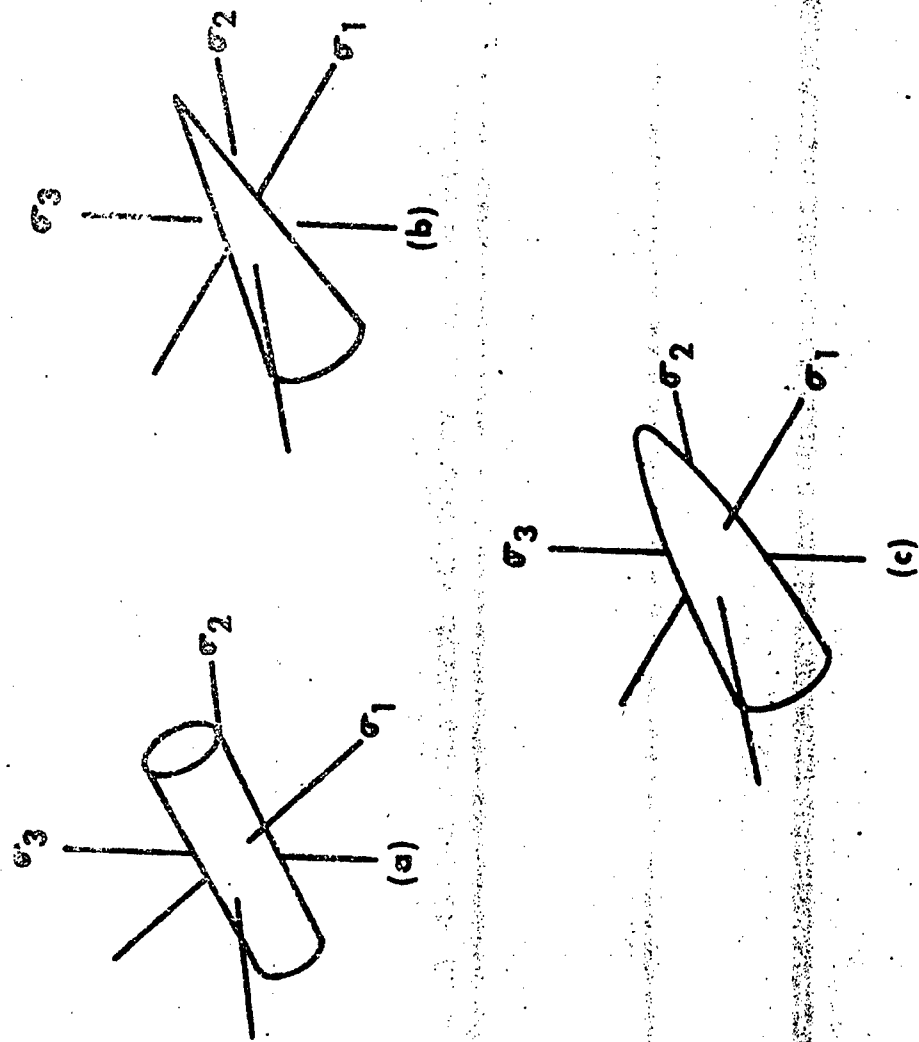


FIGURE 25. Various failure surfaces in principal stress space. (a) cylinder, (b) cone, and (c) paraboloid. Ref (106).

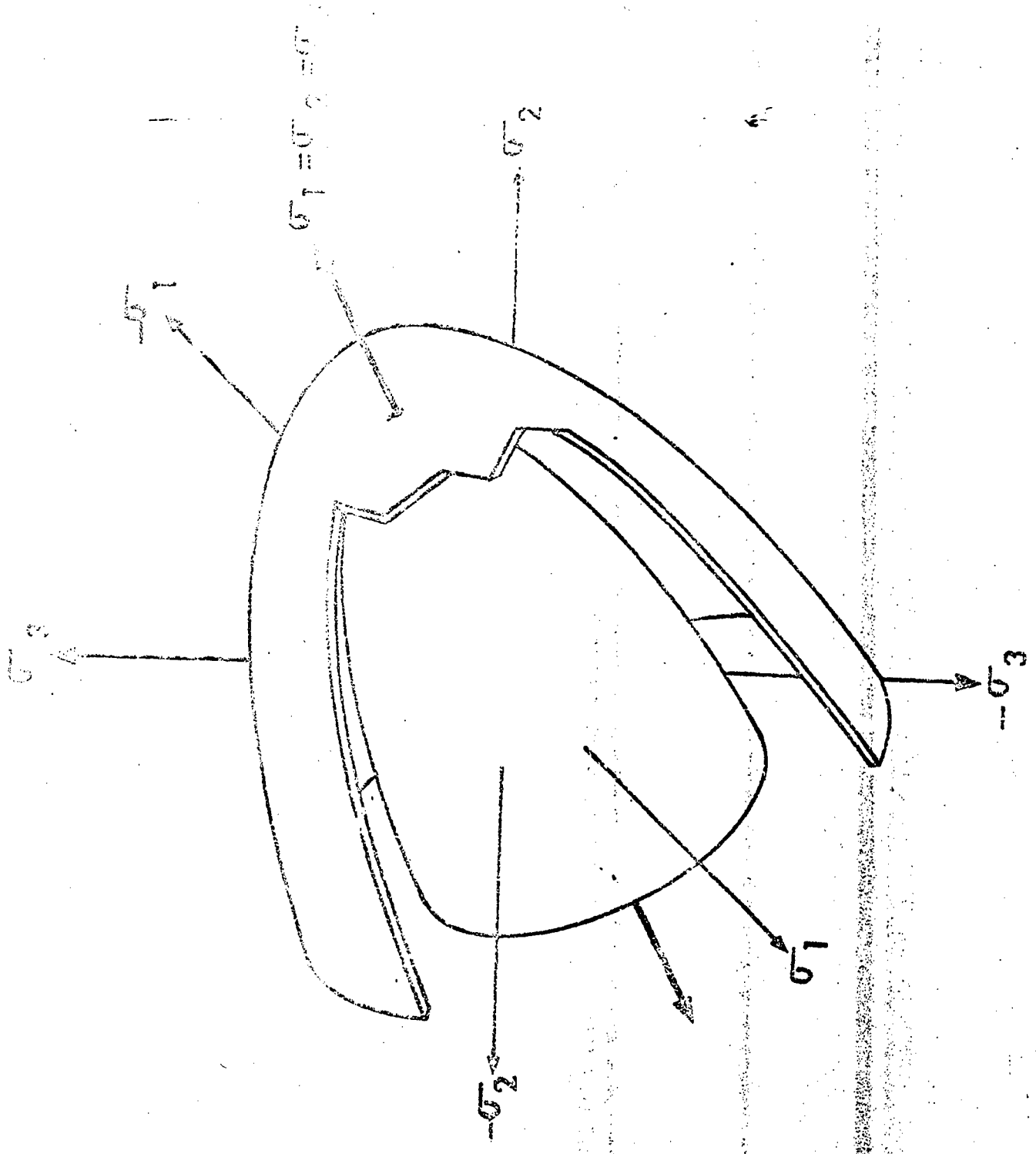
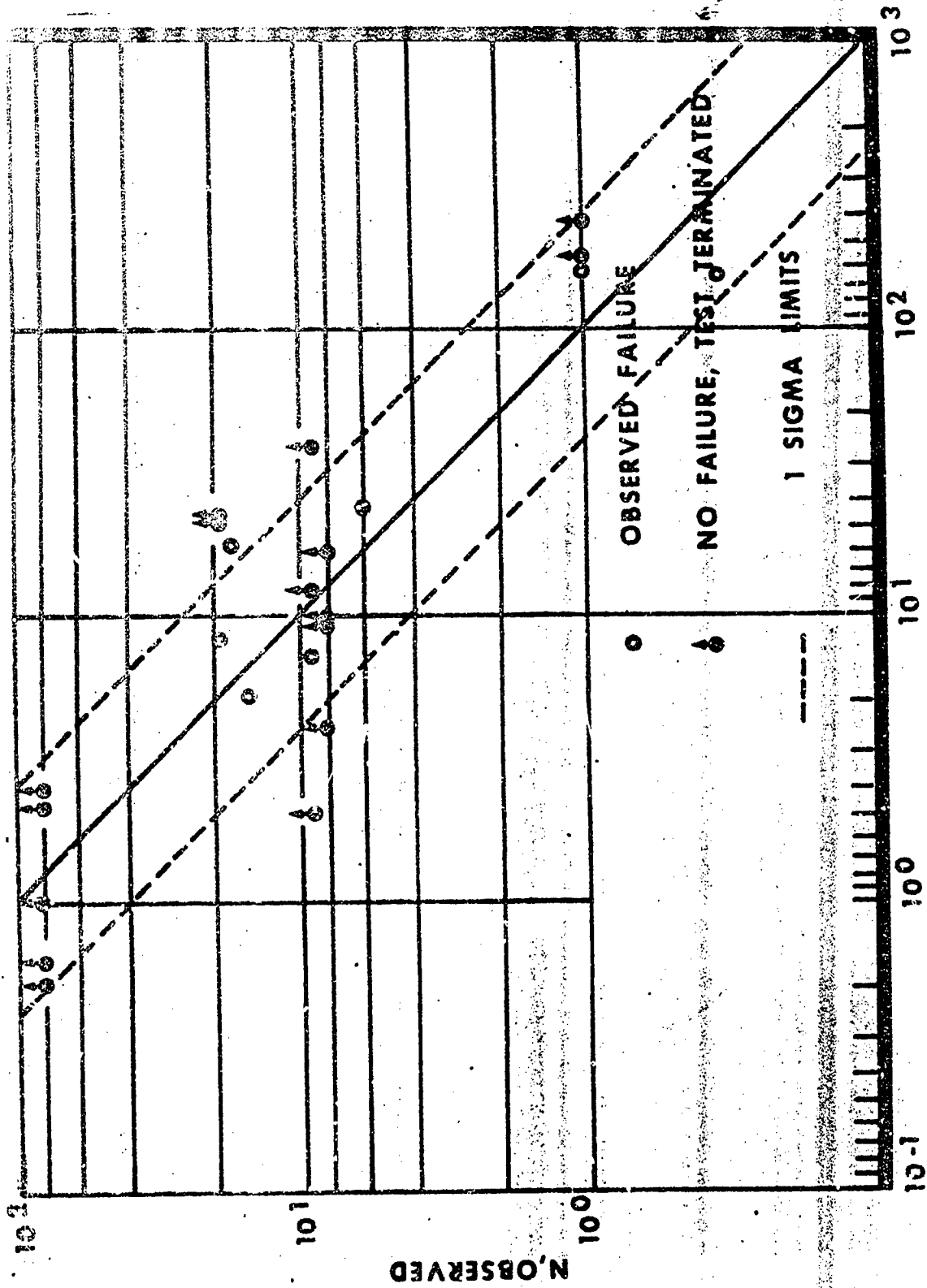


FIGURE 26. Parabolic failure surfaces co-axial to the hydrostatic axis.



N, PREDICTED

FIGURE 27. Comparison of predicted and observed number of cycles to failure for solid propellant-liner bond specimens, according to Ref (7).

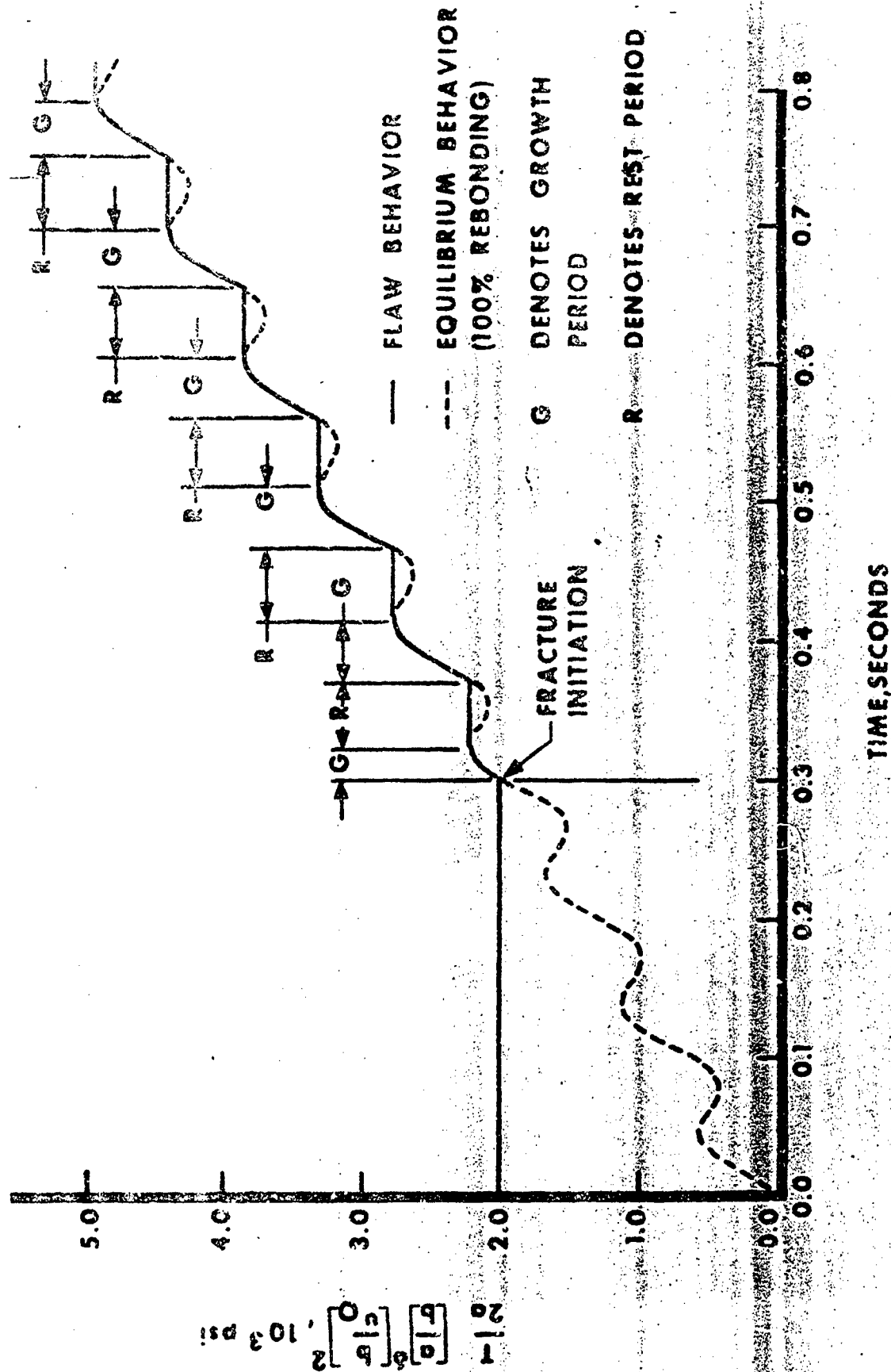


FIGURE 28. Spherical flaw growth due to oscillatory displacement $u = u_0 \sin \omega t$ for a polyurethane elastomer (5 cps). Curve generated by Eq 28.

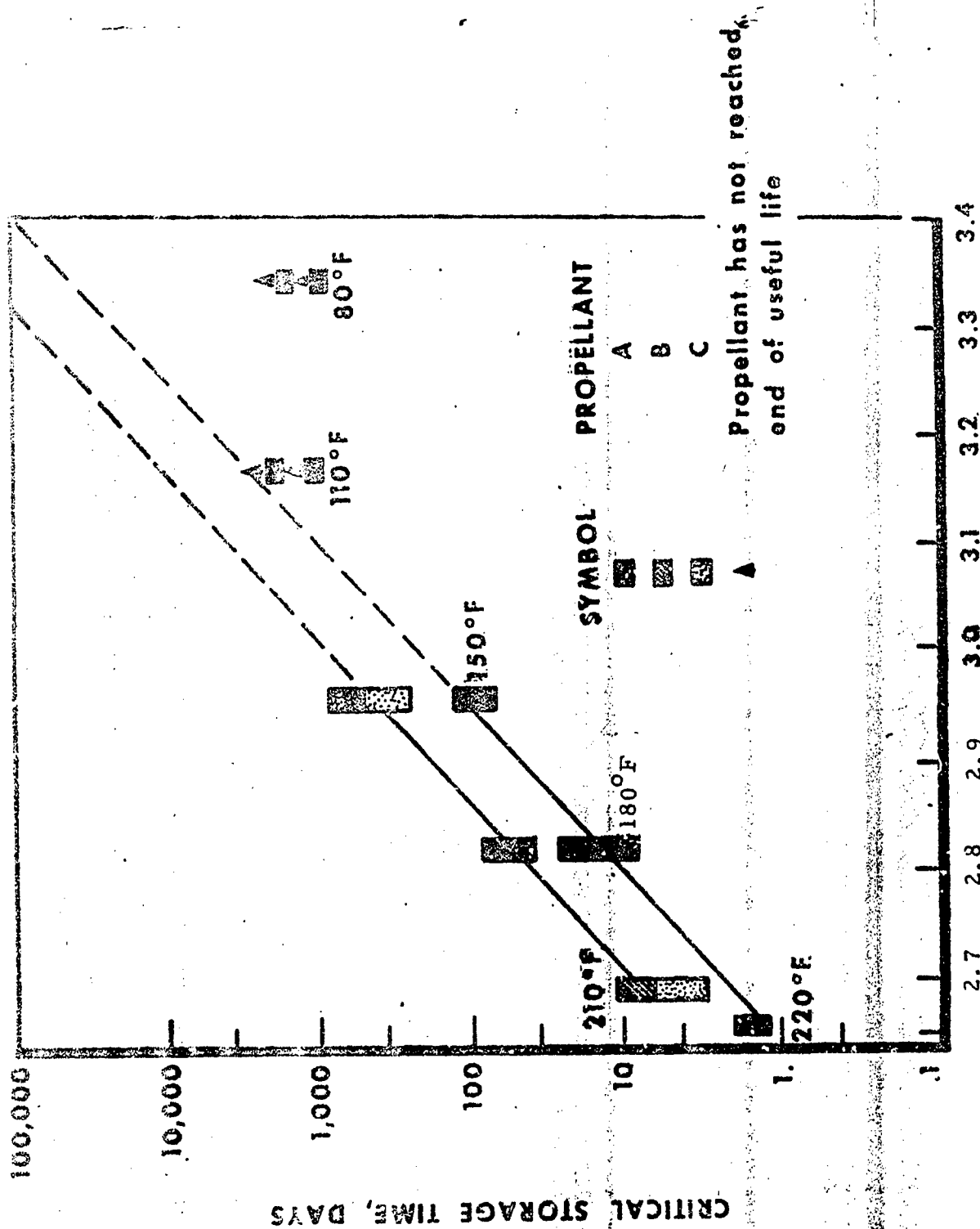


Figure 29. Plot of storage data for three propellant formulations at various temperatures. Critical storage time is defined as the time required for the

EFFECT OF DESIGN ON BOOSTER CHARACTERISTICS

(4 April 1967)

by

Artur Mager

Dr. Mager is general manager of the Applied Mechanics Division of Aerospace Corporation's El Segundo Technical Operations. Before receiving this appointment in February 1964, Dr. Mager was director of spacecraft sciences in the former Systems Research and Planning Division and has also been director of sciences at the National Engineering Science Company and on the staffs of Marquardt Corporation and NASA's Lewis Laboratories.

Dr. Mager received his B.S. degree from the University of Michigan, his M.S. from the Case Institute of Technology and his Ph.D. from Cal Tech and is the author of numerous articles, books and U.S. government publications.

INTRODUCTION

A simple and rapid method for assessing the effect of booster design variables on over-all booster characteristics is presented. This method is applicable to all boosters, regardless of whether they are expendable, reusable, rocket-powered, or airbreathing. The computations involved are minimal and many results are obtainable in a purely analytical manner. Furthermore, an all-inclusive graphical representation of booster characteristics is another by-product of this method.

Booster design procedures are given which minimize, per unit of payload weight, one of the following: gross weight, hardware weight and/or hardware costs per use. In these procedures the structural factors and the specific impulses are permitted to vary with stage size and booster velocity, respectively. All of these optimizations tend to produce larger velocity increases in those stages which have lower hardware costs per unit of weight, per use, and which have designs with lower limiting values of the structural factor and higher specific impulses at the instant of staging.

BOOSTER CHARACTERISTICS

A. Single Stage

In this analysis we use as independent variables:

1. The structural factor s_k

$$s_k \equiv \left(\frac{w_h}{w_h + w_f} \right)_k = \left(\frac{w_h}{w_g - w_p} \right)_k$$

and

2. The mass ratio $m_k^{(1)}$

$$m_k \equiv \left(\frac{w_t}{w} \right)_k$$

The mass ratio satisfies the equation of motion in the direction of the velocity

$$m_k = \exp \left[- \frac{(V_t - V_i)(1 + \bar{R})}{g \bar{I}} \right]_k$$

and is valid for any booster when the average specific impulse is given by

$$\bar{I}_k \equiv \left[\frac{V_t - V_i}{g \int_{V_i}^{V_t} \frac{dV}{gI}} \right]_k$$

⁽¹⁾ It should be noted that m_k is the inverse of the conventional mass ratio usually designated in rocket literature by symbol r .

and the average retarding-to-accelerating force ratio is given by

$$\bar{R}_k = \left\{ \frac{gI}{(V_t - V_i)} \int_{V_i}^{V_t} \left[\frac{D + w \cos \beta}{T - (D + w \cos \beta)} \right] \frac{dV}{gI} \right\}_k$$

The independent variables m_k and s_k can have any value between zero and unity. In addition, the difference $(m-s)_k$ cannot be smaller than zero. Consequently, each booster stage is represented by a point in the ms plane bounded by the intersection of the lines $s_k=0$, $m_k=1.0$ and $(m-s)_k=0$. These lines form a triangle in which the rocket-propelled vehicles are in one corner and the airbreathers are in the other corner.

Examination of design data indicates that each booster stage (e.g., first, second, etc.) tends to have its own, relatively invariant, $(m-s)_k$ value. This means that each stage tends to remain on a line parallel to the line $(m-s)_k=0$ which forms the base of the triangle. Since the magnitude of the structural factor for a given stage number and type is also usually known, therefore the values of the independent variables appropriate for the analysis of the stage characteristics can be reasonably well established.

Specifically, in such an analysis, these values permit the determination of the three dependent variables:

1. Gross-to-payload weight ratio

$$G_k = \left(\frac{w_k}{w_p} \right)_k$$

2. Hardware-to-payload weight ratio

$$H_k = \left(\frac{w_h}{w_p} \right)_k$$

3. Propellant-to-payload weight ratio

$$P_k = \left(\frac{w_f}{w_p} \right)_k$$

by the relations

$$G_k = \left(\frac{1-s}{m-s} \right)_k$$

$$H_k = \left[\frac{s(1-m)}{m-s} \right]_k = s_k (G_k - 1) = (mG)_k - 1$$

and

$$P_k = G_k - (1+H_k)$$

The lines of constant G_k and H_k may thus be conveniently plotted in the ms plane (Figure 1). Since such a representation is all inclusive, it permits an easy comparison between the various kinds of booster stages.

In addition, the knowledge of the independent variables m_k and s_k enables rapid evaluation of the sensitivity of the hardware-to-payload and gross-to-payload weight ratios to the changes of the various design assumptions. This evaluation is accomplished by use of the influence coefficients defined by

$$C_{d,q} = \frac{q}{d} \frac{\partial d}{\partial q}$$

so that the variational equations become

$$\frac{dG}{G} = C_{G,s} \frac{ds}{s} + C_{G,I} \frac{dI}{I} + C_{G,V_t} \frac{dV_t}{V_t}$$

et cetera.

The expressions for these influence coefficients are conveniently given in Table I and their magnitude may be plotted in the m -plane (Figure 2).

B. Varying Stage Size

When the design of a stage is chosen but its scale is undecided, one needs to find that size which has just the right amount of propellant sufficient for the desired acceleration. Under these conditions the structural factor varies with stage size and its variation may be given by

$$s_k = \left(\frac{a G - b}{G - 1} \right)_k$$

This relation simplifies matters considerably because H_k varies now linearly with G_k and both H_k and G_k are expressible in terms of m_k alone though the s_k is varying

$$G_k = \left(\frac{1 - b}{m - a} \right)_k$$

$$H_k = \left(\frac{a - b m}{m - a} \right)_k = (a G - b)_k$$

Although one of the independent variables is thus eliminated, the designer's choice is now reflected in the values of the constants a_k and b_k . Of these two, a_k is particularly significant because it represents the limiting value of s_k for very large gross-to-payload weight ratios (e.g., very large stages).

Obviously, these new simplified relations when differentiated may again be used to find the influence coefficients appropriate for such a stage of varying size (Table II).

C. Multistage Booster

The staging relation $w_{p,j} = w_{g,j+1}$ permits computation of the payload exchange ratio of the k th stage

$$E_k = \frac{w_{p,k}}{w_{p,n}} = \prod_{k+1}^n G_j = G_{k+1} E_{k+1}$$

This ratio is essential in the application of the previous relations to multistage boosters. Specifically, if in the previous definitions the payload is always taken as that of the complete booster and the weight contributions of the individual stages are all added together, then the dependent variables become

$$G = \frac{w_{g,1}}{w_{p,n}} = G_1 E_1$$

$$H = \frac{\sum_1^n w_{h,j}}{w_{p,n}} = \sum_1^n H_j E_j$$

$$P = \frac{\sum_1^n w_{f,j}}{w_{p,n}} = \sum_1^n P_j E_j$$

and we still have

$$P = G - (1+H)$$

Furthermore, it may be shown that if the independent variables are similarly defined so as to include the contributions from each stage

$$e = \frac{\sum_1^n w_{h,j}}{w_{g,1} - w_{p,n}} = \frac{\sum_1^n H_j E_j}{G-1} = \frac{\sum_1^n s_j (G_j - 1) E_j}{G-1}$$

$$m = \frac{w_{p,n} + \sum_1^n w_{h,j}}{w_{g,1}} = \frac{1 + \sum_1^n H_j E_j}{G} = \frac{1 + \sum_1^n (m_j G_j - 1) E_j}{G}$$

then the relations between these new dependent and independent variables remain exactly the same as for the single stage. The representation of Figure 1 is thus valid for the complete booster as well.

Furthermore, the differentiation shows that

$$\frac{dG}{G} = \frac{dG_k}{G_k}$$

so that the gross-to-payload ratio of the whole booster varies exactly like the gross-to-payload ratio of the individual stage. Or, in other words, the influence coefficients describing the variation of G_k describe also the variation of the complete booster's G .

For the over-all hardware-to-payload ratio H , the story is more complicated. We now have

$$\frac{dH}{H} = C_{H,H_k} \frac{dH_k}{H_k} + C_{H,G_k} \frac{dG_k}{G_k}$$

so that the changes of the gross-to-payload ratio of the k^{th} stage as well as the changes of the hardware-to-payload ratio of that stage affect the change of over-all H. Furthermore, the new, booster-peculiar, influence coefficients depend not only on the values of s_k and m_k for the k^{th} stage (in which the changes are assumed to be made) but also on the values of the independent variables for all the stages underneath and above it

$$C_{H, H_k} = \frac{H_k E_k}{H}$$

$$C_{H, G_k} = \frac{\sum_1^{k-1} H_j E_j}{H}$$

For this reason the graphical representation of the influence coefficients in the ms plane cannot be made although they can still be conveniently listed in tabular form (Table III).

To evaluate qualitatively the magnitude of the various changes it is often convenient to consider a special booster in which all stages have the same structural factor and mass ratio (e.g., $s_j = s^*$ and $m_j = m^*$ for all values of j). For such a booster the over-all structural factor s is the same as that of the individual stages ($s = s^*$) and the over-all difference $(m-s)$ is given by

$$(m-s) = (G^*)^{(1-n)} (m^* - s^*)$$

thus showing that the over-all value of m tends to decrease with the number of stages. Furthermore, for such a booster with similar stages, we may easily compute the multistage influence coefficients and plot these for any number of stages as a function of G^* (Figure 3).

COSTER OPTIMIZATIONS

The influence coefficients may be used to yield booster designs which have minimum values of over-all gross-to-payload or hardware-to-payload weight ratios. Furthermore, the solution so obtained for minimum H can easily be modified to yield minimum booster cost per use per unit of payload weight. In all of these solutions the optimization process results in $(n-1)$ conditions which permit finding, for each m_k , the corresponding value of m_{k+1} . In addition, since the maximum possible value of m_{k+1} is unity, these conditions also determine the special value of $m_k = m_k^0$, at which the use of the $(k+1)$ stage becomes feasible. As m_k decreases from this value towards a_k , both G_k and $V_{t,k}$ increase. Since the limiting value of $V_{t,k}$ is obtained when the stage payload is zero and $m_k = a_k$, it is important to determine the form of the optimization conditions when $m_k = a_k$.

For such a case, all three optimizations give

$$(m-a)_{k+1} = (m-a)_k \left(\frac{ac}{I_{e,i}} \right)_{k+1} \left(\frac{I_{e,t}}{ac} \right)_k \text{ with } m_k = a_k$$

where c_k is the cost per unit of hardware weight, per use, and it is understood to be unity for the G and H optimizations.

It is thus clear that the optimization process assigns higher velocity increase to those stages which have higher effective specific impulse and lower structural factors and which have lower costs per unit of hardware weight, per use. Furthermore, it is also clear that for such large velocity increases in each stage, the G and H optimizations will result in the same booster design. This, however, is not true for smaller velocity increases when the optimization conditions for minimum H are different from those for minimum G. This difference disappears when all stages underneath the stage being optimized are structurally similar and their structural factors are constant (e.g., $a_j = b_j = s^*$).

RESULTS AND CONCLUSIONS

The present investigation yielded the following results and conclusions:

1. A method for the analysis of booster performance which provides a direct insight into the dependence of over-all gross-to-payload and hardware-to-payload ratios on structural and propulsive design variables of individual stages has been formulated. This method applies to expendable and/or recoverable vehicles employing rocket or airbreathing propulsion and is especially useful in very rapid comparative evaluation and preliminary design computations.
2. A set of explicit influence coefficients is derived which permits the rapid formation of the appropriate variational equations. The solutions of such equations indicate that the effect of the specific impulse changes on the payload is independent of the stage in which these changes are made. They also show that the increase of propellant density is most beneficial, and the increase of the structural weight least harmful when made in the lowest stages of the booster.
3. Convenient, all-inclusive, graphical representation of the booster hardware-to-payload and gross-to-payload ratios is given as a function of the structural factor and mass ratio. This representation is particularly useful in understanding the fundamental differences among the many possible booster designs. In addition, the magnitude of the influence coefficients is similarly presented on graphs thus giving an indication of the sensitivity of the various designs to their inherent design assumptions.
4. New, easily calculable solutions for minimum gross-to-payload, minimum hardware-to-payload mass ratio and minimum hardware cost per unit of payload, per use, boosters with varying structural factors and varying effective specific impulses are obtained. Either of these optimization processes is shown to assign greater velocity increases to those

stages which have (at the instant of staging) higher effective specific impulses and, also, whose design leads to lower limiting (with increasing size) values of the structural factor. The differences between these two optimizations are shown to disappear when all the stages beneath the stage being optimized have equal and non-varying structural factors. Furthermore, these differences also disappear when the stages are dissimilar but designed to deliver their limiting velocity increases. The cost optimization, of course, also favors those stages which have lower hardware cost per use.

SYMBOLS

The following symbols are used in this report:

- a Constant (minimum) limiting value of the structural factor
- b Constant in expression for the varying structural factor
- C Influence coefficient
- c^{d, q} Cost, per unit of hardware weight, per use (dollars/lb)
- D Drag (lb)
- d Dependent variable
- E_k Payload exchange ratio
- G Cross-to-payload mass ratio
- g Gravitational constant (ft/sec²)
- H Hardware-to-payload mass ratio
- I Specific impulse (sec)
- m Terminal-to-gross mass ratio
- n Number of stages
- P Propellant-to-payload mass ratio
- q Varying quantity (independent variable)
- R Retarding-to-accelerating force ratio

- s Structural factor
- T Thrust (lb)
- V Booster's velocity (ft/sec)
- w Weight
- θ Angle between flight direction and local vertical (degrees)

Subscripts:

- d permutation index denoting dependent variable
- e effective
- f propellant
- g gross
- h hardware
- i initial
- j permutation index for stage designation
- k specific value of j
- p payload
- q permutation index denoting the varying quantity
- t terminal

Superscripts:

- Bar above the symbol indicates average (constant) value
- * Star indicates certain fixed constant value
- o Circle indicates the value of G_k or m_k at which the introduction of optimized (k+1) stage becomes feasible

Table I. Influence Coefficients for Single Stage.

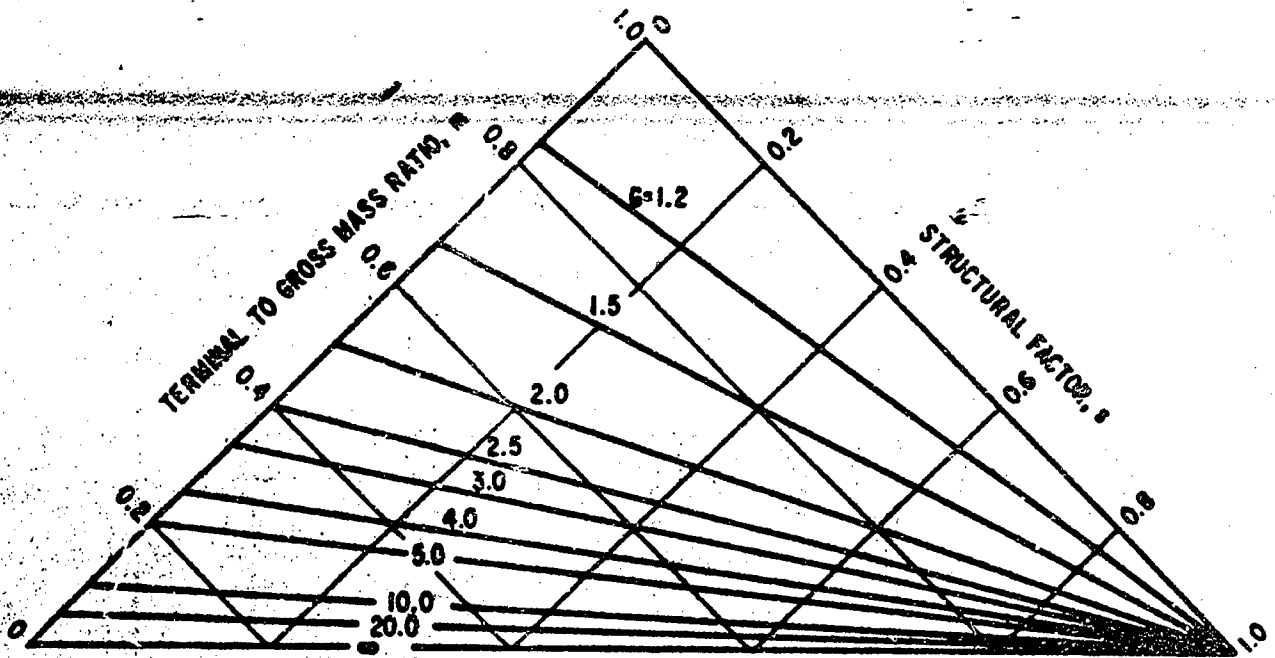
d	$(C_{d,s})_k$	$(C_{d,\bar{t}e})_k$	$(C_{d,v_t})_k$
G_k	$\frac{s(1-m)}{(m-s)(1-s)}$	$\frac{m \ln m}{m-s}$	$\frac{m}{m-s} \left[\frac{V(1+R)}{gI} \right]_{V=V_t}$
H_k	$\frac{m}{m-s}$	$\frac{m(\ln m)(1-s)}{(m-s)(1-m)}$	$\frac{m(1-s)}{(m-s)(1-m)} \left[\frac{V}{gIe} \right]_{V=V_t}$

Table II. Influence Coefficients for Stage of Varying Size.

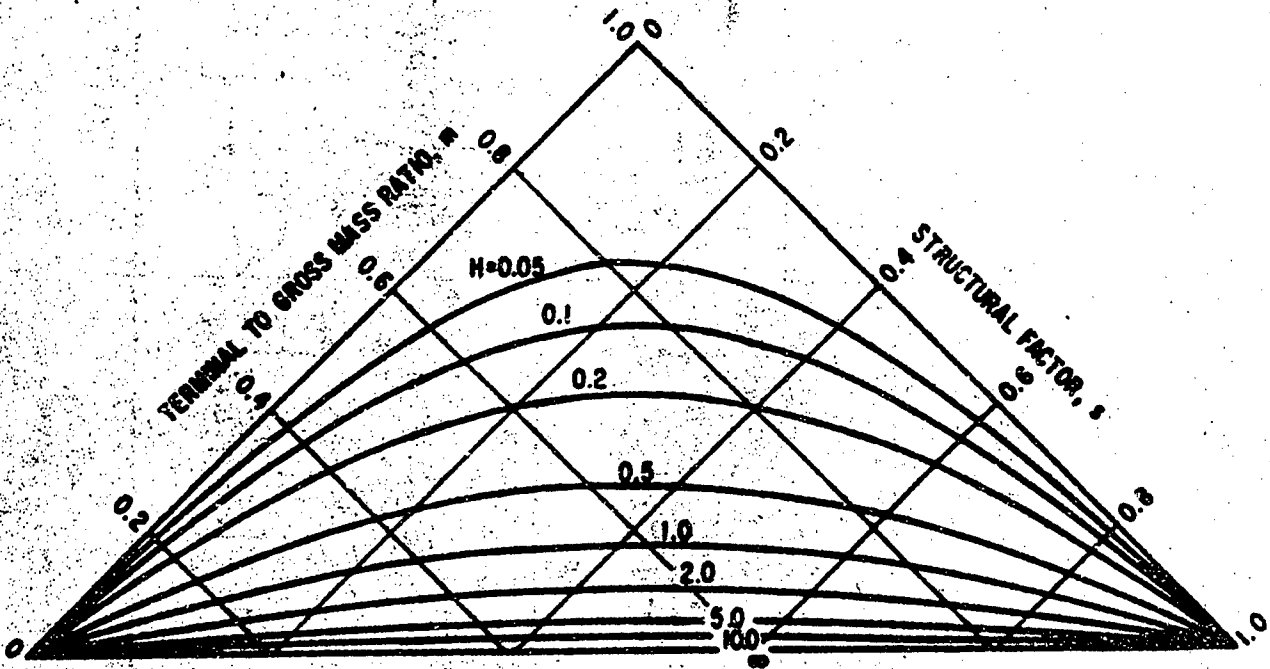
d	$(C_d, I_e)_k$	$(C_d, V_t)_k$
G_k	$\left(\frac{m \ell n m}{m-a} \right)_k =$ $- \left\{ \frac{(V_t - V_i)}{g I_e} \left[1 + \left(\frac{a}{1-b} \right) G \right] \right\}_k$	$\left\{ \frac{m}{m-a} \left[\frac{V(1+R)}{g I} \right] \right\}_{V=V_t}_k =$ $\left\{ \left[1 + \left(\frac{a}{1-b} \right) G \right] \left[\frac{V}{g I_c} \right] \right\}_{V=V_t}_k$
H_k	$\left[\frac{a(1-b)m \ell n m}{\left(1 - \frac{b}{a} m\right)(m-a)} \right]_k =$ $- \left\{ \frac{(V_t - V_i) G \left[1 + \left(\frac{a}{1-b} \right) G \right]}{g I_e \left(G - \frac{b}{a} \right)} \right\}_k$	$\left\{ \frac{a(1-b)m}{\left(1 - \frac{b}{a} m\right)(m-a)} \left[\frac{V(1+R)}{g I} \right] \right\}_{V=V_t}_k =$ $\left\{ \frac{G \left[1 + \left(\frac{a}{1-b} \right) G \right]}{\left(G - \frac{b}{a} \right)} \left[\frac{V}{(I_e)} \right] \right\}_{V=V_t}_k$

Table III. Influence Coefficients for Multistage Booster.

	$C_{d,s,k}$	$C_{d,i,k}$	$C_{d,v,k}$
d	$\left[\frac{s(1-m)}{(m-s)(1-s)} \right]_k$	$\left(\frac{mAm}{m-s} \right)_k$	$\left[\frac{m}{m-s} \left[\frac{v}{gI_e} \right]_{v=v_f} \right]_k$
G	$\frac{H_k E_k}{H} \left(\frac{m}{m-s} \right)_k + \sum_{j=1}^{k-1} \frac{H_j E_j}{H} \left[\frac{s(1-m)}{(m-s)(1-s)} \right]_k$	$\frac{H_k E_k}{H} \left[\frac{(1-s)mAm}{(m-s)(1-m)} \right]_k + \sum_{j=1}^{k-1} \frac{H_j E_j}{H} \left[\frac{mAm}{m-s} \right]_k$	$\frac{H_k E_k}{H} \left[\frac{m(1-s)}{(m-s)(1-m)} \left[\frac{v}{gI_e} \right]_{v=v_f} \right]_k + \sum_{j=1}^{k-1} \frac{H_j E_j}{H} \left[\frac{m}{m-s} \left[\frac{v}{gI_e} \right]_{v=v_f} \right]_k$
H	$\frac{H_k E_k}{H} \left(\frac{m}{m-s} \right)_k + \sum_{j=1}^{k-1} \frac{H_j E_j}{H} \left[\frac{s(1-m)}{(m-s)(1-s)} \right]_k$	$\frac{H_k E_k}{H} \left[\frac{(1-s)mAm}{(m-s)(1-m)} \right]_k + \sum_{j=1}^{k-1} \frac{H_j E_j}{H} \left[\frac{mAm}{m-s} \right]_k$	$\frac{H_k E_k}{H} \left[\frac{m(1-s)}{(m-s)(1-m)} \left[\frac{v}{gI_e} \right]_{v=v_f} \right]_k + \sum_{j=1}^{k-1} \frac{H_j E_j}{H} \left[\frac{m}{m-s} \left[\frac{v}{gI_e} \right]_{v=v_f} \right]_k$

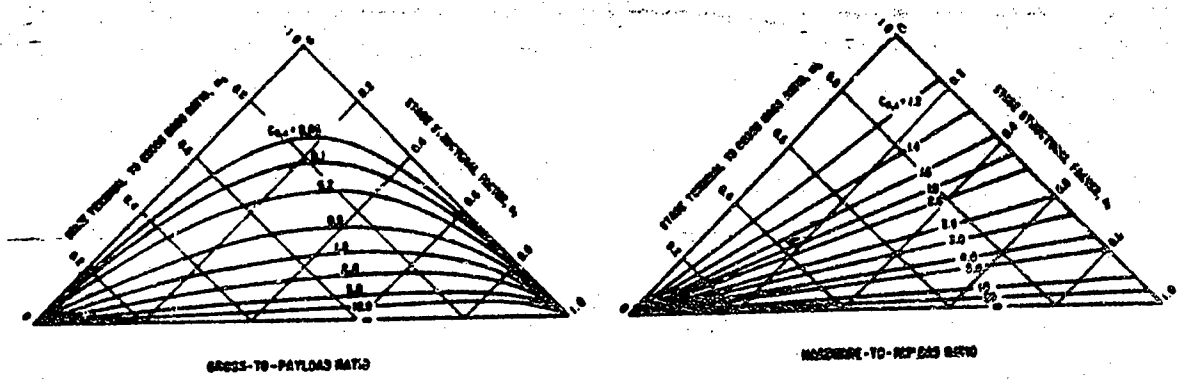


(a) Gross-to-Payload Mass Ratio

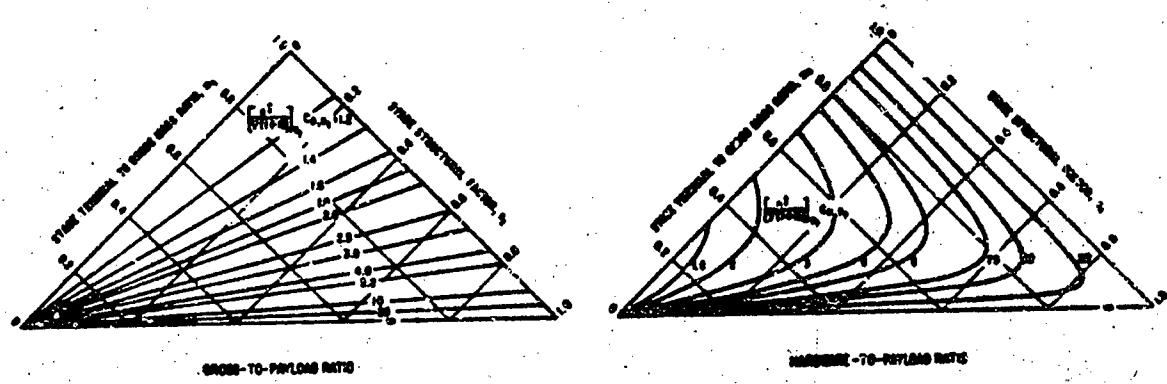


(b) Hardware-to-Payload Mass Ratio

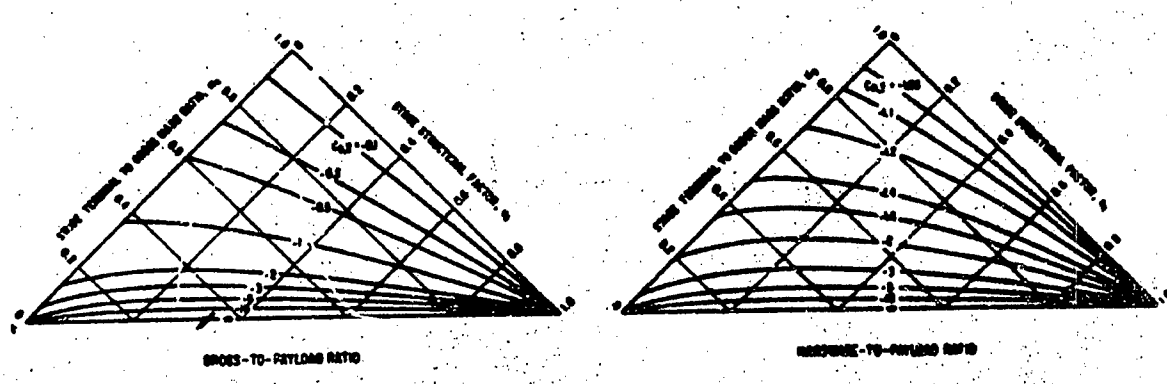
Figure 1. Booster Characteristics.



EFFECT OF STRUCTURAL FACTOR VARIATION

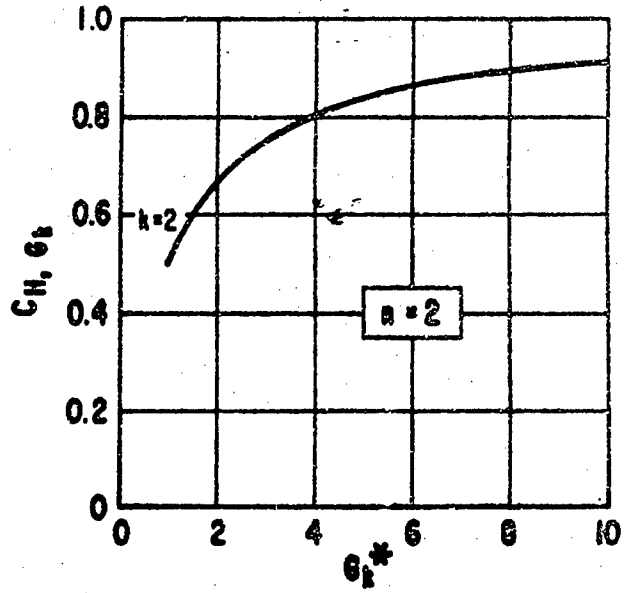
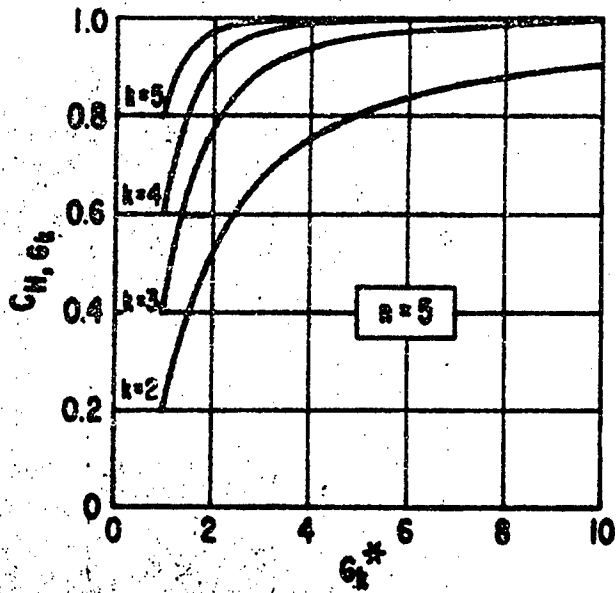


EFFECT OF TERMINAL VELOCITY VARIATION

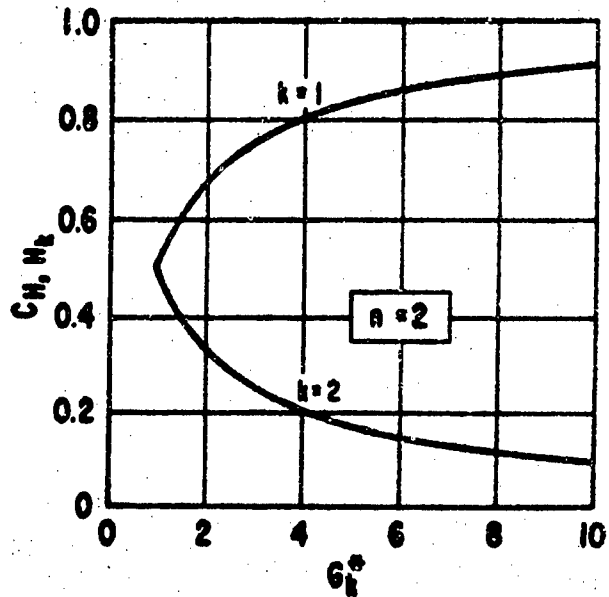
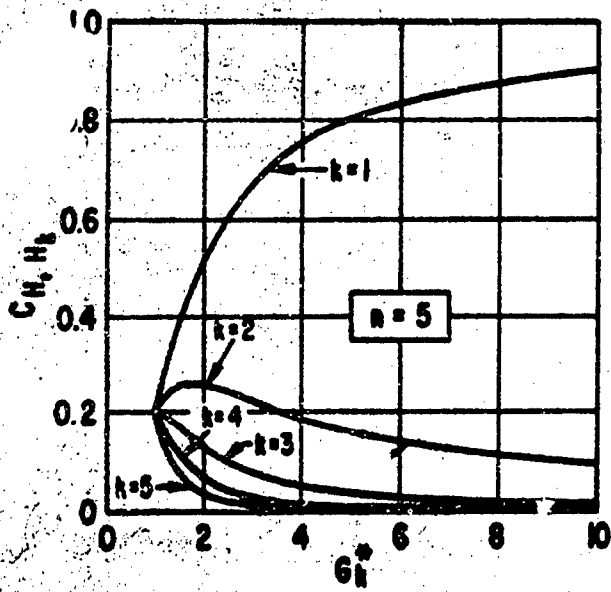


EFFECT OF AVERAGE SPECIFIC IMPULSE VARIATION

Figure 2. Single Stage Influence Coefficients.



Effect on H of Changes in G_k



Effect on H of Changes in H_k

Figure 3. Influence Coefficients for a Multistage Booster With n Similar Stages.

ADVANCED PROPELLANTS

(11 April 1967)

by

Ellis M. Landsbaum

Manager, Components and Propellants Section, Propulsion Department, Aerospace Corporation, El Segundo, California. Ph.D. in Chemical Engineering, Northwestern University, 1955. Formerly: Research Group Supervisor, Jet Propulsion Laboratory; member of ICRPG Static Test Panel and Solid Propellant Combustion Inability Working Groups, 1956-61. Technical publications in the fields of combustion, nozzles and instrumentation. Member of AIAA, ACS, Combustion Institute.

PERFORMANCE OF SOLID PROPELLANTS

Introduction

In order to understand what makes a solid propellant of high performance, let us first review the pertinent thermodynamics to determine what attributes one should seek. The standard specific impulse is equal to the exhaust velocity. For the ideal case one can write,

$$I_{sp} = \frac{v_e}{g} = \sqrt{\frac{2\gamma R T_c}{g(\gamma-1)M} \left[1 - \frac{P_e}{P_c} \right]^{(\gamma-1)/\gamma}} \quad (1)$$

The exhaust velocity is also equal to the enthalpy difference between chamber and nozzle exit,

$$v_e = 2g (H_c - H_e)^{1/2} \quad (2)$$

The enthalpy balance for the combustion process is,

$$\sum_P x_i (H_c - H_o + \Delta H_f) = \sum_R x_i (H_i - H_o + \Delta H_f) \quad (3)$$

This can also be written in terms of the heat of combustion,

$$\Delta H_c \sim \sum_R x_i \Delta H_f - \sum_P x_i \Delta H_f \quad (4)$$

For the ideal case the chamber temperature should be related to the heat of combustion,

$$\frac{\gamma R}{(\gamma-1)M} (T_c - T_o) = \frac{\Delta H_c}{T_c} \quad (5)$$

This line of reasoning circumvents the usual arguments for high temperatures and low molecular weights by placing the emphasis on high heats of combustion per gram.

The heat of combustion is equal to the heat of formation of the reactants minus the heat of formation of the products. The heat of formation of the reactants can be at best zero or slightly positive. If they were significantly positive they would undoubtedly be unstable and, therefore, not be suitable for use. Therefore, there is an upper limit to the heat of formation of the reactant. The heat of formation of the products on the other hand can be as negative as possible. It is logical, therefore, to first examine products that give highly negative heats of formation and later to determine if there are suitable reactants composed of constituents of the product.

The heat of combustion per gram of products has been calculated for the lower atomic weight elements with fluorine and oxygen and is presented in Figures 1 and 2 and Table I (Ref. 1). The same calculation for an even larger number of elements has been done by Glassman (Ref. 2). It will be noted that many of the results are given for solid products. If only gaseous products had been used the numbers would have been much lower. Indeed, BeO (g) is then endothermic and would be on the negative side of the scale. However, if one reconsiders Equation 2, it will be noted that one is interested in the enthalpy difference between chamber and nozzle exit. Therefore, in considering heats of combustion one is interested in the heats of combustion of the products as they will exist at the nozzle exit. Unfortunately, these products that supply good heats of combustion are not good working fluids and other ingredients of the propellant will have to supply the working fluids. The major advantage of liquid propellants over solid propellants is primarily the fact

that they supply a much better working fluid, one of a lower molecular weight.

In practice only the metal oxide as products will be of interest. The fluorines would be of interest, but it is difficult to get fluorines in a solid propellant. There are some fluorocarbon compounds, but they do not make good binders. If the metals would preferentially combine with chlorine this would be desirable as this might then free hydrogen to provide more working fluid. It is quite obvious that if one desires a metal oxide as a product the metal can be added as an ingredient. The metals as ingredients are examined in Table II. The table contains some other metals besides those given in the Figures. Scanning the list one sees that there is not a great deal of choice. Hydrogen is a gas. Lithium has a low density and is very reactive. Beryllium does not have too low a density but the products are toxic. The density of boron is good but it is slow burning and difficult to handle. (Ref. 2). Magnesium has a low density compared to aluminum. Aluminum has the best density of the lower atomic weight elements and has no other problems. Silicon has a lower density and phosphorus is poisonous. The heavier metals are primarily distinguished by their high density but they have lower heats of combustion and are approximately equivalent to carbon. The carbon, of course, is added as part of the binder. It is reasonably obvious why aluminum was one of the first propellant additives. Of the other elements, it is difficult to tell whether boron or beryllium would be a better additive.

One can also add the metals to the propellant as hydrides. There is no point in considering other inorganic compounds since these will all have large negative heats of formation. One might also consider some of the metal organic compounds; however, these are usually rather unstable. A number of solid metal hydrides are listed in Table III (Ref. 1). It is not quite so simple to determine which might be the better metallic hydride. Beryllium hydride has a possibility of having a slightly positive heat of formation, therefore, it would be like having beryllium with the added advantage of the hydrogen. On the other hand, it has a very low density. At this time it might be a good idea to point out that it is not entirely clear whether the favorable properties should be based on per gram basis or on a unit volume basis, since with propellant manufacture, density plays such a significant role. Aluminum hydride has a much better density, therefore, it is not clear which of these two would be best, assuming that heats of formation are correct. There is another group of materials with slightly lower ΔH_f . These are LiAlH_4 , LiH , $\text{Mg}(\text{AlH}_4)_2$ and MgH_2 . The $\text{Mg}(\text{AlH}_4)_2$ looks best because of its high density and good hydrogen content. To make a better evaluation, detailed performance calculations would have to be made since the differences between any of the above ingredients would be small.

Oxidizers

The current and earlier oxidizers are well known. First came KCl , followed by KClO_4 and then by NH_4ClO_4 which is in extensive use today. NH_4NO_3 is also in current use. The double-base propellants are primarily microcellulose and nitroglycerine with some additional higher energy additives. Aluminum and NH_4ClO_4 are also being added to double-base propellants. It

appears worthwhile to try to increase ΔH_c by reducing the ΔH_f of the reactants, primarily the oxidizer. Another possibility would be to have an oxidizer built around fluorine since as the figure indicated the metallic fluorides have very favorable ΔH_f . This, however, does not seem to be with good oxygen contents and possibly increased hydrogen content and added energy.

A great number of nitrate and perchlorate compounds are listed by Urbanski (Ref. 3). Some of their properties are given in Table IV. Unfortunately, there is a great deal of missing data. It does not appear that there are any nitrates that are particularly better than NH_4NO_3 . Hydrazine nitrate has a better ΔH_f but has a relatively low melting point and even lower density. The lower density of ammonium nitrate as opposed to NH_4ClO_4 is one of the problems in using it. The hydrazine nitrate is also sensitive. Thiourea nitrate has a better ΔH_f but its molecular constituents are not too favorable. A similar situation exists with the perchlorates. Hydrazine perchlorate has a good density and ΔH_f has been improved. However, it is probably more sensitive, similar to hydrazine nitrate. Nitrosyl perchlorate has even a better density but decomposes at rather low temperatures. Nitronium perchlorate has a positive heat of formation and a very good density. It is, however, very hygroscopic. It does have the disadvantage that it is removing hydrogen, although it is replacing it by oxygen. Ethylenediamine diperchlorate does not appear to have any significant advantages over NH_4ClO_4 . It does appear that there are many oxidizers to choose from.

Theoretical Impulse Calculations

Theoretical impulse calculations have been made for a number of the hydrides with NH_4ClO_4 and NO_2ClO_4 (Ref. 4). These are presented in Figures 3 through 6. The specific impulses increase with increasing exothermicity except that LiH appears to be out of place. This is probably due to its low ΔH_f which with its low molecular weight when placed on a gram basis is more significantly different. It will be noted, Figure 4, that AlH_3 produces a higher chamber temperature than BeH_2 and the higher specific impulse of BeH_2 is due to its lower molecular weight gases. The results with NO_2ClO_4 are given in Figures 5 and 6. There appears to be little change in specific impulse with the metal hydrides, although the maximum shifts to lower oxidizer requirements. It will be noted that in general higher temperatures and higher molecular weights are obtained with the metal hydrides plus NO_2ClO_4 . Apparently, as discussed under the oxidizer section, the increase ΔH_f is balanced by the loss of hydrogen. There is an increase with CH_2 . This is probably due to a more favorable balance in the water gas reaction. The comparison between NH_4ClO_4 and NO_2ClO_4 also holds true at higher expansion ratios.

The effect of γ (specific heat ratio) has been of interest since lower γ give higher vacuum impulses. Fig. 7 is a plot of the ratio of the vacuum thrust coefficient to the thrust coefficient at standard conditions against expansion ratio. The specific impulse will have the same ratio. The effect of gamma is rather small. However, if specific impulse measurements are made at low ϵ the estimation of high ϵ value can be overly optimistic if too low a gamma is assumed. This type of estimation is rather crude by today's standards. The thermodynamic calculations should be used to estimate efficiencies and coupled with two-phase flow losses for extrapolation purposes.

Additional insight into the effects of ΔH_f and added H_2 may be obtained by taking a composition and arbitrarily varying these quantities. This has been done with propellants consisting of 20 percent CH_2 , 16 percent Al and 64 percent NH_4ClO_4 . The assumptions and the results of the calculation are given in Table V and Figure 8. The ΔH_f of NH_4ClO_4 was varied from 0 to -140 Kcal/mole. Averaging the results gives a change in I_{sp} of 30 sec for a change of 38 Kcal/100 gms of propellant. The effect of changing the hydrogen was surprisingly less. This indicates that the effects of changing to Al or AlH_3 or to Be to BeH_2 in a real propellant will be much less than the effects indicated in Figures 3 and 5.

This can readily be seen by examining the results of calculations from Siegel and Schieler (Ref. 1) shown in Table VI. The chamber and exhaust products are shown in Table VII. Unfortunately, these calculations are for solids loading that will be difficult to obtain. Nevertheless, one can see that the differences between propellants are considerably less than that indicated in Figure 3. Note that the gains of adding metals to the polyethelene are primarily due to increases in chamber temperature. The gains due to adding the hydrides are a result of decreases in molecular weight.

Real Propellants

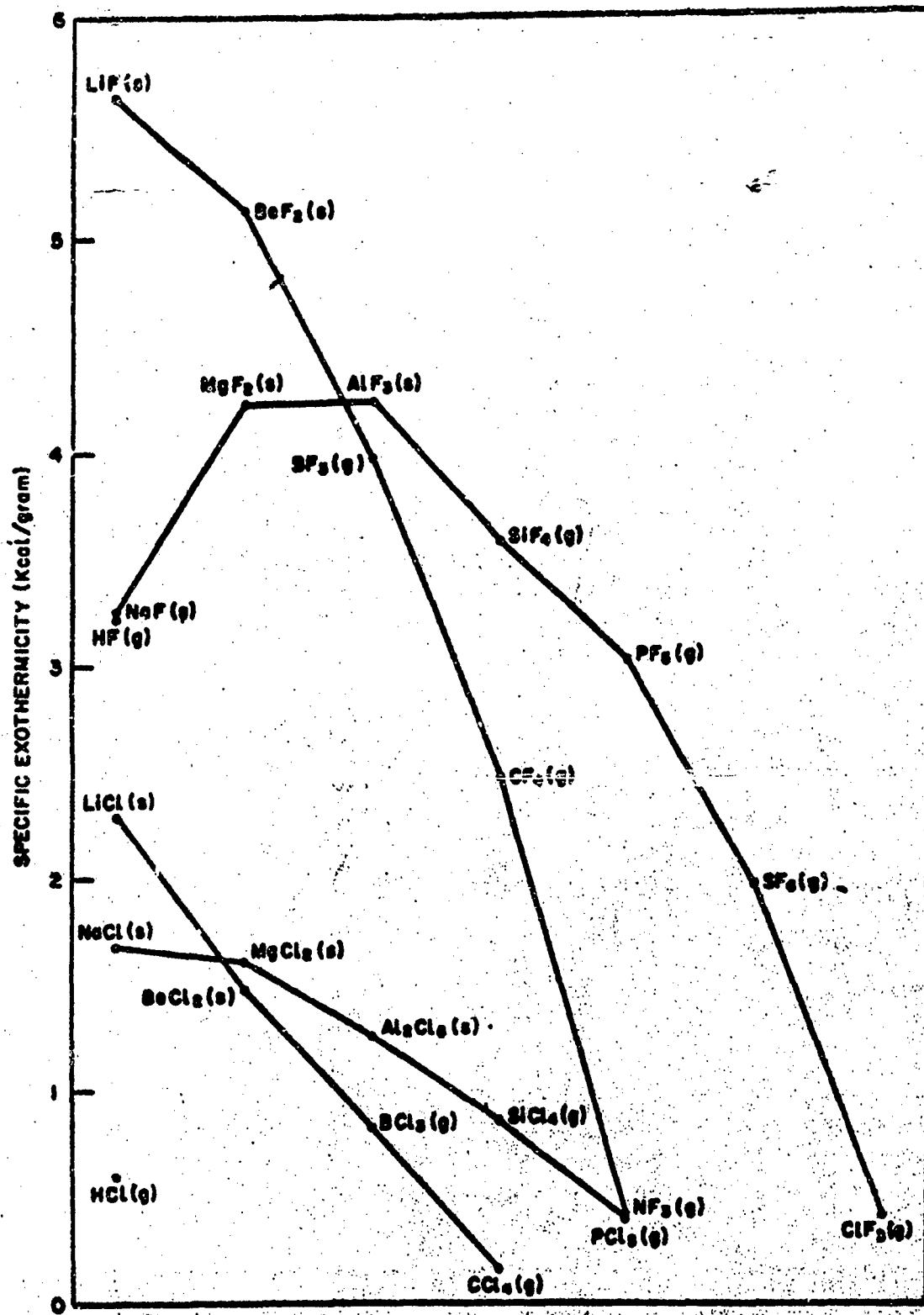
The first binders were asphalt resins. The first polymeric binders were the polysulphides. The initial polysulphide binders were not too good due to the low hydrogen content and a high sulphur content leading to high molecular weight exhaust gases. Performance was gradually increased with a polysulphide propellant by increasing the hydrogen content and reducing the sulphur content. It was, also, difficult to incorporate metals because of the water formed during the curing reaction. Polyurethane binders were the next major development. Polyurethanes are formed by the condensation polymerization of an isocyanate and a diol. This eliminates the secondary problem of water elimination. The polyurethane polymerization is better characterized than that of the polysulphide so that one can much more accurately construct the desirable physical properties and control them.

The polybutadiene type binders are the most recent and currently the most widely used. The advantage of this type of binder over the polyurethane type is a lower density and a better hydrogen content. An additional discussion of the binders can be found in Siegel and Schieler (Ref. 1). Typical binder types are compared in propellant systems containing aluminum and ammonium perchlorate in Figure 9 (Ref. 5). As one moves from the pure fuel polybutadiene to binders containing increasing amount of oxygen, peak I_g is reached at progressively lower solids loadings. Polybutadiene is a better fuel than polyurethane showing a peak I_g approximately 3 units higher; however, the solids loading requirements to obtain peak I_g poses problems in propellant processing.

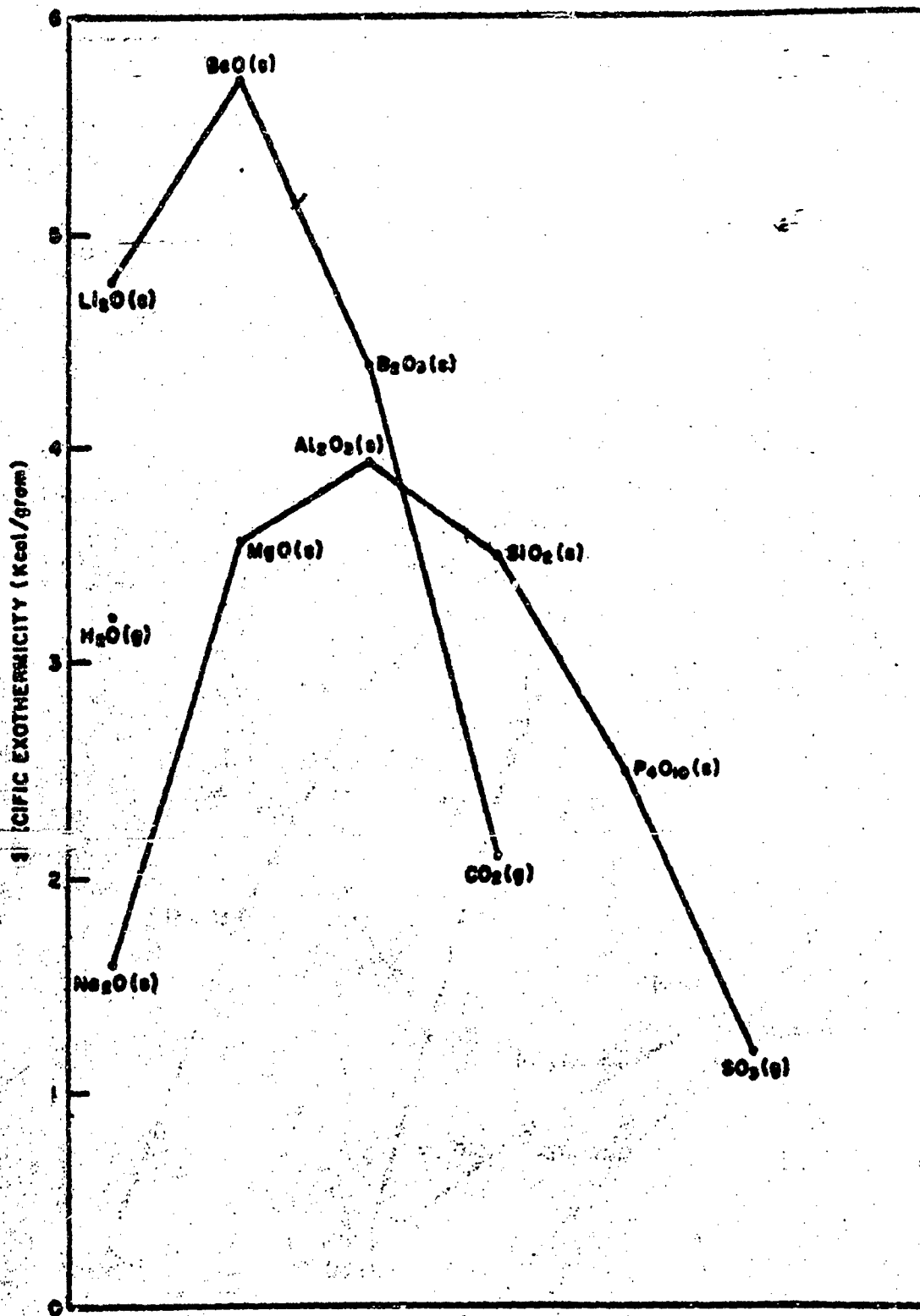
When nitroplasticizers of high oxygen content are added to polyurethane the magnitude of the peak I_g does not change but is achieved with a lower portion of solid oxidizer. The use of nitrate plasticizers and polymers, such as nitroglycerine and nitrocellulose, not only shifts the peak I_g to a lower solids loading, but also increases the peak value (compared with polyurethane). The disadvantage of propellants with peak I_g and low solids loadings is lower density and consequently lower impulse per unit volume as the solids have higher density than the binder. This is extremely important in volume-limited rocket motors. Theoretical specific impulse contours for a PBD propellant are shown over a range of compositions in Figure 10.

REFERENCES

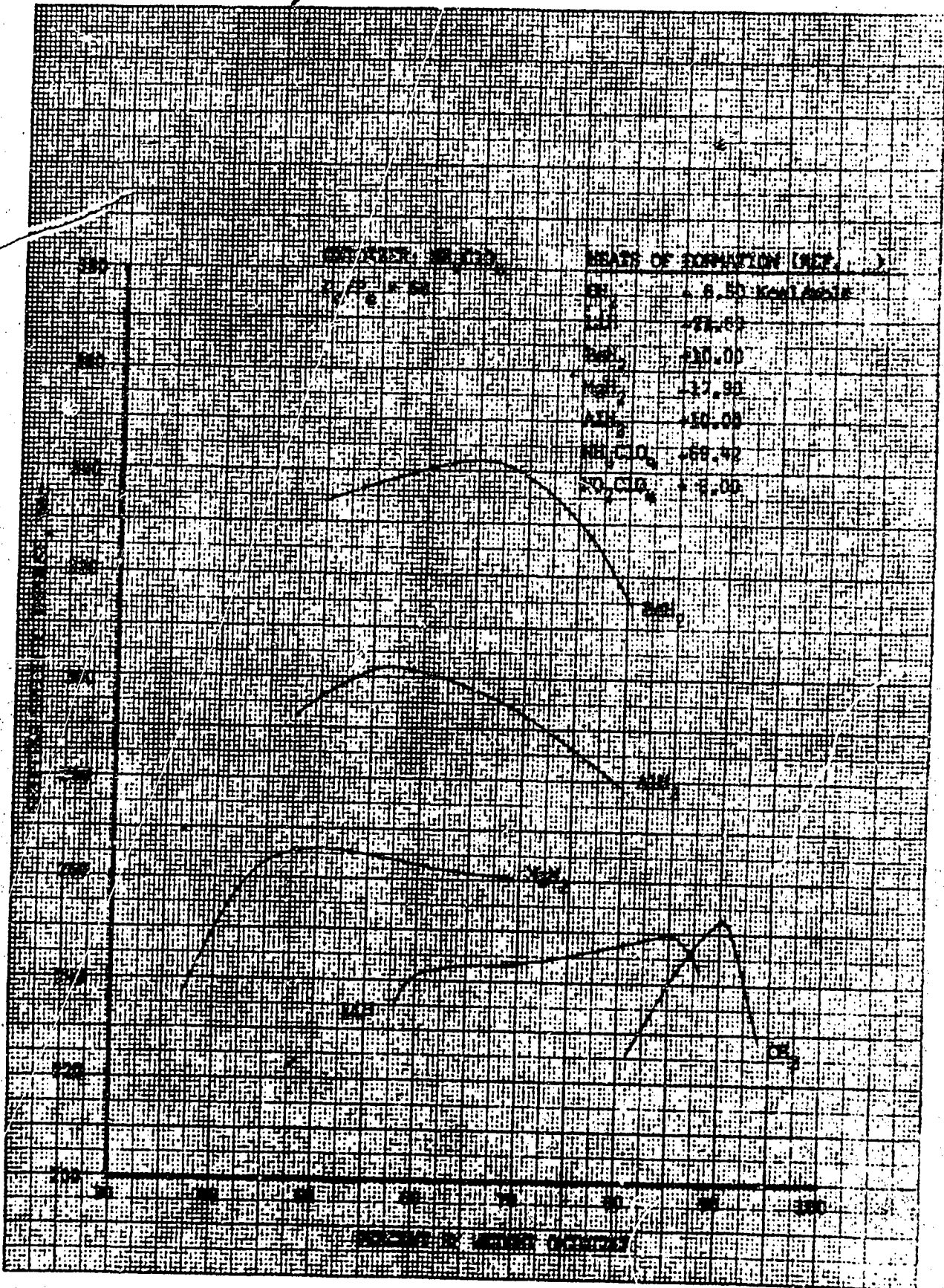
1. Siegel, B. and Schieler, L. "Energetics of Propellant Chemistry," Wiley, 1964.
2. Glassman, I. - "The Chemistry of Propellants," American Scientist, 53 (4) pages 508-524, December 1965.
3. Urbanski, T. G., "Chemistry and the Technology of Explosives," Volume II, pages 450 - 495, Pergamon Press, 1965.
4. Dobbins, T. O., "Thermodynamics of Rocket Propulsion and Theoretical Evaluation of Some Prototype Propellant Combinations," WADC TR-59-757, December 1959, ASTIA AD-232-465.
5. Klager, K. and Wrightson, J. M., "Recent Advances in Solid Propellant Binder Chemistry," International Conference Mech. Chem. Solid Propellants, Purdue, University, April 1965.



SPECIFIC EXOTHERMICITY OF THE FLUORIDES AND CHLORIDES OF THE LIGHT ELEMENTS



**SPECIFIC EXOTHERMICITY OF THE OXIDES
OF THE LIGHT ELEMENTS**



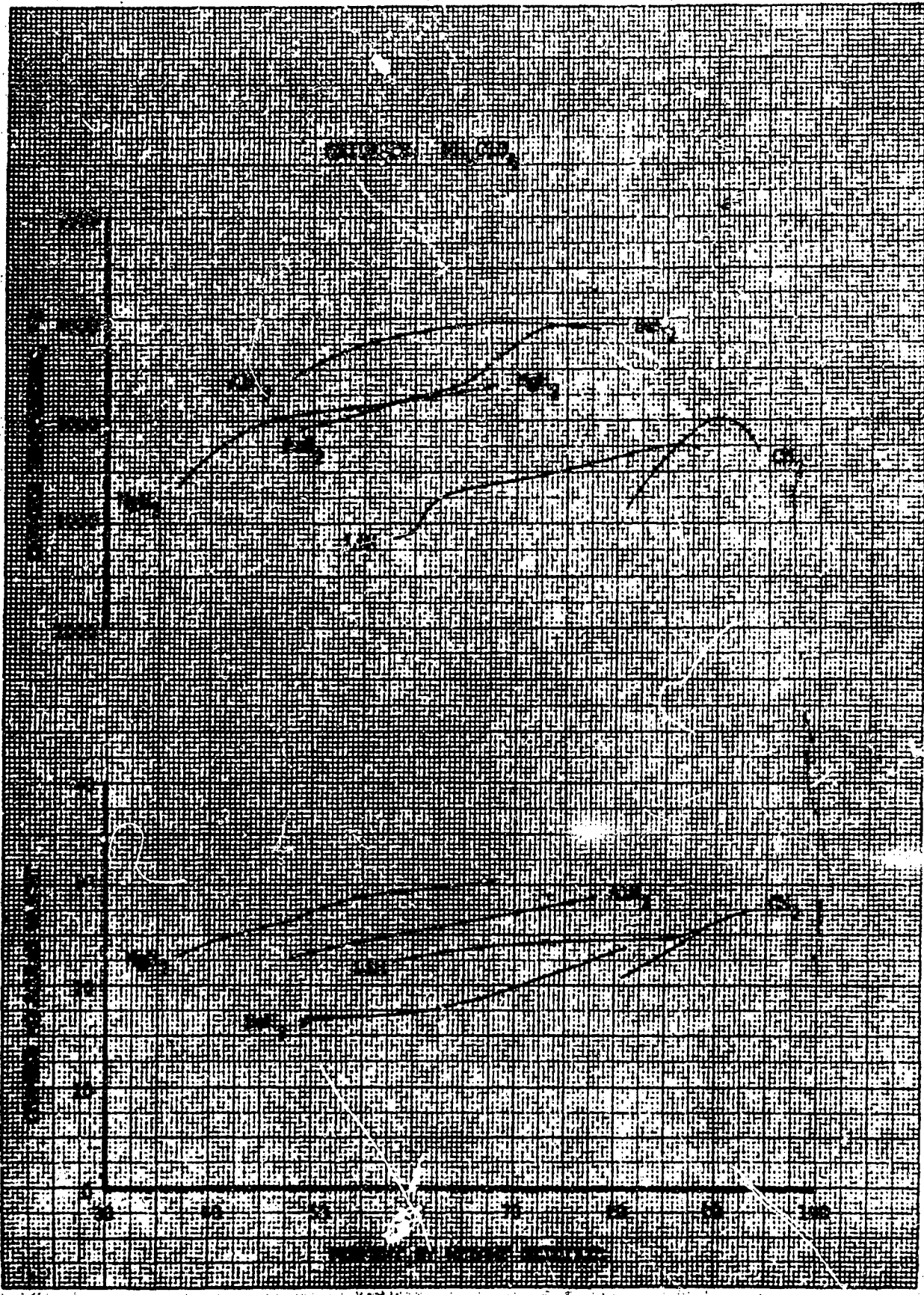
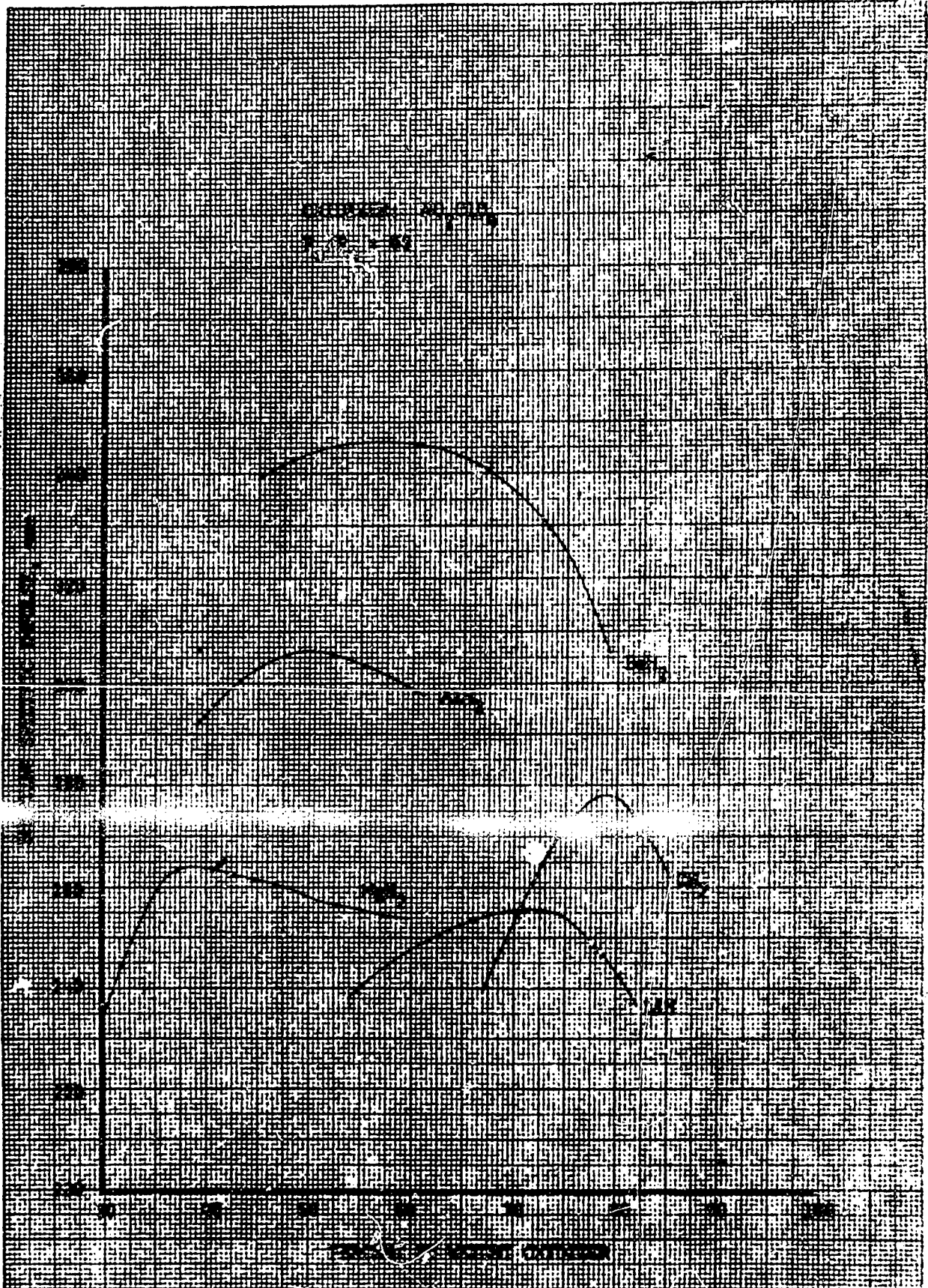


FIGURE 4



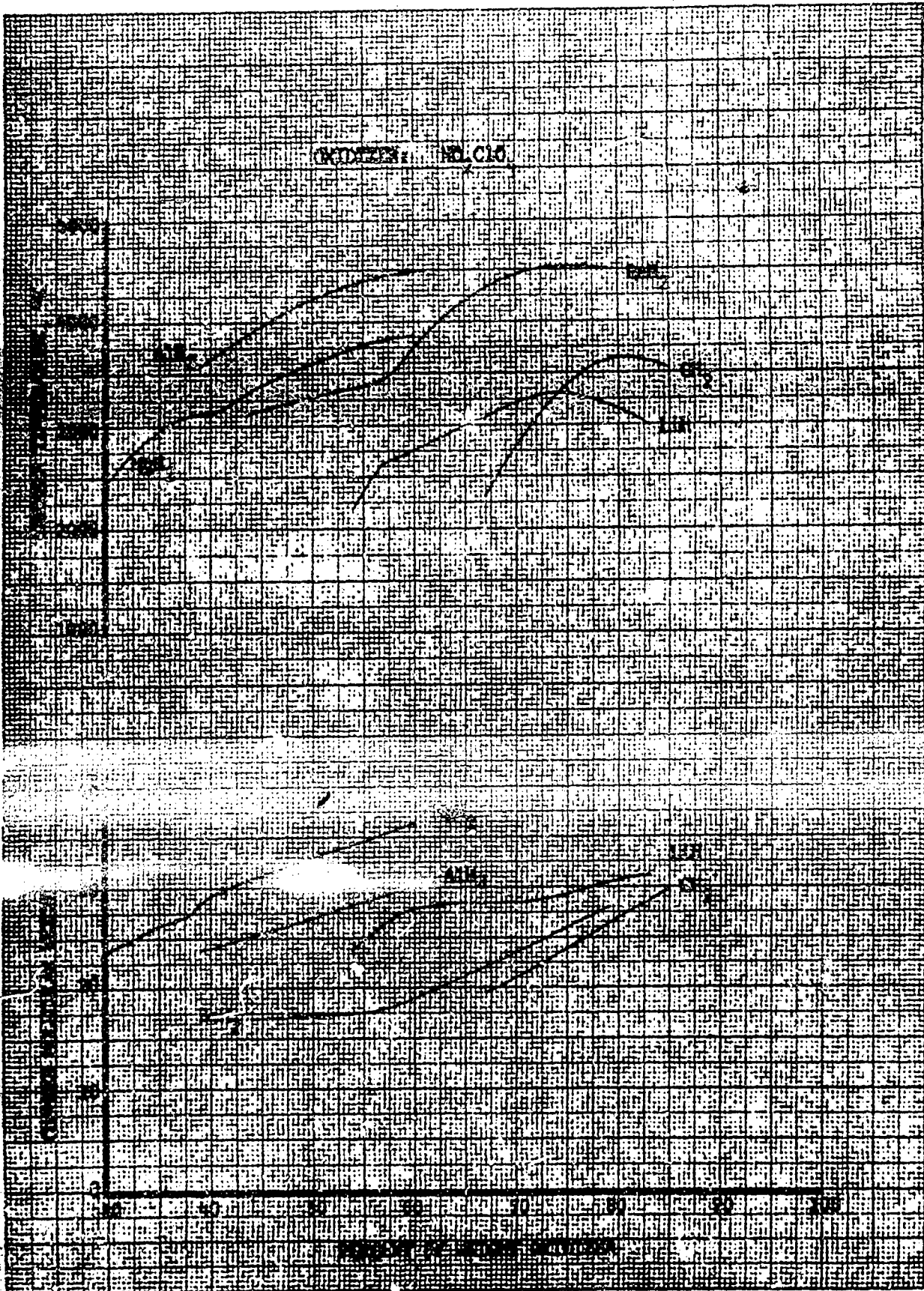
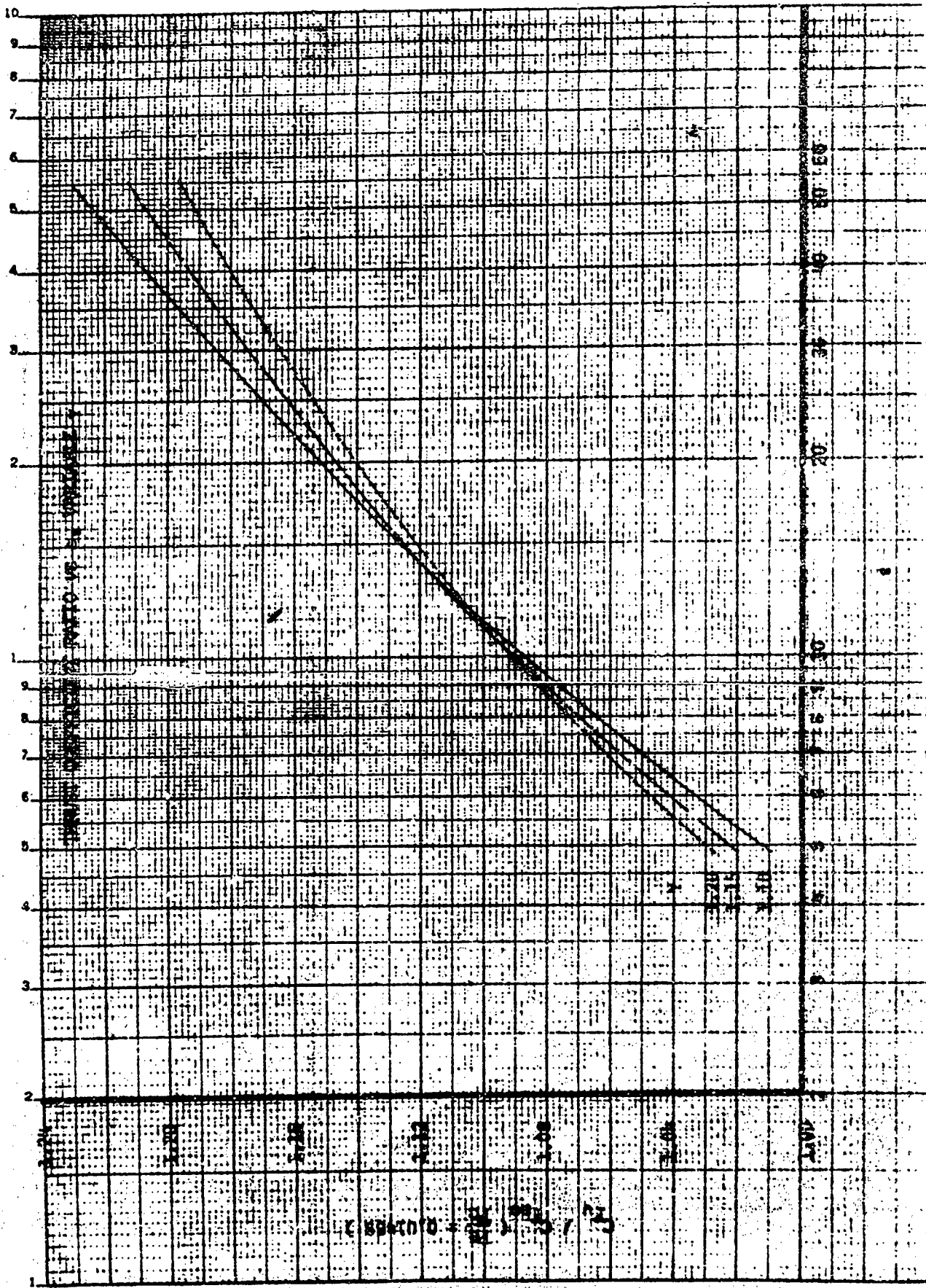
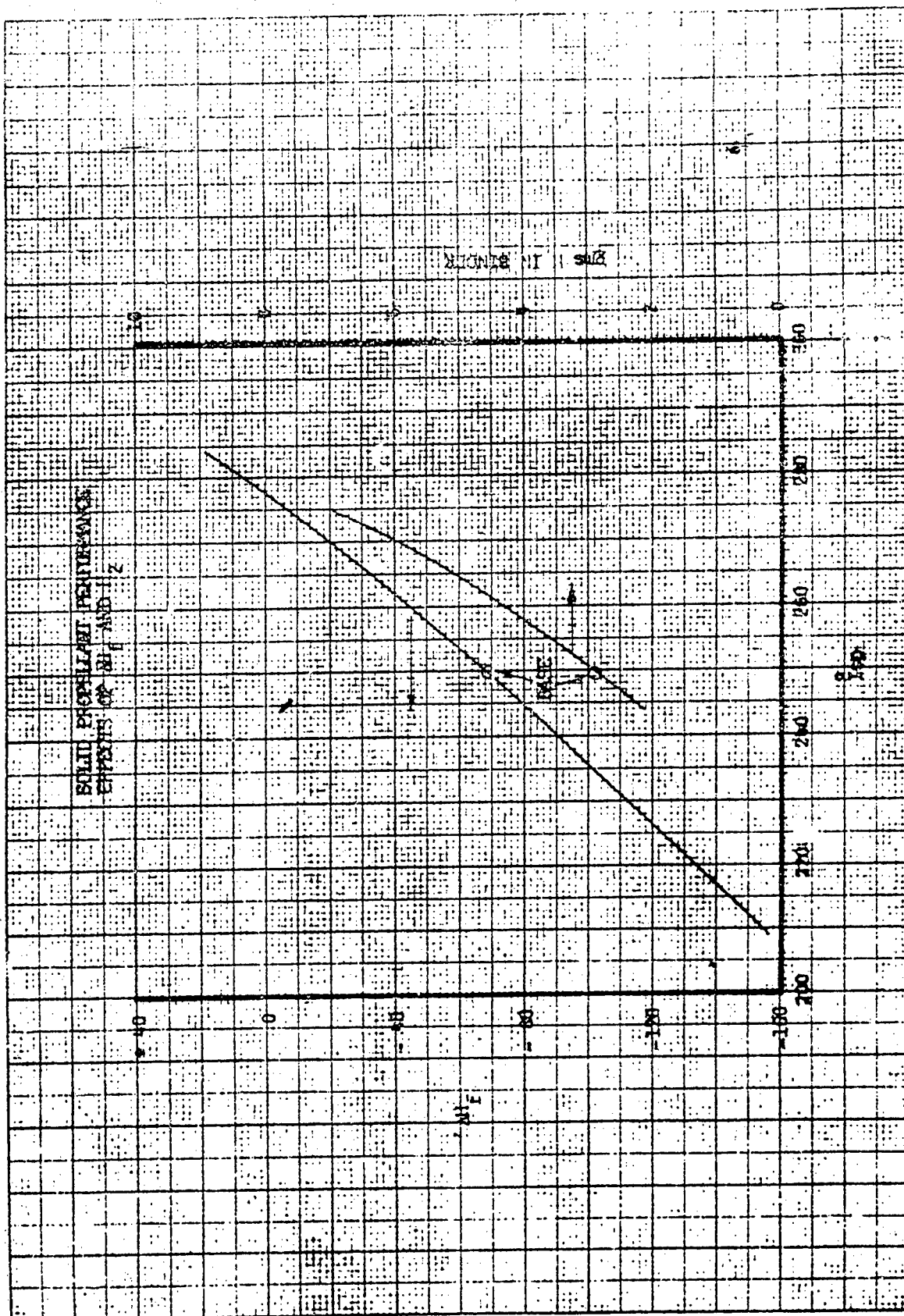


FIGURE 6





THEO. λ_s VS WT% SOLIDS
 OPT. AL: NH_4ClO_4

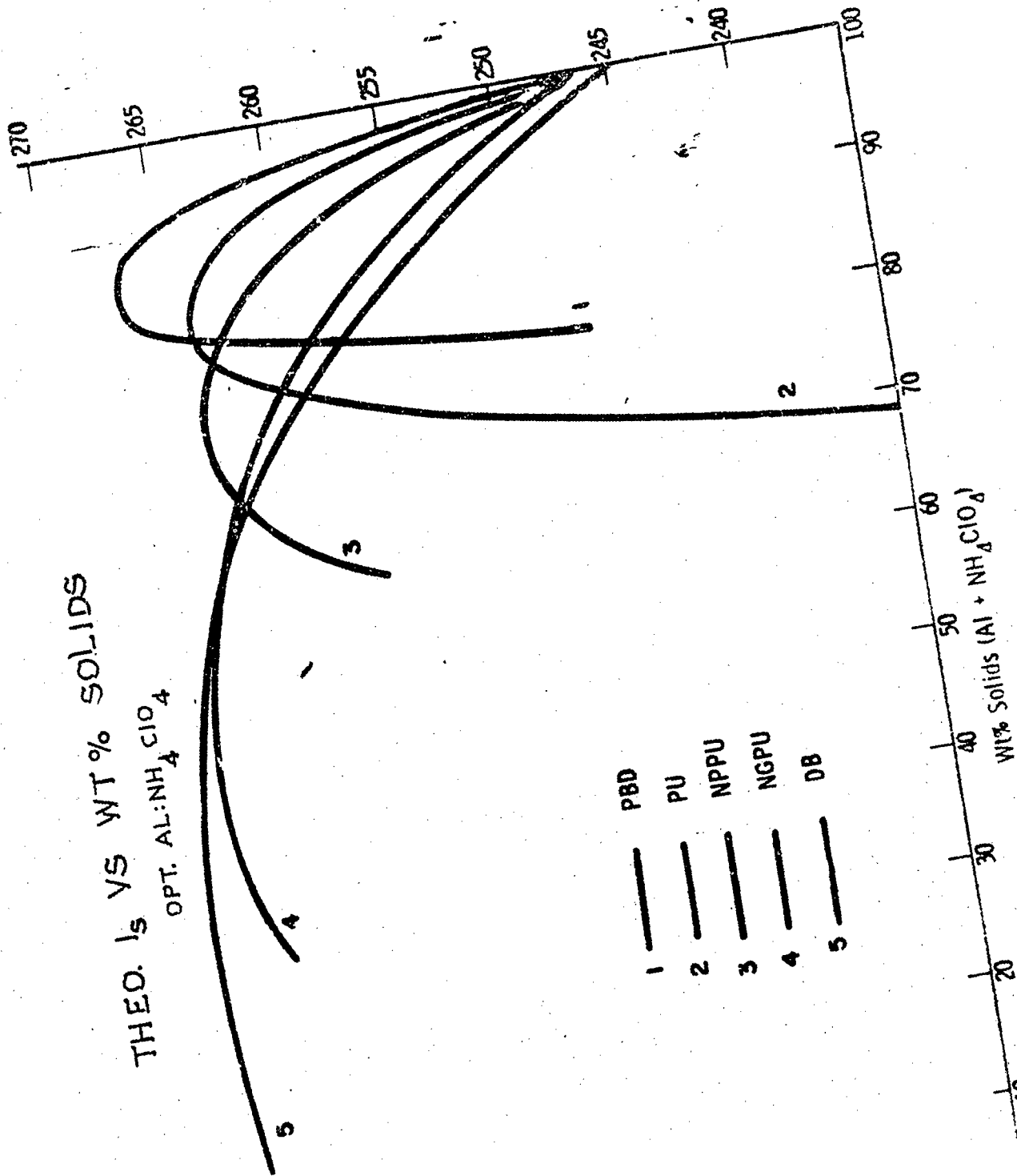


FIGURE 9

THEO. I_s AP-AI-PBD PROP.

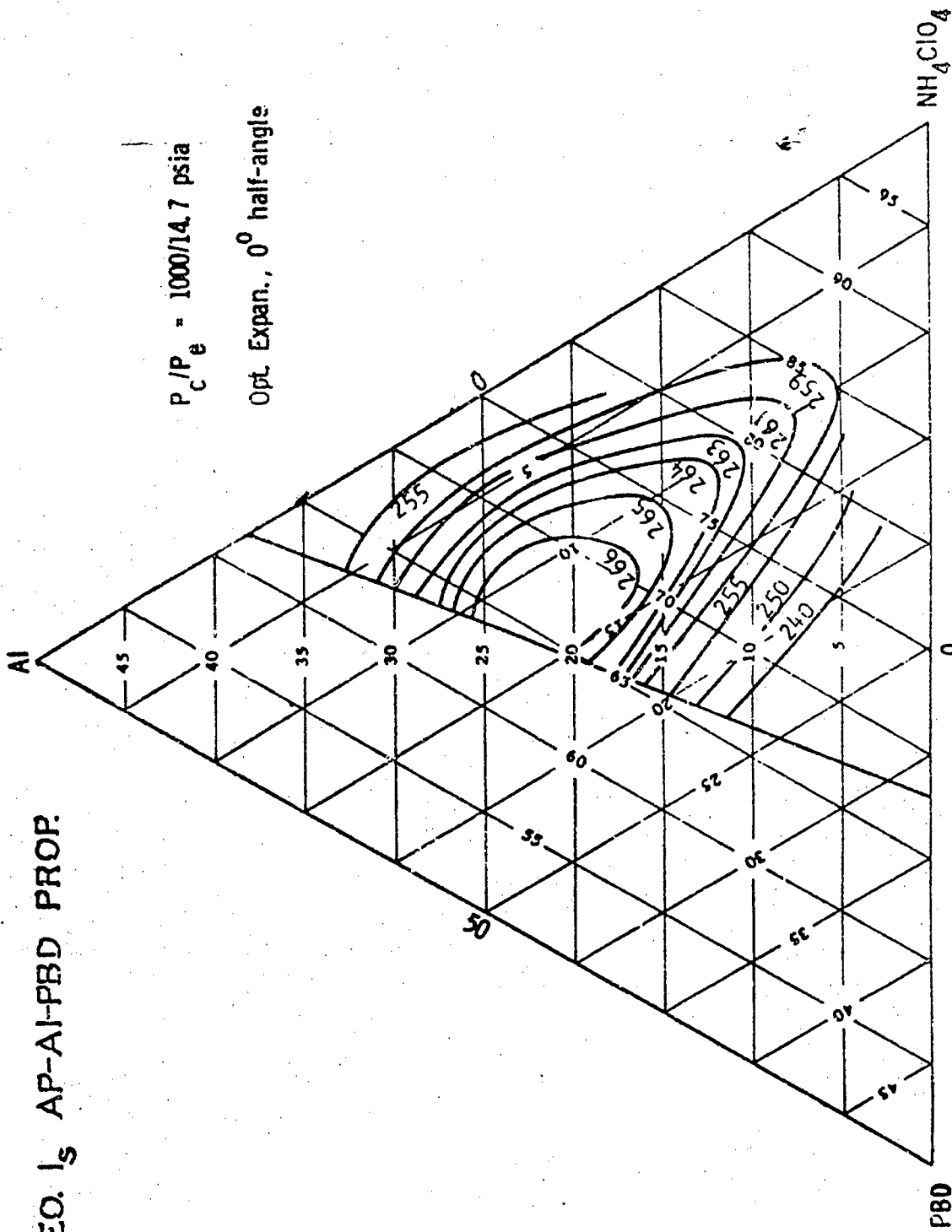


FIGURE 10

TABLE I

Components of Standard Heats of Formation at 25°C°

Compound	Binding energy (kcal/mole)	(Crystallization) energy (kcal/mole)	Standard ΔH_f (kcal/mole)	Standard ΔH_f (kcal/gram)
LiF(s)	137 ± 2.5	66 ± 2.5	-146	-5.63
NaF(s)	112	69	-136	-3.24
i.l. ₂ O(s)	170 ± 6	109 ± 5	-142.5	-4.77
Na ₂ O(s)	—	—	-99.4	-1.60
BeF ₂ (s)	301 ± 5	57 ± 5	-241 ± 5	-5.13
MgF ₂ (s)	250 ± 4	85 ± 7	-262.5 ± 3	-4.21
BeO(s)	108	174	-143	-5.72
MgO(s)	91	148	-144	-3.57
BF ₃ (g)	459 ± 6.5	Gas	-270 ± 2	-3.98
AlF ₃ (s)	420 ± 6	71 ± 5	-356 ± 5	-4.24
B ₂ O ₃ (s)	654 ± 9	95	-305	-4.38
α-Al ₂ O ₃ (s)	—	—	-400	-3.92
CF ₄ (g)	465 ± 2	Gas	-218 ± 1	-2.48
SiF ₄ (g)	559 ± 13	Gas	-373	-3.58
CO ₂ (g)	384.2 ± 0.5	Gas	-94.1	-2.14
CO(g)	257 ± 0.6	Gas	-26.4 ± 0.6	-0.94
SiO ₂ (s)	303 ± 12	136	-210	-3.49
NF ₃ (g)	199 ± 3.5	Gas	-29.7 ± 2	-0.42
PF ₃ (g)	595.7 ± 2	Gas	-381	-3.62
PF ₅ (g)	346 ± 11	Gas	-209 ± 10	-2.38
NO(g)	151 ± 1	Gas	+21.7	+0.72
P ₂ O ₅ (s)	—	—	-703 ± 3	-2.48
SF ₆ (g)	467.5 ± 2.5	Gas	-288.5 ± 0.7	-1.98
SO ₂ (g)	339 ± 1	Gas	-94.5	-1.18
ClF ₃ (g)	124.5 ± 3.5	Gas	-39 ± 1	-0.42
ClO ₂ (g)	123 ± 3.5	Gas	+25 ± 1.5	+0.34
F ₂ CO(g)	419 ± 4	Gas	-151 ± 3	-2.29
(OBF ₂) ₂ (s)	1201 ± 21	20 ± 4.5	-588 ± 2.5	-4.28
BN(s)	94.5 ± 18	211 ± 14	-60.3 ± 0.8	-2.43

* The data in this table, with the exception of PF₅, were calculated from data in the JANAF Thermochemical Tables, Dow Chemical Co., Midland, Mich., December 31, 1961. The standard heats of formation of the gaseous molecules can be calculated from the data on binding energies by use of the appropriate heats of atomization of the elements. The latter, in kcal/mole, are as follows: Li, 38.4 ± 4; Na, 25.8; Be, 78.3 ± 0.5; Mg, 35.3; B, 132.6 ± 4; Al, 78 ± 0.4; C, 170.9 ± 0.5; Si, 110 ± 12; N, 113 ± 1; P, 79.8; S, 65.7 ± 0.6; Cl, 29 ± 2; F, 18.9 ± 0.2; O, 59.6. The heat of formation for PF₅ was taken from J. T. Armstrong and L. A. Krieger's, *Progress in International Research on Thermodynamics and Transport Properties*, Academic Press, New York (1962).

TABLE II

Metal Additives

	Density ρ (gm/cc)	Comments
H, Hydrogen	—	Gas
Li, Lithium	0.53	Reactive
Be, Beryllium	1.85	Toxic products
B, Boron	2.45	Slow Burning
Mg, Magnesium	1.74	Low Density
Al, Aluminum	2.70	—
Si, Silicon	2 - 2.4	—
P, Phosphorous	2.20 (Red) 1.82 (Yellow)	Poisonous
Ca, Calcium	1.55	Reactive
Ti, Titanium	4.50	—
C, Carbon	~ 2	—
V, Vanadium	5.96	—
Zr, Zirconium	6.4	—

TABLE III
 SOLID HYDRIDES
 (Ref 8)

		Hydrogen g/cc	Density g/cc	ΔH_f kcal/mole
Aluminum hydride	AlH_3	0.130	1.3	- 3 ± 10
Beryllium hydride	BeH_2	0.109	~ 0.6	10 (?)
Lithium aluminum hydride	$LiAlH_4$	0.097	0.92	- 24.1
Lithium amide	$LiNH_2$	0.103	1.18	- 43.5
Lithium borohydride	$LiBH_4$	0.122	0.66	- 44.6
Lithium hydride	LiH	0.104	0.82	- 21.7
Magnesium aluminum hydride	$Mg(AlH_4)_2$	0.151	1.63	- 23.1
Magnesium hydride	MgH_2	0.110	1.45	- 18 ± 5

TABLE IV. OXIDIZER DATA

NITRATES	M.P. °C	Density gm/cm ³	ΔH_f kcal/cm mole	Stability	Hygroscopicity	Grade
Ammonium Nitrate NH_4NO_3	169.6	1.725	- 87.3	Excellent	Slightly	None
Ethylenediamine Dinitrate ($CH_2NH_3NO_3$) ₂	—	1.49	—	Excellent	Very high	—
Ethanolamine Dinitrate $NO_3NH_3(CH_2)_2NO_3$	103	—	—	Low	Higher	Low
Guanidine Nitrate ($(NH_2)_3NO_3$)	~ 215	—	- 91.1	—	—	Slight
Hexamethylenetetramine Dinitrate ($(CH_2)_6N_4(HNO_3)_2$)	160	—	—	—	—	—
Hydrazine Nitrate $NH_2NH_3NO_3$	70.7	1.62	- 59.0	Good	Less	Like 20
Methylaminenitrate $CH_3NH_3CAO_4$	195 (d)	0.9	—	Good	Higher	Low
Oxonium Nitrate $COHNO_3$	—	—	—	—	—	—
Tetramethyl Ammonium Nitrate (CH_3) ₄ NNO ₃	410	1.25	—	—	—	None
Thiourea Nitrate $C(NH_2)_2SNO_3$	410 (d)	—	- 74.5	—	—	—
Urea Nitrate $C(NH_2)_2OHNO_3$	125 (d)	1.59	- 114.8	Poor	—	None
<u>PERCHLORATES</u>						
Ammonium Perchlorate NH_4CAO_4	240 (d)	1.95	- 69.4	Excellent	—	—
Dicyandiamidine Perchlorate $C(NH)_3CONH_2H_2CAO_4$	—	—	—	—	—	—
Ethylenediamine Diperchlorate ($CH_2NH_3CAO_4$) ₂	—	—	- 68.5	—	High	High
Guanidine Diperchlorate $C(NH_2)_3CAO_4$	250	—	—	Excellent	None	Moderate
Hexamine Perchlorate (Hexamethylenetetramine) ($C_6H_{12}N_4H_3NHCAO_4$)	—	—	—	Low	—	Like Mercuric Picrate
Hydrazine Perchlorate $NH_2NH_3CAO_4$	~ 137	1.94	- 39.0	—	—	—
Lithium Perchlorate $LiCAO_4$	236	2.429	- 98	Very	High	None
Methylamine Perchlorate $CH_3NH_3CAO_4$	210	—	—	—	—	High
Nitrooyl Perchlorate NO_2CAO_4	< 100 (d)	2.169	- 41.8	Low	—	—
Nitronium Perchlorate NO_2ClO_4	135 (d)	2.22	8	—	Very	—
Potassium Perchlorate $KCAO_4$	—	2.524	- 103.6	Excellent	—	None
Pyridine Perchlorate	245	—	—	—	—	Moderate
Triphenylcarbonium Perchlorate (C_6H_5) ₃ CClO ₄	150	—	—	—	—	—

NOTE: Absence of data means not available in standard reference.

TABLE 1

SOLID PROPELLANT PERFORMANCE

Effects of ΔH_f and H_2

Run	ΔH_f kcal/mol	Binder	I_{SP}° , sec	T_c , °K	
1	-69.4	$[CH_2]_n$	249.7	2546	22
2	0	$[CH_2]_n$	277.7	3120	21
3	-140	$[CH_2]_n$	216.9	1996	22
4	-69.4	$[CH_4]_n$	264.5	2458	18
5	-69.4	$[CH_6]_n$	273.7	2375	16

TABLE VI

Performance of Solid Composite Propellants

Propellant (weight ratios)	T_c (°K)	M_c	T_b (°K)	M_b	I_p (max) (lb sec/lb, 1000/14.7 psi)
0.5 NH ₄ ClO ₄ , 0.5 (CH ₂) _n	1175	20.63	790	22.76	181
0.6 NH ₄ ClO ₄ , 0.4 (CH ₂) _n	1242	19.42	840	21.74	191
0.7 NH ₄ ClO ₄ , 0.3 (CH ₂) _n	1312	18.41	883	20.97	200
0.8 NH ₄ ClO ₄ , 0.2 (CH ₂) _n	2036	20.43	924	20.99	221
0.9 NH ₄ ClO ₄ , 0.1 (CH ₂) _n	3013	26.13	1615	26.85	252
0.95 NH ₄ ClO ₄ , 0.05 (CH ₂) _n	2529	27.47	1690	27.72	219
0.81 NH ₄ ClO ₄ , 0.09 (CH ₂) _n , 0.10 Al	3433	28.54	2147	29.78	261
0.765 NH ₄ ClO ₄ , 0.085 (CH ₂) _n , 0.15 Al	3621	29.83	2349	31.42	264
0.72 NH ₄ ClO ₄ , 0.08 (CH ₂) _n , 0.20 Al	3784	31.17	2490	33.21	266
0.81 NH ₄ ClO ₄ , 0.09 (CH ₂) _n , 0.10 Ba	3653	27.87	2619	29.23	278
0.765 NH ₄ ClO ₄ , 0.085 (CH ₂) _n , 0.15 Ba	3860	28.61	2838	30.83	282
0.72 NH ₄ ClO ₄ , 0.08 (CH ₂) _n , 0.20 Ba	3819	28.96	2844	30.26	280
0.765 NH ₄ ClO ₄ , 0.085 (CH ₂) _n , 0.15 AlH ₃	3346	24.91	1943	25.53	273
0.765 NH ₄ ClO ₄ , 0.085 (CH ₂) _n , 0.15 BaH ₂	3330	21.44	2193	22.84	303

TABLE VII

Combustion Products Corresponding to Propellants

Propellant	Fractions of products at T_0	Mole fractions of products at T_1
0.5 NH_4ClO_4 , 0.5 $(\text{CH}_2)_n$	0.274 H_2 , 0.273 $\text{Cl}(s)$, 0.130 CH_2 , 0.103 CO , 0.096 H_2O , 0.064 HCl , 0.032 N_2 , 0.028 CO_2	0.348 $\text{Cl}(s)$, 0.224 H_2 , 0.152 H_2O , 0.123 CH_2 , 0.063 HCl , 0.043 CO_2 , 0.032 N_2 , 0.014 CO
0.6 NH_4ClO_4 , 0.4 $(\text{CH}_2)_n$	0.322 H_2 , 0.185 CO , 0.135 $\text{Cl}(s)$, 0.093 CH_2 , 0.084 HCl , 0.084 H_2O , 0.042 N_2 , 0.032 CO_2	0.279 H_2 , 0.267 $\text{Cl}(s)$, 0.145 H_2O , 0.081 HCl , 0.077 CH_2 , 0.070 CO_2 , 0.041 CO , 0.041 N_2
0.7 NH_4ClO_4 , 0.3 $(\text{CH}_2)_n$	0.370 H_2 , 0.305 CO , 0.109 HCl , 0.069 H_2O , 0.061 CH_2 , 0.034 N_2 , 0.032 CO_2	0.322 H_2 , 0.144 $\text{Cl}(s)$, 0.130 H_2O , 0.106 HCl , 0.099 CO_2 , 0.097 CO , 0.033 N_2 , 0.047 CH_2
0.8 NH_4ClO_4 , 0.2 $(\text{CH}_2)_n$	0.278 H_2 , 0.249 CO , 0.222 H_2O , 0.139 HCl , 0.070 N_2 , 0.043 CO_2	0.337 H_2 , 0.150 H_2O , 0.150 CO , 0.143 HCl , 0.136 CO_2 , 0.071 N_2 , 0.014 CH_2
0.9 NH_4ClO_4 , 0.1 $(\text{CH}_2)_n$	0.453 H_2O , 0.183 HCl , 0.126 CO_2 , 0.098 N_2 , 0.061 CO , 0.031 H_2 , 0.016 OH , 0.014 Cl , 0.004 H , 0.003 NO , 0.003 O	0.471 H_2O , 0.206 HCl , 0.161 CO_2 , 0.103 N_2 , 0.031 CO , 0.029 H_2
0.95 NH_4ClO_4 , 0.05 $(\text{CH}_2)_n$	0.435 H_2O , 0.204 HCl , 0.171 O_2 , 0.108 N_2 , 0.097 CO_2 , 0.045 Cl , 0.009 OH , 0.007 NO	0.439 H_2O , 0.216 HCl , 0.130 O_2 , 0.112 N_2 , 0.099 CO_2 , 0.004 Cl
0.81 NH_4ClO_4 , 0.09 $(\text{CH}_2)_n$, 0.10 Al	0.336 H_2O , 0.164 HCl , 0.124 CO , 0.108 H_2 , 0.092 Cl , 0.050 CO_2 , 0.056 $\text{Al}_2\text{O}_3(s)$, 0.026 OH , 0.020 Cl , 0.020 H , 0.004 O_2 , 0.004 NO , 0.003 O	0.366 H_2O , 0.193 HCl , 0.108 CO , 0.107 H_2 , 0.097 N_2 , 0.074 CO_2 , 0.052 $\text{Al}_2\text{O}_3(s)$, 0.002 Cl
0.765 NH_4ClO_4 , 0.085 $(\text{CH}_2)_n$, 0.15 Al	0.260 H_2O , 0.160 H_2 , 0.151 HCl , 0.139 CO , 0.088 N_2 , 0.075 $\text{Al}_2\text{O}_3(s)$, 0.036 H , 0.028 CO_2 , 0.027 OH , 0.022 Cl , 0.004 O , 0.003 NO , 0.003 O_2 , 0.002 AlCl_3 , 0.002 AlCl	0.293 H_2O , 0.184 HCl , 0.153 H_2 , 0.133 CO , 0.094 N_2 , 0.000 $\text{Al}_2\text{O}_3(s)$, 0.042 CO_2 , 0.004 Cl
0.72 NH_4ClO_4 , 0.08 $(\text{CH}_2)_n$, 0.20 Al	0.213 H_2 , 0.184 H_2O , 0.145 CO , 0.134 HCl , 0.098 $\text{Al}_2\text{O}_3(s)$, 0.085 N_2 , 0.057 H , 0.025 OH , 0.024 Cl , 0.016 CO_2 , 0.006 AlCl , 0.004 AlCl_3 , 0.003 NO	0.233 H_2 , 0.204 H_2O , 0.175 HCl , 0.147 CO , 0.119 $\text{Al}_2\text{O}_3(s)$, 0.091 N_2 , 0.022 CO_2 , 0.011 H , 0.006 Cl , 0.002 OH
0.81 NH_4ClO_4 , 0.09 $(\text{CH}_2)_n$, 0.10 Be	0.218 $\text{BeO}(s)$, 0.178 H_2O , 0.132 H_2 , 0.129 HCl , 0.123 CO , 0.074 N_2 , 0.036 H , 0.019 Cl , 0.019 OH , 0.017 CO_2 , 0.016 BeOH , 0.003 O , 0.002 NO	0.242 $\text{BeO}(s)$, 0.197 H_2O , 0.169 H_2 , 0.143 HCl , 0.120 CO , 0.076 N_2 , 0.022 CO_2 , 0.016 H , 0.009 Cl , 0.004 OH
0.765 NH_4ClO_4 , 0.085 $(\text{CH}_2)_n$, 0.15 Be	0.290 $\text{BeO}(s)$, 0.226 H_2 , 0.119 CO , 0.106 HCl , 0.066 N_2 , 0.059 H_2O , 0.060 H , 0.031 BeOH , 0.019 Cl , 0.008 OH , 0.004 CO_2 , 0.004 BeCl_2	0.322 $\text{BeO}(s)$, 0.243 H_2 , 0.119 CO , 0.117 HCl , 0.066 N_2 , 0.062 H_2O , 0.038 H , 0.013 Cl , 0.009 BeOH , 0.005 CO_2 , 0.003 OH , 0.002 Be_2O_3
0.72 NH_4ClO_4 , 0.08 $(\text{CH}_2)_n$, 0.20 Be	0.325 $\text{BeO}(s)$, 0.272 H_2 , 0.111 CO , 0.060 N_2 , 0.059 H , 0.059 HCl , 0.036 Be , 0.030 BeOH , 0.025 BeCl_2 , 0.008 Cl , 0.005 BeH , 0.003 H_2O , 0.003 BeCl , 0.002 Be_2O_3	0.352 $\text{BeO}(s)$, 0.301 H_2 , 0.112 CO , 0.060 N_2 , 0.049 HCl , 0.042 H , 0.033 Cl , 0.033 Be , 0.010 BeOH , 0.005 Cl
0.765 NH_4ClO_4 , 0.085 $(\text{CH}_2)_n$, 0.15 AlH_3	0.268 H_2 , 0.268 H_2O , 0.141 HCl , 0.126 CO , 0.076 N_2 , 0.058 $\text{Al}_2\text{O}_3(s)$, 0.025 H , 0.017 CO_2 , 0.010 OH , 0.009 Cl	0.286 H_2 , 0.273 H_2O , 0.136 HCl , 0.119 CO , 0.078 N_2 , 0.060 $\text{Al}_2\text{O}_3(s)$, 0.026 CO_2
0.765 NH_4ClO_4 , 0.085 $(\text{CH}_2)_n$, 0.15 BeH_2	0.377 H_2 , 0.216 $\text{BeO}(s)$, 0.182 HCl , 0.102 H_2O , 0.098 CO , 0.053 N_2 , 0.027 H , 0.010 BeOH , 0.005 Cl , 0.006 CO_2 , 0.003 OH	0.395 H_2 , 0.231 $\text{BeO}(s)$, 0.110 HCl , 0.103 H_2O , 0.098 CO , 0.053 N_2 , 0.005 CO_2 , 0.003 H

TABLE VIII

Physical and Thermodynamic Properties of Propellant Ingredients

Compound	Formula	MP (°C)	BP (°C)	Density		ΔH_f		
				State	g/cc	°C	State	kcal/mole at 25°C
Acetylene	C_2H_2	-81.8	-83.6 (subl.)	(l)	0.621 ¹⁴	-84	(g)	54.2 ± 0.2
Aluminum	Al	659.7	2467 ¹⁵	(s)	2.70 ¹⁶	20	(g)	78.0 ± 0.4
							(s)	2.4
							(l)	0
Aluminum borohydride	$Al(BH_3)_3$	-64.5 ¹⁷	44.5	(l)	0.545 ¹⁸	32.5	(g)	-65 ¹⁹
							(s)	-72 ¹⁹
Aluminum hydride	AlH_3	—	—	(s)	~1.3 ²⁰	—	(g)	18 ± 10 ²¹
							(s)	-3 ± 10 ²¹
Ammonia	NH_3	-77.7	-33.4	(l)	0.817 ²²	-79	(g)	-11.0
							(s)	-16.6 ²³
Ammonium nitrate	NH_4NO_3	169.2 ²⁴	210 (d.) ²⁵	(s)	1.725 ²⁶	25	(s)	-87.3 ²⁷
Ammonium perchlorate	NH_4ClO_4	(d.)	—	(s)	1.95 ²⁸	20	(s)	-69.4
Beryllium	Be	1278	2677 ²⁹	(s)	1.85 ³⁰	25	(g)	78.5 ± 0.5
							(s)	2.9 cal
							(s)	0
Beryllium hydride	BeH_2	—	—	(s)	~0.6 ³¹	—	(g)	30 cal
							(s)	10 cal. ³²
							(s)	3.7
Boron	B	2300	3677 ³³	(s)	2.33 ³⁴	20	(s)	133 ± 4
							(s)	0
							(s)	0
Bromine pentafluoride	BrF_5	-61.3	40.5	(l)	2.465 ³⁵	25	(g)	-10.5
Chlorine dioxide	ClO_2	-59 ³⁶	11 ³⁷	(l)	—	—	(g)	25 ± 1.5
Chlorine heptoxide	Cl_2O_7	-91.5	82	(l)	1.86 ³⁸	0	(g)	63
							(s)	57 ³⁹
Chlorine trifluoride	ClF_3	-83	11.3	(l)	1.209 ⁴⁰	25	(g)	-39 ± 1
							(s)	-44.4 ⁴¹
Cyanogen	$NCCN$	-34.4	-20.5	(l)	0.866	17	(g)	73.9 ± 0.04
Decaborane	$B_{10}H_{12}$	99.7 ⁴²	213 ⁴³ (d.)	(s)	0.94 ⁴⁴	20	(g)	2.8 ± 1.5
							(s)	-15.8 ± 1.4 ⁴⁵
Diborane	B_2H_6	-163.5 ⁴⁶	-92.5 ⁴⁷	(l)	0.447 ⁴⁸	-112	(g)	7.5
							(s)	2.9 ⁴⁹
Dicycloacetylene	NCO_2OCN	23.5 ⁵⁰	76.5 ⁵¹	(l)	0.97 ⁵²	25	(s)	118 ⁵³
Dioxygen difluoride	O_2F_2	-163.5 ⁵⁴	-57 ⁵⁵	(l)	1.45 ⁵⁶	-57	(g)	4.7 ⁵⁷
Ethyl alcohol	CH_3CH_2OH	-117.3	78.3	(l)	0.789 ⁵⁸	20	(g)	-50.2 ⁵⁹
Ethylene	$CH_2=CH_2$	-109.4	-103.9	(l)	0.66 ⁶⁰	-169	(g)	12.5 ⁶¹
Ethylene oxide	C_2H_4O	-111.3	10.7	(l)	0.87 ⁶²	20	(g)	-12.2 ± 1
Fluorine	F_2	-223	-188	(l)	1.50 ⁶³	-189	(g)	0
							(s)	-3.0 ⁶⁴
Hydrazine	N_2H_4	1.4	113.5	(l)	1.011 ⁶⁵	20	(g)	22.8
							(s)	12.0 ⁶⁶
Hydrazinium nitrate	$N_2H_5NO_3$	70.7	140 (subl.)	(s)	1.68 ⁶⁷	25	(s)	-59.0 ⁶⁸
Hydrogen	H_2	-252.8	-252.8	(l)	0.071 ⁶⁹	-252.7	(g)	0
							(s)	-2.0 ⁷⁰
Hydrogen peroxide	H_2O_2	-0.41	150.2	(l)	1.463 ⁷¹	20	(g)	-32.5
							(s)	-44.8 ⁷²
Lithium	Li	181 ⁷³	1363 ⁷⁴	(s)	0.534	25	(s)	38.4 ± 0.4
							(s)	0.6
							(s)	0
Lithium aluminum hydride	$LiAlH_4$	125 ⁷⁵	—	(s)	0.92 ⁷⁶	25	(s)	-24.1 ⁷⁷
Lithium amide	$LiNH_2$	375	430	(s)	1.18 ⁷⁸	25	(s)	-43.5 ⁷⁹
Lithium borohydride	$LiBH_4$	277 ⁸⁰	—	(s)	1.66 ⁸¹	25	(s)	-44.6 ⁸²
Lithium hydride	LiH	689	—	(s)	0.82 ⁸³	25	(s)	32.1
							(s)	-21.7
Lithium nitrate	$LiNO_3$	255	—	(s)	2.38 ⁸⁴	25	(s)	-115.3 ⁸⁵

TABLE VIII
(Continued)

Compound	Formula	MP (°C)	BP (°C)	Density			ΔH _f kcal/mole at 25°C	
				State	g/cc	°C		
Lithium perchlorate	LiClO ₄	236	300 (d.)	S	2.429 ^a	25	S	-82.1
Magnesium	Mg	651	1107	S	1.74 ^a	20	S	-98 ^a
Magnesium aluminum hydride	Mg ₂ (AlH ₅) ₃	140 (d.†)	—	S	1.63 ^a	25	S	15.3
Magnesium hydride	MgH ₂	230 (d.†)	—	S	1.45 ^a	25	S	2.1
Monomethylhydrazine	CH ₃ NHNH ₂	-32.4 ^a	57.5 ^a	l	—	—	S	0
Nitric acid	HNO ₃	-42	86	S	1.502 ^a	25	S	-23.1 ^a
Nitric acid, red fuming	72.6% HNO ₃ 24.0% NO ₂ 3.4% H ₂ O	-50 ^a	—	S	1.583 ^a	23.9	S	-18 ± 5 ^a
Nitric acid, white fuming	86.3% HNO ₃ 6.54% NO ₂ 13.1% H ₂ O	-45 ^a	—	S	1.476 ^a	23.9	S	13.1 ^a
Nitrogen dioxide	NO ₂	-11.2	21.2	S	1.447 ^a	2	S	12.7 ^a
Nitrogen pentoxide	N ₂ O ₅	30 ^a	45-50 ^a	S	—	—	S	-41.4 ^a
Nitrogen trifluoride	NF ₃	-216.6	-120	S	1.537 ^a	129	S	-41.0 ^a
Nitrogen tetroxide	N ₂ O ₄	-11.2	21.2	S	1.45 ^a	20	S	2.3
Nitroglycerin	C ₃ H ₅ (ONO ₂) ₃	2.9	260 (d.)	S	1.60 ^a	25	S	0 ± 0.5
Nitromethane	CH ₃ NO ₂	-29	101	S	1.13 ^a	20	S	-18 ^a
Nitronium perchlorate	NO ₂ ClO ₄	125 (d.†)	—	S	2.22 ^a	25	S	-26.7 ^a
Nitrosyl fluoride	NOF	-134	-36	S	1.320 ^a	-39.9	S	8 ^a
Oxygen	O ₂	-218.4	-183.0	S	1.42 ^a	-182	S	-15.7 ± 0.4
Oxygen difluoride	OF ₂	-223.8	-144.8	S	1.528 ^a	-147.3	S	0
Ozone	O ₃	-192.1	-181.9	S	1.70 ^a	-183	S	34.1 ± 0.4
Pentaborane	B ₅ H ₉	-46.0 ^a	—	S	0.630 ^a	16.2	S	15.0 ± 0.4
Perchloryl fluoride	ClO ₃ F	-148 ^a	—	S	1.390 ^a	20.9	S	7.8 ^a
Polyethylene	(CH ₂) _n	—	—	S	0.92 ^a	25	S	-3.1
Potassium perchlorate	KClO ₄	—	—	S	2.524 ^a	11	S	-19.1 ± 0.7 ^a
RP-1	kerosene	-40 ^a	160-200 ^a	S	0.7 ^a	25	S	67 ± 3
Sodium nitrate	NaNO ₃	306.2	380 (d.)	S	2.257 ^a	20	S	-5.5 ^a
Tetrafluorohydrazine	N ₂ F ₄	-163 ^a	-73 ^a	S	1.65 ^a	-73	S	-101.5 ^a
Tetra nitromethane	C(NO ₂) ₄	13	123.7	S	1.64 ^a	25	S	-2 ± 2.5 ^a
Triethylamine	N(CH ₂ CH ₃) ₃	-114.8	89.5	S	0.723 ^a	25	S	-5.2 ^a
Ura-dimethylhydrazine	(CH ₃) ₂ NNH ₂	-57.8 ^a	63 ^a	S	0.790 ^a	15.6	S	5.2 ^a

^a Melting points, boiling points, and densities are taken from the *Handbook of Chemistry and Physics*, 42nd Ed., The Chemical Rubber Publishing Co., Cleveland, Ohio, 1960, unless otherwise indicated. Heats of formation are taken from the JANAF Thermochemical Tables, Dow Chemical Co., Midland, Mich., 1960, unless otherwise indicated.

† The reference numbers refer to the reference list that follows this page.

HUMAN FACTORS AND MAINTENANCE
IN SPACE

(18 April 1967)

by

John Lyman

John Lyman holds a joint appointment as Professor of Engineering and Professor of Psychology at UCLA where he is Head of the Biotechnology Laboratory. He received his A.B. degree in 1943 with a major in mathematics and psychology; his M.A. in psychology in 1949; and his Ph.D. in psychology in 1951, all from UCLA. He and his collaborators have published over 75 articles which have appeared in psychological and engineering journals and as reports for government sponsored projects conducted in the Biotechnology Laboratory.

The increasingly higher price paid in system inefficiency as the result of maintainability problems with each new generation of projects is well known. The growth in complexity of both current and projected space projects, civilian as well as military has been accompanied by a "critical mass" effect which has focused on maintainability functions. It is generally accepted that on a dollar cost basis alone, from ten to thousands of times the original cost of a given system is spent on maintenance during its operating life. Despite increased use of automatic checkout procedures and other aids for simplified troubleshooting and repair it remains a fairly defensible rule-of-the-thumb that approximately one-third of the personnel assigned to operational systems are principally engaged in maintenance functions. The role of human factors engineering in maintainability is directed toward economically reducing the number of personnel and skill levels required in maintenance functions, by providing direction for hardware design that makes the fullest possible use of knowledge about human behavioral patterns. A basic assumption is that even with the maximum practical use of redundancy, reliability improvement of components and advanced self repair techniques, an ultimate level of overall system reliability can only be obtained by the directed use of man's

versatility and ingenuity as a decision maker in matters of failure detection, replacement and repair.

Particular areas where major contributions of human factors engineering may occur include the following:

1. Development of criteria for evaluating and comparing alternate maintainability programs.
2. Development of maintenance plans and schedules within the framework of an overall maintainability philosophy for a particular system.
3. Determination of maintenance personnel requirements in terms of manpower and skill levels.
4. Development of training and evaluation procedures for maintenance personnel.
5. Determination of environmental tolerance and work load limits and requirements for maintenance personnel.
6. Development of trouble-shooting strategies for fault detection and determination of optimal placements of test point locations.
7. Provision of information concerning design constraints based on such factors as human body part sizes and sensory input requirements.
8. Development of job aids, special supports and other supplementary equipment.

As with other subsystem aspects of complex system design a key necessity is specialized participation by maintenance engineers in collaboration with human

factors engineers (in some cases they may be the same people) from the earliest stages of design and development. An integrated maintenance management concept suitable for the particular system mission and overall design approach should evolve simultaneously with the elimination of alternative candidate approaches in the preliminary design stage. Specific human factors considerations should cover at least the following items:

1. A preventive maintenance and a contingency maintenance plan based on the operational plan.
2. A maintenance training program based on a maintenance schedule arrived at by a "best available information" logical analysis and prediction of which components are likely to fail and when.
3. A list with quantitative estimates of the men, equipment, tools and publications that accurately reflects what maintenance facilities each subsystem will require and at what organizational level the maintenance is to occur.

To provide the necessary detail for implementing the human factors engineering contributions as the system is designed and developed, a maintenance engineering analysis is required. Minimally it should provide the following:

1. A part-by-part analysis which describes each component, outlines its function and tells why and how it is to be maintained. Each maintenance task should be described in detail.
2. A tool and equipment summary which lists both routine and special tools required along with ground support equipment and

material needs. This summary should specify the maintenance level at which the work is to be performed to ensure that proper tools, parts, and equipment is available in the right location.

3. Time and error studies which will intensify the number of man-minutes required to perform each maintenance task and indicate human initiated errors that may occur. An efficiency factor may be assigned to allow for different working conditions and new skill levels.
4. A manning specification which sets up personnel requirements necessary to put a sufficient number of men with proper skills into the systems support program placing them at the proper maintenance level.

The effects of the simultaneous conduct of a maintenance analysis with the rest of the design and development program and its continuation throughout the lifetime of the system will be to provide data that will directly affect the hardware design and operational procedures. For example, if the analysis shows that more than half the economically available man-hours are committed before half the maintenance tasks are described, the need for design changes or changes in the maintenance parameters should become obvious. A restudy of the most time-consuming or high skill level consuming tasks should then provide a decision basis for choosing between the redesign of a given subsystem to include new features or the programming in of more man-hours and supplies to the system's support plan.

Naturally the cost of providing a complete integrated maintenance management plan will vary with the complexity of the system and the number purchased. The return on the investment will be in the form of cost savings during the

operational phases of the program. Increased probability of predictable system availability, reduction in total number and overlap of the manuals and technical directives associated with each maintenance level and data which will help provide increased efficiencies during design and development of each future system directed toward related missions will all contribute to such savings.

Even though planning, designing and evaluating for maintainability have become more or less accepted as fundamental to the development of complex space systems, there are many problem areas where our specific knowledge is not adequate. In the human factors field this is especially true with respect to our knowledge of human maintenance performance in space both in IVA (intra vehicular activity) and EVA (extra vehicular activity). As missions become more prolonged, maintenance problems will multiply. It is particularly important that new knowledge about man's capabilities be developed in anticipation of the increased load that will be placed on him during long missions. Some particular areas which seem to require special research efforts are as follows:

1. Anthropometric measures concerned with man working in a space suit in the weightless state for purposes of establishing accessibility, sizing standards, need for special tools, restraint and maneuvering equipment, etc.
2. Motor skills such as assembling, packaging and applying torque from unusual postures.
3. Perceptual capacities requiring special coding of information to avoid effects of sharp lighting contrasts, visual illusions, etc.
4. Memory storage limitations where special performance aids may be required in complex repair tasks, especially in EVA where

instruction manuals may be hard to refer to.

5. **Human stereotypes (habits) in space which will affect task sequences and optimal spatial relationships between information inputs and work outputs.**
6. **Decision capabilities with respect to time pressures, information feedback requirements, testing procedures and other task stress factors.**
7. **Tolerance to environmental factors and work loads requiring high metabolic costs over both short time, high intensity conditions and longer time, moderate intensity conditions.**

It is evident that even those elements and the implementation procedures that can now be anticipated with respect to maintenance in space will require much experience to evolve a full viable set of standards. In the meantime the fullest use of man's abilities and the understanding of the design constraints which surround them must remain a high priority responsibility of not just the human factors engineers but also the many other engineers with whom the "people part" of a space system has interfaces.

CONCEPTS OF HYPERSONIC ABLATION

by

Sinclair M. Scala

Dr. Scala received a Bachelor's degree (cum laude) in Mechanical Engineering at the College of the City of New York in 1950, an M.S. in Mechanical Engineering at the University of Delaware in 1953 and an M.A. and Ph.D. at Princeton University in 1955 and 1957 respectively. From 1953 to 1956, he was a Guggenheim and Bakhmeteff Fellow at the James Forrestal Research Laboratory of Princeton University and contributed to the theory of combustion instability in rocket motors. He joined the General Electric Company in 1956 where he pioneered the theory of hypersonic ablation. In 1964, Dr. Scala was appointed Manager of the Theoretical Fluid Physics Section and now directs research in gas dynamics, atomic, radiation and plasma physics, fluid mechanics, aerothermophysics and applied mathematics. He has published more than fifty papers in technical journals and books.

INTRODUCTION

At the present time, new conceptual advances are being made in understanding the complex interaction between refractory materials and the high-temperature, chemically reacting, environment in which they are required to perform as thermal insulators while retaining their structural integrity.

Graphite is of particular interest to us since it is itself a refractory material capable of carrying a structural load at high surface temperatures and also because many plastics will form an outer char layer upon exposure to severe heating rates.

The oxidation of carbon, coal and graphite has been studied extensively for over one hundred years, and much attention has been given to the reaction-rate-controlled, transition, and diffusion-controlled oxidation regimes. The oxidation

rate of carbonaceous materials in these regimes is dependent upon the surface temperature, the reactivity of the particular type of graphite utilized, and the diffusion processes in the gaseous boundary layer.

At still higher surface temperatures, one must be concerned not only with the homogeneous and heterogeneous chemical reactions occurring between the oxygen present in the boundary layer and the carbon, but also the nitrogen. In this ultra-high surface temperature regime, sublimation of the graphite is the mode of mass loss.

Here it is noted that the upper limit of the applicability of conventional boundary-layer theory is determined at the extreme surface temperature when the sublimation rate of the vaporizing graphite induces pressure gradients normal to the gas-solid interface.

ABLATION REGIMES OF GRAPHITE

We will now summarize the results of a unified theoretical treatment of the graphite ablation process over the entire range of pressures and surface temperatures of interest, i. e. from room temperature up to $10,000^{\circ}\text{R}$ (see references 1-5).

At the lowest surface temperatures, the oxidation process is reaction rate controlled and hence the mass loss increases exponentially with surface temperature. At intermediate surface temperatures, the overall rate of mass loss depends both on gas dynamic processes and the specific chemical reactivity. Eventually, as the surface temperature rises beyond a certain point the mass loss becomes limited by the rate at which oxygen-bearing species can diffuse to the surface. This is known as the diffusion-controlled regime. In this regime,

it can be shown that the mass loss is independent of the surface temperature, but varies directly as the square root of the stagnation pressure.

The mass transfer and heat transfer results for the diffusion-controlled regime and sublimation regime which are discussed are based on exact numerical solutions of the boundary layer equations which include the conservation of mass, momentum, energy, and chemically reacting species. In the diffusion-controlled regime, a six-component gas model has been utilized, including CO and CO₂, plus the four primary species found in high temperature dissociated air (i.e. O, O₂, N, N₂). In the sublimation regime, three additional species (namely C, C₃ and CN) are introduced, bringing the total number of chemical species to nine.

Based upon a large number of numerical solutions to the boundary layer equations, correlations have been obtained for the heat transfer rate and the mass transfer rate including the specific effects of enthalpy, pressure, geometry and surface temperature.

DISCUSSION OF RESULTS

In figure 1, one observes the various mass transfer regimes which have just been described. In the region on the extreme right hand side, boundary layer theory begins to become inapplicable.

In figure 2, one observes the correlated heat transfer rate as a function of the effective mass fraction of the element carbon at the surface, $C_{<C>_w}$. Note that $\left(K \frac{\partial T}{\partial y} \right)_{S,w}$, the heat transferred to the solid, has been normalized by the heat transfer in the diffusion-controlled regime, Q_0 .

Finally, figure 3 shows the normalized mass loss as a function of surface temperature and stagnation pressure. Here it is seen that the chemical kinetics at the surface, which are a function of the grade of the graphite, have a pronounced effect at surface temperatures below 3000°R. Above this temperature, the surface reaction rate is sufficiently fast so that the overall process is governed by gas-phase transport phenomena.

CORRELATION FORMULAS FOR MASS LOSS

In the reaction rate controlled regime, at low surface temperatures, the mass loss is given by the Arrhenius expression:

$$\dot{m}_R = K_o e^{-E/RT_w} (P_{O_2})_w^n \quad (1)$$

where K_o , E and n depend on the properties of the graphite.

In the diffusion controlled regime, the mass loss is given by:

$$\dot{m}_D \left(\frac{R_B}{P_e} \right)^{1/2} = 6.35 \times 10^{-3} \frac{\text{lb.}}{\text{ft.}^{3/2} \text{ sec. atm.}^{1/2}} \quad (2)$$

At intermediate surface temperatures, the mass loss is given by

$$\dot{m} = \left[\frac{1}{\dot{m}_R} + \frac{1}{\dot{m}_D} \right]^{-1/2} \quad (3)$$

Finally, in the sublimation regime, the normalized mass loss is given by:

$$\frac{\dot{m}_S}{\dot{m}_D} = 6.67 C_{<C>_w} \quad (4)$$

where

$$C_{<C>_w} = 0.15 + 2.4 \times 10^6 P_e^{-0.67} \exp \left[-11.1 \times 10^4 / T_w \right] \quad (5)$$

where P_e is in atmospheres, and T_w is in $^{\circ}R$. For cones, spheres and wedges the above formulas may in the diffusion controlled and sublimation regimes be generalized (see Ref. 5) to:

$$\frac{\dot{m}_w (\epsilon_S H_e)^{1/4}}{C_{<C>_w \left[2 P_e \left(\frac{d\epsilon_e}{dx} \right) / \beta \right]^{1/2}} \approx \left(1.20 + 0.42 \frac{\beta u_e^2}{g J T_e} \right) \times 10^{-3} \frac{\text{lb. (BTU/lb)}^{1/4}}{\text{ft.}^2 (\text{sec-atm})^{1/2}} \quad (6)$$

CORRELATIONS FOR HEAT TRANSFER

In the rate controlled and diffusion controlled regimes, the heat transfer to an ablating graphite surface is given by:

$$Q_o (R_B / P_e)^{1/2} = 33.3 + 0.0333 (H_e - h_{w, \text{Air}}), \quad \frac{\text{BTU}}{\text{ft.}^{3/2} \text{sec. atm}^{1/2}} \quad (7)$$

In the sublimation regime, the heat transfer rate to the surface becomes

$$\frac{\left(K \frac{\partial T}{\partial y} \right)_{S,w}}{Q_o} = 1 - \tilde{S} (C_{<C>_w - 0.15) \quad (8)$$

where $C_{<C>_w$ has been defined in equation (5) and \tilde{S} is a fifth degree polynomial which (see figure 2) decreases with increasing stagnation enthalpy.

For spheres, cones and wedges, the above formula for $\left(K \frac{\partial T}{\partial y} \right)_{S,w}$ still holds, but we find that the expression for Q_o can be generalized to:

$$\frac{Q_o (\epsilon_S H_e)^{1/4}}{(H_e - h_w) \left[2 P_e \left(\frac{d\epsilon}{dx} \right) / \beta \right]^{1/2}} = \left(1.04 + 1.35 \frac{\beta u_e^2}{g J T_e} \right) \times 10^{-3} \frac{\text{lb. (BTU/lb.)}^{1/4}}{\text{ft.}^2 (\text{sec. - atm.})^{1/2}} \quad (9)$$

The various symbols $\beta, \epsilon, \frac{d\epsilon}{dx}$ are standard nomenclature and are defined in ref. 5, for example.

CONCLUSIONS

At the present time theoretical techniques exist for the prediction of the oxidation and sublimation of graphite for the laminar hypersonic viscous flow over cones, spheres and wedges. Agreement with experimental data is reasonable. Future work should stress investigation of the effect of turbulence on the heat and mass transfer to a graphitic surface.

REFERENCES

1. Scala, S. M., "Surface Combustion in Dissociated Air," *Jet Propulsion*, Vol. 28, No. 40, pp. 340-341, 1958.
2. Scala, S. M., "A Study of Hypersonic Ablation," *Proceedings of the Xth International Astronautical Federation Congress*, London 1959, pp. 790-827.
3. Scala, S. M., "The Ablation of Graphite in Dissociated Air, Part I-Theory," *IAS Paper 62-154*, June 1962. Also GE Co., MSD TIS R62SD72, Sept. 1962.
4. Scala, S. M. and Gilbert, L. M., "The Sublimation of Graphite at Hypersonic Speeds," *AIAA Journal*, Vol. 3, No. 9, pp. 1635-1644, Sept. 1965.
5. Gilbert, L. M. and Scala, S. M., "Combustion and Sublimation of Cones, Spheres and Wedges at Hypersonic Speeds," *AIAA Journal*, Vol. 3, No. 11, pp. 2124-2131, 1965.

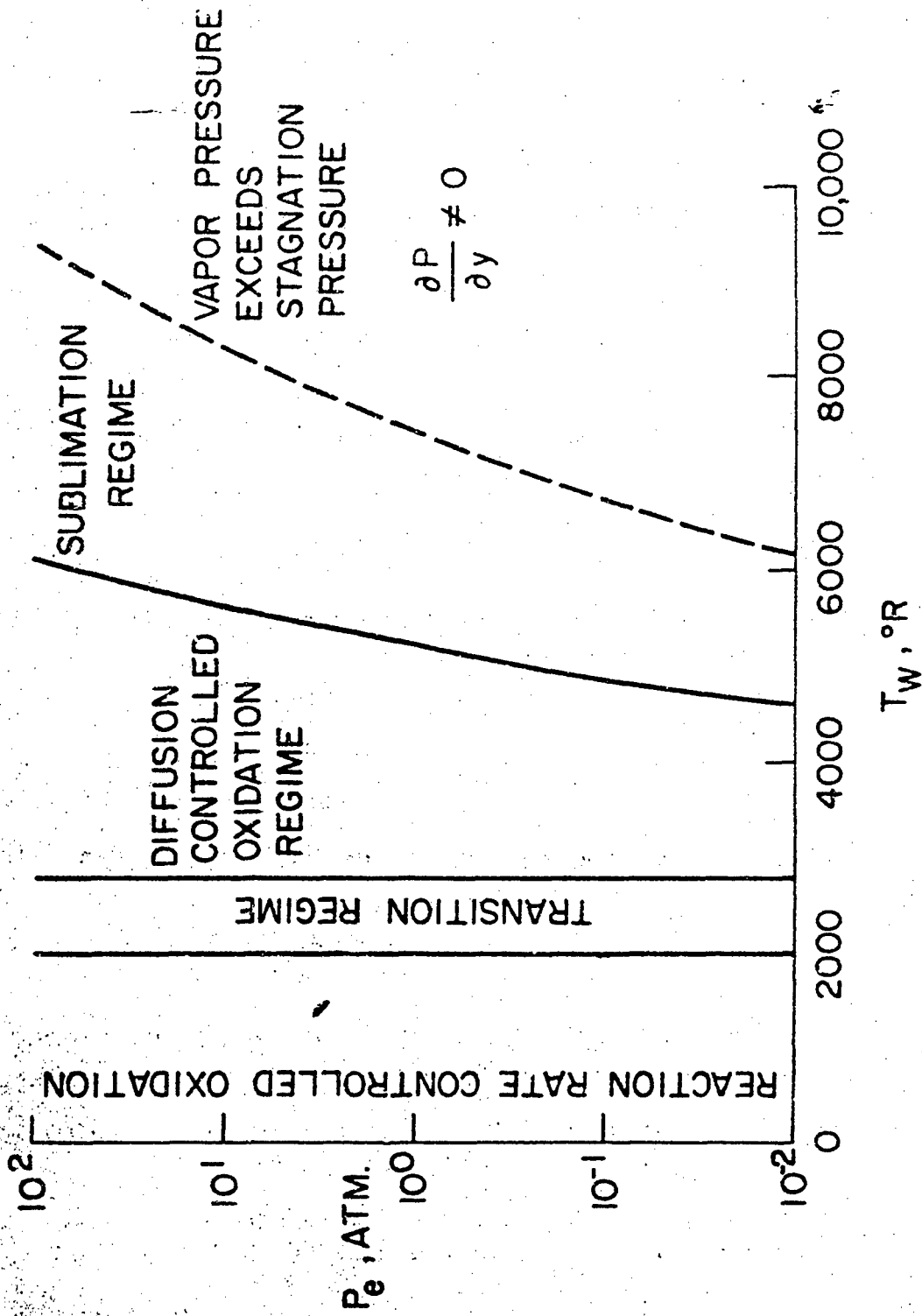


Figure 1. Mass Transfer Regimes for Ablating Graphite

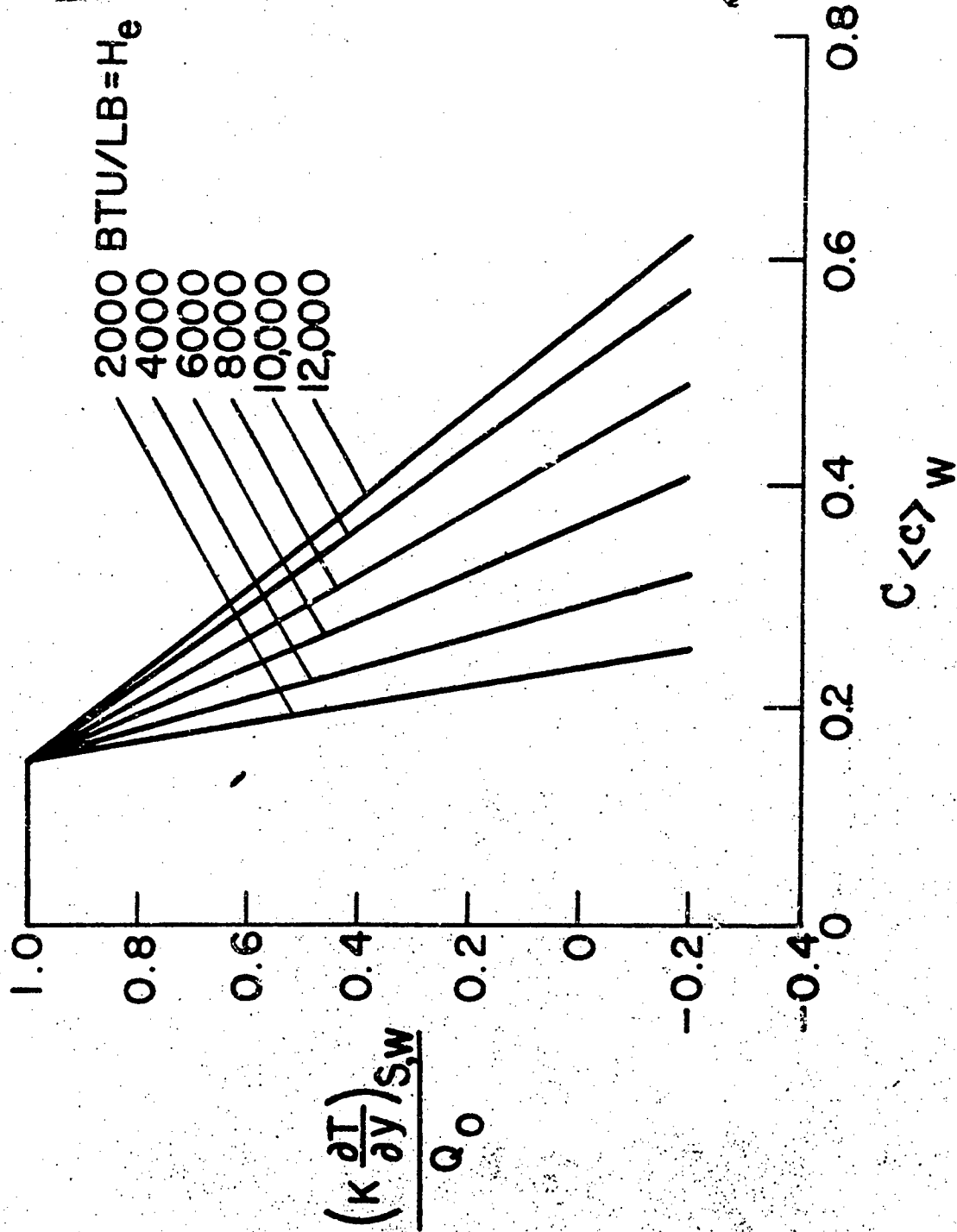


Figure 2. Heat Transfer Correlation for Graphite Sublimation

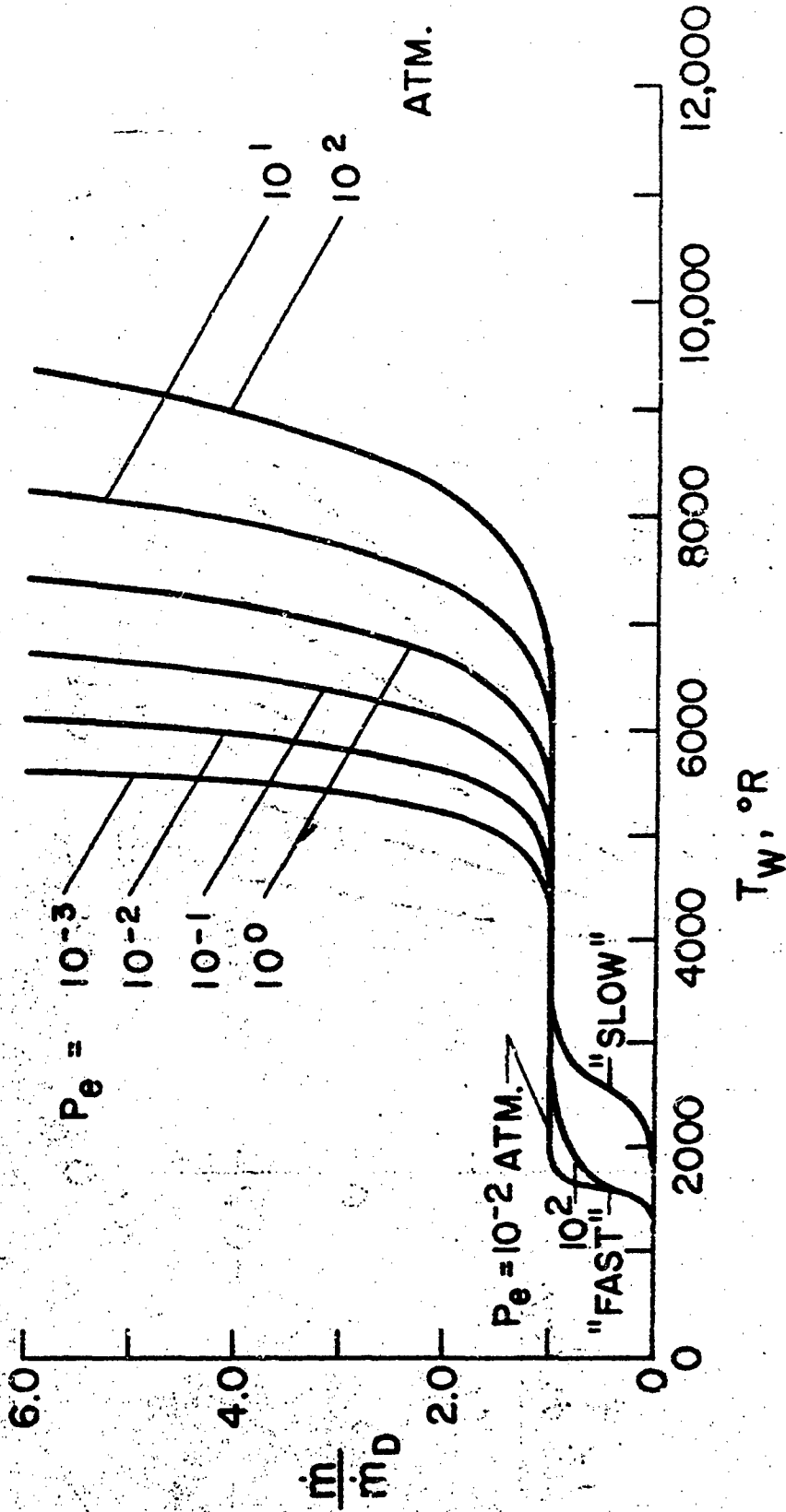


Figure 3. Normalized Hypersonic Ablation Rate of Graphite over the Entire Range of Surface Temperature

DIGITAL AND ANALOG SIMULATION OF DISTRIBUTED PARAMETER SYSTEMS
(9 May 1967)

by

W. J. Karplus

B.E.E. Cornell University; M.S.E.E. University of California, Berkeley;
Ph.D. University of California, Los Angeles. Walter J. Karplus is Professor
of Engineering at the University of California at Los Angeles where he teaches
courses in Computer Application and Circuit Theory and is also Head of the
Engineering Department Computing Laboratory.

After ~~an~~ time service in the Navy Electronics Program, he worked for Sun Oil
Company, International Geophysics Incorporated, and Hughes Aircraft Company.
Since joining UCLA, he has consulted for a number of industrial and government
organizations. He is the author of four textbooks, numerous technical papers,
and holds several patents in the computer field.

General Remarks

The solution of problems governed by partial differential equations
constitutes a special challenge both to the analog computer and to the digital
computer. Analog methods are complicated by the fact that such problems have
two or more independent variables, whereas analog computers are restricted to
one independent variable: time. Moreover, field problems are usually formulated
as boundary-value problems, whereas analog computers are particularly useful for
initial-value problems. The application of digital computer techniques demands
stepwise integration in the time domain and most often leads to unacceptably
long computer runs if reasonable accuracies are required.

This discussion begins with a brief survey of conventional analog and
digital techniques for treating transient field problems characterized by partial
differential equations; several hybrid computer methods are then described.
These techniques offer some important advantages over conventional methods and
indicate the potentialities of computers in which analog and digital hardware
are interconnected.

Probably the most widely occurring partial differential equation is
Laplace's equation:

$$\nabla^2 \phi = 0$$

(1)

where Δ^2 is the Laplacian operator, which in two Cartesian dimensions takes the form

$$\nabla^2 = \frac{\partial^2}{\partial x^2} + \frac{\partial^2}{\partial y^2} \quad (2)$$

Equation (1) is one of the family of elliptic partial differential equations, whose solutions are not time-dependent.

The parabolic partial differential equation

$$\nabla(\sigma \nabla \phi) = S \frac{\partial \phi}{\partial t} \quad (3)$$

occurs in the study of transient heat transfer, the flow of fluids through porous media, and a wide variety of diffusion phenomena. σ and S are field parameters which may be functions of time, space, or the potential function ϕ . For constant parameters and in one-space dimension, Equation (3) becomes

$$\frac{\partial^2 \phi}{\partial x^2} = \frac{1}{\alpha} \frac{\partial \phi}{\partial t} \quad (4)$$

Fields governed by Equation (4) are usually characterized as initial-value problems. In addition to the partial differential equation, the specifications include an initial condition $f(x,0)$ for all points in the field at $t = 0$ and two boundary conditions $f_1(0,t)$ and $f_2(X,t)$ applying to the two extremities of the field for $t > 0$.

Other partial differential equations that are of frequent interest include the hyperbolic wave equation

$$\nabla^2 \phi = \frac{\partial^2 \phi}{\partial t^2} \quad (5)$$

and the biharmonic equation

$$\nabla^4 \phi = \frac{\partial^2 \phi}{\partial t^2} \quad (6)$$

governing the vibration of beams.

In order to treat transient field problems of the type of Equations (3) to (6) by electronic differential analyzer or by digital techniques, it is essential to effect a transformation to reduce the number of independent variables. This is accomplished by means of finite-difference approximations in which a continuous variable such as x , y , z , or t is replaced by an array of discretely-spaced points. Solutions are then obtained for these points, and interpolation techniques are used to construct continuous equipotential or stresslines. When an independent variable is discretized in this manner, the corresponding partial derivative is replaced by an approximate algebraic expression. In computer terms, this means that the operation of integration is replaced by additions and subtractions.

Consider as an example of a very simple transient field problem, the parabolic equation (4). This equation has two independent variables, the space variable x and the time variable t . In applying analog methods, either of these two variables can be kept in continuous form or discretized by the application of finite difference approximations. There exist therefore four basic analog approaches:

1. ~~Continuous-space-continuous-time (CSCT)~~. Both the time variable and the space variable are kept in continuous form.
2. ~~Discrete-space-continuous-time (DSCT)~~. The left side of Equation (4) then becomes an algebraic expression, while the right side remains unchanged.
3. ~~Continuous-space-discrete-time (CSDT)~~. The left side of

Equation (4) then becomes an algebraic expression, while the right side remains unchanged.

4. Discrete-space-discrete-time (DSDT). Both the x and the t variables are discretized so that all derivatives in Equation (4) become algebraic expressions.

If a digital computer is to be employed, only the DSDT method is feasible since no continuous variables can be handled digitally. A choice must be made, however, between explicit and implicit integration formulas.

Among analog methods, the DSCT method using resistance-capacitance network models is the most important and widely-used technique. The CSCT method is particularly adapted to nonlinear parabolic equations in one space dimension, where iterative electronic analog computers can be used to advantage. The DSDT technique is the most general and powerful analog simulation method and permits the use of resistance networks in the study of nonlinear fields governed by any of Equations (1) to (6).

REFERENCES

1. Karplus, W. J., "Analog Simulation: Solution of Field Problems," McGraw-Hill Book Company, New York, 1959.
2. Fox, L., "Numerical Solution of Ordinary and Partial Differential Equations," Addison-Wesley Publishing Company, Reading, Mass., 1962.
3. Karplus, W. J., "A Hybrid Computer Technique for Treating Nonlinear Partial Differential Equations," Trans. IEEE, October 1964, Vol EC-13, pp. 597-605.

PRINCIPLES OF CRYOGENIC ENGINEERING

(16 May 1967)

by

Samuel C. Collins

B.S., M.S., University of Tennessee; Ph.D., University of North Carolina, 1927. Member of faculty of various institutions before going to the Massachusetts Institute of Technology in 1930. Retired from M.I.T. in 1964 as Emeritus Professor of Mechanical Engineering. Since 1964, a member of the engineering staff of Arthur D. Little, Inc.

Research includes thermodynamic properties of gases, liquefaction cycles, heat transfer and expansion devices for refrigeration at very low temperature levels.

Among his honors are Wetherill Medal of the Franklin Institute, Kamerlingh Onnes Gold Medal of the Netherlands Refrigeration Society, Rumford Medal of the American Academy of Arts and Sciences, and Honorary D.Sc. Degree, University of North Carolina, 1957.

INTRODUCTION

The word cryogenic is generally associated with very low temperatures ranging from the liquid air level downward in contrast to ordinary refrigeration in the range employed for food storage, air conditioning and the like. Refrigeration systems for both high and low levels require compressors and coolers for removing the heat of compression and possible heat of condensation. They also require expansion devices in the refrigerated zone for reducing the pressure. The equipment for low level refrigeration includes one other important item, the counterflow heat exchanger. This device makes possible the steady flow of refrigerant from the compressor which must operate at room temperature to the coldest part of the system and back again with minimal loss of refrigeration. The heat exchanger is comprised of two elongated conduits side by side and thermally bonded to each other. The outgoing cold stream flowing in one channel simply picks up the thermal energy from the incoming warm stream flowing in the second channel.

There are two types of expansion device, one of them a simple valve or capillary for isenthalpic expansion, the other an engine in which the expanding gas does useful work against a piston or the blades of a turbine. In this case the expansion is essentially isentropic.

Some of the thermodynamic relations needed for a discussion of low-temperature processes are given below.

Kelvin or absolute scale of temperature defined by the relation

$$\frac{q_1}{q_2} = \frac{T_1}{T_2} \quad (1)$$

in which q_1 and q_2 are respectively the heat received and the heat rejected by a reversible engine working between the absolute temperatures T_1 and T_2 . The equation applies equally well to reversible heat pumps. The only difference is in the direction of the flow of work, namely, out of the engine, into the pump. The magnitude of the work, of course, must be equivalent to the difference between the two heat quantities.

Enthalpy is defined as the sum of the internal energy u and the pressure-volume product pv , $h = u + pv$. Another useful relation is concerned (2)

with the change of enthalpy with temperature

$$dh = c_p dT \quad (3)$$

where c_p is the specific heat at constant temperature.

The Joule-Thomson coefficient is defined by the equation

$$\mu = \left(\frac{\partial T}{\partial P} \right)_h \quad (4)$$

The First Law energy equation for steady flow is

$$Q = h_2 - h_1 + W_x \quad (5)$$

where Q is the flow of heat and W_x the flow of usable work respectively across the boundary of the system.

Changes in entropy are given by the relation

$$ds = \frac{dq}{T} \quad (6)$$

along a reversible path.

HISTORY

Significant events in the development of apparatus for producing and maintaining very low temperatures. Four distinct approaches to the problem were made, all leading to important developments.

1. Isenthalpic expansion of a compressed gas possessing a positive Joule-Thomson effect with aid of counterflow heat exchanger.

1895 Carl von Linde in Germany liquefied air in quantity in a continuous process for the first time.

1898 James Dewar in England liquefied hydrogen with the aid of liquid air. The Joule-Thomson coefficient of hydrogen is negative at room temperature but becomes positive at lower temperatures.

1908 Kamerlingh-Onnes in the Netherlands liquefied helium with the aid of liquid hydrogen.

2. Isentropic expansion of compressed gas with assistance of a counterflow heat exchanger.

1838 - 50 Dr. John Gorrie of Florida devised and built an ice-making machine in which the refrigerative effect was secured by an engine working on compressed air. Gorrie's system also included an elementary counterflow heat exchanger.

1897 - 1902 Georges Claude, French inventor, made substantial improvements in Gorrie's system by way of adapting it to the liquefaction of air.

1925 - 26 du Pont engineers in the United States used compressed hydrogen as the working fluid in an expansion engine-heat exchanger cycle for refrigeration in the 60° to 70° K range for purifying gases.

1934 P. Kapitza in England, using helium as the refrigerant and with the aid of liquid air and a Joule-Thomson addendum, liquefied helium.

1946 S. C. Collins developed new cycle with multiple expansion engines thermally staged. Improved engines and heat exchangers for greater reliability and ease of maintenance. Precoolants not required.

1964 Collins introduced expansion engine with plunger-type pistons and crosshead with sealed bearings.

3. Isentropic expansion of compressed gas with assistance of a thermal regenerator.

1814 - 27 Rev. Robert Stirling of Scotland developed a new heat engine using a regenerator for recovering heat that might otherwise be wasted.

1862 - 65 Alexander Kirk of Scotland converted Stirling's heat engine into an efficient heat pump by reversing it. Although intended for refrigeration near the ice point, Kirk's machine actually achieved temperatures below -40°C .

1954 Kühler and others in the Netherlands improved Kirk's machine and adapted it first for the liquefaction of air and later for refrigeration down to 20°K .

1959 W. E. Gifford and H. O. McMahon modified the Stirling cycle to separate the compression machinery from the regenerator and expansion device. A standard type of compressor is used. The refrigerating portion is compact, small in weight and adaptable to unusual conditions.

4. Free expansion of highly-compressed gas from a flask which has been precooled to the lowest available temperature. At any time during the "blow-down" the gas remaining in the flask will have expanded reversibly and cooled accordingly. Depending upon conditions such as degree of precooling, initial pressure, heat capacity of the flask and identity of gas used, a fraction of the gas will condense within the flask.

1877

Cailletet in France obtained a mist of liquid oxygen when he released the pressure in a vessel charged with oxygen at very high pressure and at an initial temperature of -40°C .

1923

F. E. Simon in Germany liquefied helium in useful quantities by means of Cailletet's method. Simon used liquid and solid hydrogen as the precoolant. At the start of the expansion, the pressure was 100 atm and the temperature 11°K . A large yield of liquid was obtained.

1967

Collins liquefied helium by cooling the vessel with gas discharged from an expansion engine. The starting pressure and temperature were 100 atm and 19°K respectively.

DISCUSSION OF LOW TEMPERATURE CYCLES

1. Isenthalpic Expansion

The primary requirement of a refrigerant to be used in this type of cycle is that it must possess a positive Joule-Thomson coefficient at the warm end of the counterflow heat exchanger. Said in another way, the enthalpy of the outgoing low pressure gas must be greater than that of the incoming high pressure stream. From Equation 5 above, as applied to the heat exchanger-expansion valve system, it is seen that the refrigerative load Q is equal to the gain in enthalpy, there being no useful work done.

Figure 1a represents diagrammatically the Linde cycle for the liquefaction of air. Since the J-T coefficient for air at room temperature is small, it is desirable to compress to 150 to 200 atm. At 300°K the enthalpy of air under a pressure of 200 atm is less than that at 1 atm by 8 cal/gram. Initially, the temperature drop at the valve will be approximately 34° . The colder gas returning through the heat exchanger extracts heat from the incoming high pressure air so that the latter arrives at the valve at a progressively lower temperature until the liquid phase appears. When a steady state has been attained, a fraction of the

stream drops out as liquid. In this instance the maximum possible value of the fraction is 0.08. The final temperature drop at the valve is somewhat more than 90° . It is characteristic of Joule-Thomson heat exchangers to operate with relatively high ΔT 's at the cold end. This coupled with the fact that because of partial liquefaction the cold stream is deficient in mass makes it easy for the counterflow heat exchanger to recover nearly all of the available refrigeration possessed by the outgoing stream.

2. Isentropic Expansion

In an isentropic expansion the temperature drop resulting from the work done by the gas is usually large in relation to the Joule-Thomson effect. The refrigerant can, therefore, be any gas that is otherwise acceptable.

Gorrie's ice machine of 1851 is indicated in Figure 1b. Because of the high temperature level of refrigeration, it was more appropriate to place the counterflow heat exchanger in the path of the incoming water which was to be frozen rather than the compressed air. Air was used as the refrigerant. Gorrie's expansion engine was a modified steam engine.

Figure 1c is a flow diagram of an air liquefier designed and built by Claude in 1902. Note that the heat exchanger is divided into two parts, the engine receiving a large fraction of the compressed air from the intermediate zone and delivering the expanded air to the cold end of the colder section. The remaining fraction of compressed air, still at the higher pressure, is further cooled and completely condensed by the action of the stream of expanded air. At the expansion valve V, the pressure drops to substantially 1 atm; and a small part of the liquid flashes into vapor which joins the engine exhaust for the return trip through the heat exchanger.

In an earlier model Claude had placed his engine at the end of the heat exchanger with the intent of forming liquid in the engine and separating it from the vapor in the discharge pipe. The yield of liquid was very low because of the irreversible cooling of each new charge of compressed air by the film of liquid on the cylinder wall.

The schematic diagram of Figure 1d represents Kapitza's helium liquefier of 1934. In addition to changing the working fluid from air to helium, Kapitza found it necessary to precool with liquid air or nitrogen and to add a Joule-Thomson exchanger for the temperature interval 10° to 4.2° . Because of the extraordinarily narrow pressure and temperature range of the two-phase region of helium, the overall efficiency is greater when a fraction (of the order of 25%) of the compressed helium is expanded isenthalpically.

In the cycle shown in Figure 1e the liquid nitrogen precooling has been replaced by a second engine. There is justification for having a multiplicity of engines thermally staged along the heat exchanger in that the principal heat load in a helium liquefier arises from the specific heat of the gas rather than the latent heat of condensation. One liquefier with four engines has been successfully operated.

Figure 2 is a partial sectional view of the helium liquefier at M.I.T. It is of interest here because of the engine pistons and crosshead. It is the first engine of its kind. The plunger-type piston is made of micarta. One end of the piston is at the average temperature of the working helium, about 60°K for one and 11°K for the other; and the other end is at room temperature. Sealing of the piston is accomplished by an "O" ring at the warm end. All of the moving parts of the crankshaft and crosshead are carried by sealed ball bearings.

A similar liquefier, recently completed at Arthur D. Little, Inc., for Brookhaven is shown in Figure 3. This machine has a capacity of 60 l/hr as a liquefier or a refrigerative output of 245 watts at 4.3°K .

Apparatus as used in the reversed Stirling cycles is shown in Figure 4. Kirk's machine of 1862, Figure 4a, features a cylinder within which a piston C and a regenerator-displacer D slide. The piston is power driven through a definite cycle causing the pressure to rise and fall rhythmically. The displacer is made of a stack of woven wire disks. It is moved up and down with the same frequency as the piston but not in phase with it. When the piston is at its lowest position and the pressure is at maximum, the displacer must be at the bottom of the cylinder. The temperature of the gas is high at this time, and heat flows

out from the finned area near the middle of the cylinder. Before the piston moves appreciably, the displacer is moved quickly to a position near the piston. The compressed gas charge passes through the porous displacer to fill the cavity at the bottom of the cylinder. Then the piston and the displacer move upward, the pressure falls to its minimum value and the temperature of the gas falls. The displacer is then returned to the bottom. The gas is transferred to the intermediate space, and a thermal gradient is set up in the regenerator. On the next cycle the compressed gas begins its expansion at a lower temperature, and the final temperature is lower.

Kohler and others have developed an elegant small air liquefier based on this principle. By adding a second stage, refrigeration in the 20°K range has been achieved.

Figure 4b illustrates the modification introduced by Gifford and McMahon. The compressor has been divorced from the cooling equipment. Mechanically-operated valves at room temperature expose the regenerator and displacer chambers alternately to the discharge and the suction pipes of the compressor.

With displacer in the down position, the system is pressurized. The charge of gas is heated appreciably by flow work during filling. The displacer is then moved to its uppermost position. This action causes the gas charge to flow through the regenerator in which it is cooled to the space below the displacer. The pressure is then relieved, isentropic expansion of the charge takes place; and the temperature falls. After many cycles, a steady state is reached. The upper end of the regenerator will be above room temperature, the lower end will be very cold.

Figure 5 is a schematic drawing of the ADL Cryodyne Refrigerator which is based on the Gifford-McMahon cycle. In addition to the three stages of cooling by means of regenerators and displacers, a Joule-Thomson loop has been added for the purpose of having refrigeration at the liquid helium level. The heat capacity of all substances falls off as the temperature approaches the absolute zero. Regenerators depend upon the heat capacity of the material they are made of to absorb heat from the gas being cooled. Below 12°K regenerators are quite ineffective.

USES OF LOW TEMPERATURES

The value of liquefied gases in basic research is inestimable. Liquid helium itself has received much attention from many of our ablest physicists, but the environment it provides for the study of the properties of matter in general is much more important. The current usage of liquid helium for this purpose at M.I.T. is approximately 6000 l/month.

Liquid nitrogen and oxygen in commerce have become one of the heavy industries. Liquid hydrogen and liquid helium have achieved a place of importance in space technology.

A significant number of helium refrigerators are devoted to cryo-pumping and to cooling superconducting magnets.

Figure 6 is a photograph of a coil winding apparatus and a finished coil of finned tubing for use in a novel heat exchanger for the recovery of refrigeration from a stream of helium gas at about 12 mm of mercury pressure. This is part of a 300 watt refrigerator for 1.85°K.

The physical properties of many substances are altered at very low temperatures. In general, matter becomes stronger and more brittle. Figures 7, 8 and 9 illustrate the effect upon stainless steel.

Electrical resistance of conductors decreases and, in some cases, becomes zero.

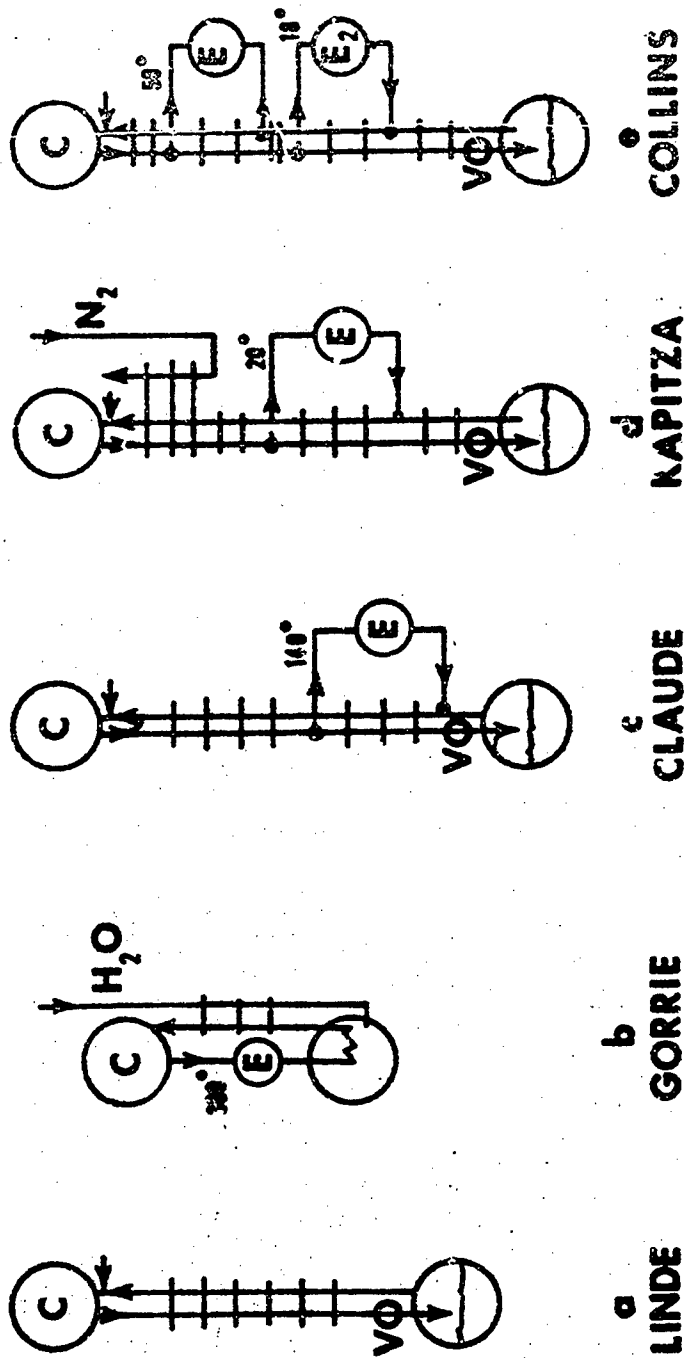


FIG. 1 COMPARISON OF LIQUEFACTION CYCLES

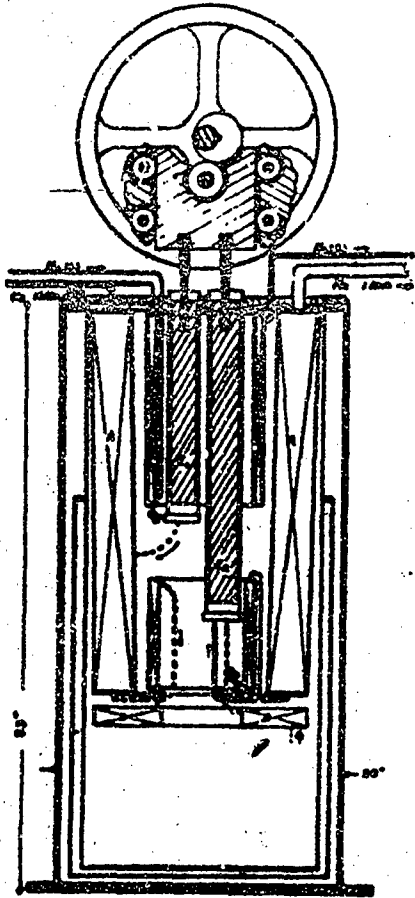


Figure 2
Partial Sectional View of M.I.T. Liquefier

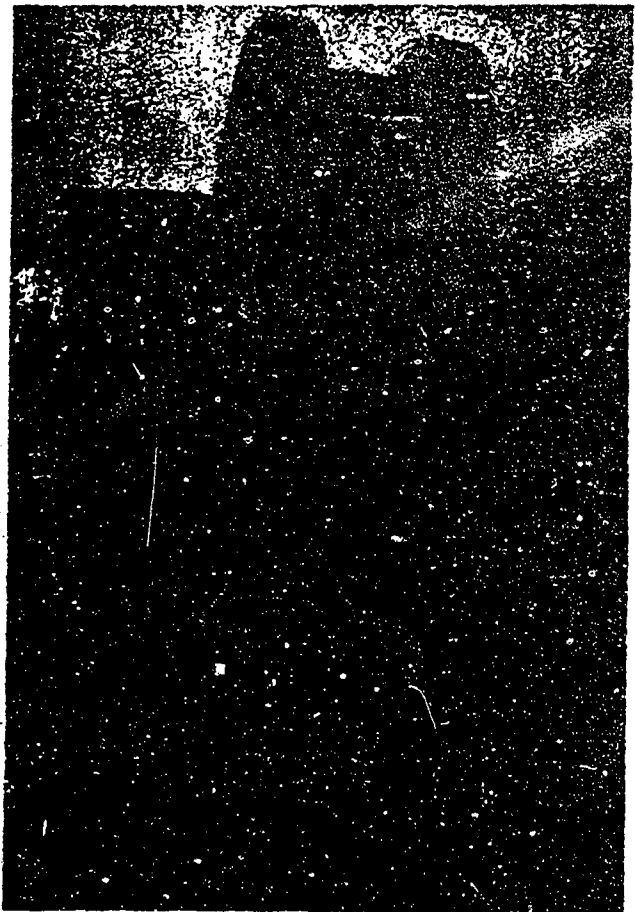
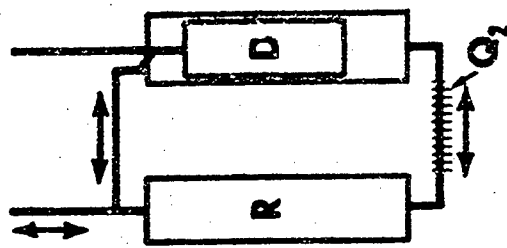
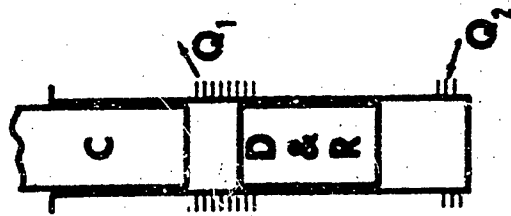


Figure 3
ADL-COLLINS HELIUM
REFRIGERATOR/LIQUEFIER



b GIFFORD-McM. HON



a KIRK

Fig. 4 REVERSED STIRLING CYCLES

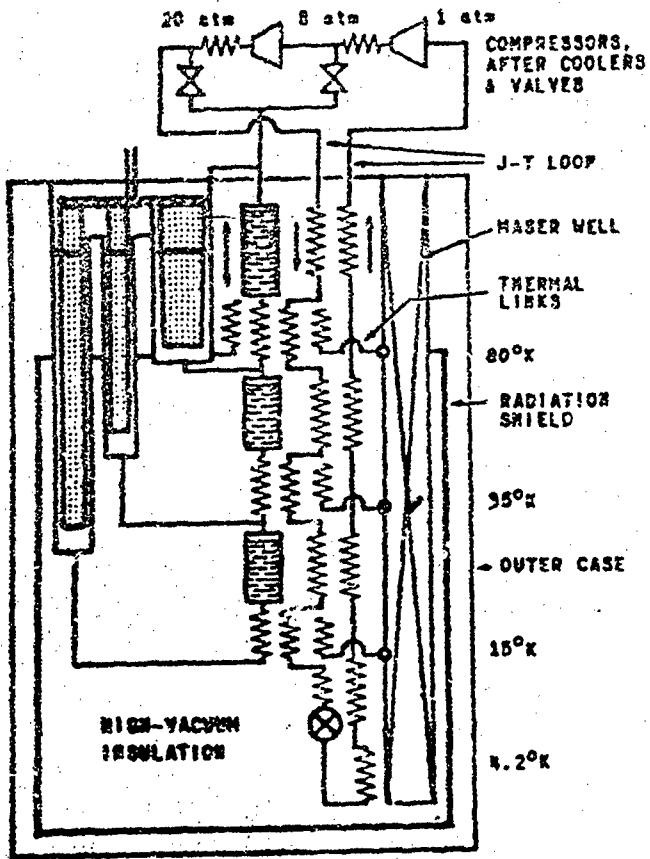


Figure 5
 ADL CRYODYNE^(R)
 HELIUM REFRIGERATOR



Figure 6
 Manufacturing Coils for
 1.85°K Refrigerator

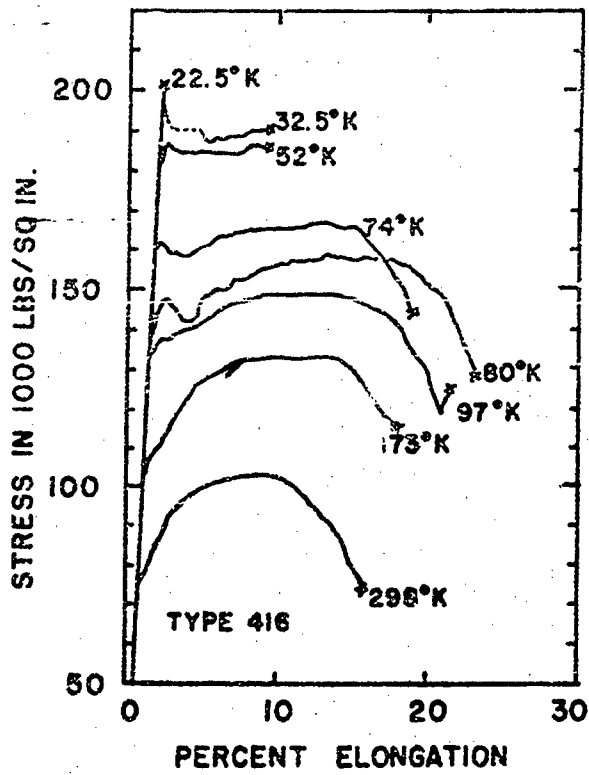


Figure 7

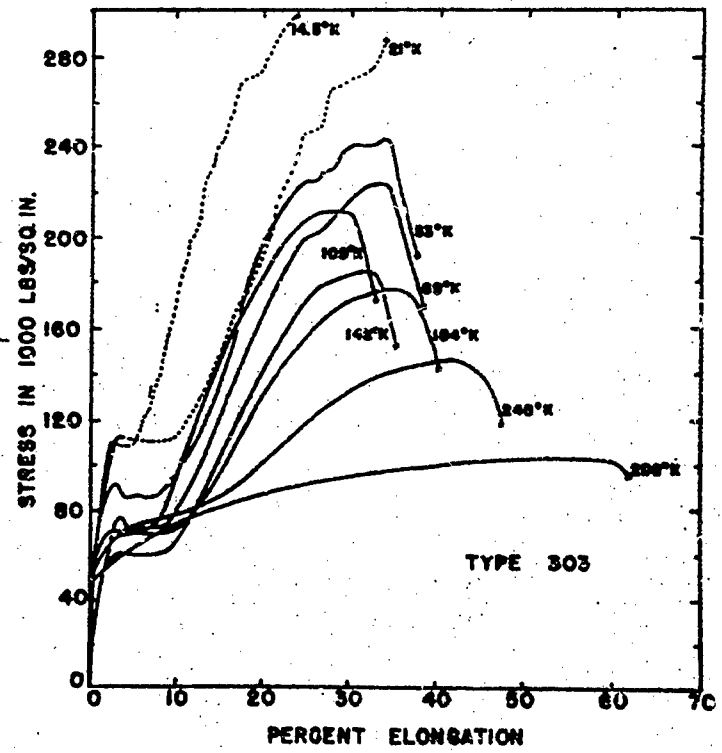


Figure 8

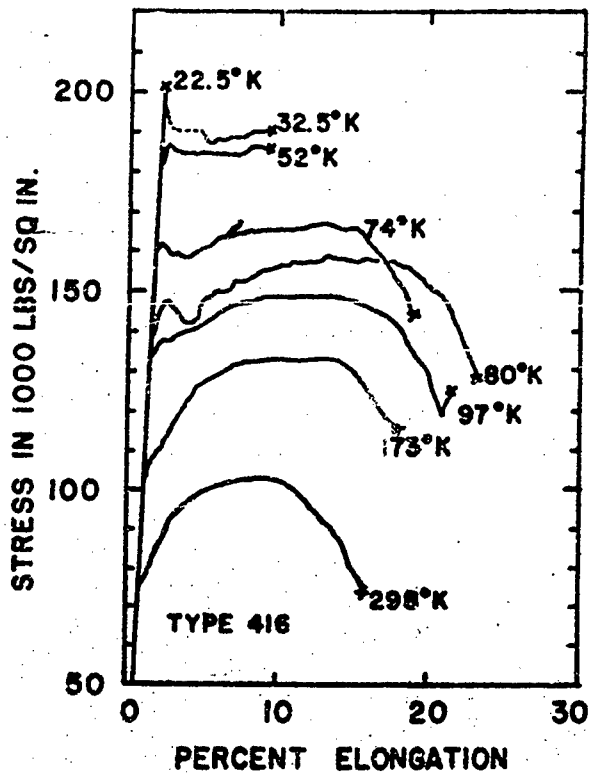


Figure 7

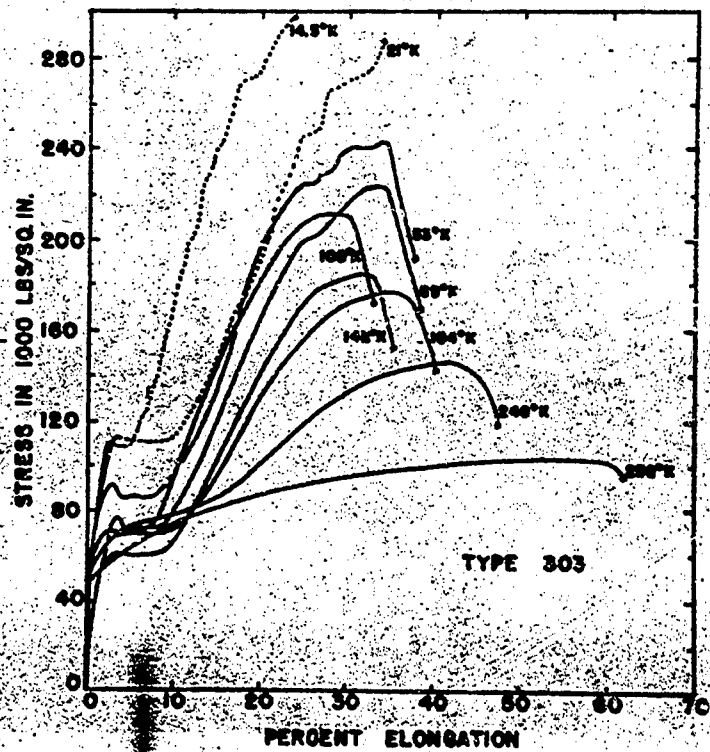


Figure 8

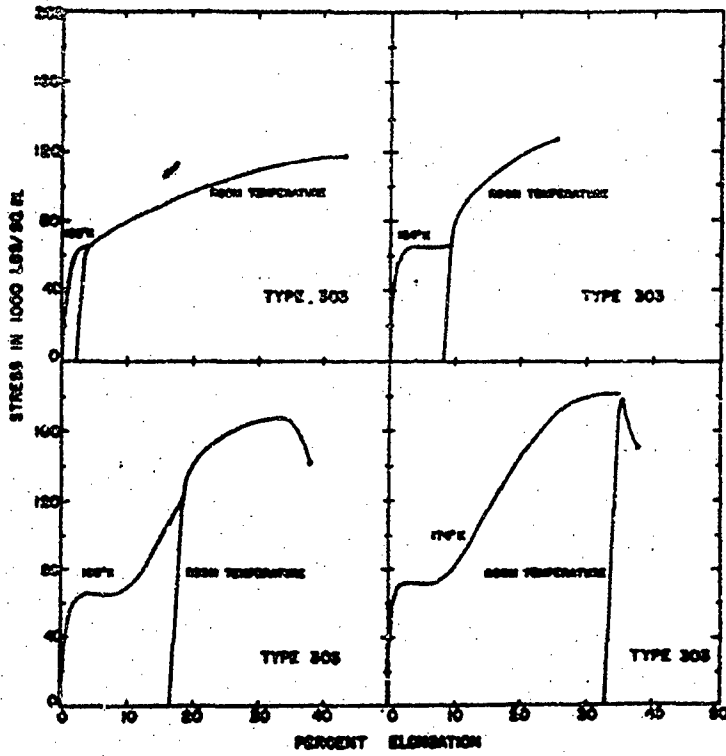


Figure 9

DEFORMATION AND FRACTURE OF VISCO-ELASTIC
MATERIALS

(23 May 1967)

by

A. N Gent

Dr. A. N. Gent joined the British (now Natural) Rubber Producers' Research Association in 1949 as Research Physicist, and carried out investigations of the mechanical behavior of rubber under large elastic deformations, under vibratory forces and under extreme temperature conditions. In April 1961 he took up a dual appointment as Research Associate (now Assistant Director) of the Institute of Polymer Science and Professor of Polymer Physics at the University of Akron, where he and his students are investigating a wide range of problems in the mechanics of rubberlike substances.

1. Introduction

Elastomers are not perfectly elastic; some part of the energy spent in deforming them is dissipated due to a variety of causes. The principal energy-dissipating mechanisms are:

- (i) Internal friction or viscosity, as the molecular chains rearrange their positions and segments of them slide past each other.
- (ii) Strain-induced crystallization. Under the orienting influence of a deformation, sufficiently regular molecules may form microcrystalline assemblies. Any further deformation can only be accomplished by disrupting the crystallites with a corresponding dissipation of energy.
- (iii) Structural breakdown of a filled elastomer (two-phase) system. Hard filler particles, generally of carbon black, stiffen elastomers in two ways: by forming long associated chains of particles and by adhering strongly to the molecules in contact with each particle. Both of these associations are destroyed at least partially by a deformation, the particle chains at quite small deformations and the elastomer-particle bonds at large ones.

The dissipation of energy internally has usually been regarded as a serious disadvantage of elastomers. Recently, however, it has been shown to be responsible for the resistance to a wide variety of fracture processes; tensile rupture, tearing, surface cracking by ozone, and abrasion. These findings are reviewed here. Also, the existence of unstable states is pointed out, at which an elastic deformation becomes inhomogeneous. Small regions then become highly deformed, often to the point of rupture. In these cases the criterion for fracture is an elastic one involving the relations between applied loads and deformations.

2. Tensile Rupture

Strength measurements at different rates of elongation $\dot{\epsilon}$ and temperatures T are found to depend upon a single variable $\frac{\dot{\epsilon}}{\eta}$, where η is the segmental viscosity (Smith, 1958). Variations with temperature are thus due to corresponding viscosity changes. Moreover, the master curve under iso-viscous conditions has the form expected of a viscosity-controlled quantity; it rises sharply with increased rate of elongation to a maximum value at high rates when the segments do not move and the material breaks as a brittle glass (Bueche, 1955). The breaking elongation at first rises with increasing rate of elongation,

reflecting the enhanced strength, and then falls at higher rates as the segments become unable to respond sufficiently rapidly.

An alternative measure of tensile rupture is the work W_b required to break the rubber per unit volume. It varies with the rate of elongation in a similar manner to the elongation at break, passing through a maximum value with increasing rate, or with decreasing temperature at a constant rate. The variation closely resembles that obtained for energy dissipation under small deformations, indicating the close parallel between energy dissipation and energy required to rupture. A more striking demonstration is afforded by the recent observation of Grosch, Harwood and Payne (1966) that a direct relationship exists between W_b and the energy dissipated W_d in stretching to the breaking elongation, irrespective of the mechanism of energy loss, i.e., for filled and unfilled, strain-crystallizing and amorphous elastomers. Their empirical relation is

$$W_b = 4.1 W_d^{2/3},$$

W_b and W_d being measured in joules/cm³. Those materials which require the most energy to bring about rupture, i.e., the strongest elastomers, are precisely those in which the major part of the energy is dissipated before rupture.

3. Tear Strength

It is important to recognize that the tear strength T is also not a constant value for a particular material; it depends strongly upon the temperature and rate of tear, i.e., the rate at which material is deformed to rupture at the tear tip. Several critical values of T may be distinguished. The smallest possible value is given by the surface energy, about 50 ergs/cm² for non-polar hydrocarbons. This value is indeed found to govern the growth of surface cracks due to chemical scission of the elastomer molecules (by atmospheric ozone), when the function of the applied forces is merely to separate molecules already broken (see section 6). Another critical value of T is that necessary to break all the molecules crossing a random plane. This has been estimated to be of the order of 10⁴ ergs/cm² for typical hydrocarbon elastomers (Thomas, 1966). Measurements of the minimum value of T necessary to cause any cut growth by mechanical rupture are in reasonable agreement with this value (Lake and Lindley, 1965).

In simple tearing measurements the observed values of T are considerably larger, ranging from 10⁵ to 10⁸ ergs/cm². The reason for the enhanced strength is made clear by considering the process by which the energy T is dissipated at the tear tip. Thomas (1955) has shown that T can be expressed in terms of the effective diameter q of the tip of the tear and the

"intrinsic" breaking energy \bar{W}_b of the material by the approximate relation

$$T = d \bar{W}_b .$$

The "intrinsic" breaking energy may be defined as the energy required to break unit volume of the material in the absence of a significant nick or flaw. It will be generally similar to, but larger than, the value of W_b determined for carefully prepared tensile test-pieces in which chance edge flaws are minimized. Both \bar{W}_b and d depend upon the conditions of tear. However, for unfilled non-crystallizing elastomers, d remains small (of the order of 0.01 cm) and relatively constant. In these cases Greensmith (1960) has shown that T is proportional to \bar{W}_b and changes in a parallel fashion with temperature and rate of tearing (rate of extension). Mullins (1959) has also shown that T is proportional to a measure of the viscous stress component. Thus the internal viscosity determines the intrinsic breaking energy and the tear resistance for such materials. The effective diameter d of the tip of a growing tear also depends upon the elastic and viscous properties to some degree (Gent and Henry, 1967) so that the tear energy T shows a complex temperature dependence. It is still governed by the internal energy dissipation, however, and is found to be the same for elastomers of widely-different chemical composition under conditions of equal segmental mobility (Mullins, 1959).

In strain-crystallizing elastomers (for example, natural rubber) the tear resistance and tensile strength are greatly enhanced. Such materials show mechanical energy dissipation as discussed in the Introduction, and their strength has been accounted for in this way (Andrews, 1963). Adding reinforcing particulate fillers to non-crystallizing elastomers brings about a similar strengthening. This effect is principally due to a pronounced change in the character of the tear process, from relatively smooth tearing in unfilled materials to a discontinuous stick-slip process, in which the tear develops laterally or even circles around under increasing force until a new tear breaks ahead and the tear force drops abruptly. The process then repeats itself. This form of tearing has been termed "knotty" tearing (Graessmuth, 1956).

The mechanism of tear deviation is still obscure. It may occur because the maximum stresses lie off the tear axis, due to anisotropic elastic behavior of the strained material around the tear tip or to a "frozen" stress mechanism proposed by Andrews (1963), or because the filled materials have anisotropic strength. Pronounced knotty tearing occurs only within a limited range of tear rates and temperatures, depending upon the particular filler and elastomer employed (Graessmuth, 1956). There are some indications that this effect is associated with the viscoelastic response of the polymer, but the conditions required involve much higher temperatures and lower rates of extension than the main rubber-to-glass transition region.

4. Sliding Friction

Friction is naturally associated with energy dissipation. The principal mechanism of dissipation again turns out to be energy losses within the elastomer, but the connection between the coefficient of friction μ and the internal viscosity, for example, is complex; two distinct modes of deformation having been distinguished (Grosch, 1963). The first is due to indentation by surface asperities on the track and the second arises from molecular adhesions which are formed and broken during sliding.

On a lubricated rough track the value of μ increases with increasing sliding velocity and then passes through a maximum. The relation closely resembles the dependence of the energy absorption per deformation cycle upon the frequency of deformation. Indeed, the speed of sliding at which μ has a maximum value, divided by the spacing between asperities, corresponds accurately to the frequency of deformation at which the energy dissipation is a maximum at the same temperature. The dominant role of energy dissipation in lubricated sliding friction is thus established. For sliding over a clean smooth surface the relation for μ is found to be similar, but displaced toward lower velocities. It corresponds, therefore, to "asperities" of much closer spacing than those in the rough surface.

The spacings are calculated to be only about 60\AA , by comparing the velocity for maximum friction with the frequency for maximum energy absorption. Thus, friction between dry smooth surfaces is associated with deformations on a molecular scale. It has therefore been attributed to transitory molecular adhesions between elastomer and track. The high frictional coefficient is, however, again due to dissipation of energy in the rubber as it undergoes local shearing deformations around the temporary bonds, and not due to the strength of the bonds themselves. This is shown by the characteristic dependence on speed and temperature.

On dry rough surfaces the effects of both surface asperities and molecular adhesions are evident in the master relation for μ as a function of the speed of sliding. On lubricated smooth surfaces both deformation processes are minimized and the coefficient of friction is correspondingly small.

5. Wear Due to Sliding

As both the tear resistance and the tearing (frictional) force depend upon temperature in accord with viscosity-controlled processes, it is not surprising that the abrasive wear as a function of speed of sliding should do so. A suitable measure of the rate of wear is provided by the ratio A/μ of the volume A abraded away per unit normal load and unit

sliding distance to the coefficient of friction μ . This ratio, termed the abrasibility, represents the abraded volume per unit energy dissipated in sliding.

It is found to decrease with increasing speed, pass through a minimum and then rise again at high speeds. This behavior resembles the variation of the reciprocal of the breaking energy W_b with rate of deformation (a reciprocal relationship because high abrasibility corresponds to low strength). Indeed, Grosch and Schallamach (1965) found a general parallel between A/μ and $1/W_b$. Moreover, the coefficient of proportionality was found to be similar, about 10^{-3} , for all the unfilled elastomers examined. This coefficient represents the volume of rubber abraded away by unit energy applied frictionally to a material for which unit energy per unit volume is necessary to cause tensile rupture. It may be regarded as a measure of the inefficiency of rupture by tangential surface tractions; large volumes are deformed but only small volumes are removed.

6. Resistance to Ozone Cracking

In an atmosphere containing ozone, stretched strips of unsaturated elastomers develop surface cracks. These cracks grow in width and depth and either sever the strip or cause a serious loss of strength. From experiments with initial cuts of different length and with elastomers of different degrees

of crosslinking, and hence different values of Young's modulus, Braden and Gent (1960, 1961) found that the minimum stresses for cracking to occur corresponded to a critical energy requirement of about 50 ergs/cm² of new surface. This suggests that the critical condition is a very simple one: the stored elastic energy must be sufficient to meet the surface energy requirements. The critical stresses to cause cracking in uncut test-pieces corresponded to cuts about 10⁻³ cm deep, using the same energy criterion. It was therefore deduced that normal ozone cracks start from surface nicks or flaws equivalent to cuts of this size.

Provided the critical stress was exceeded, the rate of crack growth did not depend significantly upon the applied stress over a wide range of stresses. However, it depended markedly upon temperature. The rates of growth were determined over a wide temperature range for a series of butadiene-styrene rubbers containing from 0 to 80 per cent styrene (Gent and McGrath, 1965). When plotted against the temperature difference $T - T_g$ between the test temperature and the glass temperature for each material, they were found to form a single relation, suggesting that the segmental mobility is the primary factor determining the rate of growth of an ozone crack. The Williams, Landel and Ferry relation for the segmental mobility (Ferry, 1961) was found to describe the experimental

results well at low temperatures. At higher temperatures the observed rates did not continue to increase with increasing segmental mobility but approached a constant value. This was due to the limited concentration of ozone; the incidence of ozone molecules had become rate-determining, rather than the segmental mobility. However, over a temperature range up to about $T_g + 60^\circ\text{C}$ at this particular ozone concentration, the rates of ozone crack growth were clearly determined by the internal viscosity of the rubber, rather than by strictly chemical factors. This is apparently due to the need for movement of the rubber molecules in and near the crack tip to yield new surfaces for reaction (Gent and McGrath, 1965).

7. Elastic Instabilities

Novel instabilities can occur for materials capable of undergoing large elastic deformations. For example, the uniform inflation of a long rubber tube becomes unstable at a critical degree of inflation and the tube develops a pronounced "blister". In such cases, where the deformation becomes markedly non-uniform, the specimen will obviously rupture prematurely. For materials of limited extensibility fracture can therefore be calculated quantitatively from purely elastic considerations, and will be largely independent of the detailed fracture properties of the material. The cavitation of elastomers

under a negative hydrostatic pressure (triaxial tension) is an example of this type of fracture. Gent and Lindley (1958) have shown experimentally that the critical stress at which cavitation occurs is not greatly dependent on the tensile strength or extensibility of the elastomer. Instead it is directly proportional to the elastomer modulus. Indeed, quantitative agreement was obtained with the calculated stress at which the elastic expansion of a hypothetical small hole in the elastomer would become indefinitely large.

Acknowledgments

This review was prepared in connection with a program of research supported by the National Science Foundation. A brief version was presented at the Conference on Elasto-Plastics Technology, Detroit, in May, 1965. The author is indebted to an earlier review by Grosch and Mullins (1962), in which the general relationship between hysteresis and various strength properties was outlined. Other recent reviews by Greensmith, Mullins and Thomas (1963), Landel and Fedors (1964) and Halpin (1965) should be consulted for further details.

References

- Andrews, E.H. (1963) *Rubb. Chem. Technol.*, 36, 325.
- Braden, M., and Gent, A.N. (1960) *J. Appl. Polym. Sci.*, 3, 100.
- Braden, M., and Gent, A.N. (1961) *Kautschuk U. Gummi*, 14, WT157.
- Bueche, F. (1955) *J. Appl. Phys.*, 26, 1133.
- Ferry, J.D. (1961) "Viscoelastic Properties of Polymers", Wiley, New York.
- Gent, A.N., and Henry, A.W. (1967) in press.
- Gent, A.N., and Lindley, P.B. (1958) *Proc. Roy. Soc. (London)*, A249, 195.
- Gent, A.N., and McGrath, J.E. (1965) *J. Polym. Sci.*, A2, 1473.
- Greensmith, H.W. (1956) *J. Polym. Sci.*, 21, 175.
- Greensmith, H.W. (1960) *J. Appl. Polym. Sci.*, 3, 183.
- Greensmith, H.W., Mullins, L. and Thomas, A.G. (1963) Chap. 10 in "The Chemistry and Physics of Rubberlike Substances" ed. by L. Bateman, Wiley, New York.
- Grosch, K.A. (1963) *Proc. Roy. Soc. (London)*, A274, 21.
- Grosch, K.A., Harwood, J.A.C., and Payne, A.R. (1966) *Nature*, 212, 497.
- Grosch, K.A., and Mullins, L. (1962) *Rev. Gen. Caoutch.*, 39, 1781.
- Grosch, K.A., and Schallamach, A. (1965) *Trans. Instn Rubb. Ind.*, 41, T80.
- Halpin, J.C. (1965) *Rubb. Chem. Technol.*, 38, 1007.
- Lake, G.J., and Lindley, F.B. (1965) *J. Appl. Polym. Sci.*, 9, 1233.
- Landel, R.F., and Fedors, R.F. (1964) Chap. IIIB in "Rupture Processes in Polymeric Solids" ed. by B. Rosen, Interscience, New York.
- Mullins, L. (1959) *Trans. Instn Rubb. Ind.*, 35, 213.
- Smith, T.L. (1958) *J. Polym. Sci.*, 32, 99.

Thomas, A.G. (1955) J. Polym. Sci., 18, 177.

Thomas, A.G. (1966) Unpublished work.

THE CHALLENGE OF EFFECTIVE TECHNICAL SPEAKING
(6 June 1967)

by
Harry E. Hand

Dr. Harry E. Hand is Associate Professor and Head of the Department of Humanities, School of Engineering, Air Force Institute of Technology. He earned the B.S. degree from Ohio University and Ph.D. from University of Michigan. Previously an instructor in English at the Air Force Academy, Dr. Hand now teaches technical writing, speech and American literature. He has written many articles and reviews for professional journals and is also the author of a textbook Professional Speaking for the Technical Man to be published in 1968.

Technical speaking can be defined as the formal oral presentation of purposeful technical information to an audience who is technically knowledgeable to some degree, or at least interested in technical matters. In any communications system there are three principal components: a sender, a communication channel, and a receiver. The effectiveness of the communications system depends on the effectiveness or the quality of all three components: the sender or speaker must analyze the audience and the purpose of his message, and he must carefully select and organize the material he transmits; the message must be transmitted or delivered in ways that the audience can understand--often the channel of communication, words, is reinforced by many kinds of audio-visual aids; and the receiver or listener must have all of its communication networks open and alert. These requirements offer a considerable challenge to any technical speaker, and if all components of the system are effective, then the receiver will understand the message of the sender. Often there is desirable feedback from a receiver who wants additional information. Noise is anything that interferes with the sending and receiving of a message, for example, the use of words or visual aids that the listener does not understand. The sender or speaker must accept the

following responsibilities to insure effective oral communication:

(1) analyze the audience for their knowledge and interest in the subject;
(2) determine the purpose of the message; (3) carefully select and
organize the material for easy aural and visual comprehension, including
audio-visual aids; and (4) practice delivery of the material to help
eliminate unwanted noise. If the sender performs these functions
effectively, the reliability of any communications system is increased.

The speaker must first analyze the audience for their technical knowledge and experience, and for their interest in the subject or their need to know the material. An audience listening to a technical presentation may consist of fellow specialists, specialists in another technical field, or decision makers, who are intelligent but uninformed about technical matters. A speech explaining the latest developments in the manufacture of transistors would include and emphasize different data for audiences of reliability engineers, aeronautical engineers, and system managers. The speaker must also remember that different audiences do not always want to know or need to know the same information. The system manager may not need to know or want to know about the physics of transistors in a speech describing the latest developments in transistors. Audiences may also differ in their attitudes toward the subject and the speaker, and in their fixed beliefs. An electrical engineer may be unsympathetic toward psychologists or motivation research--unless its importance to his field can be demonstrated. If a speaker first analyzes his audience for their technical knowledge and interests, he can better select and present meaningful information.

Secondly, a speaker must determine the purpose of his presentation.

A decision as to the exact purpose of the technical talk helps the speaker to select and to organize the data so that it fulfills his communication objective. The general communication objective may be to inform, to convince, or both. After the general objective has been decided, the specific objective must be decided and written down to guide the speaker.

A purpose statement is to the speaker preparing a speech as the North Star is to a celestial navigator; it helps give him his bearing and keeps him on course. A speech on the new design of a wing configuration might be (a) to explain why and how the wing was designed; or (b) why the wing configuration must be used in all future fighter aircraft; or (c) both (a) and (b), that is, both informative and persuasive. Until a speaker has decided his exact purpose, he cannot properly select significant, relevant information.

Next the speaker must carefully select and organize information which suits his audience and his purpose--and the time limits imposed. He may elect to use several audio-visual aids to help him send his oral message. The information should be organized into a sentence outline. A sentence outline forces the speaker to be concrete, and it helps him to arrange his ideas logically, clearly, concisely, and emphatically. The outline also enables the speaker to check the selection and organization of the information against his stated purpose. Later the outline can be put on 3 x 5 cards for easy handling in delivering the speech extemporaneously, or the outline can be expanded into a complete written manuscript. Writing out a speech, whether later delivered from a manuscript or not, allows the speaker the advantage of seeing the whole relationship and development of the ideas.

Every speech has three vital sections; an introduction to prepare the listener for the topic; a body to develop the topic; and a closing to recall important points. Specifically, the function of an introduction is to state the subject and purpose of the talk; to state the scope of the talk, that is, what will be covered and what will not be covered; to state how the talk is organized--its plan of development; and to state the importance and application of the information (a motivating device). The specific function of the body of the speech is to develop, clarify, and emphasize principal points; and the specific function of the closing is to summarize important information, state conclusions reached about the data, or offer recommendations or solutions.

In organizing and developing the data in the body of the speech, several rhetorical devices can be used to help make the message clear; (1) repetition of important points, preferably in varied ways; (2) transitions which summarize long sections of statistics, formulas, raw material, or material new to the audience, and transitions which set the stage for the next important point to be covered; (3) definition and description of special or unfamiliar terms, mechanisms, and processes; (4) comparison and contrast between the new and the old or between the abstract and the concrete; (5) examples and illustrations of abstract or new ideas.

Audio-visual aids such as charts, blackboards, slides, vu-graphs, handouts, films, models, and tapes offer the speaker a valuable means of presenting figures and equations, showing relationships, illustrating forms and shapes, and reinforcing lists and conclusions. Eighty-five

per cent of our learning comes through the eyes, and eye learning is 35% faster. There is 55% better retention of eye-learned data. Aids should be limited in number, relevant to the topic, and necessary to understanding (not a parade of unnecessary props competing with the speaker for the attention of the audience); easy to comprehend (simple in form, stripped to essentials, with adequate labels); limited to one idea per display; pictorial rather than verbal or statistical whenever possible; presented precisely at the moment needed (because earlier distracting and later ineffective), and removed immediately after discussion to prevent distracting competition with the speaker; visible to everyone; and thoroughly discussed by the speaker.

Lastly, the speaker must practice, practice, practice the delivery of his oral information and the use of his audio-visual aids. If the speaker is thoroughly familiar and at ease with his topic, he should try to deliver his speech extemporaneously, that is, from 3 x 5 note cards. Extemporaneous delivery allows for naturalness, spontaneity, and audience contact or feedback. Repeated practice of the speech and the use of note cards usually gives the speaker the confidence he needs. Speeches should not be memorized word for word--if the speaker forgets a line, all may be lost! If the situation demands the immediate and precise understanding of information (e.g., a briefing on how to unload a fuel tank), the speaker may elect to read from a carefully prepared manuscript. He should read slowly, carefully, and audibly, pausing before and after important points, stressing important words, and looking up at his audience whenever possible. If he is writing the

manuscript himself, he must remember that he is writing a paper for a listener and not a reader; hence he must repeat principal ideas in several different ways. In most technical speaking situations, however, except the most formal or professional, extemporaneous delivery seems to be preferred by most audiences. The extemporaneous talk must be practiced several times aloud to avoid memorizing and to check on timing and sound of voice. Dry running the speech before a friend who matches the audience profile not only gives the speaker confidence, but it also gives him the opportunity to revise openings, closings, order of presentation, use of graphic aids, selection of data, and word choice. Words should be simple but accurate. The accuracy of technical terms must not be sacrificed, but new or difficult terms can be defined. At all costs the speaker must avoid technical shoptalk or jargon which is familiar to one technical group but unfamiliar to another group. Eighty percent of the words in technical communication are found in the vocabulary of our everyday life; 15% are found in the vocabulary of any technical person; and only 5% are found in the vocabulary of a specialized technical person. There seems little need to exceed this ratio of technical terms in most presentations. The voice should be conversational, and gestures, posture, and mannerisms as natural as possible. Nervousness before and during a speech is natural. It can be alleviated by reading the opening or closing, by thoroughly knowing and preparing the topic, and by practicing the speech.

If the speaker accepts his responsibilities of (1) analyzing the audience for their knowledge and interest in the subject; (2) determining

the purpose of the talk; (3) carefully selecting and organizing the material for easy aural and visual comprehension; and (4) practicing the delivery of the talk, then he will have done his part in guaranteeing successful communication. Little has been said in this presentation about the responsibilities of the listener, but if the sender does his job well, the receiver will be motivated to keep all of his networks open and alert.

June 13, 1967

FM SYSTEMS
DR. JACK H. CROW
DIRECTOR OF ENGINEERING
SONEX, INC.

INTRODUCTION

Frequency modulation has been widely used for transmission and storage of data because of four principal advantages:

1. DC response with an AC system
2. Signal amplitude variations cause a secondary effect
3. Ability to trade data bandwidth for accuracy and signal-to-noise performance
4. Compatibility with tape recording techniques

The FM/FM technique using proportional bandwidth subcarrier channels was standardized for data transmission by the Research and Development Board in 1948. Essentially the same system has been continued as the IRIG standard system. The principal change has been the addition of constant bandwidth subcarrier channels in the 1966 revision.

THEORY

A sinusoidal carrier that is frequency modulated by a single frequency signal may be expressed as

$$S = \sin(\omega_0 t + \frac{\Delta\omega}{\omega_m} \sin \omega_m t)$$

where: ω_0 = frequency of unmodulated carrier.
 $\Delta\omega$ = peak frequency deviation of carrier due to the modulating signal.
 ω_m = frequency of the modulating signal.

The above expression may be rewritten in terms of the carrier and sideband frequencies as

$$S = J_0(M) \sin \omega_0 t + \sum_{k=1}^{\infty} J_k(M) [\sin(\omega_0 + k\omega_m)t + (-1)^k \sin(\omega_0 - k\omega_m)t]$$

where: $M = \Delta\omega/\omega_m$ = modulation index.
 $J_k(M)$ = value of the Bessel function of the first kind and k th order with argument M .

This equation shows that in theory the bandwidth of a frequency modulated signal extends without limit.

Furthermore, any phase or amplitude change of the sidebands relative to the carrier should cause an error in the demodulated signal. In practice symmetrical

attenuation of the sidebands causes a reduction of demodulated signal amplitude but very little harmonic distortion. Conversely the phase relations of the sidebands and carrier are extremely critical in regard to harmonic distortion.

Thus the filters in the frequency modulated portion of the system are a practical compromise between narrowband filter with steep sided response which improves interference rejection and signal-to-noise response and broadband filter with constant time delay which improves data accuracy. The constant time delay is also a prime requirement for effective tape speed error compensation. The result is that the most critical filters, the receiver IF and discriminator input filter, should be state-of-the-art filters.

MULTIPLE FREQUENCY MODULATION

The expression for a sinusoidal carrier that is frequency modulated by sinusoidal signals may be written as

$$S = \sin \left[\omega_c t + \sum_{k=1}^n M_k \sin (\omega_k t + \theta_k) \right]$$

where: ω_k = k th modulating frequency.
 M_k = modulation index of the k th modulating frequency.
 θ_k = phase angle of k th modulating frequency.

The above expression may be written in terms of Bessel functions as

$$S = \sum_{n=-\infty}^{\infty} \left[\prod_{k=1}^n J_n(M_k) \right] \sin \left[\omega_c t + \sum_{k=1}^n i_k (\omega_k t + \theta_k) \right]$$

This expression shows that the sideband spectrum contains sidebands separated from the center frequency by the modulating frequencies, their harmonics and the sum and difference frequencies of the modulating frequencies and their harmonics.

This is shown more clearly in the case of two modulating frequencies with zero phase angle. The general expression reduces to

$$S = \left[\sum_{n=-\infty}^{\infty} J_n(M_1) \right] \times \left[\sum_{m=-\infty}^{\infty} J_m(M_2) \right] \sin (\omega_c + i_1 \omega_1 + i_2 \omega_2) t$$

SQUAREWAVE MODULATION

Squarewave modulation is commonly encountered with PCM, PAM and PDM signals. A convenient technique is to consider the modulated signal as the sum of two 100% squarewave amplitude modulated signals. The expression may then be written as

$$S = \cos \omega_c t + \frac{1}{2} \left(\frac{4}{\pi} \sum_{n=1}^{\infty} \frac{1}{n} \sin \frac{n\pi}{2} \right) \left[\cos (\omega_c - n\omega_s) t + \cos (\omega_c + n\omega_s) t \right] \\ + \cos \omega_c t - \sum_{n=1}^{\infty} \sin \frac{n\pi}{2} / \frac{n\pi}{2} \left[\cos (\omega_c - n\omega_s) t + \cos (\omega_c + n\omega_s) t \right]$$

where: ω_{o1} = carrier frequency at one side of the squarewave.
 ω_{o2} = carrier frequency at the other side of the squarewave.
 ω_s = fundamental frequency of the squarewave.

SINGLE FREQUENCY INTERFERENCE

The output of an FM detector with two input signals may be expressed as

$$e = K_D(\omega_d - \omega_o + (\omega_d - \omega_i)[A \cos(\omega_d - \omega_i)t + A^2 \cos 2(\omega_d - \omega_i)t + A^3 \cos 3(\omega_d - \omega_i)t \dots])$$

where: A = ratio of the amplitude of the smaller signal to the larger signal
 K_D = gain constant of the FM detector.
 ω_o = zero output frequency of the FM detector.
 ω_d = frequency of the input signal with the larger amplitude.
 ω_i = frequency of the input signal with the smaller amplitude.

The derivation of this expression assumes a perfect limiter before the detector and also assumes that the detector output is affected by the signal throughout the entire cycle of signal.

There are three important aspects of the interference equation:

1. The amplitude of the interference at the output of the detector is proportional to the frequency difference between the two signals.
2. If A is considerably less than one, the interference frequency is essentially equal to the frequency difference between the two input signals.
3. If A is considerably less than one, the amplitude of the interference is proportional to the amplitude of the interfering signal.

A simplified form of the interference equation is very useful because it gives a close approximation of the worse case interference condition. If the DC term $\omega_d - \omega_o$ is neglected and A is considerably less than one the result is

$$e = K_D(\omega_d - \omega_i)A \cos(\omega_d - \omega_i)t$$

The output filter of the demodulator attenuates the interference beat frequency, $\omega_d - \omega_i$, if this frequency is greater than the cutoff frequency, thus the worse case interference occurs when the difference frequency is approximately the 3 db frequency of the output filter. The peak output of the demodulator due to the interference may then be written

$$\left| \frac{e}{e_n} \right| = \frac{\omega_d A}{2\Delta\omega_p} = \frac{A}{2D}$$

where: $\Delta \omega_p$ = full-scale output due to frequency change of.
 $D = \Delta \omega_p / \omega_c$ = deviation ratio of the channel.

This result must be modified to include the effect of the filters in the system.

HARMONICALLY RELATED INTERFERENCE

Classical interference theory does not completely account for interference because of the assumption that the detector output is affected by the signal throughout the entire cycle of the signal. This assumption is not valid after the signal has been limited. Therefore it is possible to have low frequency beats caused by interfering signals which are nearly harmonically related to the desired signal. This effect is negligible in practical data systems due to the filters in the systems.

SIGNAL-TO-NOISE PERFORMANCE

FM

The generalized expression for FM signal-to-noise performance is

$$S/N|_{out} = S/N|_{in} \times \Delta \omega_p \left[\frac{3\omega_{in}}{2(\omega_c^2 - \omega_{in}^2)} \right]^{1/2}$$

where: $S/N|_{out}$ = rms signal-to-noise ratio at the output of an FM demodulator with an output bandwidth
 $S/N|_{in}$ = rms signal-to-noise ratio at the input to the demodulator after an input filter with a noise bandwidth.
 $\Delta \omega_p$ = peak frequency deviation.
 ω_{in} = input filter noise bandwidth.
 ω_c = upper noise cutoff frequency of output filter.
 ω_c' = lower noise cutoff frequency of output filter.

In many data systems the $\omega_{in} = 2 \Delta \omega_p$ and $\omega_c' = 0$. Thus the generalized expression reduces to

$$S/N|_{out} = S/N|_{in} \times \sqrt{3} D^2$$

These expressions are valid if the input signal-to-noise ratio is greater than approximately 9 db. Below this threshold level the output signal-to-noise ratio decreases very rapidly.

FM/FM

A useful approximation to the generalized signal-to-noise equation for operation above threshold is

$$S/N|_o = S/N|_i \times \frac{\Delta \omega_{c2}}{\omega_i} \times \left(\frac{\omega_{in}}{2\omega_{out}} \right)^{1/2}$$

- where: $S/N|_s$ = rms subcarrier signal-to-noise ratio at the output of the input filter of the subcarrier discriminator.
- $S/N|_c$ = rms carrier signal-to-noise ratio measured at the output of the receiver IF filter.
- ω_s = center frequency of subcarrier.
- $\Delta\omega_{cs}$ = peak carrier deviation due to the individual subcarrier.
- ω_{cs} = effective noise bandwidth of subcarrier discriminator bandpass input filter.
- ω_{in} = effective noise bandwidth of receiver IF filter.

Combining this with the previous expression for subcarrier signal-to-noise performance yields

$$S/N|_{out} = S/N|_c \times \sqrt{3D^{1/2}} \times \frac{\Delta\omega_{cs}}{\omega_s} \left(\frac{\Delta\omega_{in}}{2\omega_{cs}} \right)^{1/2}$$

PAM/FM

Extension of the basic FM signal-to-noise equation to include an instantaneous sampler and interpolation filter yields

$$S/N|_{out} = S/N|_c \times \left[\frac{3\omega_{cs}}{2\omega_{cs}} \right]^{1/2} \times \frac{\Delta\omega_{cs}}{\omega_{cs}} \times \left[\frac{\omega_f}{2\omega_d} \right]^{1/2}$$

- where: ω_f = frame rate.
- ω_d = noise bandwidth of interpolation filter.

FM SYSTEM ANALYSIS

The System accuracy is surprisingly difficult to define. The more commonly used definitions are based on rms, average or peak error. Regardless of the definition of error it is necessary to combine the errors due to the various parts of the system in some manner. Careful consideration must be given to the system conditions that cause the errors because many of the errors are interrelated.

There is little technical justification for the use of any particular definition of error or the type of data signal for which the error is defined. However, from an analytical viewpoint about the only feasible data signal is sinusoidal and the only justifiable error definition is peak error. As a practical matter this approach can yield a worse-case error and thus represents a bound on system accuracy.

TYPES OF FM DATA SYSTEMS AND A CUMULATIVE LIST OF SOURCES OF ERROR

System Description	Cumulative Sources of Error
<p>I Single channel FM system consisting of a modulator without an output filter and a demodulator with an output filter but without an input filter.</p>	<ol style="list-style-type: none"> 1. Modulator and demodulator zero drift. 2. Modulator and demodulator sensitivity changes. 3. Modulator and demodulator nonlinearities. 4. Modulator data feed-through. 5. Carrier feed-through in demodulator. 6. Demodulator output filter.
<p>II Multiple channel FM system with each channel consisting of a modulator with an output filter and a demodulator with an input and output filter. There is also a mixer amplifier in the multiplex path.</p>	<ol style="list-style-type: none"> 7. Modulator output filter. 8. Demodulator input filter. 9. Nonlinearities in the multiplex path. 10. Crosstalk due to modulation feed-through from other channels. 11. Crosstalk due to interference from the sidebands of other channels. 12. Crosstalk due to harmonics of the modulator output.
<p>III System II with a tape recording and playback system.</p>	<ol style="list-style-type: none"> 13. Additional nonlinearities in the multiplex path. 14. Tape recorder noise. 15. Tape speed errors. 16. Tape dropouts. 17. Tape recorder frequency response. 18. Beat frequencies due to the bias signal of the tape recorder.
<p>IV System III with constant bandwidth channels requiring translation and detranslation.</p>	<ol style="list-style-type: none"> 19. Filters in the translators and detranslators. 20. Image frequencies response of the detranslator. 21. Drift of translation and detranslation reference frequencies. 22. Beat frequencies due to imperfections of mixer circuits in the translators and detranslators.
<p>V System II and System IV with a frequency modulated rf link.</p>	<ol style="list-style-type: none"> 23. Additional nonlinearities in the multiplex path. 24. Transmitter filters. 25. Receiver filters. 26. Noise in the rf link and receiver. 27. Frequency modulation of the transmitter due to its environment.

With modern telemetry equipment operating within specifications there are a few key sources of error that provide considerable information about system accuracy.

Zero signal or dc accuracy is primarily determined by the airborne VCO. The oscillator temperature stability is typically $\pm 1.5\%$ and other environmental conditions reasonably add $\pm 1.0\%$. Calibration just prior to and during flight can greatly reduce this error.

Harmonic distortion of the data should be primarily due to the discriminator input filter and should be less than 0.3% for a deviation ratio of 5 and 1.2% for a deviation ratio of 2. The data distortion due to the VCO output filter is seldom specified but should be checked carefully because the filter is typically non-symmetrical.

Data amplitude error is primarily caused by airborne VCO sensitivity error and the discriminator output filter, input filter and phase-locked loop detector. The VCO deviation sensitivity stability is seldom specified but may easily change 0.5% .

The discriminator output filter obviously causes a data amplitude error which may be 30% due to its amplitude response. The discriminator bandpass input filter causes a data amplitude error due to attenuation of the FM sidebands. This error may be calculated to good accuracy for symmetrical deviation by $1/k M^2$ where k is the attenuation of the filter at the peak deviation under consideration and M is the modulation index. The response of a typical wideband phase-locked loop at the cutoff frequency will rise approximately 0.2 db for $D = 5$ and 1.4 db for $D = 2$. This increase in amplitude response may be partially compensated by the output filter response.

Crosstalk in a well designed multichannel system is almost entirely due to equipment imperfections. The VCO output distortion specification is typical 1% . This distortion can cause an error of 1% without pre-emphasis. Mixer amplifier, transmitter and receiver nonlinearities can cause beat notes at the sum and difference frequencies of the subcarriers and their harmonics. Typically these units are linear to within 1% and the resultant amplitude of the beat frequencies are not troublesome for deviation ratio of greater than four. However, care should be taken that linearity is properly defined. The receiver IF filters are another source of crosstalk due to the subcarrier distortion created by phase non-linearities across the passband. This aspect of receiver performance is seldom specified in sufficient detail to be useful. Tape recorder performance is necessarily a compromise between signal-to-noise and linearity. The optimum record level is not specified or indicated in sufficient detail to be useful. The problem is further compounded by recording subcarrier multiplexes without de-emphasis.

FUTURE FM SYSTEMS

Improvements in FM systems are primarily dependent upon improvement of the system components. Recent development work points to improvement in the

following areas:

1. Airborne VCO temperature stability, $\pm 1/2\%$ from -20° to $+85^\circ$.
2. Improved VCO output filters; permits spacing channels as close as four times the data frequency at a deviation ratio of one.
3. Improved transmitter linearity; permits with rf links operation at lower deviation ratio without excessive crosstalk.
4. Improved receiver filters and detector linearity; permits operation with rf links at lower deviation ratios without excessive crosstalk.
5. Improved subcarrier discriminator input filters; permits operation at lower deviation ratios and closer channel spacings.
6. Improved phase-locked-loop detectors; reduces FM threshold signal-to-noise level.

HEY, WAIT FOR ME; I'M YOUR LEADER

(20 June 1967)

by

Frank J. Jasinski

Frank Jasinski received his Ph. D. in Anthropology from Yale University where he taught in the Schools of Engineering and of Medicine also doing organizational research in a variety of business and industrial firms. At TRW Systems, Dr. Jasinski has been involved in organizational improvement including managerial and technical development and optimal utilization of professional, technical and support personnel. His articles reflect an interest in the influence of technological, administrative, and cultural factors upon organizational behavior. He is a member of the American Anthropological Association and the Society for applied Anthropology.

A very prevalent and pervasive image of what a "good leader" is in business and industry evokes the characteristics of:

- forceful
- strong
- decisive
- initiating
- self-sufficient, and
- "in control"

We all have succumbed - perhaps still do - to such an image.

Our folklore in industry, our learned articles in professional journals, and indeed, even our academic research focuses on these and similar characteristics of "leadership". In years back, as an "interactionist", I was very concerned with the then seemingly important variable of: Who initiated action for whom? For me - and many, many other researchers - a high level of initiation designated leadership with the big "L". In short, anyone who acted in response to others could not possibly be forceful, strong, decisive, self-sufficient--or, a leader.

I would like to explore how we tend to react, given that image, in our individual behavior as managers and how we might experiment with behavior that rests on a somewhat different base. Toward that end, I would like to discuss:

- Why we tend to behave to make that image come "true".

- What the forces are which threaten that image.
- How we react to those threats to our image.
- Ways in which we can work ourselves out of the apparent dilemma of the several conflicting forces.
- Initial, first steps to undertake a change in our behavior to achieve more effective leadership.

I Am Your Leader!

Given the notion that leadership is central and localized in one individual - me - and accepting the elements that contribute to that leadership, I try to behave in ways that live up to that standard. Unless I do, you may not consider me as an effective leader.

These elements are so generally applicable that I, as an individual, have little choice in how I behave. I evaluate myself, my superiors evaluate me (look at most performance evaluation forms) and I feel my peers and my subordinates evaluate me along the same dimensions.

Unless I behave in ways to meet those prescribed qualities of leadership, I am not a leader. Therefore, as I choose how I behave as a manager, or as a leader, I tend to select patterns that prove I am forceful, strong, decisive, initiating, self-sufficient and "in control". Further, I tend to resist attempts which have me behave differently.

Forces Sapping My Leadership

Unfortunately, for my image of myself, others not only do not share that image, but, very often, challenge my image. They want to contribute to my decisions, they want autonomy, they ask me to do things; when I say "jump", they sometimes ask "why?" instead of "how high?".

The trouble with this challenge to my image is that groups using this new way of operating often are more effective. Not only do they get jobs done more easily, but the people involved feel more productive! They not only do more, but they seem to grow more.

Increasingly, I get into the dilemma either of being a traditionally "effective" leader, or of having an effective group.

When, on occasion I give into letting my subordinates take the bit into their teeth, I feel like shouting after them: "Hey, wait for me: I'm your leader".

On these occasions, it has been hard for me to accept their getting something done without my being quite central to those efforts. Even worse, they sometimes come up with a better way of getting the job done; that's even harder to accept.

On those occasions, I get to feel that I am lacking in my leadership - that I'm losing control.

My Attempts to Control

We rely on a variety of mechanisms to establish and maintain control: They vary from the very subtle to the ludicrous. They may involve:

- Only ourselves
- Our relations with another person
- Our relating to a group

I would like to give a few illustrations from my personal experience.

Altogether too often, I find myself deluding me in an effort to control my self image. Sometimes I do so through selective screening of my environment and my experience. At times I do so at the expense of others.

An illustration of the latter was a pattern I had established with my son some time back. It had to do with my helping him with his Algebra homework. I would spend two and three hours a night "helping him". One day I suddenly realized that the one I was really helping was me - and my self image of a loving, devoted, dedicated father.

In the process of creating this self-deception, I was really making my son pay; with anxiety, frustration and guilt. (By the way, I was learning Algebra, not he!)

While I was controlling my self-image, I was also controlling my son. He couldn't pin responsibility for his sorry state of affairs on a "loving, devoted, dedicated father".

We have all met those "super nice guys" whom we can't criticize: "But he's such a nice person."

Be alert to these "helpers" and nice-guys": They can manipulate you - ever so nicely - into a pretty confining corner.

A variant on "helping" is to indulge in "nit-picking" - keeping the other person off balance. I know I can always find something wrong in a document or presentation if I've a mind to. I'm sure you can do equally well.

People do find ways to deal with nit-pickers and helpers. (How else are we going to learn?) I got my "come-uppance" once when I slipped into a blue pencil period: I edited the hell out of documents my subordinates passed by me for review. In an effort to please me, my subordinates gave me more and more to edit. I finally got the message when they began submitting professional papers virtually on the backs of envelopes.

Recently a student of mine - a manager in the aerospace industry - learned from other managers that his subordinates were "planting" nits for him to find. They had learned that he stopped hunting for nits in their work after he caught one. They were nice about it though. They planted the nit fairly early in the paper and saved time and effort for everyone.

A former colleague of mine learned how to handle a "helping" boss. It became downright ridiculous; he had the boss hand-carry his personal medical claims through the company benefits office, or track down in the company library why a certain book hadn't arrived as yet.

This, then is the dilemma: Industrial folklore defines leadership in positive aggressive terms, individuals increasingly demand greater participation in decisions about their work-life. We managers, and would-be leaders, tend to fight off attempts to reduce our control; we tend to be more and more controlling.

Which Way Out?

In recent years a change has been occurring in concepts about leadership and productive groups.

More is being written about a leadership function rather than the big "L" leader. The leadership function is performed variously by several, if not all, members of the group. (In a way, the task determines appropriate and effective behavior.)

We are changing our assumptions about people. Less frequently do we see them as things who have to be manipulated or forced to perform

effectively. The tendency is to assume that individuals seek the following characteristics in a work situation:

- Challenge
- Freedom
- Worthwhile work
- Recognition
- Responsibility
- Competent/Congenial colleagues
- Opportunity to grow

Given the foregoing models of leadership and of individuals, the tendency is to define a healthy work climate or culture as having the following characteristics:

- | | |
|--|--|
| - Focus on the task
(problem solving) | - Organic |
| - Structure around task | - In process |
| - Openness | - Deal in here and now |
| - Trust | - Responsibility for choice |
| - Confrontation | - Day-to-day coaching |
| - Caring for others | - Bias toward optimism |
| - Introspective (step out
of culture) | - Ability to cope with conflict |
| - Role flexibility | - Internalized controls and rewards |
| - Spontaneous | - Growth at all levels in organization |

To the extent we can establish and maintain these qualities in a work situation, we will create opportunities for effective performance and continued growth. Much of our leadership might well be invested in developing such an environment.

I can attest, from personal experience that it is not easy. Moreover, the job is never really done. The results, however, can be astounding!

To Begin

The path is not an easy one - yet, it is potentially a very rewarding one. And the first step is the most difficult one. It has to be; it begins with you as an individual.

I had to begin - as will you - by becoming authentic. I had to learn about me. I had to acknowledge what was "with me" at the current point in time - in the here and now.

A large part of the process of learning about me was to observe my behavior and people's reaction to my behavior. I had to act, critique that act (often with the help of others) and then act. Too often we perform a series of continuous acts without pausing for introspection. Too often we don't learn from our experience.

The task may sound awesome and too hard to do. But, if I think in terms of five-minute segments of behavior - not a major self-overhaul - the job is "do-able". I may not be able to undo five, ten or twenty years of past behavior, but I can learn from the last five minutes and behave more appropriately for the next five.

Remember that one of the qualities of a healthy climate is a bias toward optimism.

TRAJECTORY AND ORBITAL MECHANICS
(11 July 1967)

by
W. T. Thomson

Dr. William T. Thomson, who earned the Ph. D. at University of California, Berkeley, is Professor and Chairman of Mechanical Engineering, University of California, Santa Barbara as well as consultant to TRW Systems, Inc. He was Professor of Engineering at UCLA for 15 years and has also held academic positions at University of Wisconsin, Cornell University and Kansas State University. His industrial experience includes several years as Head of Vibration and Flutter at Ryan Aeronautical Company and a position as research engineer at Boeing Aircraft Company. In addition he has been consultant to U. S. Navy Electronics Lab, San Diego; Rand Corporation; Ramo Wooldridge Company; Space Technology Labs. Among his honors were a Guggenheim Fellowship to Germany, 1961-1962; Fulbright Research Professorship, Kyoto University, Japan, 1957-58 and appointment as University Fellow in Electrical Engineering UC Berkeley, 1935-36.

(1) Historical Introduction

The Motion of heavenly bodies has interested the minds of great thinkers for many centuries. It is believed that the early Greeks such as Pythagoras (569-470 B. C.) and Aristarchus (310-250 B. C.) believed in the heliocentric theory; however, with the authoritative influence of Aristotle (384-322 B. C.) the geocentric theory became accepted and went unchallenged until early Renaissance.

During the years 1500 to 1630, great strides were made in celestial mechanics. A Polish astronomer, Nicolaus Copernicus (1473-1543) broke away from the geocentric theory of Aristotle when he proposed the heliocentric reference for the motion of planets. Tycho Brahe, (1546-1601) a Danish astronomer, made extensive observations of the motions of planets and in particular, the motion of Mars. Johannes Kepler (1571-1630) of Weil, Germany, who assisted Brahe, noted that the planetary motions around the sun were not circles but ellipses and formulated his three empirical laws of motion, known as Kepler's laws. These are:

- Law 1. The orbit of each planet is an ellipse with the sun at a focus.
- Law 2. The radius vector drawn from the sun to the planet sweeps over equal areas in equal times.

Law 3. The squares of the periods of the planets are proportional to the cubes of the semi-major axes of the elliptical orbit.

Galileo Galilei (1565-1642) introduced a new approach to science by founding his theories on experimental observation. He was a supporter of the Copernican theory, lectured on Kepler's "New Astronomy" published in 1609, and in 1610 built the first telescope and discovered four of the moons of Jupiter.

The year Galileo died, Isaac Newton (1642-1727) was born. He introduced the concept of mass, the law of gravitation, and laid the foundation for the entire field of classical mechanics with his three laws of motion published in his Principia in 1686. His development of the infinitesimal calculus enabled the prediction of the Kepler's laws of planetary motion as a consequence of his laws of motion.

Since Newton's time, mathematical methods of analysis were developed with great skill by people like Leonard Euler (1707-1783) and Joseph Louis Comte de Lagrange (1736-1813). Under such masters the subject of celestial mechanics was placed on a high level of sophistication.

(2) The Two Body Problem

The motion of two bodies under the influence of their mutual gravitational force, excluding all other forces, can be solved exactly. It is the only multibody problem which can be solved exactly by analytical

means, and its study is of importance in providing an understanding of the approximations which are made for the limiting case where one mass is much larger than the other.

Newton's laws of motion for m_1 and m_2 can be set up in inertial coordinates \vec{r}_1 and \vec{r}_2 . It can be shown that the center of mass of the system (called the barycenter) remains at zero acceleration. When the relative coordinate $\vec{r} = \vec{r}_1 - \vec{r}_2$ is introduced we find that the system obeys the equation $\vec{F}_{12} = \frac{m_1 m_2}{m_1 + m_2} \ddot{\vec{r}}$ which establishes the equivalent mass for the two body system as $\frac{m_1 m_2}{m_1 + m_2}$. If one of the masses is very large (i.e. $m_2 \rightarrow \infty$) compared to the other, the equivalent mass reduces to that of the smaller mass moving relative to the center of the larger mass. The problem is then referred to as the motion of a body in a central force field. The motion of planets about the sun (whose mass is 98% of the total mass of the Solar system) and the motion of satellites about the Earth are essentially central force problems.

(3) Motion in a Central Force Field

Using polar coordinates r, θ , with origin at the center of the large body, the equation of motion of the small body about the large body can be presented in the radial and transverse components.

Radial force

$$\ddot{r} - r\dot{\theta}^2 = -\frac{k}{r^2} \quad (1)$$

Transverse force

$$h\ddot{\theta} + 2\dot{h}\dot{\theta} = \frac{1}{r} \frac{d}{dt} (h^2 \dot{\theta}) = 0 \quad (2)$$

Equation (2) leads to the theorem of conservation of moment of momentum

$$h^2 \dot{\theta} = H \quad (3)$$

A third equation giving the total energy per unit mass of the orbiting body (sometimes referred to as the "vis viva" equation) is

$$E = \frac{1}{2} v^2 - \frac{k}{r} \quad (4)$$

The equation (1), (3), and (4) will completely describe the motion of the body in a central force field. Its geometric path is described by the equation of a conic section

$$r = \frac{l}{1 + e \cos \theta} \quad (5)$$

where: l = semi-latus rectum
 e = eccentricity which depends on total energy E .

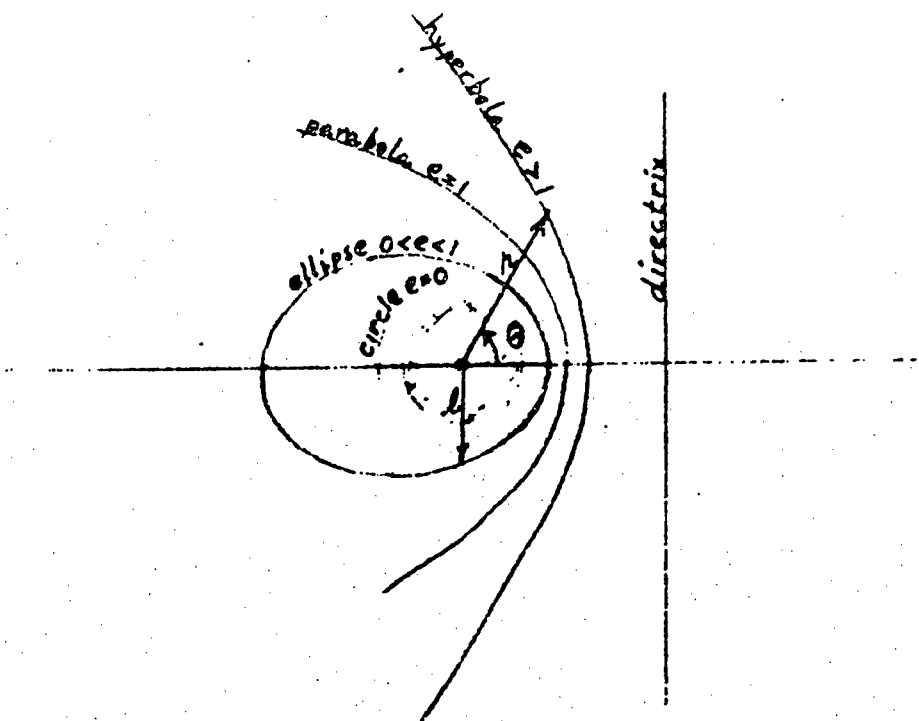


Fig. 1. Orbits under central force

Figure 1 illustrates the class of orbits which satisfy Eq. (5) and Table 1 gives some of the information pertaining to each class.

TABLE 1

	Circle	Ellipse	Parabola	Hyperbola
Equation	$r = a$	$r = \frac{(1-e^2)a}{1+e \cos \theta}$	$r = \frac{2r_p}{1+\cos \theta}$	$r = \frac{a(e^2-1)}{1+e \cos \theta}$
Periapsis	a	$r_p = a(1-e)$		$r_p = a(e-1)$
Apoapsis	a	$r_a = a(1+e)$		
Energy		$\epsilon = \frac{-K}{2a}$	0	$\epsilon = \frac{K}{2a}$
Moment of Momentum		$H = \sqrt{Ka(1-e^2)}$		$H = \sqrt{Ka(e^2-1)}$
Semi Major Axis = a				

(4) Orbit Established from Initial Conditions

The type of orbit which a satellite will go into is completely established from initial conditions at injection which are: r_0 , v_0 and β_0 shown in Fig. 2.

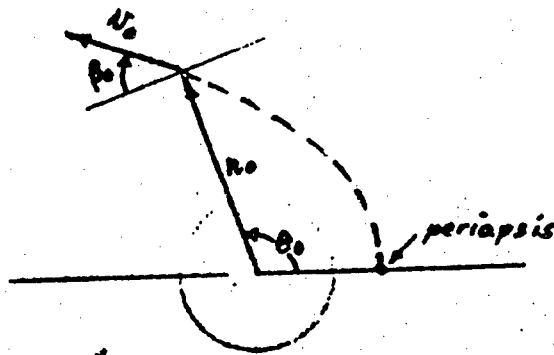


Fig. 2. Initial conditions at injection

The eccentricity of the orbit and the location of perigee can then be determined from the equations

$$e^2 = \left(\frac{r_0 v_0^2}{K} - 1 \right)^2 \cos^2 \beta_0 - \sin^2 \beta_0 \quad (6)$$

$$\tan \theta_0 = \frac{\left(\frac{r_0 v_0^2}{K} \right) \sin \beta_0 \cos \beta_0}{\left(\frac{r_0 v_0^2}{K} \right) \cos^2 \beta_0 - 1} \quad (7)$$

By dropping the subscript o , these equations hold for any point on the orbit, and parametric charts relating these quantities are given by Figs. 3 and 4.

(5) Time of Flight

The time of flight computations are generally more tedious. One approach is to start from the equations of polar coordinates substituted into the moment of momentum equation, Eq. (3),

$$dt = \frac{r^2}{H} d\theta \quad (8)$$

and performing the integration. This leads to a complicated equation whose results are presented by curves in Figs. 5 and 6.

The second approach, applicable to elliptic orbits, is to use the equation of the ellipse in terms of the eccentric anomaly E which is

$$r = a(1 - e \cos E) \quad (9)$$

Again substituting into (8) and letting $M = 2\pi \frac{t}{T}$, a term called mean anomaly, the solution is available from

$$M = E - e \sin E \quad (10)$$

The solution of Eq. (10) is shown graphically in Fig. 7.

(6) Transfer Between Orbits and Interplanetary Travel

We consider here only the case for transfer between two circular orbits. Also we discard the classical equations and solve the problem from the energy equation and the moment of momentum invariance. Assuming a velocity change under impulsive thrust, a transfer orbit (Hohmann trajectory) and its departure and arrival velocity can be found. The results are immediately applicable as preliminary calculations for interplanetary missions based on segments of three central force problems. Important to the procedure is the theory of the corridor which is pertinent to the capture conditions of the particle.

References:

1. W. T. Thomson, Introduction to Space Dynamics, Ch. 4, John Wiley and Sons, N. Y., 1961
2. "Trajectory Selection Considerations for Voyager Mission to Mars During 1971-72," Jet Prop. Lab., Pasadena, Calif., Document No. 281, September 15, 1965
3. Loh, W. T. H., Re-Entry and Planetary Entry, Ch. 15, Springer-Verlag, Inc., New York, 1967

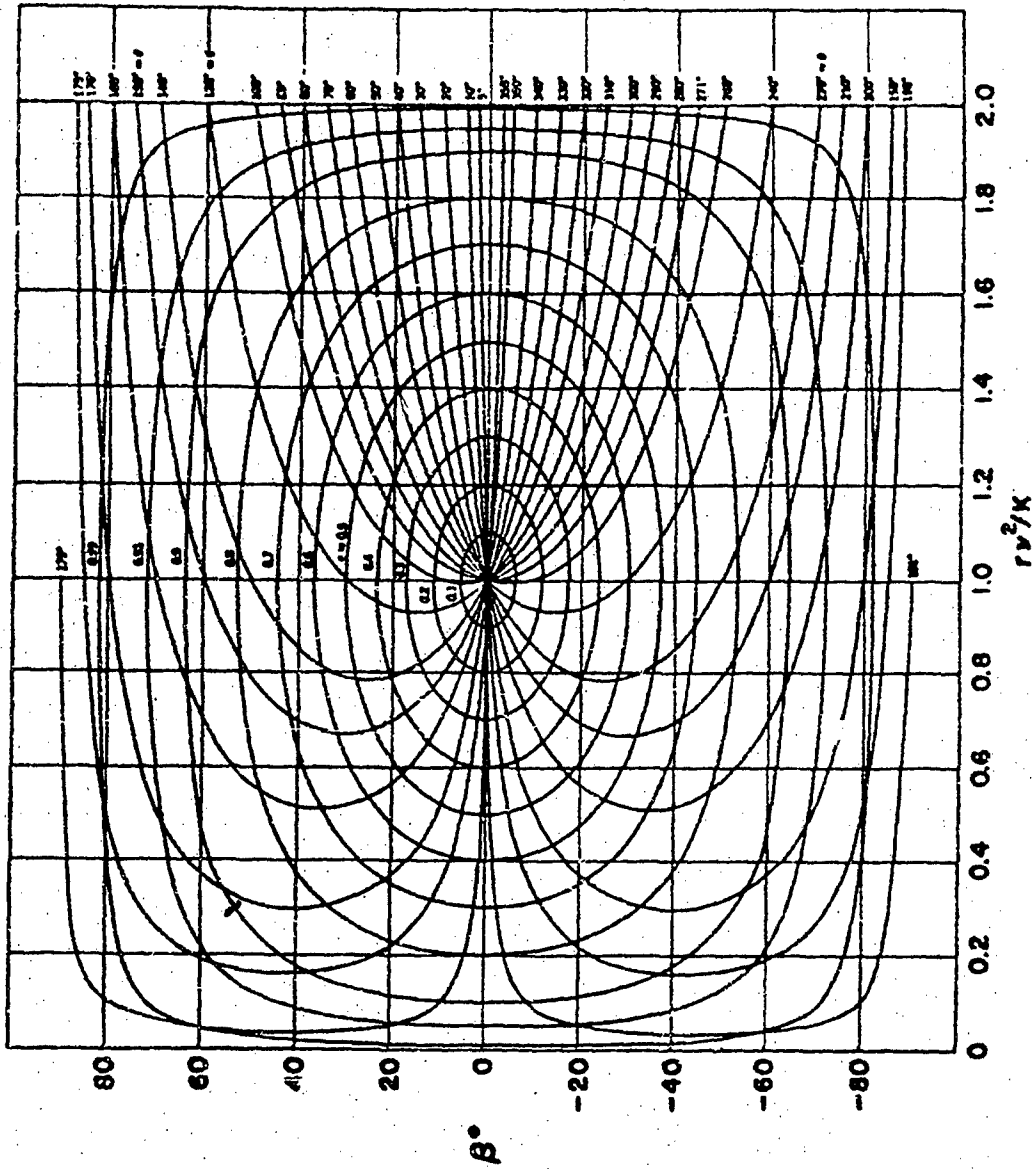


FIGURE 3

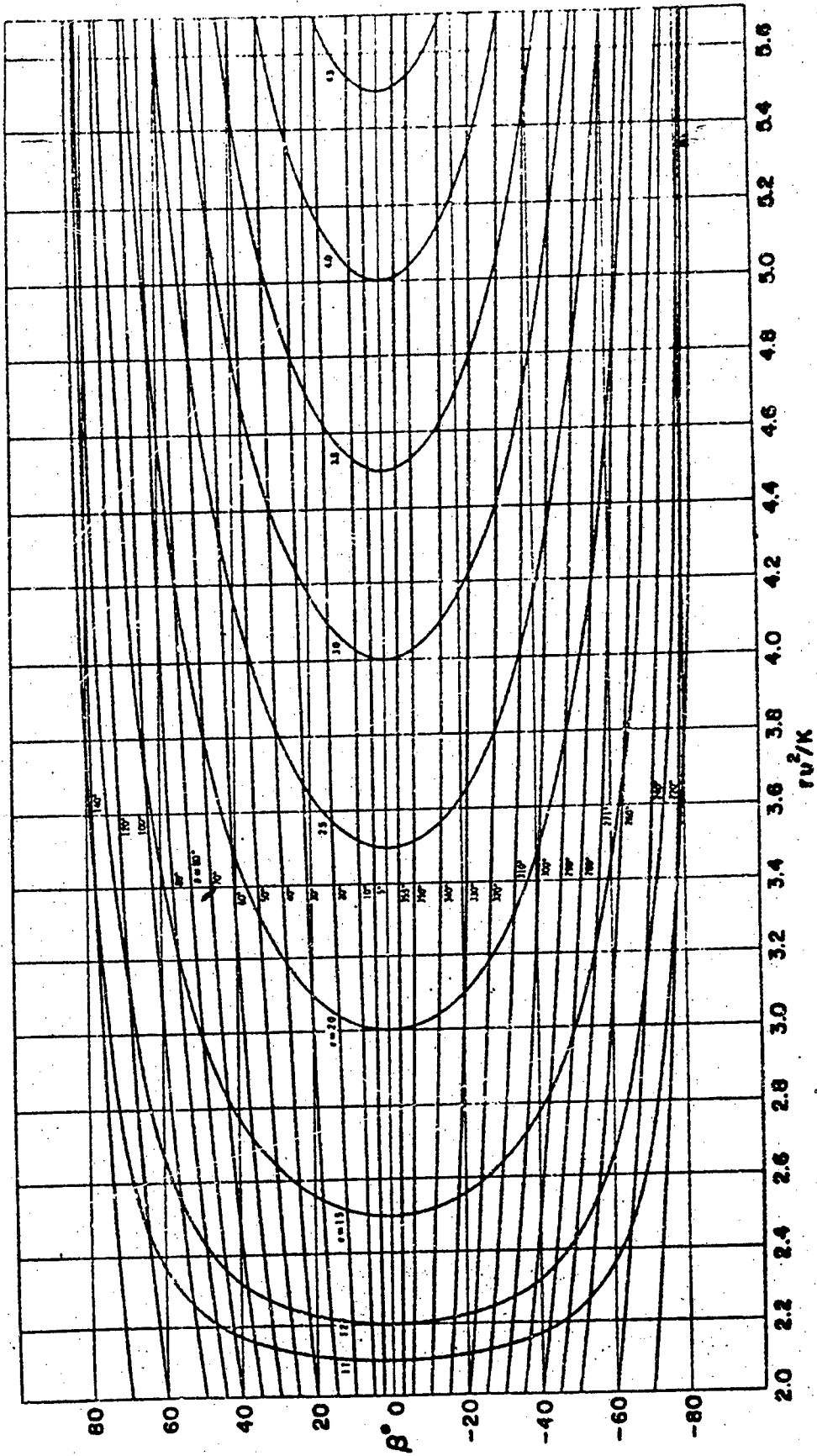


FIGURE 4

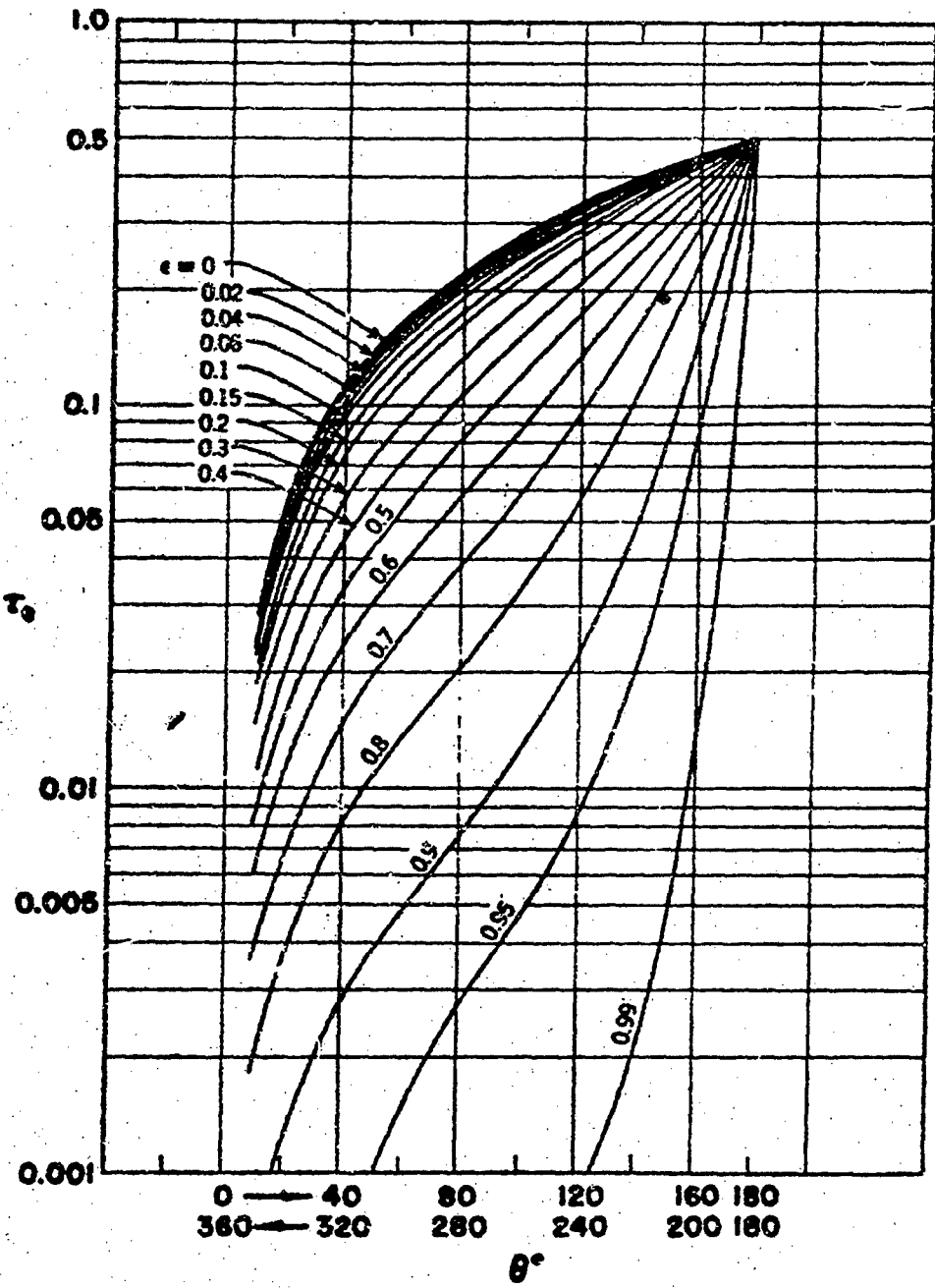


FIGURE 5

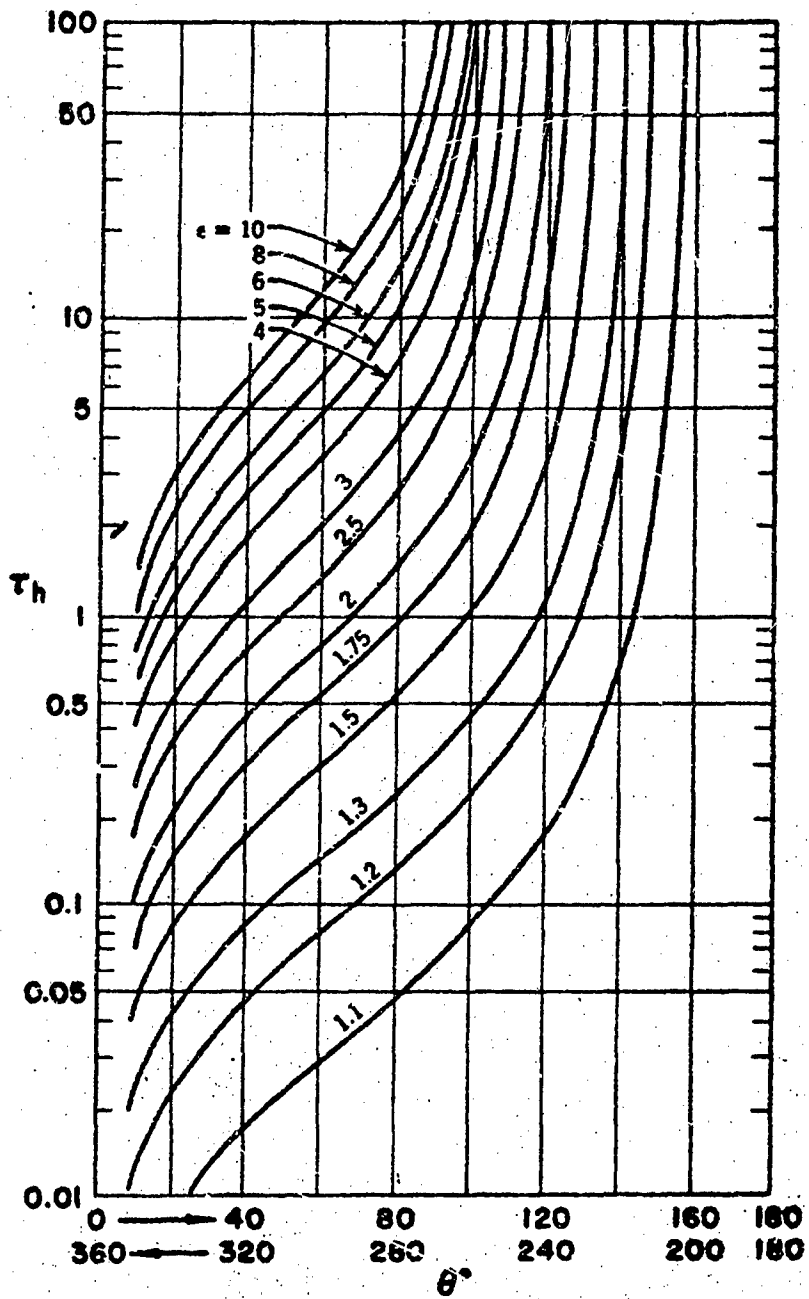


FIGURE 6

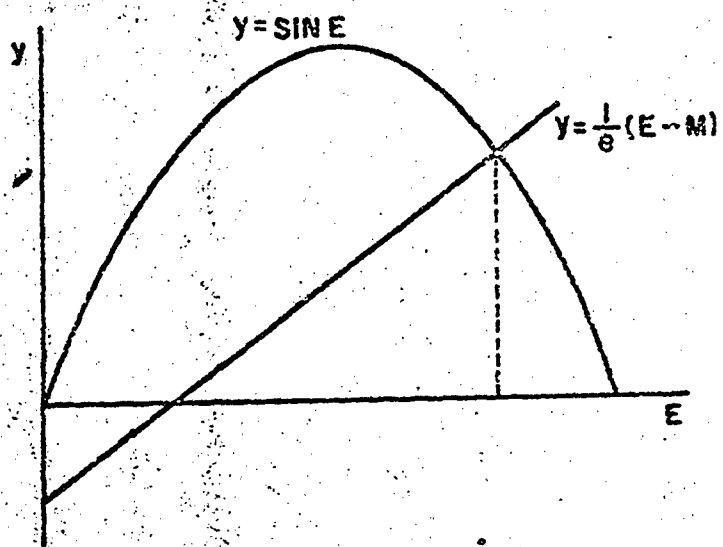


FIGURE 7

OPERATIONS RESEARCH AND DECISION MAKING
(18 July 1967)

by
David C. Dellinger

Lt. Col. David C. Dellinger, USAF, is an Operations Research Analyst in the office of the Assistant Secretary of Defense for Systems Analysis. He was formerly an Associate Professor of Statistics and Operations Research at the Air Force Institute of Technology. He is a graduate of Duke University (Mechanical Engineering) and holds a Ph.D. in Operations Research and a Master's degree in Industrial Engineering, both from Stanford University.

Mr. August A. Busch, III, Vice President and General Manager of Anheuser-Busch, Inc., in his remarks to a recent Annual Meeting of Shareholders, stressed the fact that operations research was being used to guide company decisions concerning plant location, product research and development, and estimates of future demand for their products. President Johnson recently directed that all government departments apply systems analysis to major programming decisions. A recent series of articles in Management Science expressed concern over the problem of communication with top management. What is the significance of these, and many other similar events? To me, it's an indication that operations research is becoming a significant influence in the decision-making process at the higher levels of industry and Government. Traditionally, (if a field only 20 years old can have a tradition) operations research has been--as the name suggests--operationally oriented. Some of the earliest applications of operations research were military, having to do with improving the efficiency of going operations. Increasing the effectiveness of bombing systems, the effective utilization of radar, or problems of anti-submarine warfare were some of the early problems addressed in World War II by operations researchers. These were problems concerning operating procedures--not so much equipment problems. In industry, early applications were directed toward improving production through changes in operating procedures rather than changes in equipment. These applications emphasized improvements in such things as inventory or production control systems but had little to do with basic company policy decisions. The change that is taking place is this: operations research is being applied more and more to high level policy decisions. Decisions which

are more difficult, harder to formulate, concerned with greater uncertainty, and which are far more significant than production or operating problems are being treated as operations research problems. It is this trend--the reasons for it and the changes in decision processes resulting from it--that I want to discuss with you this morning.

But first, I want to explain what I mean by operations research. It is not a very well defined term. A professor of mine once defined it as "the thing operations researchers do." I find this an unsatisfactory definition but it indicates the difficulty of defining the term.

If you were to examine a few copies of The Journal of the Operations Research Society of America (ORSA), you would find that a preponderance of the articles are highly mathematical. Most of them are concerned with mathematical techniques for solving well defined, abstract problems. For example, you are apt to find several articles proposing more efficient algorithms for solving linear or non-linear mathematical programming problems. I think you would be left with the impression that operations research was simply a form of applied mathematics concerned with optimization techniques.

I view operations research in a much broader sense. It encompasses applied mathematics, as the Journal of ORSA suggests, but it also encompasses the broader spectrum which includes management science and systems analysis. While areas of specialization have developed around each of these three aspects of operations research (specialized journals are published, societies have been formed, and books have been published in each of these areas) they have much more in common than the specialization might suggest.

It's not these differences that I want to emphasize. It is the encompassing philosophy or approach to decision problems common to all these areas of specialization which is significant. It is this broader concept that I associate with the term operations research. It matters little whether we agree on the use of this title--but it is important that we have a mutual understanding of the concept.

Operations research, then, as I am using the term, is a disciplined approach to decision problems which involves:

- a. the use of a formal analytical framework for the systematic comparison of alternatives;
- b. an explicit statement of the criterion of choice--or the objective which guides the decision-maker;
- c. a methodology for dealing with uncertainty.

It is further characterized by the fact that it is usually concerned with institutional systems (rarely with pure physical systems) and, moreover, with the optimization, in some sense, of these systems.

The use of a formal analytical framework or model serves two important purposes. First, it identifies the variables, both exogenous and endogenous, assumed to be relevant to the decision and states explicitly the relationships assumed to exist among the variables. Second, it provides a predictive device which relates the decision-maker's alternatives to the expected future consequences of choosing each one. The explicit statements about the relevant variables is essential for a disciplined approach to decision-making. It provides a way of checking results against assumptions and a way for persons other than the analysts to follow the analysis. It is little more than the openness and explicitness expected in any credible analysis.

The predictive nature of the analytical framework, or model, is at the heart of operations research approach to decision-making. Decisions, by their very nature, are (1) choices from among alternatives and (2) attempts by the decision-maker to alter the future by choosing an alternative which leads to a stream of future consequences which is more desirable than other alternatives. It is essential, then, that one attempt to predict what these consequences are likely to be for each alternative considered. Only by relating the expected future consequences of the alternatives can one compare and choose rationally.

The requirement for an explicit statement of the criterion of choice--or the basis for determining the preference of one alternative over another--becomes more important and more complex as the institutional level of the decision problem is raised. In personal decision problems this explicitness is not too important. One can simply state that he desires one alternative over another without stating, or even fully understanding, why. His choice somehow reflects his personal value system which, after all, is the only relevant criterion in personal decisions. This is not the case in institutional

decision problems. The personal likes and dislikes of the decision-maker are not relevant and should be forcibly excluded from the decision process by explicitly stated organizational goals. This may not be too difficult at the lower levels of an organization. At the higher levels, however, the problem becomes increasingly more difficult. Even in industrial organizations, where the profit motive is supposed to dominate, the criterion problem is complicated by multiple objectives such as long-run vs. short-run profits, institutional survivability, etc. In Government, the problem is even more complex. In either case, however, the criterion problem must be faced and the operations research approach tends to force the decision-maker to face it.

Finally, since no one can predict the future with certainty, and since decision problems are inextricably associated with predictions of the future, uncertainty in decision-making is a certainty! There is, of course, no way of completely overcoming this problem. The operations research approach does, however, provide methodology for reducing the risk associated with the uncertainty. The two most widely used methods are sensitivity analysis and probabilistic models.

Sensitivity analysis is merely the testing of the results of an analysis to variations in the basic set of assumptions. Through sensitivity analysis, one can identify those variables to which the results are most sensitive so that further study can be focused on the relevant questions. It can also aid the decision-maker in choosing an alternative which guards against undesirable consequences even under the most adverse set of assumptions, if he desires such a solution. For example, it may be more rational in choosing a military system, to select one which is capable of coping with a wide range of threats than to select one which is most efficient for a single, most likely, threat (if it turns out that these are mutually exclusive choices).

The other method of dealing with uncertainty--the use of probabilistic models--requires that one select a probability distribution to describe a random variable in the model. This approach has been used successfully in the analysis of queuing problems, inventory problems, and many other problems where the nature of the stochastic system being modeled is

reasonably well understood.

Both of these methods of dealing with uncertainty are dependent upon having the formal analytical framework or model and an explicit statement of criterion characteristic of the operations research approach.

Having examined the characteristics of the operations research approach to decision-making, let's now turn to the reasons for its being applied to higher level decision problems in government and industry. Recent changes in both the decision-making environment and in the operations research field have brought about this increased application.

In both government and industry, high level decision problems have become more complex over the past few years. The technological explosion of the last two or three decades has offered decision-makers a far greater number of alternatives than they previously had. The number of alternative military systems which could be developed from today's technology, for example, staggers the imagination. The pace of technology also makes today's alternatives obsolete in a very few years. Moreover, the costs of these systems is so high that one cannot avoid the problem of choice by selecting several to try out; he must choose! In addition, the uncertainties of the problem are magnified because the systems are so radically new and because obsolescence comes so rapidly. These factors combine to create a situation where the number of alternatives is large, the cost of each is high, the consequences of a poor choice are catastrophic, and the uncertainty is great. Similar conditions exist in industry and other government agencies. Experience and unaided judgment are simply inadequate for guiding decisions under these circumstances. Decision-makers are turning to analysis to aid their judgments.

Changes have also occurred in the field of operations research during the past few years which have made this approach practical for high level decision problems. For one thing, a great deal of work has been done in developing the methodology for solving a wide class of optimization problems. Probably the most important, however, is the availability of electronic computers which make it relatively easy to solve such problems. This makes it possible for the analyst to concentrate on the analysis and leave most of the routine calculations for the computer.

Finally, the change which is probably the most important single reason for the increased use of operations research to these types of problems has been changed in the decision-makers themselves! More and more the decision-maker is somewhat of an analyst himself. His education has generally included a formal exposure to economic principles and methods of analysis. He has observed the value of analysis in such decision problems. In short, he understands the approach, whether he understands the detailed methodology or not, and he can understand and believe the results of a good analysis. It has been said that a decision-maker would rather live with a problem he can't solve than to accept a solution he can't understand. The number of decision-makers who understand and will accept analysis as an aid to judgment is increasing.

The view of operations research which I have presented to you is that of a disciplined approach to decision-making. While operations research was developed in an operational environment, its greatest benefits can be realized in applications to high level policy decision problems. In spite of the difficulties of formulating precise statements of these problems, this approach can be, and is being, used to improve the decision-making process at the highest levels of government and industry. It is not a panacea, but is far superior to the implied alternative--unaided judgment and intuition.

THE NEW INDUSTRIAL ECONOMICS - AN ADJUSTMENT PROCESS

TEXT OUTLINE

Dr. M. E. Salvesson

July 25, 1967

INTRODUCTION

Economic activity revolves about three key elements : (1) human wants, which are varied and insatiable (2) resources which are limited, versatile and capable of being combined in various proportions to produce a given commodity (3) techniques for utilizing resources to produce goods and services which satisfy wants. (1)

The social science of economics has devoted itself to the analysis of this activity in order to measure, explain, predict and control, observed phenomena. Models have been created to simplify the complex reality of an existing economy to the essential determinants in order to observe and evaluate the effects of an introduced change.

As a result we tend to place labels on a given economy such as the "Free Enterprise System", predominant in the Western World or "The System of State Capitalism" of the Iron Curtain countries. With a free enterprise system we associate a consumers choice of selection, a resource owners freedom of resource deployment, an entrepreneur's ability to enter or leave the business of his choice, and a price system that at least in the short run, depends upon supply and demand, with money as an essentially neutral medium of exchange. Equating management with entrepreneurship and accepting the profit motive as the guiding force of such a system, we have now a model of the American economy which was essentially valid for the early part of this century.

In the meantime the federal budget involves some 20 % of the nation's income. The Government has replaced the private entrepreneur in large sections of the economy by assuming the risks of new production and by making the decision to employ resources. Today's topic is this effect of Government entrepreneurship on private industry.

*

* *

(1) Richard H. Leftwich "The Price System and Resource Allocation". Holt, Rinehart and Winston, New-York, 1960, p. 10

-GOVERNMENT EXPENDITURES AND THE STRUCTURE OF AMERICAN INDUSTRY

The growing significance of Government expenditures on the structure of American industry can be demonstrated by the number of large defense contractors in the 100 largest industrial corporations group.

TABLE I (2)

Overlap between the 100 Large Defense Contractors and the 100 Largest Industrial Corporations:

<u>Period</u>	<u>Number of Firms on Both Lists</u>
World War II Defense Contractors and 1939 Industrial Ranks	29
World War II Defense Contractors and 1945 Industrial Ranks	53
Korea Defense Contractors and Industrial Ranks	41
Missile Age Defense Contractors and Industrial Ranks	40

The State of California received approximately \$6 billion worth of prime contracts or 18.3 % of the total \$32 billion spent by the Department of Defense during fiscal 1966.

Employment in the aerospace industry provides another interesting statistic: In 1939 the aircraft industry accounted for .6 % of total manufacturing employment and in 1944 for 7.6 %, making it the largest single industry in the economy in that year.

(2) Merton J. Peck, Frederick M. Scherer. "The Weapons Acquisition Process". Division of Research, Graduate School of Business Administration, Harvard University, Boston, 1962, p. 120

Case 1: The immediate requirement for large increases of existing production.

Actually this type of problem can occur in a normal free enterprise market system in the case of a sudden shift in consumer's tastes. The result is an immediate rise of price of the product, reflecting the increased demand at given levels of supply, with rapid buildup of capacity and gradual lowering of price until equilibrium has been achieved.

While the problem is similar, the effect is quite different. Take the case of Norris Industries, Inc. a major ordnance supplier since World War II. The firm is the country's largest producer of artillery cartridge cases. During peace time, it averages about \$20 million worth of military business annually. In the fiscal year ended July 31, 1965, its military sales edged up to \$23 million, but in the following months they more than doubled to \$50 million. This year, Norris expects these sales to reach \$120 million. (6)

The differences between a non-defense rapid increase in production and the case of Norris are primarily the complete impossibility to predict demand level or duration - normal predictive tools such as market research cannot be used - and since surges in defense buying are usually large enough to affect the total economy, the labor market also becomes tight, with an accompanying pressure on wages and salaries, especially for skilled resources.

In contrast to earlier emergencies, the Government no longer operates in the rather haphazard fashion of World War II days. Specifications for standard items have become very detailed, very precise. Higher inspection standards have significantly improved the quality of the produced item and competitive bidding has resulted in a price level for defense goods which requires excellent management of the contractor to maintain peacetime profit margins, since most defense contracts for such standard hardware as ammunition, are based on

(6) Business Week, June 3, 1967, p. 147

a fixed-price basis or on a cost-plus-fixed-fee basis in which all costs are tightly controlled.

Even though the Government carries the largest part of the risk, there is no automatic provision to cover all closing costs when the emergency has passed. Companies such as Norris have therefore adopted a policy of simultaneous expansion of non-defense business during the emergency. This is reflected in the fact that output of commercial goods has risen from almost nothing in 1946, to \$15 million at the time of Korea, to an expected \$78 million this year - the latest figure includes the very recent acquisition of a group of commercial, non-defense companies with a combined sales total of \$21 million.⁽⁷⁾

Summary: The impact upon private industry by large sporadic increases in demand by the Government has become less disruptive as inspection standards have improved the basis for evaluation of products manufactured by competitive firms. Changes in contract arrangements and tighter control of costs have resulted in more effective management and thus a lesser cost to the total economy. The awareness of the contractor, that he has to participate in the risks and costs of closing down operations after the emergency has resulted in provisions made by management to facilitate later transition to peace-time operation.

Case 2: While Case 1 deals with an emergency expansion of capacity, there are few technological problems in such relatively simple production processes as the making of standard ordnance. The matter becomes much more difficult when we consider the development and production of advanced weapons or space systems.

Expenditures can easily exceed the \$1 billion level. Given the high expenditures in individual programs and the difficulty of making accurate cost, development-time and end-product quality predictions, private industry is usually not willing to assume the huge financial

risks especially since political decisions, changes in military strategy, breakthroughs in technology, can cause entire programs to be shelved. As a consequence the Government has accepted the financial risks in most cases through cost reimbursements; it assumes the initiative for product decisions and participates in managerial functions which normally are performed exclusively by sellers.

The problem the Government faces is to maintain incentives for efficient and optimal program execution in an essentially non-market environment and yet maintain the competitive element in the selection process.

Triggered by threatened set-backs in the arms race between Russia and the U.S., crash programs such as the development of inter-continental and intermediate range ballistic missiles are being initiated, or the special conditions imposed by a new theater of war call for the development of a new type of weapon, or the technological advances of other nations threaten important markets of American industry, such as the development of a Super Sonic Transport by Britain, France and Russia.

The first requirement is to find and to describe a system that will satisfy the obvious need. This first preliminary description is then used to find and identify the potential creators of the implemented system by a Request for Proposal.

It has been recognized by the Government, that such proposals are extremely costly for any major system. Because of this a new procedure has been developed. The original Request for Proposal is only a rather gross preliminary specification of the system. The Government screens all responses and selects at least two potential contractors. A more detailed RFQ is then sent to these selected firms with a request for a very detailed technical plan and cost proposal. This response is financed by the Government, if not completely, at least to a major proportion.

A typical case for this kind of selective process was the Advanced Aerial Fire Support System, a combat and fire support helicopter specifically designed for Vietnam type jungle warfare. Among about a dozen qualified contractors, Lockheed and Sikorsky were chosen by the U.S. Army Materiel Command, the contracting agency, to submit the more detailed proposals. At the same time - as a parallel effort - the Army selected two contractors to submit more detailed proposals for the management of the prime contract data: Booz-Allen Applied Research and TRW Systems. Also as a funded effort the actual contract given was for the development of hardware through prototype development with the production contract to follow after presumably another round of competitive bidding.

A similar type of selection was used for the prime contractor for the American version of the Super Sonic Transport: After preliminary selection of both Lockheed and Boeing, both firms received funding to further develop detailed specifications and technical approach.

There are a number of questions raised in connection with this new approach of Government to work with private industry:

- Are the costs associated with choosing more than one initial contractor excessive in comparison to the resulting benefits.
- Will it reduce the time gap between conceptual and operational stage of the system.
- Would it be perhaps more economical for the Government to rely entirely on Government-owned facilities to carry development efforts all the way from conception, through research and development, to the beginning of production.

From an economists' point of view the new approach by Government agencies to the selective process increases perhaps the development cost by duplicating efforts to an extent; on the other hand the Government gets the advantage of at least two different approaches in management and technological advancement. Also, each potential

contractor normally has areas of special skills and background. The Government has the option to use obvious better approaches and solutions to speed-up development or to improve overall cost and reliability. This tends to reduce the time gap between conception and operation of the system. Furthermore, should the Government decide that the contractor chosen for the development effort does not perform satisfactorily, at least one alternate contractor is available for the production phase.

The argument that it might be more economical to use Government facilities exclusively for development, is not valid for a number of reasons: It becomes very costly for the Government to maintain the huge staff of skilled employees necessary to cover all needs. The Governmental employment system is rather inflexible and does not allow readily for the necessary mobility of resources. It is very difficult to motivate Government management to the same extent as private industry management since by the very standards set for Government employees, monetary incentives can only play an insignificant role. And finally the Government cannot, like private industry, decide to invest additional funds for a development contract in anticipation of the expected technological fall-out for other products generated or planned for by the commercial firm.

In special situations the Government has however created facilities for participation in major development efforts such as the Air Force Space Systems Division or the Commodity Commands of the Army Materiel Command. It has however almost always been a close co-operative effort between industry and those agencies. Only very few exceptions are known.

Summary: The Government has found new effective ways to maintain competition for complex weapons and space systems. Availability of the total scope of skilled personnel has been accomplished by expanding funds for occasional duplication of efforts. Elapsed time to system operation has been reduced by a faster application of new technology and management methodology. Actual cost control has been improved.

because comparison of cost on a task basis can now be made on the basis of more than one estimate.

Case 3: Incentive Contracting:

One problem faced by the Government is that it gets more and more involved in the very detailed control and supervision of contracts. This is very essential for all cost-plus-fixed-fee type of contracts to assure that the contractor is indeed operating in a cost-effective manner.

Increasingly a new type of contracting is used to insure emphasis by the contractor on the area most important to the contracting agency. For example the armed services have placed great emphasis on expected end-product quality, (technical performance and reliability) somewhat lesser emphasis on time of availability and relatively little emphasis on cost of quality control throughout the defense industry, (for example, higher inspection costs have boosted the cost of artillery shells in the previously mentioned Norris case by 10 %) and a much greater demand for management of the lower and middle levels. The results were reliability ratings that assured the status of the antiballistic missile system in the expected state of operational readiness, an extremely low hardware failure rate under field conditions, lower maintenance requirements and presumably lower overall system cost.

During the production phase the incentive plan was extended to cover cost reduction, but so far the program has not been overly successful because of the fact that anticipated savings through cost-effective production could not compensate for the high cost of setting up new producers and the risk of quality failures.

Ever since 1963, after a change in procurement regulations, a new type of incentive program has been used by ex-post evaluation of contractor performance. Specifically the Navy in their anti-submarine warfare program has made use of this program. A board of evaluators

is created and a set of performance goals and criteria set up. After completion of a task, or a series of tasks, values are assigned to each of the criteria and then computed against a predetermined formula. The actual fee is determined according to the degree of performance effectiveness established and applied to the predetermined percentage. (See figure 1)

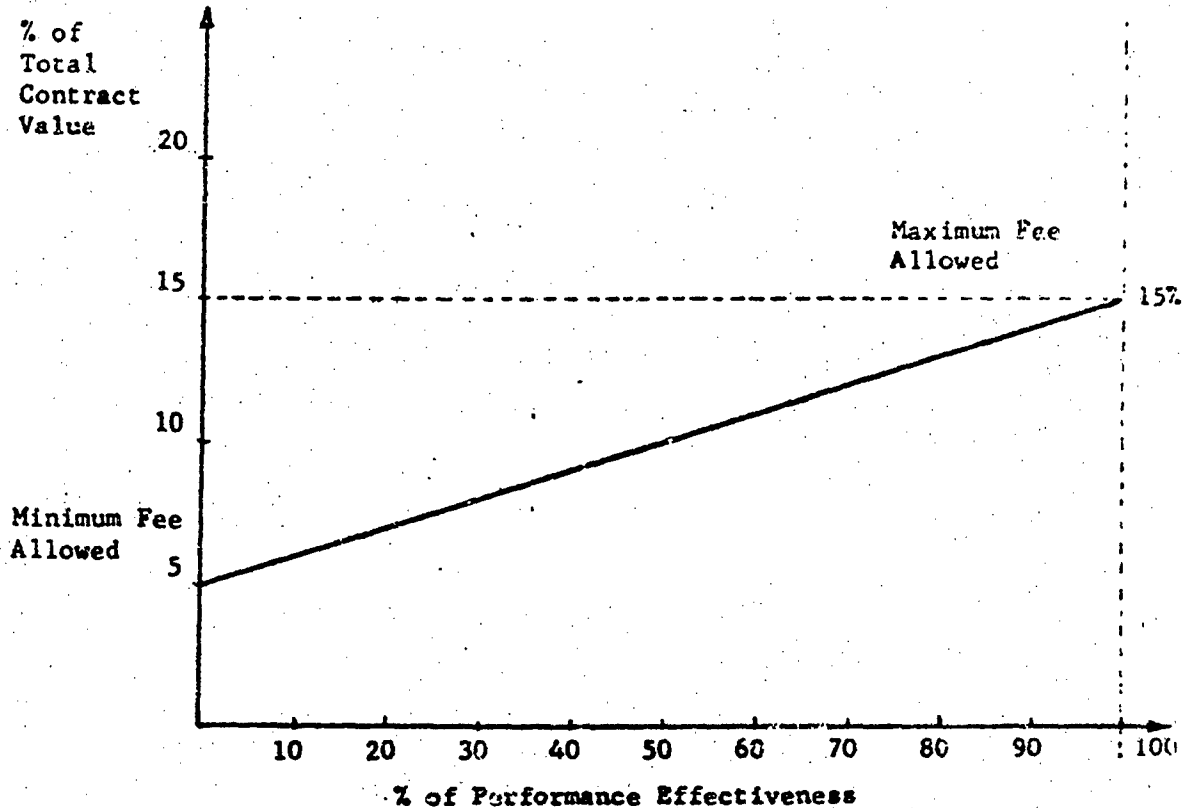


(Figure 1)

The difficulty, of course, is the definition of performance standards to measure with. Already significant advances have been made in this area and it can be expected that measuring criteria will soon be available to evaluate contractor performance in all areas.

Summary: Cost-plus-fee incentive contracting is becoming the preferred method in Government-private industry contractual relationships. As methods and criteria for measurement become more precise and relevant, governmental participation in contract management can be

reduced for an overall increase in cost effectiveness.

Case 4: Specialized areas in which it is, or would be, preferable for the Government to own and operate facilities.

While in most areas of large-systems development technological fall-out can be produced for the developing firm, such as the know-how gained to build satellites for NASA, can be exploited to develop a commercial communication satellite or the heat-resistant material used for the nose cone of a rocket is equally well-suited as the material for all sorts of cooking ware as demonstrated by the Corning Company. But unfortunately in some areas of technological development no immediate fall-out can be expected and not even the normal requirement for more product for the operational phase, as is normal.

Specifically we could mention the area of rocket propulsion. Let us first look at a typical demand curve for a new product during the various phases of its life cycle: (Figure 2)

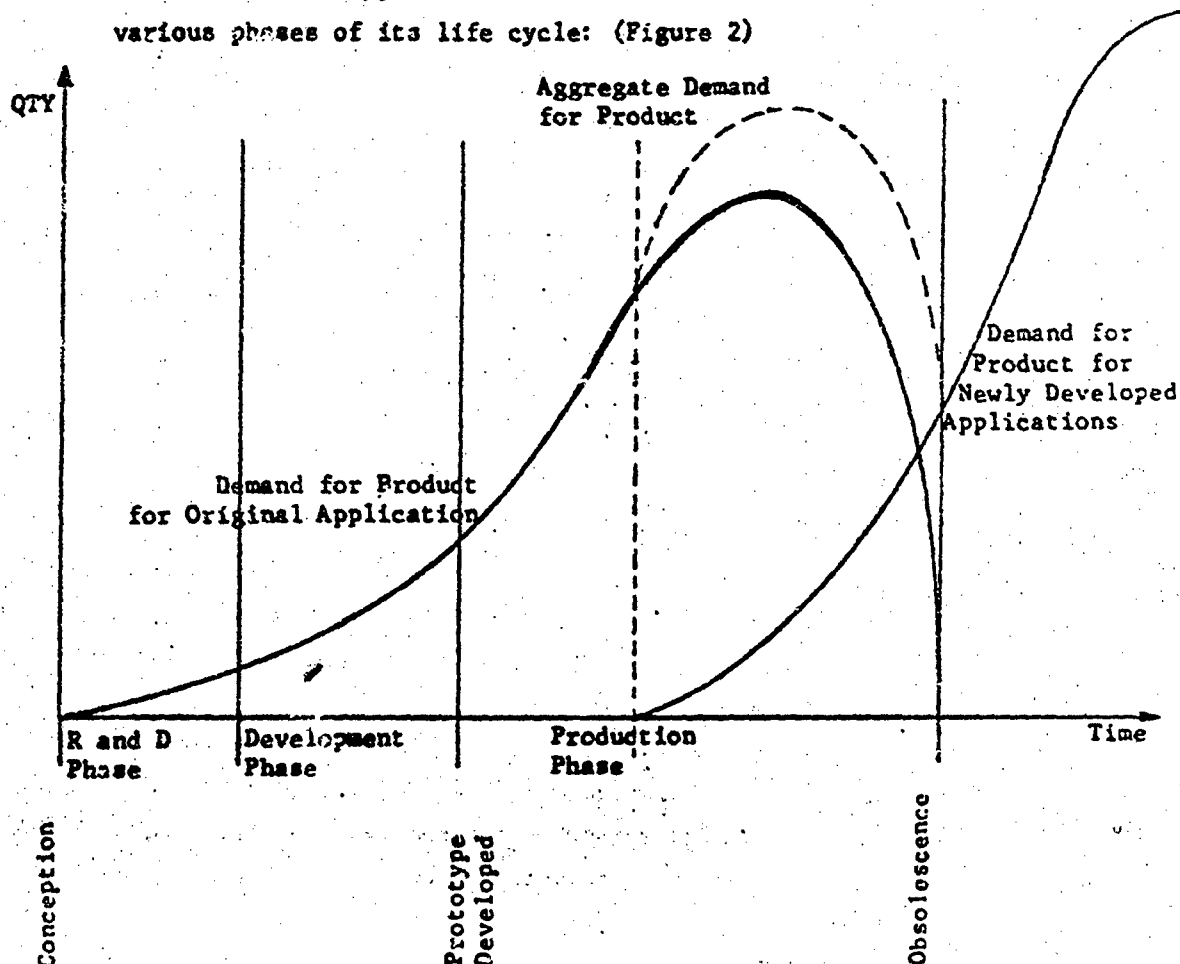


(Figure 2)

There is a small initial demand for the product through development of prototype. The heavy demand is during the production phase. While use for the prime requirement subsides, alternate uses for the product are being identified and marketed, so that the aggregate demand for the product is sustained at high levels over a significant time period.

A contractor can recoup total cost of development and realize a profit during that phase, with expectations of more profit as alternate product use continues.

Let us compare this now with the typical demand curve for a rocket propellant:

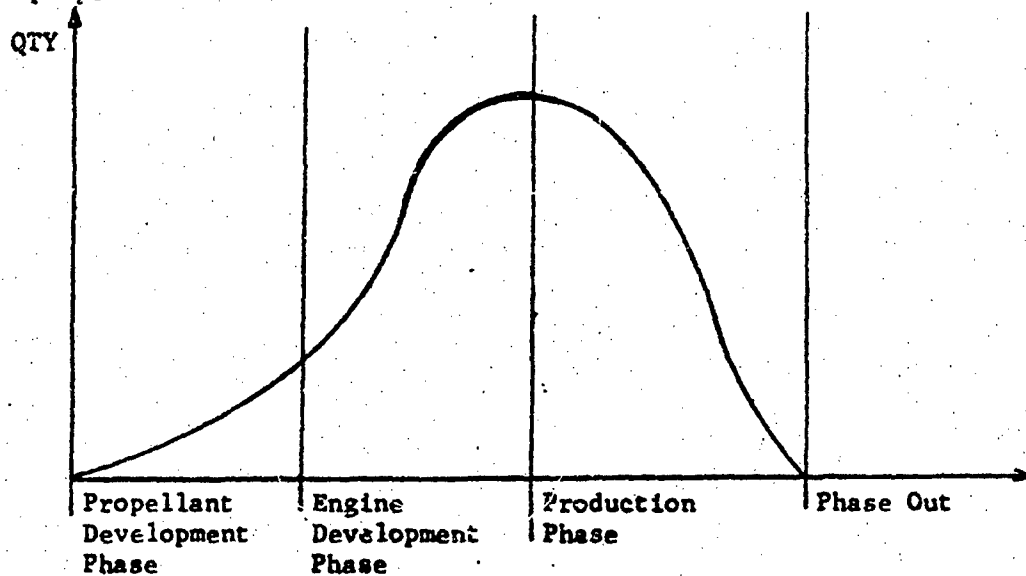


(Figure 3)

The requirements for the product are high during propellant development and even higher during engine development, with very little additional needs during the operational phase. There are usually no alternative uses for the product, ergo there is no possibility for a private firm to recover the cost of development or make a profit.

In addition to the atypical distribution of demand, alternative propellants for a given purpose may completely scrap an existing

program. Take for example the solid propellant booster developed by the Aerojet-General Corporation: In a recent test 1,645,000 pounds of propellant produced 5.4 million pounds of thrust in a 75-second burn.⁽⁸⁾ The idea is to prove the great potential use in multi-stage launch vehicle systems to carry heavy payloads into space at a cost per pound less than that delivered by clustered liquid engines.

However, the Space Agency contends that nuclear upper-stage rockets coupled with the liquid-fueled Saturn V booster, will be capable of lofting any foreseeable payloads.

The outcome of the test - not yet evaluated at the writing of this paper - will decide whether or not the program will be adequately financed or discontinued.

It is obvious that risks such as these are a burden which cannot be carried by a contractor. In addition to the cost-recovery problem, it would appear advantageous for the Government to own and operate such a facility.

Summary: In special cases of product development, Government-owned and -operated facilities appear to be not only economically feasible, but actually advantageous in an economic sense.

⁽⁸⁾L.A. Times, June 16, 1967, p. 6, part II

CONCLUSION

The effect of Government on private industry has been very evident in a number of areas, but does not reflect the full impact of Government expenditures in percent of gross national product.

Examples:

- Wage and salary policies of the Government follow patterns established by private industry.
- The Government does not monopolize - at least not on a large scale - products or processes developed under Government contracts.

On the other hand, Government expenditures have caused significant changes in American industry:

- A large number of enterprises have newly been created solely or primarily on the basis of Government contracts. Many of them have grown into large industrial complexes, such as North American Aviation, TRW Systems, PRC.
- Methodology, processes and products developed for or by the Government, have been adopted throughout the American industry for a wide scope of applications in the public and private sector of the economy. Examples are (1) PERT - a Project Evaluation and Review Technique, developed by the Navy for the planning and control of the Polaris program. (2) The Systems Engineering Concept developed jointly by the Aerospace Industry and the Air Force for the Ballistic Missile program.
- Pools of skilled resources have been developed flexible and mobile, not only between industries and applications, but also geographically to respond to the many varying needs of the Government.
- Development of industrial centers of gravity with vast impacts upon the employment, educational facilities, land use and other aspects of a given region, such as the centralization of the aerospace industry in Southern California, the Manned Space Flight Program in Houston, Missile Ranges in Florida and Southern California.

- The growing participation of Government in the managerial function of industry and the development of Government as an entrepreneur.

There are also important problem areas which should not be overlooked.

- There are definite limits in the economics of size. Centralization can only be justified up to a point.
- It is difficult to provide incentives for creative entrepreneurship in a system that is too heavily dependent upon Government influence.
- An economy significantly dependent upon Government expenditures could easily lose stability and stagnate or expand too rapidly as a result of political decision-making.

In Summary

American industry has adapted itself to the increasing effects of Government expenditures without losing its identity of a modified free enterprise system in contrast to the stricter system of state capitalism. Economic and social changes have come about through evolution rather than revolutionary upheaval. Without the availability and thorough analysis of large masses of statistical data, it is not possible to state conclusively that the results of increased Government expenditures have caused a change in industry that has both caused a better deployment and combination of resources and a better distribution of income. However, the rise in personal incomes and growth of GNP seem to indicate a positive effect on the total economy.

COMMUNICATION AND THE MANAGERIAL PROCESS

(1 August 1967)

by
Warren H. Schmidt

Dr. Warren H. Schmidt received his A.B. from Wayne University, his B.D. from Concordia Seminary, St. Louis, the M.A. and Ph.D. in psychology from Washington University, St. Louis. His career at UCLA, which began in 1955, has involved both administrative and faculty positions. He was Director of Statewide Conferences and Community Services for University of California Extension, and is now Director of the Master of Business Administration Program in the UCLA Graduate School of Business Administration. He has written extensively in the fields of human relations, leadership and conference planning, and is co-author of the book "Techniques that Produce Teamwork."

I. Critical Importance of Communication in Management

Communication is the process by which we share our thoughts and feelings. Since a manager, by definition, depends on others to carry out his decisions and policies, communication is a central aspect of his job. A manager is paid for not only identifying problems, making decisions and giving instructions, but also for gaining acceptance of those instructions so that they will be implemented. All of the time and energy which goes into planning and decision making is worthless unless the decisions are implemented. Recognition of this fact has increased managers' interest in the processes of communication and influence.

II. Purpose of This Session

- A. To deepen our understanding of what is involved in getting an idea from one person to another.
- B. To identify common blocks to effective communication.
- C. To explore ways of overcoming these blocks.
- D. To better understand factors which help or hinder communication in a work situation.

These processes will be achieved through a combination of experiments, lectures and discussion.

III. Perception - A Basic Aspect of Communication (demonstration and lecture)

Perception is a basic concept of psychology which managers need to keep in mind in order to understand the complexity of communication. An individual's perception of any event is determined by two major factors: a) outside stimuli and b) his past experience which is evoked by the stimuli. Since each individual carries with him a different kind of past experience, it follows that each person will have a somewhat unique perception of a single event.

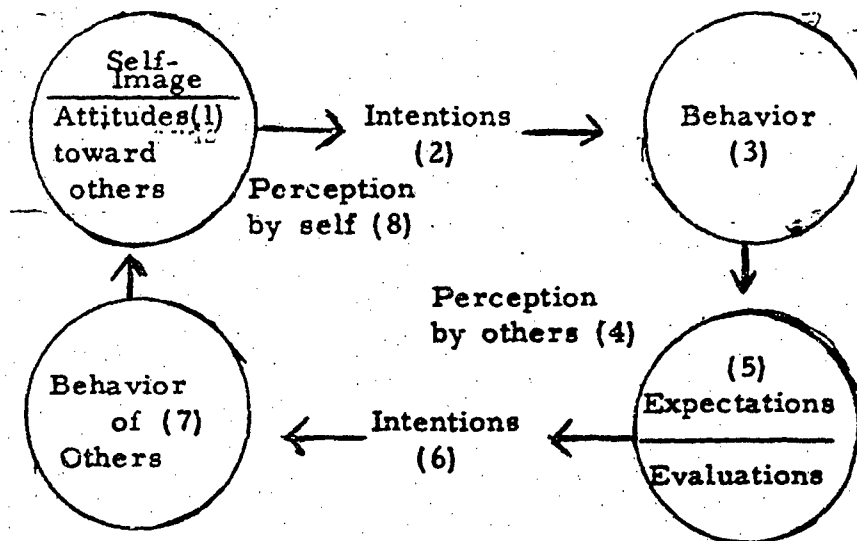
IV. Comparison of One-Way and Two-Way Communication (Experiment and lecture)

In an experiment of one-way and two-way communication, the following differences tend to emerge with predictable regularity: a) One-way communication takes less time than a two-way process, b) two-way communication produces significantly greater accuracy of understanding, c) the sender tends to over-estimate the accuracy of his one-way communication and to under-estimate the accuracy of his two-way communication, d) the receivers are usually more frustrated during the one-way communication process, and e) receivers have more control over the pace and quality of two-way communication.

All of the studies made of communication emphasize the importance of a feedback system which enables the sender to correct misunderstandings which almost inevitably arise in this complex process.

V. The Circular Process of Communication (a conceptual model)

The following construct diagram, although obviously over simplified, provides a framework for looking at the interaction process between two or more persons:



This might be described step-by-step as follows:

- A. The individual has some feelings about himself (self-image) and has a set of attitudes toward the others with whom he wishes to interact.
- B. These feelings and attitudes become intentions toward the others. For example, if his feelings are that his ideas are wanted and appreciated, and if his attitudes toward others are that he would like to make a contribution, we can predict that he will have the intention of making positive contributions in a group situation.
- C. These intentions cause our individual to initiate some behavior toward the others in the group. His behavior is governed by:
 1. his intentions, and
 2. his past responses to behavior from the other people. We might think of this whole phase of the process as leading up to BEHAVIOR OUTPUT.
- D. The behavior which is put out then passes through a screen which exists in the others. This screen includes their value systems, expectations of how he should behave in this situation, and experience with how he has behaved in similar situations.
- E. The behavior which the individual has put out is then evaluated by the others in terms of these expectations, which tends to either support the expectations or to vary from them.
- F. As a result of this evaluation, the members develop some intentions toward the individual.
- G. These intentions again serve to motivate their behavior back to the

individual, and so they initiate some behavior.

This whole phase might be called the BEHAVIOR INPUT.

- H. This behavior goes through a screen which the individual has, that is, his feelings about himself and his attitudes (the ones we started with), and he receives feedback which either supports or modifies his expectations.

VI. Communication and Organizational Climate

The degree to which communication flows easily in an organizational system is heavily influenced by the climate of trust or distrust in that system. Dr. J. R. Gibb has emphasized this fact in his studies of defensive and indefensive climates. Gibb makes the point that every individual has four primary and continuing psychological concerns:

- A. Acceptance: (The degree to which the person feels accepted and respected by himself and others).
- B. Data Flow: (Determining what influences he exposes himself to and what data he shares with the people around him).
- C. Goals: (Determining toward what purposes he is directing his energy).
- D. Control: (How he disciplines himself and influences his environment to achieve his purposes).

In a group or organizational system, each individual develops some feeling about the extent to which he is accepted and respected. This feeling then determines the extent to which he expresses his ideas freely and spontaneously or the extent to which he presents a "polite facade" or bases his comments on strategic considerations. If a group is made up predominantly of people who are playing a strategic game, the decisions they make tend to be superficial and to carry little commitment on the part of those who made them. Such a group then tends to become apathetic, requiring a control system characterized by dependency rather than interdependency.

The central implication of Gibb's model is that the principle way to achieve a creative and highly integrated group is to develop a climate of trust which then opens the way for easy data flow and realistic goal

formation.

VII. Some Requirements for Effective Communication

- A. An awareness that I am a person with feelings and that I can live with the fact that my feelings influence me and my communication.
- B. A tolerance of other people's feelings and an awareness that their feelings, which may be different from mine, affect their sending and receiving communications.
- C. The intention as sender to build feelings of security in the receiver.
- D. The intention as a receiver to listen from the senders' point of view rather than evaluating the communication only from his point of view.
- E. The willingness to take more than half the responsibility for the effectiveness of communication whether as sender or receiver.
- F. The conscious effort to build feedback into all communications.
- G. The ability to resist acting on and reacting to my assumptions about another person's reasons behind a particular communication.
- H. A recognition that communications at best are imperfect and the avoidance of undue cynicism from difficulties or failures to communicate.
- I. Viewing my own functions in the organization as one of maintaining the process of communication with people who are fully capable of facing and resolving problems. Having confidence in those with whom I communicate.

SOLID PROPELLANTS: OSCILLATORY AND UNSTABLE COMBUSTION
(8 August 1967)

by

Norman W. Ryan

Mr. Ryan, who is Professor of Chemical Engineering at University of Utah, earned the B. Chem. and Chem. E. Degrees at Cornell University, and Sc. D. at Massachusetts Institute of Technology. He has been Chemical Engineer on the staff of the Research Department of Standard Oil Company and consultant to major chemical and rocket companies as well as agencies of the Department of Defense in the areas of rocket propulsion. His research includes areas of rheology, gas dynamics, combustion and condensation.

GENERAL CONSIDERATIONS

When significant excursions from the steady-state pressure level occur in a rocket chamber and we cannot attribute them to something else, we attribute them to combustion instability. As the combustion process is the means of producing sensible energy in the rocket system, we presume that combustion must somehow amplify pressure disturbances. Oscillatory combustion is the term applied to instability in which the pressure oscillates periodically or quasi-periodically. In all kinds of instability we can reproduce for study, oscillatory combustion is present.

Instability is a systems concept and has no meaning in application to elementary processes. Instability can arise if elementary processes that proceed simultaneously are coupled; that is, if fluctuations in one can influence the others. Instability does arise if a disturbance in one process produces an amplifying response in one or more others.

Combustion itself is not an elementary process but is a set of coupled sub-processes. If we follow the history of a particle of propellant, we note that it starts out as a cool solid mixture of reactive materials; it is preheated, may undergo solid-phase reactions in the final stages of preheating, then engages in a complicated set of reactions and diffusional operations at the gas-solid interface, and finally proceeds to near adiabatic equilibrium in the gas phase. There is feedback of reactive species and energy from the gas phase to the surface and part of the energy to the sub-surface material.

We see that the combustion process itself contains the necessary ingredients for instability--feedback and mass and energy capacitances. It is interesting to postulate an isolated combustion process and ask if it can exhibit intrinsic instability. We don't know the answer. We do know that under some conditions, we cannot make the propellant burn, and some investigators have suggested that under certain conditions propellants undergo oscillatory combustion at preferred frequencies. Suitable experiments have yet to be performed. On the other hand, the subject of intrinsic instability may be irrelevant. The dominant view among investigators is that we can explain all instances of instability as interaction between combustion and other processes in the rocket system. That view will be taken in the remainder of this lecture.

There are two questions to be asked: "In what ways can combustion interact with other processes in the system?," and "Under what conditions do the interactions result in instability?"

With respect to the first, we consider three kinds of stimuli that can be provided by the surroundings of the combustion zone--heat removal or supply, gas motion, and pressure. Heat removal from the combustion zone, by radiation for instance, would reduce the feedback flux from the gas phase to the gas-solid interface. As the reaction steps are strongly temperature dependent, one would expect the results to be dramatic. It happens, however, that simple thermal coupling between combustion and other processes is very weak in a rocket combustion chamber. It may be significant in some experimental burners.

Gas motion induced in the combustion zone by the contiguous flow field can give rise to what is known as velocity coupling. An instance of the effect of this stimulus is erosive burning. A related phenomenon is the variation of ignition time with gas velocity when ignition is achieved by convective heat transfer. Gas motion parallel to the burning surface affects, usually but not always in a way to enhance, the mixing and feedback processes in the gas-phase region of the combustion process.

Finally, pressure, in an effect known as pressure coupling, can influence the rate of combustion by compressing the gas-phase zone, thus

providing both compression heating and steepened concentration and temperature gradients. The rates of the feedback sub-processes are thereby altered. So also are pressure-dependent, energy-limited surface reactions such as the dissociative vaporization of ammonium perchlorate. Here we must be careful to distinguish between the normal effect of steady pressure, which is a primary variable in determining the steady-state combustion rate, and transient pressure, which is the symptom of instability.

To answer the second question concerning the conditions needed for the response to result in instability, we find it convenient to think in terms of a periodic stimulus, its characteristic time being the reciprocal of its angular frequency. If the characteristic time of a transient stimulus is very large compared with the greatest characteristic time of the combustion sub-processes that can respond, then the combustion process remains essentially in a steady state dictated by the instantaneous conditions of constraint.

Put another way, the response is in phase with the stimulus--a nonamplifying situation. As the combustion zone is the sole source of energy, the unamplified transient will be damped out by the available dissipative processes in the rocket system. If, on the other hand, the characteristic time of the stimulus is very short compared with the characteristic times of responsive sub-processes, then the response will be 180 degrees out of phase--also a nonamplifying situation. If the stimulus and the response characteristic times are of the same order of magnitude, then we have the possibility of amplification or attenuation.

If it is of interest, then, to estimate the characteristic times of the combustion process. As an upper limit, we can take the time of residence of propellant material in the combustion wave; and that time is from 0.5 to 50 msec for ammonium-perchlorate composite propellants, typically from 1 to 10 msec. The largest of the characteristic times is usually that of the preheating thermal wave in the solid. Given by the ratio of thermal diffusivity to the square of the steady-state burning rate, its value is typically from 1 to 8 msec. We suspect that the combustion may be an effective amplifier for signals in the frequency range of 100 to 1,000 rad/sec.

Our ignorance of the nature of the surface and gas-phase events makes

estimating other characteristic times difficult. The mass and energy transport times in the gas phase would be the residence time if plug flow conditions were obtained. We would estimate a time of the order of 10 to 100 microseconds and expect a sensitive response to stimuli in the frequency range of 10,000 to 100,000 rad/sec.

It is generally agreed that reaction times are very short indeed, one estimate being 0.1 microsecond. If oscillations at frequencies of the order of 10^7 rad/sec are amplified to significant amplitudes, they have not been observed and reported. The reactions are probably distributed in a chaotic gas-phase region, and their effect is probably to accentuate the sensitivity of the mixing and transport sub-processes.

Having identified two frequency regimes in which we would expect the combustion process to be a sensitive amplifier, we inquire about the source and selection of the disturbances to be amplified. Pressure pulses of complex form, therefore containing components of many frequencies, are not uncommon. More reliable as a source is the combustion process itself, which generates noise with a wide spectrum of frequencies.

The selection of frequencies to be amplified is made by the non-combustion processes in a negative way. As these processes are attenuating in nature, they favor some frequencies simply by being less capable of absorbing energy at those frequencies. If the loss due to attenuating processes is less than the gain due to combustion, then oscillations will grow.

The ideas that have been expressed so far will be applied to two kinds of instability--acoustic instability and L^* instability.

ACOUSTIC INSTABILITY

Acoustic instability acquired its name from the fact that the observed oscillations are acoustic waves at frequencies determined by the properties of the gas and the geometry of the gas cavity. The frequency range encountered in practice is about 5,000 to 100,000 rad/sec, where one expects the sensitive sub-process of combustion to be the feedback of energy and mass.

The gas cavity is sharply selective with respect to the frequencies

observed. Many shapes of gas cavity have been employed in rockets and test burners, and all the types of acoustic modes compatible with the geometries have been reported. The combustion process is not so discriminating; it behaves as a broad-band amplifier over large frequency and pressure ranges.

The acoustical description of this kind of instability attributes to the combustion zone an acoustic admittance which is simply related to the coupling function connecting gas generation rate to pressure. One obtains one or the other of these quantities from the measured growth rate of the pressure oscillations adjusted for the losses in the experimental system employed. One of the interesting predictions of the acoustical description concerns the role of the solid propellant grain in the acoustical system. It represents a significant sink for the energy of the oscillations at frequencies such that it can vibrate in resonance.

The T-burner, a cylindrical, center-vented burner employing end-burning grains, is the principal tool for evaluating the tendency of a propellant to amplify pressure-coupled oscillations. Because the instability seems to be more severe in some rocket systems than in T-burners, it is believed that velocity coupling also contributes. There is not, at the present time, a suitable method for obtaining values of the coupling function from experimental measurements.

L* INSTABILITY

The phenomenon of L* instability occurs when L^* , the gas cavity volume divided by the nozzle throat area, is small. A second condition for its occurrence is that the normal burning rate of the propellant be a small value. The frequency range observed with a small class of composite propellants carefully studied is about 200 to 1,200 rad/sec, where one expects the sensitive sub-process to be the thermal wave in the solid.

The most severe form of this kind of instability is chuffing--alternating ignition and extinguishment. As the propellant burns back, L^* increases; and the fraction of burning time in the chuff cycle increases. Oscillations of characteristic frequency appear on the crests of the chuffs and grow in

amplitude until burning ceases again. As L^* increases still more, stable conditions appear. Even then, oscillations, which damp out, can be triggered by a disturbance; and the frequency can be measured.

At the present time, the frequency of the oscillations cannot be predicted. Attempts to construct a descriptive theory, at present in a primitive state, suggest that the gas residence time determines the frequency.

SUPPRESSION OF INSTABILITY

Effective suppression of acoustic instability in the frequency range where it has been commonly encountered has been achieved by including aluminum in the propellant. The most popular view of the manner in which it acts is that the fine alumina produced dissipates the acoustic energy in the gas cavity. The particle size of the alumina is determined by the combustion characteristics of the metal, and the damping effectiveness is dependent on particle size. At the much lower acoustic frequencies one would expect in very large solid-propellant rockets, the fine particle damping mechanism may not be effective.

On the other hand, if at least part of the effectiveness of the aluminum results from a spoiling of the pressure-burning rate coupling at the combustion zone, it is exerting its influence in the thin combustion zone gas phase. At lower frequencies, however, the sensitive sub-process is in the solid phase; and again we conclude that there is no reason to expect aluminum to be effective. It is clear from experiments with experimental burners operating at low L^* levels that aluminum does not affect stability except insofar as it influences the burning rate.

ARPA Liquid Programs - A Critical Review
(15 August 1967)

by

Forrest S. Forbes

Forrest Forbes is the Chief of the Liquid Propellant Branch, Propellant Division, Air Force Rocket Propulsion Laboratory. He received his B.S. in Chemical Engineering in 1951 from the University of Iowa. He began his career at Wright Air Development Center, Wright-Patterson AFB, Ohio in 1951; then transferred to AFRPL in 1959 where he managed the liquid oxidizer research, development and evaluation programs including the effort that resulted in the development of chlorine pentafluoride. Mr. Forbes has also acted as chairman, advisor, and consultant for many boards and committees working in fields related to rocket propellants.

The ARPA liquid propellant program covered a very broad spectrum of propellant technology with the emphasis concentrated in four major areas: homogeneous oxidizers, heterogeneous fuels, heterogeneous monopropellants, and combustion of metallized fuels.

Many propellants and ingredients were screened for performance, compatibility and physical properties. The promising propellant combinations were formulated; of prime interest were N_2F_4 , ClF_5 , TNM and Compound "T" $[C(NF_2)_4]$. Attempts to reduce the vapor pressure of N_2F_4 were not successful. The most attractive mixture, N_2F_4/ClF_5 , from the standpoints of both performance and physical properties, was reactive.

Mixtures containing sufficient amounts of Compounds "T", "R", or other NF materials having acceptable performance or vapor pressure, were too sensitive for practical use. N_2O_4 can be upgraded by about 10 seconds with 30% "T"; the resulting mixture appears to meet acceptable safety standards, but the availability and difficulty

of handling "T" will limit further development. A low-temperature N_2O_4/NO gel was formulated that has acceptable properties and stability. It was successfully flowed at $-30^\circ F$. Its performance with hydrazine is 290 seconds.

Heterogeneous fuels containing aluminum, beryllium, AlH_3 , and BeH_2 were successfully formulated. The EDH-A and EDH-B compositions have good low-temperature utility and reasonable high-temperature stability. These two fuels, and a Be/N_2H_4 gel, are now ready for larger scale development studies. BeH_2 -based fuels exhibited high reactivity with MMH although some improvement was made. Recent Aerojet material appears, however, to meet our gas evaluation requirement. Replacing some of the hydride with beryllium metal merits additional study because of the higher weight loadings attainable. The use of agents to thicken, rather than to gel, may reduce or eliminate bulk expansion due to gas evolution. Satisfactory fuels can be formulated using hydrocarbon carriers.

Several high-density heterogeneous monopropellants based on boron carbide appear to be very attractive candidates for volume-limited applications. High-energy monopropellants based on BeH_2/H_2O_2 and other components were also satisfactorily formulated. Some water is required for desensitization and some decomposition occurs with BeH_2 formulation. From the combustion results in the small test equipment, it appears that the burning of metallized fuels with high

efficiency is possible. Since C^* measurements require precise hardware dimensions, future tests should be conducted at higher thrust levels. Both Al and AlH_3 propellant combinations appear very attractive, although throat erosion may be a problem.

As expected, the combustion of N_2F_4 /"R" and N_2F_4/ClF_5 mixtures with hydrazine went smoothly and resulted in high efficiency. The data reported for the BeH_2 systems indicated high C^* efficiency, while for Be gels, a lower efficiency. Sufficient variations in metal combustion efficiency under different conditions have been observed to indicate that substantial combustion improvement should be attainable. Combustion studies of BeH_2 gels are being continued by Aerojet-General Corp. under an AFRPL contract.

The ARPA liquid propellant program will serve as a guide for future propellant efforts. Many propellant mixtures were formulated and found unsuitable. Satisfactory formulations have been identified and should receive further consideration.

23 August 1967

SHOCKS AND THEIR EFFECTS ON PROPELLANTS

Leslie B. Seely, Jr.

Poulter Laboratory for High Pressure Research
Stanford Research Institute
Menlo Park, California

The subject of shock waves is quite simple. An adequate discussion of the subject can be carried on with recourse to no more than the most basic mechanical laws, and the major features of shocks can be analyzed with mathematics no more complicated than algebra. There is considerable merit in treating shocks in this simple way in order to set forth their important properties as clearly as possible; the assumptions made will be readily perceived. It is also possible to arrive at the same result (and gain, it is true, the capability of considering very complicated cases) by using involved mathematical methods and developing shock theory from the differential equations of compressible flow. In this case we are apt to overlook the true difficulties because they are hidden in the basic assumptions of differential calculus; we assume that it is legitimate to integrate equations dealing with infinitesimals to arrive at equations governing finite differences occurring at what is, from a practical point of view, a discontinuity in the variables.

Let us start from an intuitive point of view. We must first state what we are considering: A shock is a compressive wave of finite amplitude. The words "compressive wave of finite amplitude" already tell us a great deal about the properties of the shock. For instance, compression means that the volume of the material in which the wave is traveling becomes smaller. This implies the existence of particle motion, a concept which

is basic to shocks but usually difficult to grasp by those considering the subject for the first time.

A computer-generated movie was shown during the talk to illustrate what must happen when a material is rapidly compressed by a finite amount. The picture showed a 50 x 50 array of evenly spaced dots representing in two dimensions the mass points in the material. It was then imagined that a piston compressed the field of dots from left side, moving the first row of dots to one half their original distance from the second row. In the second frame the motion was continued and the distance between the second and third rows decreased by one half. The piston had by this time moved a distance equal to the original spacing between two dots, whereas the effect of the compression, evidenced by the change in spacing, had moved two dots. When the film was continued at normal framing speed, the changed average light intensity in the compressed region indicated the increased density. The front of this region progressed across the screen at a constant velocity in a plausible representation of a compressive wave of finite amplitude.

At the right side of the field of dots the wave was considered to encounter an absolutely rigid wall. This prevented motion of the last column of dots. It was noted that the piston had moved half way across the field (compression of two) at this time, and that therefore the particle velocity (equal to the piston velocity) was one half the shock velocity.

The representation shown in the movie was then changed to give a more compact representation of the phenomenon by abandoning one spatial dimension. A single row of dots can be used to represent the compression

in full completeness although it cannot give as realistic an impression of the progress of the wave. A row of dots was taken from each frame of the movie and placed one above another in order. (The number of dots in each row was cut in half because the author was not as tireless as the computer.) In this way the (x,t) plot shown in Fig. 1 was constructed. The piston velocity can be seen as the slope of the left-hand edge of the dots. The velocity of each dot is the same as the piston since we used the piston velocity constant. The front of the shock is seen as the front of the compressed region. It is clear intuitively from this picture that the compression is related to the distance between the shock front and the piston; that is, the difference between the shock velocity and the particle velocity. The relationship is:

$$V = V_0 \frac{U_s - u_p}{U_s} \quad (1)$$

where V = the compressed volume

U_s = the shock velocity

u_p = the particle velocity.

The subscript zero refers to conditions ahead of the shock.

The shock system treated here is obviously a simple one (a plane flat-topped shock with constant velocity). However, it is the type of system we need in experiments to measure the compressive shock properties of materials.

In order to simplify our considerations, we place our reference axes on the shock front and consider the material to be flowing toward the shock with velocity U_s , as it would toward a standing shock in a wind

tunnel. The laws of conservation of mass and momentum are then applied simply to 1 cm^2 of a very large plane shock. The volume of material entering this area in 1 sec is U_s , and the mass is obtained by multiplying by the density $\rho_0 = \frac{1}{V_0}$. Equating the mass flowing into the shock region to that flowing out of the shock region gives

$$\rho_0 U_s = \rho(U_s - u_p), \quad (1a)$$

which is identical with Eq. 1. Similarly, Newton's second law can be applied to the material flowing through the shock.

$$\begin{aligned} \text{Force} &= \text{mass} \cdot \text{acceleration} \\ &= \text{mass} \cdot \text{change in velocity} \end{aligned}$$

The force is the difference in pressure P . Therefore,

$$P - P_0 = \rho_0 U_s [U_s - (U_s - u_p)],$$

$$\text{or } P = \rho_0 U_s u_p, \quad (2)$$

since P_0 is small relative to P .

This relationship, based on the two most fundamental laws of mechanics, is as powerful as it is simple. It holds regardless of the energy processes that may be occurring in the shock.

Equation 2 is particularly useful for dealing with what happens at interfaces between materials. In order to perform shock experiments we must introduce shocks into test specimens from other materials. At such an interface a shock is reflected either as a shock or a rarefaction depending on the shock compressibility of the specimen material relative to the compressibility of the material in which the shock was originally traveling. It can and has been demonstrated experimentally that for the

type of shocks we have been considering no separation is produced at the boundary; that is, after shock reflection the particle velocity is the same on both sides of the boundary. It also has been observed that the interface assumes a velocity when struck by the shock and that this velocity remains constant as long as the original shock can be considered flat topped. Slightly more complicated considerations involving the conservation laws than those used to develop Eq. 2 can demonstrate that this must be so. For present purposes we will assume that it is an experimental fact that

$$\begin{aligned}
 u_{p,1} &= u_{p,2}, \\
 \text{and } P_1 &= P_2,
 \end{aligned}
 \tag{3}$$

where the numerical subscripts are used to discriminate between the two materials forming the interface.

Because of this important behavior of interfaces, the usefulness of Eq. 2 is greatly enhanced. For the same reason, interface problems should be plotted in the (P, u_p) plane. Written in the form

$$\frac{P}{u_p} = \rho_0 U_s,
 \tag{2a}$$

the equation can be used to determine the shock pressure and particle velocity in the test specimen. The procedure is indicated in Fig. 2. The upper positively sloped curve is the locus of all possible shocked states in the material of the shock generating system (in this case brass). This curve has previously been obtained and is available in the literature. The point S is the state point of the shock in the brass before the interface with the test specimen is encountered. It may be determined

in each experiment by one shock measurement on the brass. The negatively sloped line through S is the locus of all state points that can be reached by expansion in the brass starting at point S . Now if we measure the shock velocity U_s induced in the test specimen by the shock in the brass, we see from Eq. 2a that a line can be drawn with slope $\rho_0 U_s$ through the origin which will contain all values of P and u_p attainable in the test specimen as the result of a shock with velocity U_s . The intersection of this straight line with the expansion curve of the brass is the only point at which the relations (3) hold, and therefore the point I is the desired state point in the test specimen.

Thus, one shock experiment producing a particular shock velocity U_s in the sample enables us to plot one point in the (P, u_p) plane. By performing other experiments with shock generating systems designed to produce shocks of various strength we can generate other state points for the specimen material. They will be on a positively sloped curve through the origin with curvature concave upward similar in shape to the dynamic compression for brass shown in Fig. 2. Such a curve is called the Hugoniot curve for the substance in question. It can be transposed to the (P, V) plane by use of Eq. 2 which is the more usual plane in which to plot it. We have so far not invoked use of conservation of energy, but by its use additional properties of the Hugoniot can be developed. In particular, an expression for the internal energy of the shocked material can be obtained.

There are at least three experimental designs for performance of shock experiments to yield shock velocities:

1. High explosive shock generating systems with the pressure adjusted to the desired value by the "mismatch-attenuator" system. These shocks are not precisely flat topped, but accurate experiments can be performed, particularly at high pressures.
2. High explosive shock generating systems employing a "flyer plate." This system is capable of generating flat topped shocks for periods up to 5 μ sec.
3. Light gas gun systems in which the flyer plate is the flat end of a projectile. This system is particularly accurate in the low pressure regime.

In addition, shock measurements may be made of parameters other than the shock velocity. The particle velocity may be measured and used with the Hugoniot of the adjoining material in the shock-generating system to derive the pressure or used with a simultaneously measured shock velocity to derive the pressure independently. Alternatively, quartz or manganin gages may be used to record the transit time through the specimen and in addition record the time structure of the pressure pulse if the wave in fact is not a simple discontinuity (as we have so far assumed).

In summary, the theory of shocks is simply derived from the most basic physical laws. True, we have induced the simplicity by our assumptions, but this induced simplicity is appropriate to the problem of measuring the dynamic compressive properties (Hugoniot curves) of materials. In order to measure the Hugoniot curves of new materials, we must in fact use plane fronted, flat-topped shocks. The objection might be raised that in practical cases of interest we are confronted with thin irregular fronted shocks with a steep pressure gradient behind

the front. This is true, but nevertheless the measurements should be carried out with the simple shocks to which our analysis applies. There are two reasons for this. First, the simple dynamic compressive properties of materials must be determined before we can calculate how fast any shape of shock wave will move in them or how shock reflections will occur at the interfaces between them. Second, it is much more difficult to make measurements on a thin shock than on a flat-topped shock because the thin shock changes continually in velocity; no steady state is possible. It must, of course, be admitted that eventually we must deal with the thin shocks that are of interest in many practical situations. At that time we must obtain enough information about the expanded states of the materials to predict sound velocity at all points in the flow, and when we consider free surfaces of the materials we must study their dynamic tensile properties to predict spalling and similar effects. But of primary and prerequisite importance is the measurement of dynamic compressive properties. The detailed shape of the Hugoniot curves can indicate much about shock-induced changes in the materials.

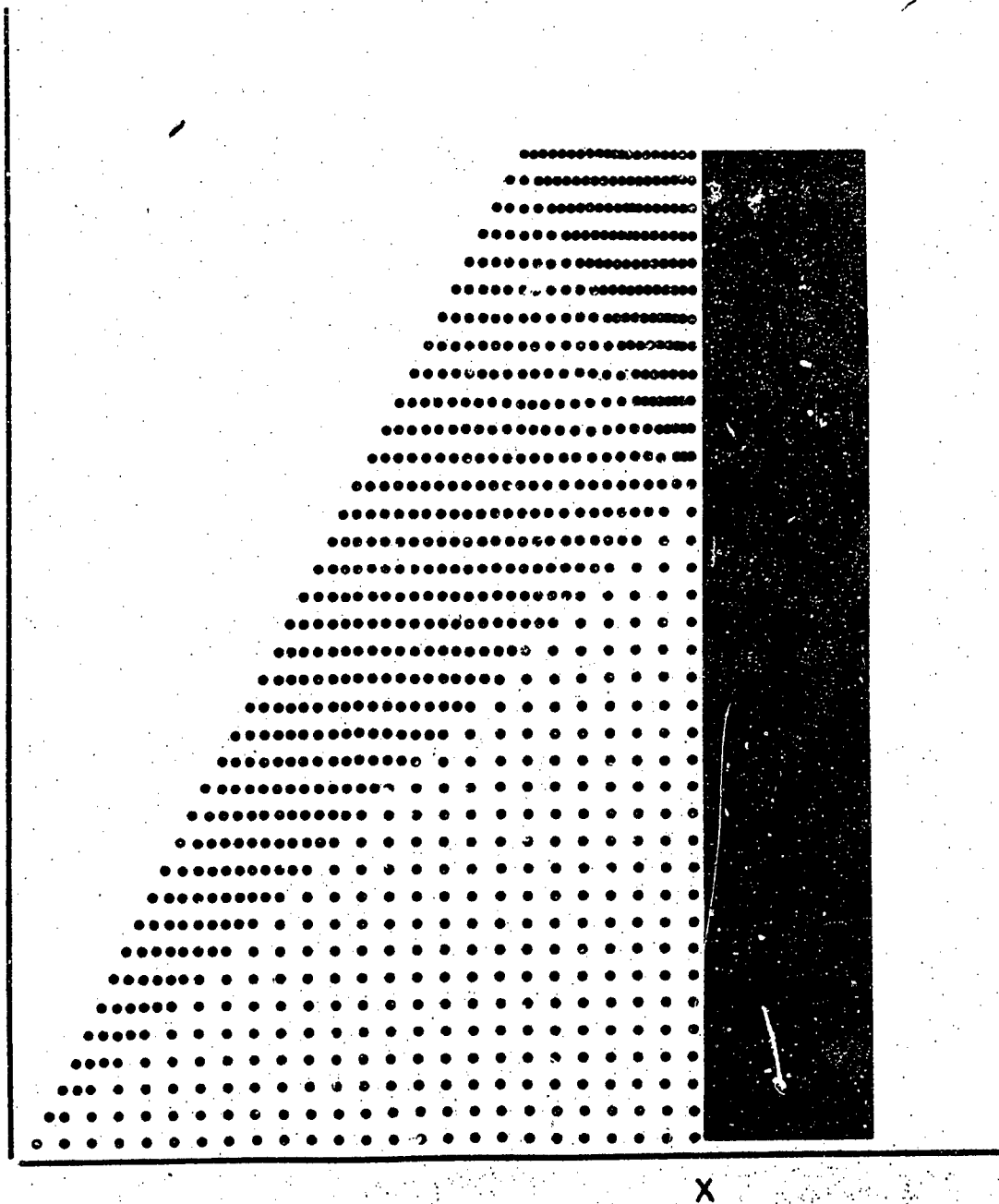


Figure 1. Plot of Mass Points in the (x, t) Plane. A shock is shown moving through a compressible material and reflecting from an incompressible wall.

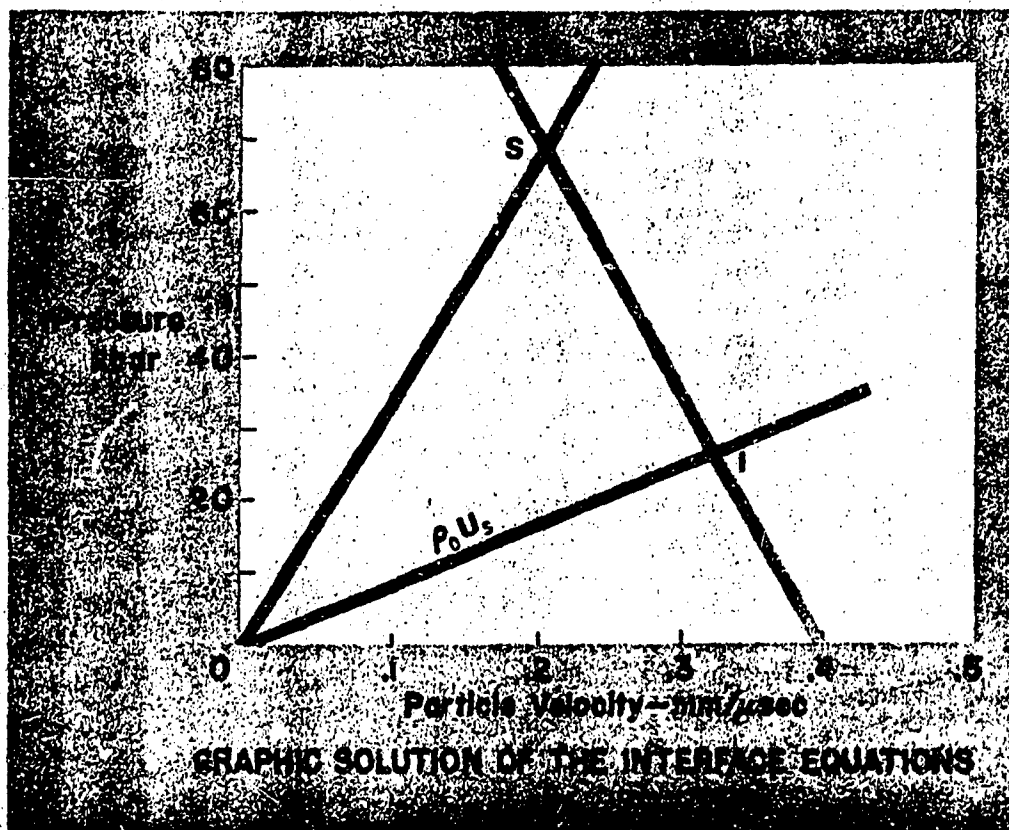


Figure 2. Method for Determination of the Pressure in a Test Explosive.

Unclassified

Security Classification

DOCUMENT CONTROL DATA - R & D

(Security classification of R&D, body of abstract and indexing annotation must be entered when the overall report is classified)

1. ORIGINATING ACTIVITY (Corporate author) Air Force Rocket Propulsion Laboratory Edwards, California 93523		2a. REPORT SECURITY CLASSIFICATION Unclassified	
		2b. GROUP	
3. REPORT TITLE AFRPL Scientific and Engineering Seminar Abstracts - 1967			
4. DESCRIPTIVE NOTES (Type of report and Inclusive dates) 10 January 1967 through 15 August 1967			
5. AUTHOR(S) (First name, middle initial, last name) Edited by Dr. Lawrence J. Edwards, and Charles M. Stone, Lt, USAF			
6. REPORT DATE February 1968		7a. TOTAL NO. OF PAGES	7b. NO. OF REFS
8a. CONTRACT OR GRANT NO.		9a. ORIGINATOR'S REPORT NUMBER(S) AFRPL-TR-68-42	
b. PROJECT NO.		9b. OTHER REPORT NO(S) (Any other numbers that may be assigned this report)	
c.			
d.			
10. DISTRIBUTION STATEMENT This document is subject to special export controls and each transmittal to foreign governments or foreign nationals may be made only with prior approval of AFRPL (RPPR-STINFO), Edwards, California 93523.			
11. SUPPLEMENTARY NOTES		12. SPONSORING MILITARY ACTIVITY Air Force Rocket Propulsion Laboratory Edwards, California 93523	
13. ABSTRACT Opportunities for personal growth through intellectual stimulation and the acquisition of new knowledge should be available to scientists, engineers and managers regardless of their field of experience or geographical location. Such opportunities are readily available when colleges and universities are located in the immediate vicinity. However, at the Air Force Rocket Propulsion Laboratory (AFRPL) the nearest university is approximately two hours distant by automobile. Accordingly, in September 1964 a seminar program was initiated as a lecture series for the scientists and engineers. In the first three years, over 100 seminars were conducted on a wide range of subjects dealing with both technical and management aspects of research and development. The emphasis in this program has been on subjects relating to the mission and the career development requirements of the Laboratory personnel. In the first three years of operation, many of the seminar speakers have been provided by UCLA on contracts from AFRPL and have included authorities from various government agencies, universities and industry. In addition, Laboratory personnel served as speakers for the program on subjects ranging from technical discussions on in-house experimental studies to reviews of management and planning activities.			

Unclassified
Security Classification

14. KEY WORDS	LINK A		LINK B		LINK C	
	ROLE	WT	ROLE	WT	ROLE	WT
Rocket Propulsion Technical Seminars						

Unclassified
Security Classification